OCS Study MMS 2009-014

cANIMIDA Tasks 3 and 4: SOURCES, CONCENTRATIONS, COMPOSITION, PARTITIONING AND DISPERSION PATHWAYS FOR SUSPENDED SEDIMENTS AND POTENTIAL METAL CONTAMINANTS IN THE COASTAL BEAUFORT SEA

Final Report Submitted to
U.S. Department of Interior, Minerals Management Service
Anchorage, Alaska
March 2009

John H. Trefry, Robert P. Trocine, Matthew B. Alkire, Carrie M. Semmler
Florida Institute of Technology, Melbourne, Florida

Mark Savoie, Kinnetic Laboratories, Inc., Anchorage, Alaska

Robert D. Rember, IARC, UAF, Fairbanks, Alaska

MMS
U.S. Department of the Interior
Minerals Management Service
Alaska Outer Continental Shelf Region

Contract Nos.
M04PC00036
M04PC00035

OCS Study MMS 2009-014

cANIMIDA Tasks 3 and 4: SOURCES, CONCENTRATIONS, COMPOSITION, PARTITIONING AND DISPERSION PATHWAYS FOR SUSPENDED SEDIMENTS AND POTENTIAL METAL CONTAMINANTS IN THE COASTAL BEAUFORT SEA

Final Report – March 2009

Submitted by:

John H. Trefry, Robert P. Trocine, Matthew B. Alkire, Carrie M. Semmler
Department of Marine & Environmental Systems
Florida Institute of Technology
150 West University Boulevard, Melbourne, Florida, 32901

Mark Savoie, Kinnetic Laboratories, Inc.
1102 West Seventh Avenue, Anchorage, Alaska, 99501

Robert D. Rember, IARC-Frontier, University of Alaska, Fairbanks
930 Koyukuk Drive, Fairbanks, Alaska 99775

(e-mail address for corresponding author: jtrefry@fit.edu)

This study was funded by the U.S. Department of the Interior, Minerals Management Service (MMS), Alaska Outer Continental Shelf Region, Anchorage, Alaska, under Contract Nos. M04PC00036 and M04PC00035 as part of the MMS Alaska Environmental Studies Program.

Table of Contents

Page

EXECUTIVE SUMMARY……..……..... xiii

1. INTRODUCTION .....……. 1

1.1 Overview and Goals …… 1

1.2 Study Area …… 1

2. METHODS ……...…… 7

2.1 Field Sampling and Initial Processing 7

2.2 Laboratory Analysis 8

2.3 Quality Assurance and Quality Control 12

2.3.4 OMP Analysis 16

3. TRANSPORT OF WATER, SEDIMENTS AND CHEMICALS FROM RIVERS DURING THE SPRING MELT …… 18

3.1 Overview ……. 18

3.2 Water and Sediment Transport from Rivers during the Spring Melt ……. 19

3.3 Particulate Metals and Organic Carbon in River Water …… 24

3.4 Dissolved Metals and Organic Carbon in River Water ……. 33

4. PARTIONING OF METALS BETWEEN PARTICULATE AND DISSOLVED PHASES IN RIVER WATER …… 38

5. DISPERSION OF RIVER WATER, SUSPENDED SEDIMENTS AND CHEMICALS UNDER ICE IN THE BEAUFORT SEA …… 43

5.1 Overview ……..…… 43

5.2 Dispersion of River Water Under Ice in the Beaufort Sea during Spring 2004 ……. 44

5.3 Dispersion of Sediments and Chemicals Under Ice in the Beaufort Sea during Spring 2004 …… 65

Table of Contents (continued)

Page

5.4 Dispersion of Water Under Ice in the Beaufort Sea during Spring 2006 ……. 83

5.5 Dispersion of Sediments and Chemicals Under Ice in the Beaufort Sea during Spring 2006 …… 88

6. THE DISTRIBUTION OF SUSPENDED SEDIMENTS AND CHEMICALS DURING THE OPEN-WATER PERIOD 93

6.1 Overview ……..…. 93

6.2 Suspended Sediments and Trace Metals in Rivers–Summer 2004-2006 ……..... 93

6.3 Suspended Sediments & Trace Metals Offshore-Summer 2004-2006 ……..…….. 99

7. BIOGEOCHEMISTRY OF ARSENIC AND MERCURY IN THE COASTAL BEAUFORT SEA …… 113

7.1 Arsenic …… 113

7.2 Mercury ……. 122

8. CONCLUSIONS ……. 130

9. REFERENCES 132

ACKNOWLEDGEMENTS …….. 140

APPENDICES ON ATTACHED CD

A. Data
B. Publications, Presentations and Posters

List of Tables

Page

Section 1

Table 1-1: The cANIMIDA Project Indicator Matrix for Decision Making for Task 3 …….. 2

Table 1-2: The cANIMIDA Project Indicator Matrix for Decision Making for Task 4 …….. 3

Section 2

Table 2-1: Summary of instrumental methods and method detection limits for metal analysis of suspended sediments and water ….…… 10

Table 2-2: Data quality objectives and criteria ……..…… 13

Table 2-3: Results for reference materials for suspended sediments …..……,… 14

Table 2-4: Results for reference materials for dissolved metals ……..……. 15

Table 2-5: Initial and final values of endmembers for water masses …… 17

Table 2-6: Error residuals for accepted values calculated for selected transects .. 17

Section 3

Table 3-1: Locations of river sampling sites …….. 22

Table 3-2: Mean, maximum and minimum concentrations of total suspended solids in the Kuparuk, Sagavanirktok and Colville rivers …… 24

Table 3-3: Concentrations of particulate metals and organic carbon in the Kuparuk and Colville rivers during May-June for the years listed … 25

Table 3-4: Concentrations of particulate metals and organic carbon in the Sagavanirktok River and mean values for the and Kuparuk, Colville, and Sagavanirktok rivers during May-June for the years listed …… 26

Table 3-5: Concentrations of dissolved metals in the Kuparuk and Colville rivers during May-June for the years listed … …….. 34

Table 3-6: Concentrations of dissolved metals in the Sagavanirktok, River and mean values for the and Kuparuk, Colville, and Sagavanirktok rivers during May-June for the years listed …….. 35

Section 4

Table 4-1: Means and standard deviations for percent of total metal in rivers that was dissolved during May-June for the years listed ……..……. 39

Table 4-2: Distribution coefficients for metals in rivers during May-June for the years listed ……. 40

Page

Section 5

Table 5-1: Coordinates, sampling dates, total depths, and ice thickness for water stations occupied during May-June 2004 …… 46
Table 5-2: Selected depth gradients for the percent of SR water between Stations along the 1 m isobaths …… 61
Table 5-3: Contribution of SR water to individual stations on June 2, 2004 ….. 64
Table 5-4: Coordinates, sampling dates, total depths and ice thickness for water stations occupied during study in May-June 2006 ……... 84

Section 6

Table 6-1: Concentrations of particulate metals and organic carbon in the Sagavanirktok River for the seasons and years listed ……..….. 94
Table 6-2: Concentrations of particulate metals and organic carbon in the Kuparuk River for the seasons and years listed …….…….…. 95
Table 6-3: Concentrations of dissolved metals in the Sagavanirktok River for the seasons and years listed ……..…… 96
Table 6-4: Concentrations of dissolved metals in the Kuparuk River for the seasons and years listed …….……...…... 97
Table 6-5: Means and standard deviations for percent of total metal in rivers that was dissolved and log K_d during summer for the years listed plus average values for May-June 2004 and 2006 ……..... 98
Table 6-6: Summary data for total suspended sediments for all stations in the ANIMIDA and cANIMIDA study areas and for a subset of stations in the area of Northstar Island ……. 104
Table 6-7: Trends in concentrations of total suspended solids in the coastal Beaufort Sea as a function of wind and ice conditions …… 105
Table 6-8: Means concentrations of particulate metals for water collected from the coastal Beaufort Sea during the open-water season …… 107
Table 6-9: Means concentrations of dissolved metals and salinity for water collected from the coastal Beaufort Sea during the open-water season …… 110

Section 7

Table 7-1: Concentrations of dissolved As in selected rivers and in seawater … 114
Table 7-2: Concentrations of As in surface seawater, phytoplankton, zooplankton, amphipods, clams and fish collected in the coastal Beaufort Sea during summer 2005 …… 121
Table 7-3: Concentrations of total dissolved Hg and dissolved CH_3Hg^+ in selected rivers, estuaries and seawater …….. 123
Table 7-4: Concentrations of Hg and CH_3Hg^+ in surface seawater, phytoplankton, zooplankton, amphipods, clams and fish collected in the coastal Beaufort Sea during summer 2005 …… 128

List of Figures

Page

Executive Summary

Figure ES-1: (a) Hydrographs during the spring floods in 2001, 2002, 2004 and 2006 for the Kuparuk River and (b) concentrations of calcium versus aluminum for suspended sediments from the Sagavanirktok, Kuparuk and Colville rivers during 2001, 2002, 2004 and 2006 ……..… xiii

Figure ES-2: (a) Photograph showing spring flow of the Sagavanirktok River northward to the ice-covered Beaufort Sea and (b) typical vertical profiles for salinity and temperature under the ice where river water was flowing over seawater ……..… iv

Figure ES-3: (a) Cross section showing the percent of Sagavanirktok River water at increasing distances from the river mouth and (b) vertical profiles for turbidity under ice at station SW4 on three different days in May 2004 as well as in August 2004 during the open-water period ……... xv

Figure ES-4: (a) Dissolved As versus salinity under ice during spring floods, May-June 2004 and (b) dissolved Ba versus salinity under ice during the spring floods, May-June 2006 …....…..… xvi

Figure ES-5: (a) Vertical profiles for salinity at station K1 in May and August 2004 and (b) values for particulate As versus Al for suspended sediments from the Beaufort Sea in summer 2004 … xvi

Figure ES-6: (a) Concentrations of particulate Pb versus Al for suspended sediments from the coastal Beaufort Sea in summer 2006 and (b) average concentrations of As in phytoplankton, zooplankton, amphipods, clams and fish collected from Stefannsson Sound during summer 2005 ……..…….…. xvii

Figure ES-7: Concentrations of (a) total Hg and CH_3Hg^+ in phytoplankton and zooplankton and (b) total Hg in phytoplankton, zooplankton, amphipods, clams, and fish collected from Stefannsson Sound during summer 2005 ……..……... xviii

Section 1

Figure 1-1: Map showing locations of sampling sites in the Sagavanirktok, Kuparuk and Colville rivers …….……..……. 4

Figure 1-2: Map showing cANIMIDA study area in the Beaufort Sea …… 5

Section 3

Figure 3-1: Annual hydrographs for the Kuparuk River in 2004 and the Sagavanirktok River in 2001 ……...……. 19

Figure 3-2: Hydrographs during the spring floods in 2001, 2002, 2004 and 2006 for the Kuparuk and Sagavanirktok rivers ……...…… 20

Page

Figure 3-3: Peak flow in the east channel of the Kuparuk River in 2006 …… 21
Figure 3-4: Annual water discharge from 1970 to 2005 for the (a) Sagavanirktok River and (b) Kuparuk River ……..……. 22
Figure 3-5: Water flow and total suspended solids for the Kuparuk and Sagavanirktok rivers for Many-June 2004 and 2006 ……..…. 23
Figure 3-6: Concentrations of Ca versus Al for suspended sediments from the Sagavanirktok, Colville and Kuparuk rivers during 2001, 2002, 2004 and 2006 …….....…… 27
Figure 3-7: Concentrations of (a) K and (b) Mg versus Al for suspended sediments from the Sagavanirktok, Kuparuk and Colville rivers during the spring floods ……..…… 28
Figure 3-8: Concentrations of Fe versus Al for suspended sediments from the Sagavanirktok, Colville and Kuparuk rivers during May-June 2004 and 2006 ……..……... 29
Figure 3-9: Concentrations of (a) Ba, (b) Cu, and (c) Cr versus Al for suspended sediments from the Sagavanirktok, Colville and Kuparuk rivers during May-June 2004 and 2006 ……..……..…… 31
Figure 3-10: Concentrations of (a) nickel, (b) lead, and (c) zinc versus Al for suspended sediments from the Sagavanirktok, Colville and Kuparuk rivers during May-June 2004 and 2006 ……. 32
Figure 3-11: Concentrations of dissolved Fe and water discharge in (a) the Sagavanirktok River for May-June, 2004 and (b) 2006 and (c) peak concentrations of dissolved Fe in the Sagavanirktok and Kuparuk rivers for May-June 2001, 2002, 2004 and 2006 … 36
Figure 3-12: Concentrations of (a) dissolved Cu, (b) dissolved Ba and (c) dissolved Ca in the Sagavanirktok River ……. 37

Section 4

Figure 4-1: Average concentrations of dissolved and particulate Ba and distribution coefficients for Ba in the Sagavanirktok. Kuparuk and Colville rivers …… 41

Section 5

Figure 5-1: Sampling sites in Stefannsson Sound …… 45
Figure 5-2: Aerial photograph with view to the north showing the spring outflow from the Kuparuk River …… 47
Figure 5-3: Aerial photograph with view to the south showing the spring outflow from the Kuparuk River …… 48
Figure 5-4: Aerial photograph with view to the north showing the spring outflow from the Sagavanirktok River ……...……... 48
Figure 5-5: Vertical profiles for salinity and temperature for stations K1, K3 on May 23, 2004 and station K4 on May 29, 2004 ……..... 49

Page

Figure 5-6: Vertical profiles of salinity for station SW4 on May 25, May 28 and May 31, 2004 ……..……...… 50

Figure 5-7: Under-ice vertical profiles of temperature, salinity and turbidity taken along the SE transect …….. 51

Figure 5-8: Under-ice horizontal contour maps of temperature, salinity and turbidity isoclines at 2-m water depth that depicts flow from both the Sagavanirktok and Kuparuk rivers ……..……. 52

Figure 5-9: $\delta^{18}O$ versus salinity for water collected in Stefannsson Sound from May 23-31, 2004 ……... 53

Figure 5-10: Concentrations of dissolved silica versus $\delta^{18}O$ for water collected from Stefannsson Sound from May 23-31, 2004 ……..... 54

Figure 5-11: Percent of water sample that was Sagavanirktok River for (a) samples from the SW transect on May 25, (b) samples from the SW transect on May 28, (c) samples from the S transect sampled on May 31 and (d) samples from the SE transect sampled on May 27 …… 55

Figure 5-12: Quasi-synoptic view of the percent Sagavanirktok River water and Kuparuk River water at 1.0 m on May 27-31 …..…… 57

Figure 5-13: Percent of water sample that was (a) Kuparuk River water and (c) Sagavanirktok River water for stations SK8, SK5 and SK2, and (b) Kuparuk River water and (d) Sagavanirktok River water for stations SK10, SK7 and SK4 …… 58

Figure 5-14: Percent of water sample that was (a) Kuparuk River water and (c) Sagavanirktok River water for stations SK8, SK9 and SK10, and (b) Kuparuk River water and (d) Sagavanirktok River water for stations SK5, SK6 and SK7 …… 59

Figure 5-15: Qualitative flow pathways for Sagavanirktok River water according to lowest negative gradients ……... 62

Figure 5-16: Total suspended solids versus salinity for the Sagavanirktok River and offshore Stefannsson Sound in May-June 2004 …….. 65

Figure 5-17: Total suspended solids versus salinity for water samples collected in Kuparuk River and along the K and SK transects …. 66

Figure 5-18: Turbidity versus total suspended solids for samples collected during Spring 2004 ……. 67

Figure 5-19: Vertical profiles of turbidity for station SW4 on May 25, May 28 May 31, 2004 ……..…. 67

Figure 5-20: Turbidity versus salinity for station SW4 on May 25, May 28, May 31, 2004 …… 68

Figure 5-21: Vertical profiles for the activities of total ^{210}Pb, excess ^{210}Pb and ^{137}Cs for sediment cores from Stations in Prudhoe Bay and east of Endicott Island ……..……..…… 69

Figure 5-22: Concentrations of dissolved As versus salinity for water samples collected under ice across mixing zones from the Sagavanirktok and Kuparuk rivers to the coastal Beaufort Sea ……...…… 70

Page

Figure 5-23: Concentrations of particulate As versus (a) particulate Al, (b) total suspended sediments and (c) dissolved As for water samples collected in the rivers and under ice in the coastal Beaufort Sea … 71

Figure 5-24: (a) Concentrations of particulate Cu versus particulate Al and (b) concentrations of dissolved Cu versus salinity for samples from the Sagavanirktok and Kuparuk rivers and coastal Beaufort Sea ……. 73

Figure 5-25: (a) Concentrations of dissolved Cu versus salinity, (b) the particulate Cu/Al ratio for suspended matter versus salinity and (c) particulate Cu/Al ratio versus concentrations of dissolved Cu 74

Figure 5-26: Concentrations of particulate (a) Fe and (b) Ba versus particulate Al for samples from the Sagavanirktok and Kuparuk rivers and the coastal Beaufort Sea …….. 75

Figure 5-27: Concentrations of (a) particulate Cr versus Al and (b) particulate Cr versus Fe from the Sagavanirktok and Kuparuk rivers and the coastal Beaufort Sea ……. 76

Figure 5-28: Concentrations of dissolved Cr versus salinity for water samples collected under ice across the mixing zones from the Sagavanirktok and Kuparuk rivers ……..…… 77

Figure 5-29: (a) Concentrations of particulate Cd versus particulate Al and (b) concentrations of particulate Cd versus salinity for samples from the Sagavanirktok and Kuparuk rivers and the coastal Beaufort Sea ……..…….. 78

Figure 5-30: Concentrations of particulate Cd as a function of (a) concentrations of total suspended solids and (b) as total mass of TSS on filter 79

Figure 5-31: Concentrations of dissolved Cu versus salinity for water samples collected under ice across the mixing zones …… 80

Figure 5-32: Concentrations of particulate Cd versus dissolved Cd for water samples collected in rivers and under ice in the coastal Beaufort Sea ……..… 80

Figure 5-33: Concentrations of particulate Zn versus particulate Al for samples from the Sagavanirktok and Kuparuk rivers and the coastal Beaufort Sea ……..……...… 81

Figure 5-34: Concentrations of particulate Pb versus particulate Al for samples from the Sagavanirktok and Kuparuk rivers and the coastal Beaufort Sea ……..……...…… 81

Figure 5-35: Concentrations of particulate Pb as a function of (a) concentrations of total suspended solids and (b) as total mass of TSS on filter … 82

Figure 5-36: Map showing sampling stations for the May-June 2006 under-ice study in the coastal Beaufort Sea …….. 83

Figure 5-37: Vertical profiles of temperature, salinity and turbidity taken at station S2 over a 10-day period in 2006 ……..…….. 85

Figure 5-38: Vertical contour map of salinity along an onshore-offshore transect extending from station S0 near shore to station S6 beyond the barrier islands, June 2, 2006 …….. 86

Page

Figure 5-39: Temperature, salinity, and turbidity obtained during a 2-week period during spring breakup of 2006 …….…….. 87
Figure 5-40: Concentrations of dissolved (a) As, (b) Cd, (c) Ba and (d) Cr versus salinity across the freshwater-seawater mixing zone from the Sagavanirktok River to the Coastal Beaufort Sea ……..…. 88
Figure 5-41: Concentrations of dissolved (a) Cu and (b) Zn versus salinity across the freshwater-seawater mixing zone from the Sagavanirktok River to the Coastal Beaufort Sea …….. 89
Figure 5-42: Concentrations of total suspended solids (TSS) versus salinity for the freshwater-seawater mixing zones from the (a) Sagavanirktok River and (b) Kuparuk River to the coastal Beaufort Sea during May-June 2006 ……..…… 89
Figure 5-43: Concentrations of Fe versus Al for suspended sediments from the (a) Sagavanirktok River and (b) Kuparuk River and respective offshore, under-ice plumes in the coastal Beaufort Sea …… 90
Figure 5-44: Concentrations of Ba versus Al for suspended sediments from the Sagavanirktok and Kuparuk rivers and their respective offshore, under-ice plumes in the coastal Beaufort Sea …… 91
Figure 5-45: Concentrations of (a) Pb, (b) Cu, (c) Cr and (d) Zn versus Al for suspended sediments from the Sagavanirktok and Kuparuk rivers and their respective offshore, under-ice plumes in the coastal Beaufort Sea ……..… 92

Section 6

Figure 6-1: Map showing the western portion of the coastal Beaufort Sea …… 99
Figure 6-2: Map showing cANIMIDA study area in the Beaufort Sea …….. 100
Figure 6-3: Vertical profiles for salinity at station K1 on May 23 and August 6, 2004 …….. 101
Figure 6-4: Vertical profiles for salinity at station SW4 during three days in May and on August 5, 2004 …… 102
Figure 6-5: Vertical profiles for turbidity for May and August 2004 …….. 102
Figure 6-6: Schematic representation of the thickness of a layer of bottom Sediments that would need to be resuspended in an 8-m deep water column to produce a value for total suspended solids (TSS) of 40 mg/L …….. 105
Figure 6-7: Turbidity versus total suspended solids for samples from the open Beaufort Sea during summer 2005 ……..……. 106
Figure 6-8: Concentrations of particulate (a) Cd and (b) As versus particulate Al for samples collected during May-June and July-August 2004 … 108
Figure 6-9: Concentrations of particulate Pb versus particulate Al for water samples collected during July-August 2006 …… 109
Figure 6-10: Concentrations of dissolved Cd and phosphate in the coastal Beaufort Sea versus the global trend for seawater …….. 111
Figure 6-11: Concentrations of nitrate versus phosphate from global data sets …… 112

Page

Section 7

Figure 7-1: Concentrations of dissolved versus salinity from the Sagavanirktok River across the freshwater-seawater mixing zone to the coastal Beaufort Sea during summer 2005 …… 114

Figure 7-2; Concentrations of dissolved plus excess particulate As versus salinity from the Sagavanirktok River and the freshwater-seawater mixing zone to the coastal Beaufort Sea ……. 115

Figure 7-3: (a) Concentrations of dissolved reactive phosphate versus salinity and (b) concentrations of dissolved As versus DRP from the Sagavanirktok River across the freshwater-seawater mixing zone to the coastal Beaufort Sea …….……..……. 116

Figure 7-4: Concentrations of (a) dissolved As and (b) dissolved reactive phosphate versus salinity from the Sagavanirktok River across the freshwater-seawater mixing zone ……. 117

Figure 7-5: Vertical profiles of (a) salinity, (b) dissolved As, (c) dissolved reactive phosphate and (d) dissolved NO_3^- on July 31 and August 3 in Stefannsson Sound ……..…… 119

Figure 7-6: Vertical profiles of the ratio of dissolved As to dissolved reactive phosphate (a) July 31 and (b) August 3 in Stefannsson Sound … 120

Figure 7-7: Concentrations of As versus (a) Al and (b) Fe in suspended and bottom sediments collected from Stefannsson Sound during summer 2005 …… 120

Figure 7-8: Average concentrations of As in phytoplankton, zooplankton, amphipods, clams and fish collected from Stefannsson Sound during summer 2005 ……..….. 122

Figure 7-9: Concentrations of total dissolved Hg versus salinity from the (a) Sagavanirktok River across the freshwater-seawater mixing zone to the coastal Beaufort Sea, and (b) Ob and Yenisei estuaries …… 124

Figure 7-10: Concentrations of total dissolved Hg versus salinity from the Sagavanirktok River across the freshwater-seawater mixing zone to the coastal Beaufort Sea and in Stefannsson Sound … 125

Figure 7-11: Vertical profiles of total dissolved Hg at stations along a transect sampled on August 3 in Stefannsson Sound …… 126

Figure 7-12: Vertical profiles of (a) dissolved CH_3Hg^+, (c) dissolved As, (d) dissolved reactive phosphate (DRP), and (e) dissolved NO_3^- at L01C on August 3 ……. 127

Figure 7-13: Concentrations of (a) total Hg and CH_3Hg^+ in phytoplankton and zooplankton and (b) total Hg in phytoplankton, zooplankton, amphipods, clams, and fish collected from Stefannsson Sound during summer 2005 …….. 129

EXECUTIVE SUMMARY

The continuation of the Arctic Nearshore Impact Monitoring in Development Area (cANIMIDA) Project was designed to determine whether offshore oil development in the coastal Beaufort Sea has had any adverse impacts on the marine environment. This report encompasses two aspects of the cANIMIDA Project, the study of suspended sediments (Task 3) and the distribution of potential metal contaminants between dissolved and particulate phases (Task 4). Samples were collected during the spring floods of May-June of 2004 and 2006 and during the open-water periods (July-August) of 2004, 2005 and 2006. The spring portion of the study was designed to investigate the flow of water, suspended sediments and dissolved and particulate metals by rivers and then trace their dispersion under ice into the coastal Beaufort Sea. The summer portion of the study was designed to investigate the distribution of suspended sediments and dissolved and particulate metals across the shelf and in the areas of active development in the open waters of the Beaufort Sea. Data from the ANIMIDA Project (1999-2002) are included in this report in some cases to help show interannual variability.

During the 2 to 3 weeks of spring floods in May-June 2004 and 2006, about 60% of the annual water flow from the Kuparuk River and about one third of the annual water flow of the Sagavanirktok River were carried to the Beaufort Sea. Interannual variability in the onset date for river flow, volume at peak flow and the duration of peak flow can be significant as shown in Figure ES1a. During May-June, maximum concentrations of total suspended solids (TSS) ranged from 60 mg/L (2006) to 120 mg/L (2002) in the Kuparuk River and 244 mg/L (2002) to 609 mg/L (2001) in the Sagavanirktok River. Differences in the chemical composition of the river particles could often be related to the mineralogy of the drainage basin as, for example, the highest Ca values were found for particles in the carbonate-richer Sagavanirktok River basin (Figure ES1b) and the highest Al values were found in the more clay-rich Colville River.

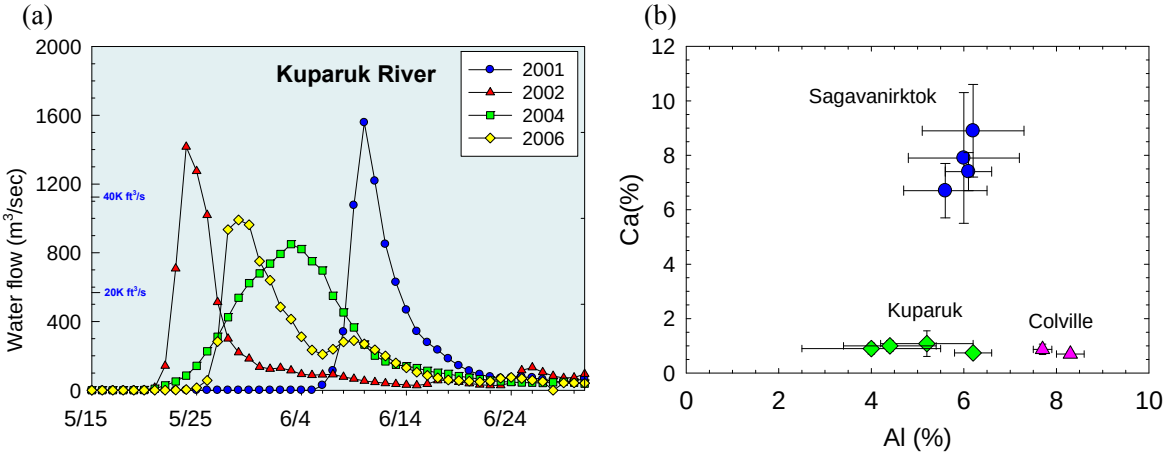

Figure ES1. (a) Hydrographs during the spring floods in 2001, 2002, 2004 and 2006 for the Kuparuk River (Data from U.S.G.S. http://waterdata.usgs.gov/ak/nwis) and (b) concentrations of calcium (Ca) versus aluminum (Al) for suspended sediments from the Sagavanirktok (circles), Kuparuk (diamonds), and Colville (triangles) rivers during 2001, 2002, 2004 and 2006. Markers show means and lines show standard deviations.

More than 85% of the data points for Ba, Cu, Cr, Ni and Pb in suspended sediments from the three rivers (Sagavanirktok, Kuparuk and Colville) during 2004 and 2006 were within predicted ratios to Al for bottom sediments from the Beaufort Sea. This overall continuity shows strong support for river particles as a key source for metals in coastal sediments as well as showing that concentrations of these metals in Beaufort Sea sediments were not significantly influenced by anthropogenic inputs or diagenetic processes.

The trend of maximum concentrations of dissolved trace metals, such as Fe and Cu, in rivers during peak flow in spring, first observed during the ANIMIDA Project, was again observed in some cases in the 2004 and 2006 data. This observation is natural and influenced by the discharge of soil interstitial water and shallow surface water that is diluted by snow melt and flushed from surrounding soils into the rivers. In contrast concentrations of major dissolved elements, such as Ca or even Ba, varied by <10% in a given river during the May-June period.

A simple distribution coefficient (K_d) was used to provide one perspective for metal partitioning between particulate and dissolved phases. For example, despite significant differences in concentrations of dissolved and particulate Ba among rivers, the K_d values calculated for Ba were statistically equal, suggesting that partitioning of Ba between dissolved and particulate phases is a quasi-equilibrium controlled process between free Ba^{2+} and suspended particles. Reasonably good agreement in K_d values among rivers and seasons was found for Cd, Cu, Cr, Pb and other metals and the relationship can be used to help explain concentrations of dissolved metals in area rivers.

The high water flow from rivers during the spring floods was carried to a Beaufort Sea that was covered with ~2-m thick, land-fast ice (Figure ES2a). The fresh and relatively warm (slightly > 0°C) discharge from the rivers flowed out onto and then under the land-fast ice where it mixed with the colder marine waters to form a 1 to 2 m thick under-ice lens of brackish water (Figure ES2b) that extended >15 km offshore. Sampling in the

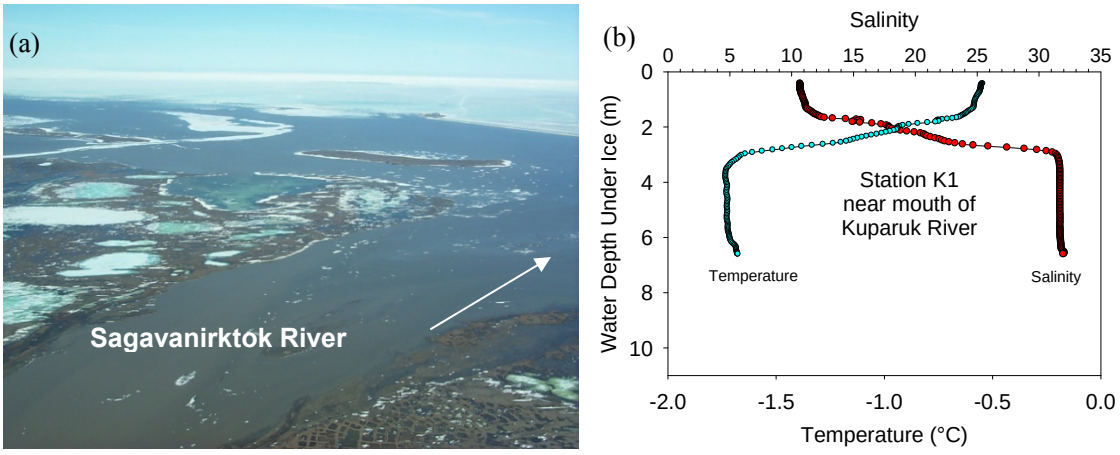

Figure ES2. (a) Photograph showing spring flow of the Sagavanirktok River northward to the ice-covered Beaufort Sea and (b) typical vertical profiles for salinity and temperature under the ice where river water was flowing over seawater.

Beaufort Sea was carried out via holes drilled through the ice in 2004 and 2006. Salinity, $\delta^{18}O$ and dissolved silica were used in 2004 to identify, trace and quantify the movement of Sagavanirktok River (SR) water beneath a 2-m thick ice layer into the coastal Beaufort Sea (Figure ES3a). The SR water was transported beneath the ice, relatively undiluted, to a distance of ~6 to 8 km offshore and ~8 to 10 km alongshore in ~3 days. The calculated total volume of Sagavanirktok River water under ice was ~0.5 km^3 across an area of ~300 km^2; this amount of freshwater was equal to about half the total discharge from the river during the study period. The westerly flowing, 1 to 1.5 m thick plume of Sagavanirktok River water interacted with the easterly flowing plume from the Kuparuk River to result in increased northward transport of freshwater. Transport of relatively undiluted river water beneath the ice provides an important source of freshwater to the coastal ocean as well as providing a pathway to the coastal Beaufort Sea for potential contaminants or spills originating from activities on the North Slope.

Concentrations of suspended sediments (shown as turbidity in Figure ES3b) were greatest in the incoming freshwater and showed both temporal and spatial variations as a function of changes in river inputs and settling of particles. Concentrations of TSS, under ice, along the freshwater-seawater mixing zone into the Beaufort Sea decreased sharply and showed settling of >50% of the river-borne suspended sediments.

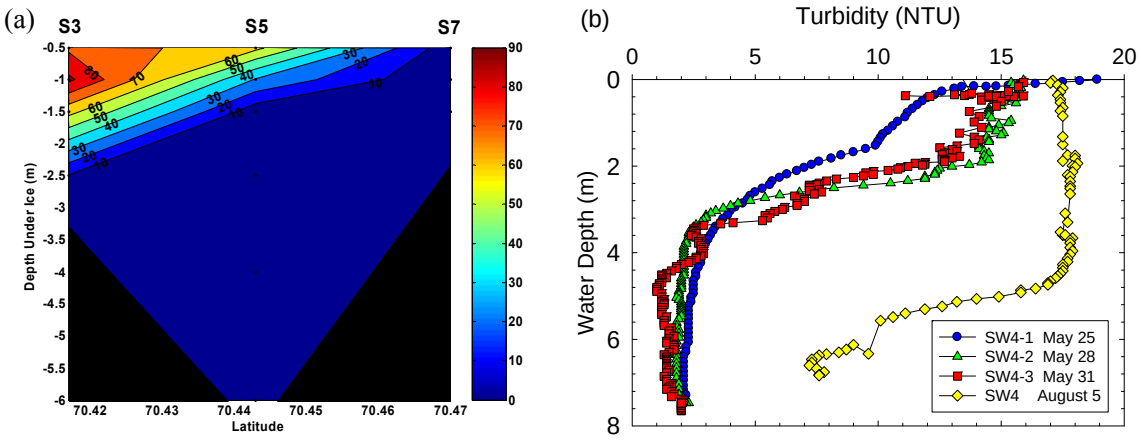

Figure ES3. (a) Cross section showing the percent of Sagavanirktok River water under ice at increasing distances from the river mouth (stations S3, S5 and S7, May 2004; two black areas at base of figure on left and right denote the seafloor) and (b) vertical profiles for turbidity under ice at station SW4 on three different days in May 2004 as well as one day in August 2004 during the open-water period.

Concentrations of dissolved As were essentially conservative (i.e., showing simple or linear mixing) along the freshwater-seawater mixing zone in spring and summer (Figure ES4a). Barium followed a conservative, but opposite, trend during mixing (Figure ES4b). Although weaker correlations were found for salinity versus dissolved Cu, Cr, Pb and Cd, relatively conservative mixing was observed across the freshwater-seawater mixing zone for these metals.

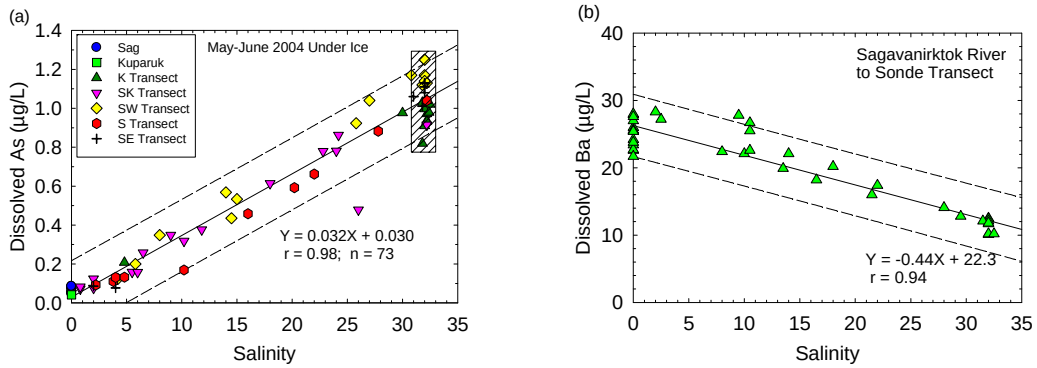

Figure ES4. (a) Dissolved arsenic (As) versus salinity under ice during spring floods, May-June 2004 and (b) dissolved barium (Ba) versus salinity under ice during the spring floods, May-June 2006. Regression lines and prediction intervals are shown for each graph. The shaded area on the As plot highlights differences in concentrations of dissolved As in offshore seawater

Vertical profiles for salinity, temperature and turbidity, as well as water samples for suspended sediments and dissolved and particulate metals, were collected during the summers of 2004, 2005 and 2006 from the coastal Beaufort Sea. Salinity in the upper layer of the water column typically increased between early June and late July as break-up of the ice cover was followed by mixing due to wind. For example, at the mouth of the Kuparuk River (station K1), the salinity in the upper 2 m increased from ~11 on May 23, 2004, under ice, to ~23 during the open-water period. However, the salinity of the bottom water was essentially unchanged and the water column remained stratified.

Concentrations of TSS in the Kuparuk River during summer 2004, 2005 and 2006 averaged 1.0 mg/L, about 25 to 60 times lower than during the spring floods. Values for TSS in the Sagavanirktok River were variable during summer with a range of 0.5 to 53.4 mg/L, with the maximum value linked to a summer rain storm. All TSS values in rivers during summer were 10 to >300 times lower than during the spring melt. Values for K_d in the summer river samples were within the range of values found for spring for As, Cd, Cr and Pb in the Sagavanirktok River, but lower in summer than spring for Ba, Cu, and Zn.

Concentrations of dissolved As, Cr and Pb were lower than reported values for surface seawater worldwide and well below the EPA water quality criteria for chronic impacts in marine waters. No significant differences in concentrations of dissolved trace metals were observed near Northstar Island relative to the overall cANIMIDA study area during 2004, 2005 and 2006. Concentrations of particulate metals during the open-water season showed enrichment of selected metals relative to Al due to scavenging by particles (e.g., As), uptake by biota and possibly some anthropogenic inputs (e.g., Pb in Figures ES5a) as explained with more specific details in the report. Concentrations of particulate metals near Northstar Island were not different than in the overall cANIMIDA area, with the exception of Cd in 2004 (plankton) and Pb in 2006 (possibly anthropogenic).

A more detailed study of the biogeochemistry of As and Hg were developed during the cANIMIDA Project. Concentrations of As in phytoplankton were enriched by a factor of ~5,000 relative to seawater, indicating that bioaccumulation of dissolved As by

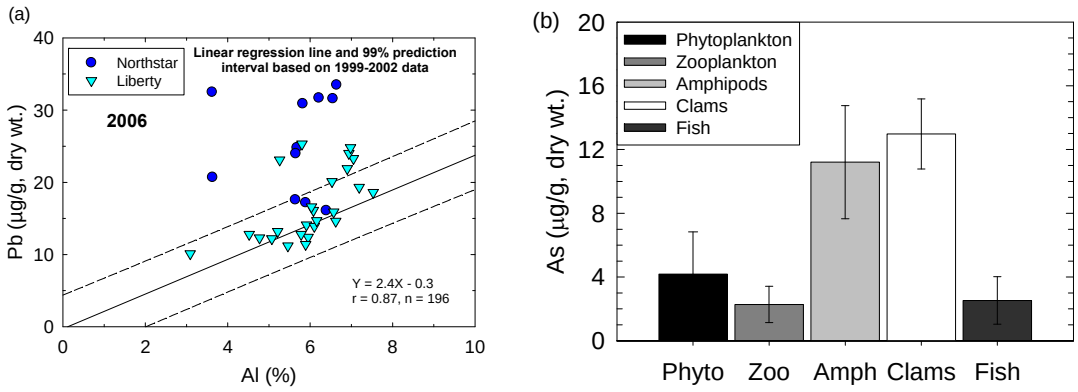

Figure ES5. (a) Concentrations of particulate lead (Pb) versus aluminum (Al) for suspended sediments from the coastal Beaufort Sea in summer 2006. Solid line, equation and prediction interval (dashed line) are from linear regression for bottom sediments collected from 1999-2003 (Trefry et al., 2003) and (b) average concentrations of As in phytoplankton, zooplankton, amphipods (*Anonyx* sp.), clams (*Astarte* sp.) and fish collected from Stefannsson Sound during summer 2005.

phytoplankton was occurring (Figure ES5b). No significant differences were observed in concentrations of As between phytoplankton and zooplankton, or between zooplankton and fish. Concentrations of As were significantly greater in amphipods than in zooplankton and also were significantly greater in clams than in phytoplankton.

Total Hg values for zooplankton (55 ± 31 ng/g, dry wt.) were significantly greater than those for total Hg in phytoplankton (19 ± 13 ng/g, dry wt.) collected from Stefannsson Sound during summer 2005 (Figure ES6a). Concentrations of CH_3Hg^+ in zooplankton (4.2 ± 1.9 ng/g, dry wt.) also were significantly greater than in phytoplankton (0.6 ± 0.6 ng/g, dry wt., Figure ES6b). Total Hg concentrations were significantly greater in clams than in phytoplankton and significantly greater in fish than in zooplankton (Figure ES6a).

With respect to potential contaminants from offshore activities, the overall conclusion of this study is that concentrations of suspended sediments, as well as dissolved and particulate metals, are at background levels throughout the study area, with a possible minor exception for Pb in some suspended particles during 2006. The data produced during cANIMIDA provide a strong baseline for future, long-term monitoring.

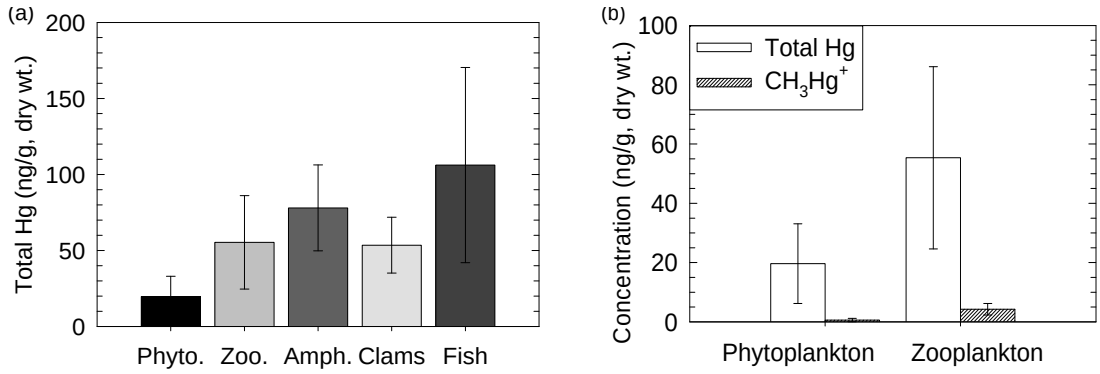

Figure ES6. Concentrations of (a) total Hg in phytoplankton, zooplankton, amphipods, clams, and fish and (b) total Hg and CH_3Hg^+ in phytoplankton and zooplankton collected from Stefannsson Sound during summer 2005.

1.0 INTRODUCTION

1.1 Overview and Goals

The cANIMIDA Project was designed to identify impacts that may have resulted from offshore oil and gas exploration and production in the coastal Beaufort Sea by developing a detailed data base for concentrations of potential contaminants and obtaining a better understanding of basic biogeochemical processes. The results from the two tasks described in this report encompass the study of suspended sediments (Task 3) and distribution of potential metal contaminants between dissolved and particulate phases (Task 4).

Field sampling for Tasks 3 and 4 of the cANIMIDA Project was as follows:

- May-June 2004: Spring river flow with under-ice transport to the Beaufort Sea.
- July-August 2004: Beaufort Sea during open-water period.
- July-August 2005: Beaufort Sea during open-water period.
- May-June 2006: Spring river flow with under-ice transport to the Beaufort Sea.
- July-August 2006: Beaufort Sea during open-water period.

The pertinent issues and hypotheses for each task are compiled on the MMS Indicator Matrices for Decision Making (Tables 1-1 and 1-2).

1.2 STUDY AREA

Sampling during May-June 2004 and 2006 was carried out in the Sagavanirktok and Kuparuk rivers and through holes drilled through the ice in the coastal Beaufort Sea (Figures 1-1 and 1-2). The Colville River was sampled during June 2006. Sampling during July-August 2004, 2005 and 2006 was carried in the rivers and offshore in the coastal Beaufort Sea. More details on specific sampling sites are provided along with the results and discussion in the appropriate sections. Methods for sampling and analysis are described in Section 2.

Details on the seasonal discharge and the specific geologic make-up of the pertinent drainage basin have been discussed or referenced by Rember and Trefry (2004). Briefly, the frozen tundra and snow pack upstream begin to melt during spring and slowly flow downstream (northward), melting the river water in route. The meltwater carries particulate and dissolved components frozen in the ice and snow from the previous year along with weathered rock and soil layers from the surrounding river banks. This thawing and weathering contribute to the specific chemical compositions of the particulate and aqueous phases carried by each river. During high discharge, that lasts only 1 to 2 weeks, Alaskan Arctic rivers typically transport 40 to 80% of their total annual discharge of water and >80% of their load of suspended sediments (Rember and Trefry, 2004).

.

Table 1-1. The cANIMIDA Project Indicator Matrix for Decision Making for Task 3.

Task Order	MMS Issue Addressed	Monitoring Hypotheses	Methods	Key Monitoring Result or Parameter for Decision Making
003 – "Sources, Concentrations, and Dispersion Pathways for Suspended Sediments in the cANIMIDA Study Area"	Will offshore oil development and production at Northstar and potential development at Liberty result in increased or chronic loadings of suspended sediments or associated contaminant metals?	H1: The chemical composition and morphology of suspended particles, as determined from natural or anthropogenic tracers, is not significantly different in areas of construction activities. H2: The amount of suspended sediments transported to the near-shore environment during spring river runoff is not a significant component of net sediment deposition that also includes inputs from shoreline erosion. H3: The contribution of particulate organic carbon (especially plankton/larvae) to the suspended sediments is not a significant fraction of the total suspended solids in the water column.	Sensor profiles and discrete sampling of rivers and the coastal Beaufort Sea during the ice-covered and open-water periods with analysis of suspended sediments for metals.	Interim and final interpretative reports with tabulated data on suspended sediments will be provided. Contractor will alert MMS COTR of any important trends or changes.

Table 1-2. The cANIMIDA Projector Indicator Matrix for Decision Making for Task 4.

Task Order	MMS Issue Addressed	Monitoring Hypotheses	Methods	Key Monitoring Result or Parameter for Decision Making
004-"Partitioning of Potential Contaminants between Dissolved and Particulate Phases in the cANIMIDA Study Area"	Will offshore oil development and production at Northstar and potential development at Liberty result in increased or chronic loadings of dissolved contaminant metals?	H1: Concentrations of dissolved and particulate metals and supporting parameters in waters near offshore oil- and gas-related activities in the coastal Beaufort Sea are not significantly different than in more remote, coastal waters of the Beaufort Sea. H2: Concentrations of dissolved metals collected across the freshwater/seawater mixing zone plot on a linear mixing curve versus salinity with concentrations in river water and seawater as end-members (i.e., conservative or linear mixing). H3: Concentrations of dissolved and particulate metals in rivers and the coastal Beaufort Sea follow measurable and predictable distribution coefficients (K_d).	Discrete sampling of rivers and the coastal Beaufort Sea during the ice-covered and open-water periods with analysis of water for metals and supporting parameters.	Interim and final interpretative reports with tabulated data will be provided, with statistical tests of potential interannual significant differences. Contractor will alert MMS COTR of any important trends or changes.

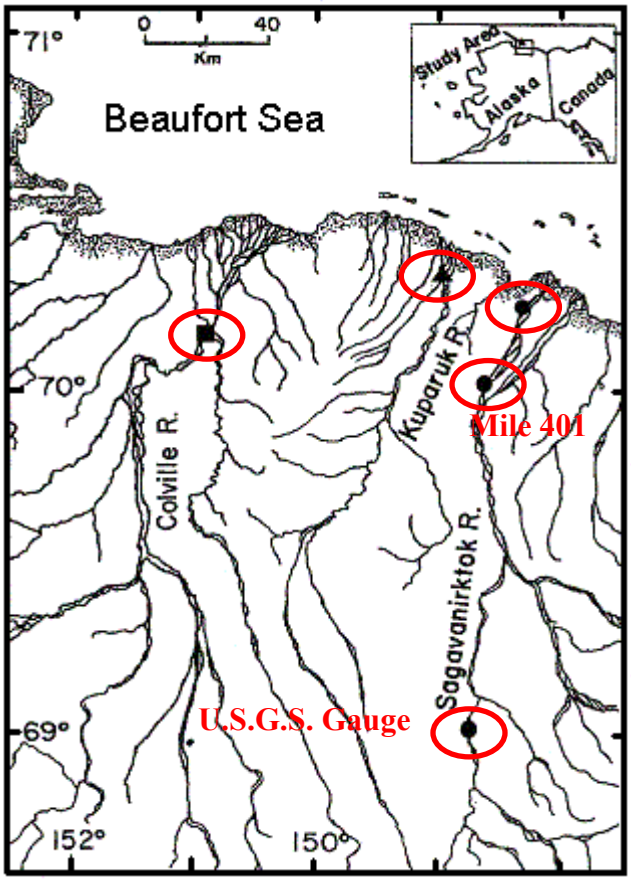

Figure 1-1. Map showing locations of sampling sites in the Sagavanirktok, Kuparuk and Colville rivers with inset map showing study area in northern Alaska. Each river was sampled at the point closest to the Beaufort Sea during the cANIMIDA Project. The location of the U.S.G.S. gauge on the Sagavanirktok River is so marked. The U.S. G.S. gauge for the Kuparuk River is about 0.5 km upstream of the sampling site. No gauge was available for the Colville River.

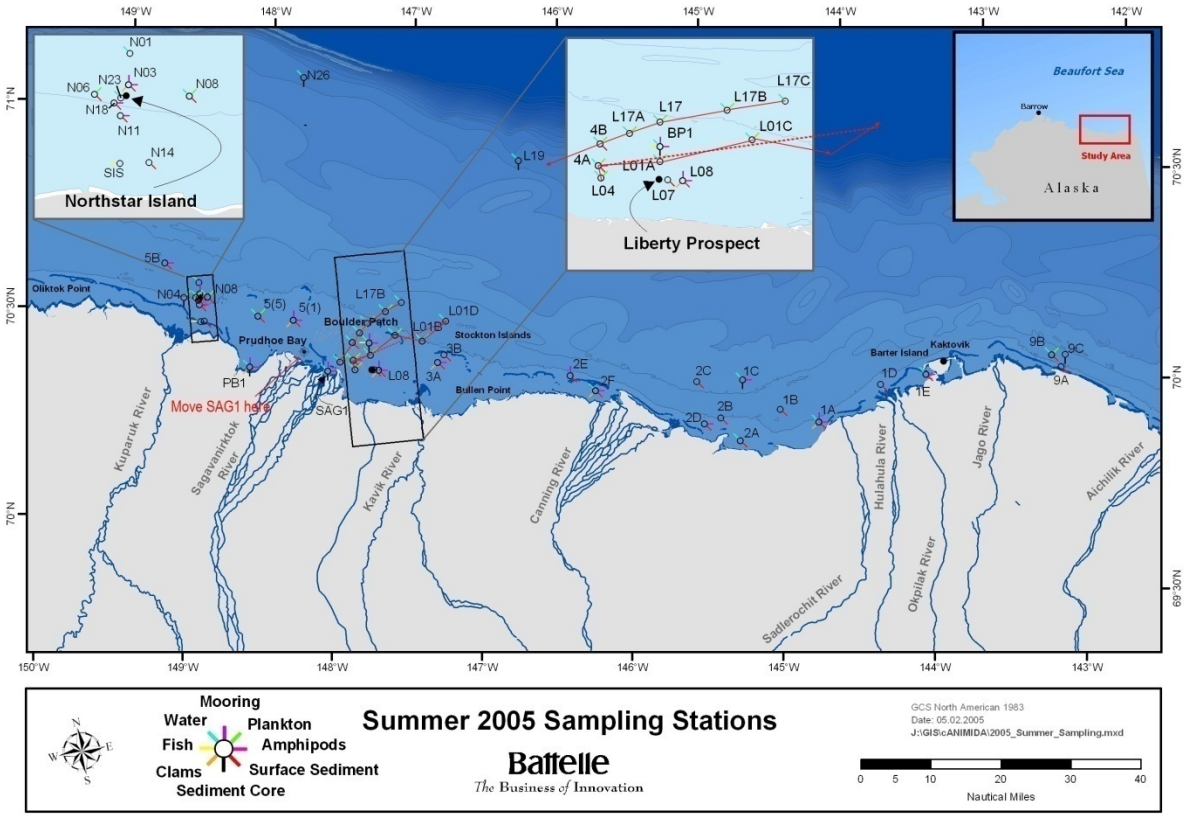

Figure 1-2. Map showing cANIMIDA study area in the Beaufort Sea along the northern coast of Alaska. Inset map in upper right-hand corner shows study area on map of northern Alaska. The other two inset maps show the area around Northstar Island and Liberty Prospect. Map shows sampling stations from 2005 summer field season. Map courtesy of Battelle.

Tracking the spring floods under-ice during 2004 and 2006 was carried out in Stefannsson Sound, a small and shallow area (average water depth <15 m) located offshore of the North Slope of Alaska and partially protected by barrier islands that separate it from the Beaufort Sea. Seasonal landfast ice (~2 m thick) that covers the area from October through April begins to melt in late May and eventually breaks up and blows offshore in July (Weingartner and Okkonen, 2001). During the spring melt, Alaskan Arctic rivers, including the Sagavanirktok River, flow at maximum discharge above and below the landfast ice. The ambient shelf water has a salinity that ranges from 28 (July-September) to 34 (mixing with brine drainage during ice formation in winter) with spring salinity values of 31 to 32 and temperatures of -1.6 to -1.8°C that increase to as high as 4°C during the summer open water period (Weingartner and Okkonen, 2001). This shelf water is referred to here as the Polar Mixed Layer (PML), a term adopted from Macdonald et al. (1989). Circulation in the study area varies with the season as the presence of the ice determines the influence of winds on water movement. The area has a tidal range of ~0.2 m with currents that range from <1 to 24 cm s^{-1} and average 2 cm s^{-1}, with <10% of the current magnitudes >10 cm s^{-1} during the landfast ice period (Weingartner and Okkonen, 2001; Matthews, 1981).

The results and discussion in this report are organized as follows:

- Transport of Water, Sediments and Chemicals from Rivers during the Spring Melt.
- Partitioning of Metals Between Particulate and Dissolved Phases in River Water
- Dispersion of River Water, Suspended Sediments and Chemicals Under Ice in the Beaufort Sea
- The Distribution of Suspended Sediments and Chemicals During the Open-Water Period
- Biogeochemistry of Arsenic and Mercury in the Coastal Beaufort Sea

2. METHODS

2.1 Field Sampling and Initial Processing

River water was collected in 1-L, acid-washed, low-density, polyethylene (LDPE) bottles using a polyvinyl chloride (PVC) water sampler that held the LDPE bottles and could be lowered from a bridge across each river. In some cases, samples were obtained by wading into the river, waiting until disturbed sediments washed downstream, and then opening an acid-washed 1- or 2-L LDPE bottle below the surface of the water. When the bottle was full, it was sealed beneath the surface, retrieved, placed in a plastic bag, labeled and stored in a cooler for return to the on-site laboratory facilities to be filtered.

During May-June, seawater was collected using a peristaltic pump (Masterflex model 75-45-30 pump with high-capacity pump head) equipped with acid washed Tygon tubing attached to a Teflon weight that was lowered through holes in the ice that were drilled with an augur. Sampling through the ice was limited to 9 days in 2004 and 12 days in 2006 by the time of onset of the floods, weather conditions and accessibility when nearshore areas flooded above the ice. Water samples for dissolved and particulate metals, as well as total suspended solids (TSS), were collected in 1-L, acid-washed, LDPE bottles. For the under-ice samples, the first two liters of water were discarded and the next two liters were pumped directly into a 2-L, LDPE bottle. Samples were collected ~20 to 30 minutes after drilling the hole to allow for re-establishment of any stratification in the water column. The sample containers were sealed in plastic bags, labeled and placed in coolers for transport back to the onshore laboratory at the Seawater Treatment Plant (STP) near West Dock.

Two snowmobiles equipped with freight sleds were used to transport personnel and sampling gear from the Prudhoe Bay STP to the sampling stations during the May-June, under-ice studies. Due to the hazardous nature and potential of being cut off from land while working offshore during river breakup conditions, emergency survival gear, communication equipment, an emergency position indicating radiobeacon (EPIRB) and other safety equipment were included on each field trip. A portable hand-held global positioning system (GPS) was used for positioning and relocation of sampling stations.

Hydrographic profiles during spring and summer were obtained using a YSI Sonde conductivity, temperature, turbidity and depth sensor. Data from the Sonde were uploaded onto a portable field computer at each site. Salinity, sigma-t (density), and depth were determined during post processing from the conductivity, temperature and pressure measurements. The Sonde was factory calibrated prior to the field season and re-checked in the field each day. During spring 2004, current magnitudes and directions were measured and averaged at selected depths for each station using an AANDERAA Doppler current meter. Data are reported only for those sites where at least three consecutive current directions differed by <30°. Precision was estimated to be ±1.6 cm s^{-1} and ±9° for speed and direction, respectively.

Sampling in the coastal Beaufort Sea during the open-water periods in 2004, 2005 and 2006 was carried out from the MMS Launch 1273. *In-situ* profiles of seawater turbidity, conductivity, temperature and depth were obtained using a YSI Sonde instrument as described above. Samples of surface seawater for turbidity and TSS were collected from the bow of a small rubber boat while rowing upstream or upwind. An acid-washed 1- or 2-L LDPE bottle was opened at about 10 cm below the surface of the water. When the bottle was full, it was sealed beneath the surface, retrieved, and placed in a plastic bag for storage. Subsurface samples were obtained using a peristaltic pumping system as previously described. Approximately 10 L of water were discarded before the sample was pumped directly into an acid-washed 5-L plastic container. All water samples were sealed in plastic bags, labeled, packed in coolers and taken to an on-site laboratory at the STP.

Ice cores were collected at 5 stations in the Beaufort Sea during May-June 2004 to determine endmember values for sea-ice meltwater. Ice cores were obtained using a Sipre corer and auger with a hollow center, then they were sectioned in the field into five 30 to 40 cm intervals and melted in separate containers in the dark over ~24 hours.

Water filtration for all sampling periods was carried out in a laminar flow hood in a chemistry lab at the STP facility. In the lab, the water samples were brought to room temperature, shaken to resuspend the particles and the turbidity of each sample was determined using a Hach Model 2100A turbidimeter. The salinity of each seawater sample also was checked using a Reichert-Jung Model 10419 optical refractometer. Water samples were vacuum filtered through polycarbonate filters (Poretics, 47-mm diameter, 0.4-μm pore size). Prior to the field effort, the filters were acid washed in 5N HNO_3, rinsed three times with distilled-deionized water (DDW), dried and then weighed to the nearest μg using a Sartorius Model M3P electronic balance under cleanroom conditions. Vacuum filtration on site was carried out in a Class-100 laminar-flow hood using acid-washed glassware. The particle-bearing filters were sealed in acid-washed petri dishes, labeled and then double-bagged in plastic and stored until dried and re-weighed at Florida Institute of Technology (FIT).

2.2 Laboratory Analysis

For the discrete seawater samples, salinity was calculated from the measured chlorinity using the Mohr titration as described by Grasshoff (1976). Calculated salinities were checked in 2004 by analyzing a subset of samples (n = 34) using a Guideline 8400-B salinometer at the National Oceanic and Atmospheric Administration (NOAA) laboratory in Miami. The correlation coefficient for the salinities determined by both methods was 0.999. Concentrations of dissolved silica, phosphate and nitrate were determined within 48 hours of collection using standard methods (Grasshoff, 1976). Reagent blanks and laboratory replicates were analyzed for quality control and precision. Values for $\delta^{18}O$ were determined for 62 samples from key under-ice stations in spring 2004 that were selected based on salinity and dissolved silica values. Analyses for $\delta^{18}O$ were carried out by Geochron Laboratories, Inc., using a VG Micromass gas source stable isotope ratio mass spectrometer and results were reported as referenced to VSMOW (Vienna Standard Mean Ocean Water).

2.2.1 Particulate and Dissolved Organic Carbon

Samples for particulate organic carbon (POC) and dissolved organic carbon (DOC) were prepared by filtration of seawater and river water through pre-combusted Gelman Type A/E glass fiber filters mounted on acid-washed filtration glassware within a Class-100 laminar-flow hood. The POC filters were sealed in acid-washed petri dishes, labeled, double bagged in plastic and then stored frozen until dried at FIT. The dissolved samples saved for DOC were placed in acid-washed glass vials with Teflon-lined caps, labeled, and frozen until analysis at FIT.

At FIT, the POC filters were treated with H_3PO_4 to remove inorganic carbon phases, rinsed with DDW, dried and their particulate mass determined. The filters were then placed in ceramic boats and combusted at 900°C in a Shimadzu TOC-5050A carbon system with SSM-5000A solid sampling module following the manufacturer's instructions. The POC content of the samples was determined using a four-point calibration curve with pure sucrose as the standard. The calibration curve was checked every 10 samples by analyzing the certified reference material (CRM) MESS-2, a marine sediment issued by the National Research Council of Canada (NRC).

The DOC concentrations of the seawater and river water samples were calculated by difference, total carbon (TC) minus inorganic carbon (IC) as determined by combustion in the Shimadzu TOC-5050A system. Four-point calibration curves were prepared using potassium hydrogen phthalate (TC) and sodium bicarbonate (IC). The calibration curve was checked every 10 samples by repeat analysis of a mid-range standard.

2.2.2 Major and Trace Metals in Suspended Sediments

Filters bearing field samples of suspended sediments, as well as separate milligram quantities of standard reference material (SRM) #2704, a river sediment issued by the National Institute of Standards and Technology (NIST), were digested in stoppered, 15-mL Teflon test tubes using Ultrex II HNO_3, HF and HCl. The sealed test tubes were placed in an 80°C water bath. Refluxing of the acids completely dissolved the particles on the filters. After processing, the resultant solutions were transferred to acid-washed, 15-mL polyethylene bottles, diluted to ~6 mL (by weighing and determining density) with DDW rinses of the Teflon test tubes and stored in a plastic bag until analyzed.

Metal concentrations for the digested particulate samples, SRMs and blanks were determined by flame atomic absorption spectrometry (FAAS), graphite furnace atomic absorption spectrometry (GFAAS) or inductively coupled plasma mass spectrometry (ICP-MS) in a manner compatible with EPA Series 7000, 6010A and 7470 (U.S. EPA, 1991), respectively (Table 2-1). Concentrations of particulate Al, Ca, Fe, K, Mg, Mn, Na and Zn were determined by FAAS using a Perkin-Elmer Model 4000 AAS. Concentrations of Cr and Cu were quantified by GFAAS using a Perkin-Elmer Model 4000 AAS equipped with an HGA-400 graphite furnace and AS-40 autosampler. Concentrations of As were determined by GFAAS using a Perkin-Elmer model 5100

Table 2-1. Summary of instrumental methods and method detection limits (MDL) for metal analysis of suspended sediments (dry weight basis) and water.

	Suspended Sediments		Water	
Metal	**Method**	**MDLs (µg metal/g, dry weight)**	**Method**	**MDLs (µg metal/L)**
Al – aluminum	FAAS	1500	-	-
As – arsenic	GFAAS	1.8	GFAAS	0.00811
Ba – barium	ICP-MS	9	ICP-MS	0.1
Ca – calcium	FAAS	230	FAAS	0.01 mg/L
Cd – cadmium	ICP-MS	0.03	ICP-MS	0.0001
Cr – chromium	FAAS	0.33	GFAAS	0.005
Cu – copper	FAAS	0.4	GFAAS	0.003
Fe – iron	FAAS	250	GFAAS	0.01
K – potassium	FAAS	250	FAAS	0.02 mg/L
Hg – mercury	-	-	CVAFS	0.03 ng/L
Mg – magnesium	FAAS	40	FAAS	0.01 mg/L
Mn – manganese	FAAS	170	GFAAS	0.1
Na – sodium	FAAS	0.7	FAAS	0.008 mg/L
Ni – nickel	ICP-MS	0.2	ICP-MS	0.02
Pb – lead	ICP-MS	82	ICP-MS	0.002
Zn – zinc	FAAS	2	ICP-MS	0.01
POC and DOC	Shimadzu Carbon System	0.01%	Shimadzu Carbon System	0.1 mg/L

Notes: CVAFS = Cold Vapor Atomic Fluorescence Spectrometry
FAAS = Flame Atomic Absorption Spectrometry
GFAAS = Graphite Furnace Atomic Absorption Spectrometry
ICP-MS = Inductively Coupled Plasma-Mass Spectrometry
MDL = Method Detection Limit

Instrument equipped with an HGA-600 graphite furnace and an AS-60 autosampler. Values for Ba, Cd and Pb were determined by ICP-MS using a Perkin-Elmer ELAN 5000 spectrometer. In all cases, the instrument manufacturers' specifications were followed and adherence to QA/QC requirements was maintained as described below in Section 2.3 (QA/QC section).

2.2.3 Dissolved Metals, Major Ions, Chlorinity and Alkalinity

The seawater concentrations of dissolved As, Cd, Cr, Cu, Pb and Zn were determined on extracts obtained using a reductive precipitation procedure derived from Nakashima et al. (1988). In this procedure, ultra-high purity Pd, Fe and $NaBH_4$ were used to precipitate the metals that were then collected by filtration and redissolved in ultra-high purity HNO_3 and HCl. This procedure was carried out using 400-mL aliquots of seawater and a seawater CRM (CASS-3 issued by the NRC) with final extract volumes of ~4 mL (by weighing and determining density), resulting in a ~100-fold concentration of the seawater metals prior to analysis. The extracts were transferred to acid-washed 7.5-mL LDPE

bottles, sealed, labeled and then stored in a plastic bag until analysis. Concentrations of dissolved Ba were determined directly on diluted aliquots of the seawater samples. River water samples were analyzed directly for Ba, Ca, Cu, Fe, K, Mg, Mn, Na and Ni as described below. Concentrations of Pb and Zn in river water were determined by reductive precipitation of 400-mL of sample water and the CRM SLRS-3 (river water issued by the NRC). Labware used in the extraction procedure and subsequent analysis was acid-washed with hot HNO_3 and rinsed three times with reagent water prior to use.

Total dissolved Hg concentrations in seawater and river water were determined on separate portions that had been treated with bromine monochloride solution (Szakacs et al., 1980) to oxidize organic ligands and preserve the samples until analysis.

The metal concentrations of the river water, river water extracts, CRMs and blanks were determined by FAAS, GFAAS, ICP-MS or cold-vapor atomic fluorescence spectrometry (CVAFS) (Table 2-1). Concentrations of Ca, K, Mg and Na in river water were determined directly by FAAS using a Perkin-Elmer Model 4000 AAS. Concentrations of dissolved As in the extracts were determined by GFAAS using a Perkin-Elmer Model 5100PC AAS equipped with an HGA-600 graphite furnace and AS-60 autosampler. Dissolved Pb and Zn concentrations in the river water extracts were quantified by ICP-MS using a Perkin-Elmer ELAN 5000 instrument. Dissolved Cu, Fe and Mn concentrations were measured directly for river water using a Perkin-Elmer Model 4000 AAS equipped with an HGA-400 graphite furnace and AS-40 autosampler. Dissolved Ba and Ni concentrations were determined directly on the river water samples by ICP-MS using a Perkin-Elmer ELAN 5000 instrument. Mercury in water samples was preconcentrated by gold amalgamation followed by analysis with CVAFS using a Brooks-Rand Model III Mercury System.

The metal concentrations of the seawater, seawater extracts, CRMs and blanks were determined by GFAAS, ICP-MS or CVAFS (Table 2-1). Concentrations of dissolved Cr and Cu in the extracts were determined by GFAAS using a Perkin-Elmer Model 4000 AAS with an HGA-400 graphite furnace and AS-40 autosampler. The As concentrations of the seawater extracts were determining using a Perkin-Elmer Model 5100PC AAS with an HGA-600 graphite furnace and AS-60 autosampler. Dissolved Cd, Pb and Zn concentrations of the seawater extracts were quantified by ICP-MS using a Perkin-Elmer ELAN 5000 instrument. Dissolved Ba concentrations were measured directly on the seawater samples by ICP-MS using a Perkin-Elmer ELAN 5000 instrument and multiple-spike Method of Standard Additions. Total dissolved Hg concentrations were determined by CVAFS using a Brooks-Rand Model III Mercury System following preconcentration by gold amalgamation.

River water chlorinity (Cl^-), sulfate (SO_4^{2-}) and fluoride (F^-) concentrations were determined by ion chromatography using a Dionex DX-600 ion chromatograph (IC). Standard curves were prepared using a Dionex Five Anion Standard certified solution. The IC column was a Dionex IonPac AS9-HC and the eluent was 9mM $NaHCO_3$. Alkalinity was determined by titration using the method of Strickland and Parsons (1972).

2.3 Quality Assurance and Quality Control

2.3.1 Sample Tracking Procedure

All sediment samples were collected by, transported by and stored by personnel from FIT. Upon return-to or arrival at the laboratory, each sample was carefully inspected to insure that it was intact and that the identification number was clearly readable.

2.3.2 Quality Control Measurements for Analysis

For this project, QC measures included balance calibration, instrument calibration (FAAS, GFAAS, CVAAS, ICP-MS, TOC analyzer, and *in-situ* instrument sensors), matrix spike analysis for each metal, duplicate sample analysis, analysis of CRMs and SRMs, procedural blank analysis and standard checks. With each batch of up to 20 samples, two procedural blanks, two CRMs or SRMs, two duplicate samples and two matrix-spiked samples were analyzed. Data quality objectives (DQOs) for these quality control measurements are provided in Table 2-2.

2.3.3 Instrument Calibration

Electronic balances used for weighing samples and reagents were calibrated prior to each use with certified, NIST-traceable standard weights. All pipets (electronic or manual) were calibrated prior to use. Each of the spectrometers used for metal analysis was initially standardized with a three- to five-point calibration with a linear correlation coefficient of $r \geq 0.999$ required before experimental samples could be analyzed. Analysis of complete three- to five-point calibrations and/or single standard checks alternated every 5-10 samples until all the analyses were complete. The relative standard deviation (RSD) between complete calibration and standard check was required to be <15 % or recalibration and reanalysis of the affected samples were performed.

2.3.4 Matrix Spike Analysis

Matrix spikes were prepared for a minimum of 5% of the total number of samples analyzed and included each metal to be determined. Results from matrix spike analysis using the method of standard additions provided information on the extent of any signal suppression or enhancement due to the sample matrix. If necessary (i.e., spike results outside 80-120% limit), spiking frequency was increased to 20% and a correction was applied to the metal concentrations of the experimental samples.

2.3.5 Duplicate Sample Analysis

Duplicate samples from homogenized field samples (as distinct from field replicates) were prepared in the laboratory for a minimum of 5% of the total samples. These laboratory duplicates were included as part of each set of sample digestions and analyses and provided a measure of analytical precision.

2.3.6 Procedural Blank Analysis

Two procedural blanks were prepared with each set of 20 samples to monitor potential contamination resulting from laboratory reagents, glassware and processing procedures. These blanks were processed using the same analytical scheme, reagents and handling techniques as used for the experimental samples.

Table 2-2. Data quality objectives and criteria.

Element or Sample Type Criteria	Minimum Frequency	Data Quality Objective/Acceptance
Initial Calibration	Prior to every batch of samples Standard Curve	3-5 point curve depending on the element plus a blank Correlation coefficient r ≥ 0.999 for all analytes
Continuing Calibration	Must end every analytical sequence; for flame, repeat all standards every 5 samples; for graphite furnace and ICP-MS recheck standard after every 8-10 samples	% RSD ≤15% for all analytes
Certified and Standard Reference Materials	Two per batch of 20 samples	Values must be within 20% of accepted values for >85% of the certified analytes and within 25% for Hg
Method Blank	Two per batch of 20 samples	No more than 2 analytes to exceed 5x MDL
Matrix Spike and Spike Method Blank	Two per batch of 20 samples	80-120%
Lab Duplicate	Two per batch of 20 samples	RSD <25% for 65% of analytes

2.3.7 CRM and SRM Analysis

A common method used to evaluate the accuracy of environmental data is to analyze reference materials, samples for which consensus or "accepted" analyte concentrations exist. The following CRMs and SRMs were used: Buffalo River sediment SRM#2704 (NIST) and Marine Sediment CRM MESS-2 (NRC). Metal concentrations obtained for the reference materials were required to be within <20% of accepted values for >85% of other certified analyses. Results for the CRMs and SRMs were well within the limits set in the DQOs (Table 2-2) as shown in Tables 2-3 and 2-4.

Results for QA/QC measurements for each data set are given along with the complete data set in the Appendices.

Table 2-3. Results for reference materials for suspended sediments.

Analyte	Certified Concentrations for SRM #2704[a] (μg/g)	This study[b] (μg/g)
Al (n = 38)	6.11 ± 0.16 (%)	6.14 ± 0.08 (%)
As (n = 38)	23.4 ± 0.8	23.4 ± 0.8
Ba (n = 38)	414 ± 12	418 ± 7
Ca (n = 8)	2.60 ± 0.03 (%)	2.59 ± 0.03 (%)
Cd (n = 30)	3.45 ± 0.22	3.44 ± 0.11
Cr (n = 30)	135 ± 5	134 ± 3
Cu (n = 40)	98.6 ± 5.0	99.7 ± 2.8
Fe (n = 40)	4.11 ± 0.1 (%)	4.13 ± 0.05 (%)
K (n = 8)	2.00 ± 0.04 (%)	2.00 ± 0.03 (%)
Mg (n = 10)	1.20 ± 0.02 (%)	1.19 ± 0.03 (%)
Mn (n = 10)	555 ± 19	566 ± 12
Na (n = 10)	0.547 ± 0.014 (%)	0.55 ± 0.03 (%)
Ni (n = 8)	44.1 ± 3.0	45.7 ± 3.8
Pb (n = 38)	161 ± 17	159 ± 9
Zn (n = 42)	438 ± 12	436 ± 8
POC (n = 25)	2.14 ± 0.03 (%)[c]	2.00 ± 0.05 (%)

[a] ± 95 confidence limits.
[b] ± 1 standard deviation.
[c] MESS-2 (NRC).

Table 2-4. Results for reference materials for dissolved metals.

Standard (SRM) or Certified (CRM) Reference Material	Certified Concentrations[a] (µg/L)	This Study[b] (µg/L)
CRM CASS-3 (NRC)		
As (n = 8)	1.09 ± 0.07	1.06 ± 0.04
Ba (n = 2)	-	8.9 ± 0.4
Cd (n = 7)	0.030 ± 0.005	0.027 ± 0.001
Cr (n = 6)	0.092 ± 0.006	0.092 ± 0.001
Cu (n = 6)	0.517 ± 0.062	0.538 ± 0.016
Pb (n = 7)	0.012 ± 0.004	0.012 ± 0.002
Zn (n = 7)	1.24 ± 0.25	1.11 ± 0.08
CRM SLRS-3 (NRC)		
Ba (n = 6)	13.4 ± 0.2	13.6 ± 0.2
Ca (n = 5)	6.0 ± 0.4 mg/L	6.1 ± 0.2 mg/L
Fe (n = 5)	100 ± 2	101 ± 2
K (n = 5)	0.7 ± 0.1 mg/L	0.7 ± 0.1 mg/L
Mg (n = 5)	1.6 ± 0.6 mg/L	1.6 ± 0.1 mg/L
Mn (n = 5)	3.9 ± 0.3	3.8 ± 0.2
Na (n = 5)	2.3 ± 0.2 mg/L	2.3 ± 0.1
Pb (n = 5)	0.086 ± 0.007	0.084 ± 0.004
Zn (n = 5)	1.04 ± 0.09	1.05 ± 0.04
CRM SLRS-4 (NRC)		
Cu (n = 2)	1.81 ± 0.08	1.82 ± 0.04
Pb (n = 3)	0.086 ± 0.007	0.086 ± 0.002
Zn (n = 3)	0.93 ± 0.10	0.89 ± 0.03
SRM #1640 (NIST)		
Ba (n = 6)	148.0 ± 2.2	147.5 ± 2.0
Cu (n = 5)	85.2 ± 1.2[c]	84.9 ± 1.8
Ni (n = 5)	27.4 ± 0.8[c]	27.7 ± 0.7

[a] ± 95 confidence limits.
[b] ± 1 standard deviation.
[c] Reference Value provided by NIST (not certified).

2.4 OMP Analysis for Data from May-June 2004

Optimum multi-parameter (OMP) analysis, a weighted, non-negative, linear least-squares mass balance, was used to calculate the relative fractions of each water mass in a discrete sample based on methods from Karstensen (2005). Briefly, the method finds the best fitting fraction (x) of (n) water types that contribute to the (n+1) observed values of the selected tracers in a water sample via solution of an over-determined system of linear equations that minimized the residual error. Boundary conditions were applied to the method to guarantee that all fractions calculated were positive and that the sum of all fractions was 100% (mass conservation). Three specific tracers (salinity, $\delta^{18}O$ and dissolved silica) were combined with the assumption of mass conservation as a fourth variable to quantify the fractions of three water masses that contributed most to each individual station.

The success of the OMP method is dependent upon accurate endmember values (Thompson and Edwards, 1981; Tomczak et al., 1981 a, b; Mackas et al., 1987). An initial endmember matrix was calculated by averaging measurements for each parameter in each water mass (Table 2-5). Final values were chosen by fine-tuning the initial endmembers within the range of analytical precision and daily variability in accordance with Mackas et al. (1987).This procedure yielded endmembers with the lowest residuals in the calculated water mass fractions (Table 2-5).

The endmember matrix and sample observations were multiplied by a diagonal weight matrix to account for differences in tracer reliability, environmental variability, and precision and accuracy of the data. Thompson and Edwards (1981) used estimates of analytical precision to determine tracer weights whereas Mackas et al. (1987) and Macdonald et al. (1989) based weights on measurement uncertainty and the variance and covariance of tracer properties in a given area. In this study, the method for allocating weights was adapted from Mackas et al. (1987) and Hinrichsen and Tomczak (1993) and involved the following: (1) multiplying the estimated analytical precision by a factor of ten, (2) dividing by the range of endmember values and (3) taking the inverse to yield weights of 30 for salinity, $\delta^{18}O$ and mass conservation (assumed equal to largest weights), and 10 for dissolved silica.

An estimate of the error associated with the calculation was necessary to determine the quality of the water mass fractions yielded from this analysis. Based on suggestions by Karstensen (2005), Macdonald et al. (1989) and Hinrichsen and Tomczak (1993) this problem was approached in the following ways: (1) varying endmember definitions and weights, (2) adding random, equally-distributed white noise (1σ) to sample observations, (3) varying the specific water masses included in each calculation, and (4) calculating water mass fractions using only salinity and silica without weighting or normalization. Using these comparisons, water mass fractions in each sample were estimated to be accurate to ±10 %, similar to the accuracy reported by Macdonald et al. (1989). Error residuals associated with the accepted water mass fraction calculations are listed in Table 2-6.

Table 2-5. Initial and final (bold) values of endmembers for water masses.

Water Mass	Salinity	$\delta^{18}O$ (‰)	Dissolved Silica (μM)
Kuparuk River	0.02 ± 0.01 (n = 7) **0.0**	-23.0 ± 0.3 (n = 4) **-23.0**	13 ± 1 (n = 8) **14.0**
Sagavanirktok River	0.12 ± 0.02 (n = 8) **0.0**	-21.7 ± 0.4 (n = 4) **-21.7**	24 ± 5 (n = 9) **25.0**
Meteoric Water[a]	0.15	-20.3	46.5
Sea-ice melt	5.0 ± 0.9 (n = 19) **5.0**	-0.8 ± 0.1 (n = 2) **-0.8**	0.9 ± 0.5 (n = 19) **0.0**
Sea-ice melt[a]	5.0	-2.4	2
Polar Mixed Layer	31.1 ± 0.6 (n = 71) **32.1**	-3.4 ± 0.1 (n = 6) **-3.4**	8 ± 1 (n = 70) **8.0**
Polar Mixed Layer[a]	31.6	-3.5	4.7

[a]from Macdonald et al. [1989].

Table 2-6. Error residuals for accepted water mass fractions calculated for selected transects. Average mass residuals (AMR) and maximum mass residuals (MMR) were calculated from the absolute values of the data set. Missing $\delta^{18}O$ residuals are for those stations that did not have any data.

Transect of stations	AMR[a] (%)	MMR[b] (%)	Salinity	Silica (μM)	$\delta^{18}O$ (‰)
SW 1,2,3,4 & SK1	0.2	1.1	0.1	0.8	0.1
SW 2,4,5 & SK1	0.3	1.6	0.1	1.3	0.2
K 1,2,3	0.2	0.7	0.0	0.4	0.1
K 3,4,5	0.3	1.1	0.0	0.8	nd[c]
SE 1,2,3,4 & S1	0.6	1.4	0.1	1.5	nd[c]
S 1,2,3,4	1.1	4.3	0.2	4.8	nd[c]
SK 2,3,4	0.2	0.7	0.3	1.1	0.1
SK 5,6,7	0.3	0.8	0.4	1.2	0.1
SK 8,9,10	0.2	0.7	0.3	1.0	0.3

[a]AMR = Average Mass Residual.
[b]MMR = Maximum Mass Residual.
[C]not determined.

3. TRANSPORT OF WATER, SEDIMENTS AND CHEMICALS FROM RIVERS DURING THE SPRING MELT

3.1 Overview

Most rivers that drain into the Arctic Ocean carry 40 to 80% of their annual volume of water at peak flow that occurs during the spring floods and in early summer (Arnborg et al., 1967; Gordeev et al, 1996; Rember and Trefry, 2004). In addition to water discharge, Telang (1985) showed the importance of the spring melt to the transport of dissolved organic carbon (DOC). He found that ~25% and ~35% of the annual discharge of water and DOC, respectively, into the Canadian Beaufort Sea from the Mackenzie River occurred during June. Studies in the Alaskan Arctic have shown that concentrations of total suspended solids (TSS) in the Colville River follow the same trend as water flow with >70% of the annual discharge of TSS occurring during May and June (Arnborg et al., 1967). Large seasonal discharges of water at high latitudes, linked with increased concentrations of TSS and DOC, emphasize the importance of annual spring floods to the arctic hydrologic cycle.

During the ANIMIDA Project, Rember and Trefry (2004) found that concentrations of DOC increased from 2.0 to 8.9 mg/L during peak discharge in the Sagavanirktok River, at the same time that river flow increased by 250%. Concentrations of dissolved Cu, Pb, Zn and Fe in the Sagavanirktok River followed trends observed for DOC with 3- to 25-fold higher levels at peak flow. Similar trends were observed in the Kuparuk and Colville rivers, where average concentrations of dissolved trace metals and DOC were even higher. These trends were related to the discharge of DOC and dissolved metals from thawing ponds and upper soil layers. Rember and Trefry (2004) found that during the peak 8 to 9 days of the 2001 melt-water event, the large pulse of water enriched with DOC and dissolved Cu, Fe, Pb and Zn, carried as much as half of the annual load of DOC and selected dissolved metals to the coastal Beaufort Sea. In contrast with Cu, Fe, Pb and Zn, concentrations of dissolved Ba were relatively constant in the Sagavanirktok (32 ± 2 μg/L), Kuparuk (23 ± 2 μg/L) and Colville (52 ± 3 μg/L) rivers.

The main purpose of this May-June portion of the cANIMIDA study was to determine concentrations of suspended sediments and the chemical composition of the particles and water in the Sagavanirktok River (SR) and the Kuparuk River (KR) during spring floods. Samples from the Colville River were collected and analyzed in 2006. The results and discussion section for the 2004 and 2006 river data begins with input of water and suspended sediments by rivers during the spring melt and then transitions to particulate and dissolved metals. The order of the presentation for the combined 2004 and 2006 spring data is as follows:

3.2 Water and Sediment Transport from Rivers during the Spring Melt.
3.3 Particulate Metals and Organic Carbon in River Water.
3.4 Dissolved Metals and Organic Carbon in River Water

3.2 Water and Sediment Transport from Rivers during the Spring Melt

During the 2 to 3 weeks of the spring floods in May-June, about 60% of the annual water flow from the Kuparuk River and about one third of the annual flow of the Sagavanirktok River are carried to the Beaufort Sea (Rember and Trefry, 2004; Figure 3-1). Although the overall trends in annual flow are similar, inter-annual variations and differences between rivers are observed in hydrographs during the spring melt (Figure 3-2).

The yellow-colored water of the Kuparuk River has been categorized as more representative of a tundra stream with most of the water derived from the tundra and foothills, not the mountains (Lock et al., 1989). Water and sediment discharge from the

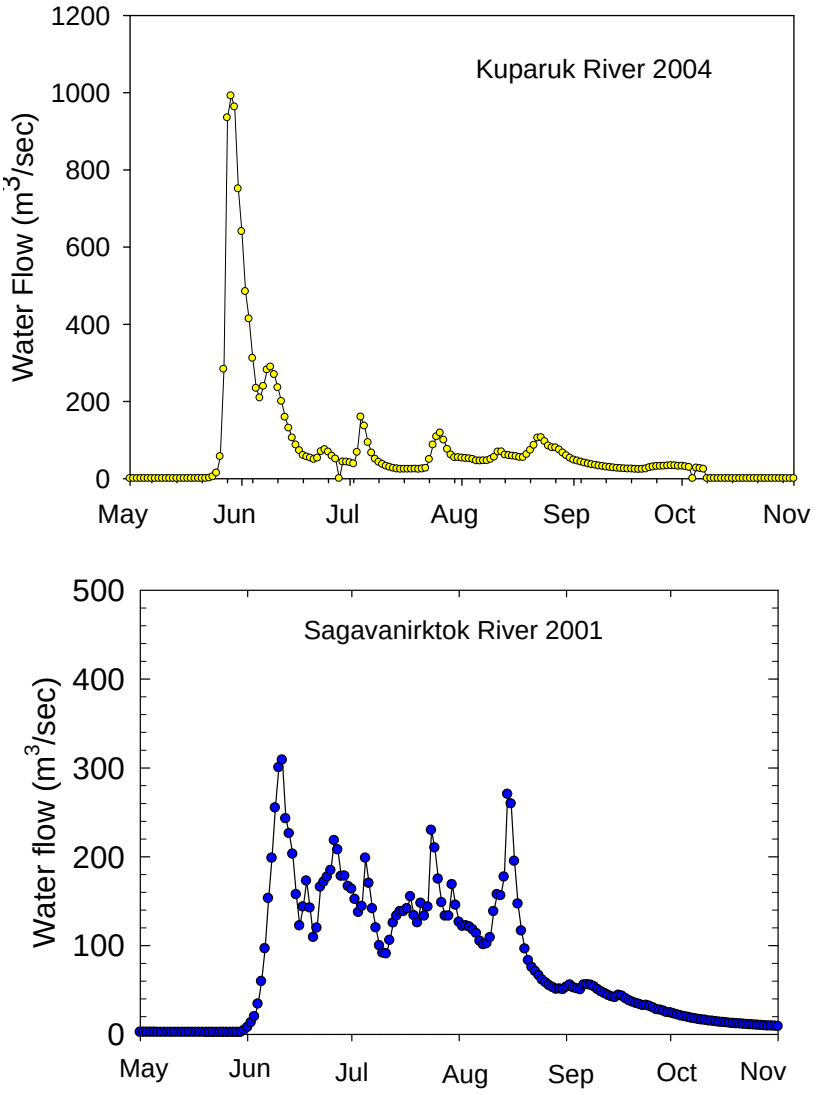

Figure 3-1. Annual hydrographs for the Kuparuk River in 2004 and the Sagavanirktok River in 2001. The rivers are completely frozen from November until May. Data from U.S.G.S. can be accessed at http://waterdata.usgs.gov/ak/nwis.

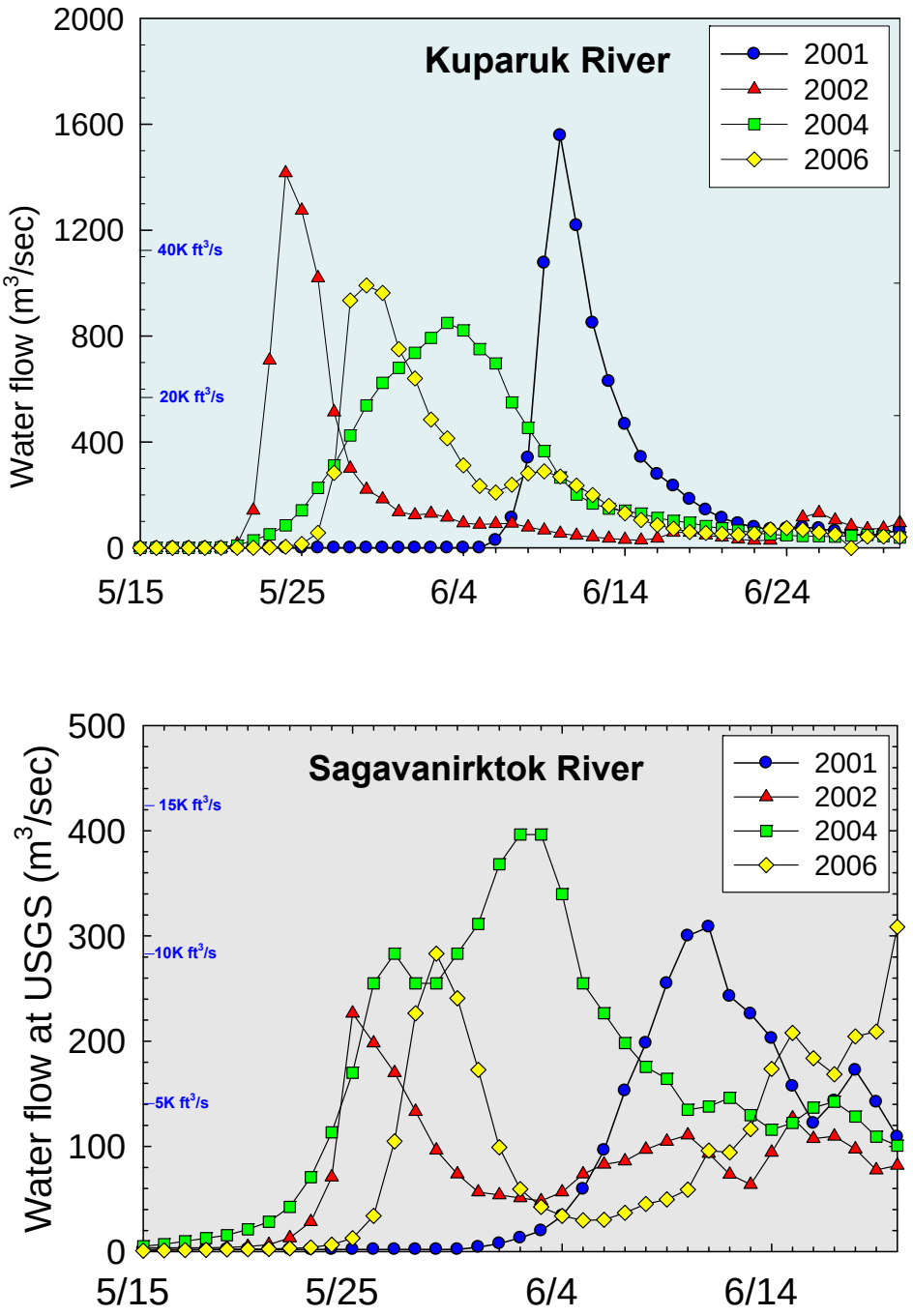

Figure 3-2. Hydrographs during the spring floods in 2001, 2002, 2004 and 2006 for the Kuparuk and Sagavanirktok rivers. Data from U.S.G.S. can be accessed at http://waterdata.usgs.gov/ak/nwis.

Figure 3-3. Peak flow in the east channel of the Kuparuk River in 2006 creates an overwash of ice and water on the causeway and bridge.

Kuparuk River has generally occurred as a brief event (3-5 days) when upstream ice jams break up and allow a large pulse of water to pass down the river. The resulting flood can close and damage causeways and bridges along the river (Figure 3-3). In contrast with the other three years, water flow in the Kuparuk River during 2004 was spread out over more than 2 weeks (Figure 3-2). Differences in the date of peak flow also can vary as shown by a 19-day separation in peak flow for the Kuparuk River for 2002 versus 2001 (Figure 3-2).

Based on the classification scheme proposed by Craig and McCart (1975), the Sagavanirktok and Colville rivers can be classified as mountain streams that drain snowfields and glaciers in the Brooks Range. Peak flow, though quite pronounced, tends to extend over a longer time period than observed in the Kuparuk River (Figure 3-2). The dates of peak flow in the Kuparuk and Sagavanirktok rivers coincided within just a few days (Figure 3-2).

The annual discharge of the Sagavanirktok River, at the USGS gauge, has increased by about 50% over the past 3 decades (Figure 3-4a) due to increased melting of ice and snow in the Brooks Range and increased precipitation in the mountains. In contrast, no discernible change in water flow has been observed for the Kuparuk River, a tundra stream (Figure 3-4b).

During the cANIMIDA Project of spring 2004, water was collected nine times from the Sagavanirktok River and 8 times from the Kuparuk River between May 22 and June 2. In 2006, water was collected 13 times from the Sagavanirktok River between May 22 and June 4 and 10 times from the Kuparuk River between May 26 and June 4. Coordinates for the sampling locations are listed in Table 3-1 and shown on a map in Figure 1-1 (page 4). In 2006, three water samples were collected for us from the Colville River by Dr. James McClelland of the University of Texas Marine Science Institute.

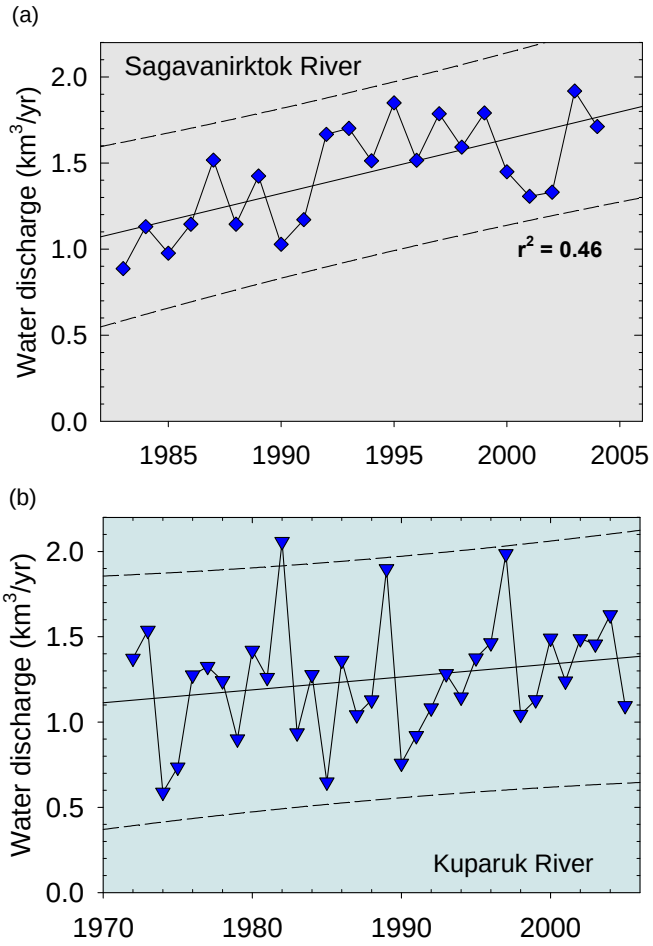

Figure 3-4. Annual water discharge from 1970 to 2005 for the (a) Sagavanirktok River and (b) Kuparuk River. Data are from the U.S.G.S. and can be accessed at http://waterdata.usgs.gov/ak/nwis.

Table 3-1. Locations of river sampling sites.

Site	Latitude (N)	Longitude (W)
Sagavanirktok River (near Prudhoe Bay)	70° 15.033′	148° 18.484′
Sagavanirktok River (U.S.G.S. gauge at mile 327 on the Dalton Highway)	69° 00.527′	148° 49.214′
Kuparuk River (U.S.G.S. gauge at this location)	70° 19.812′	149° 00.527′
Colville River (no U.S.G.S. gauge)	70° 09.519′	150° 56.791′

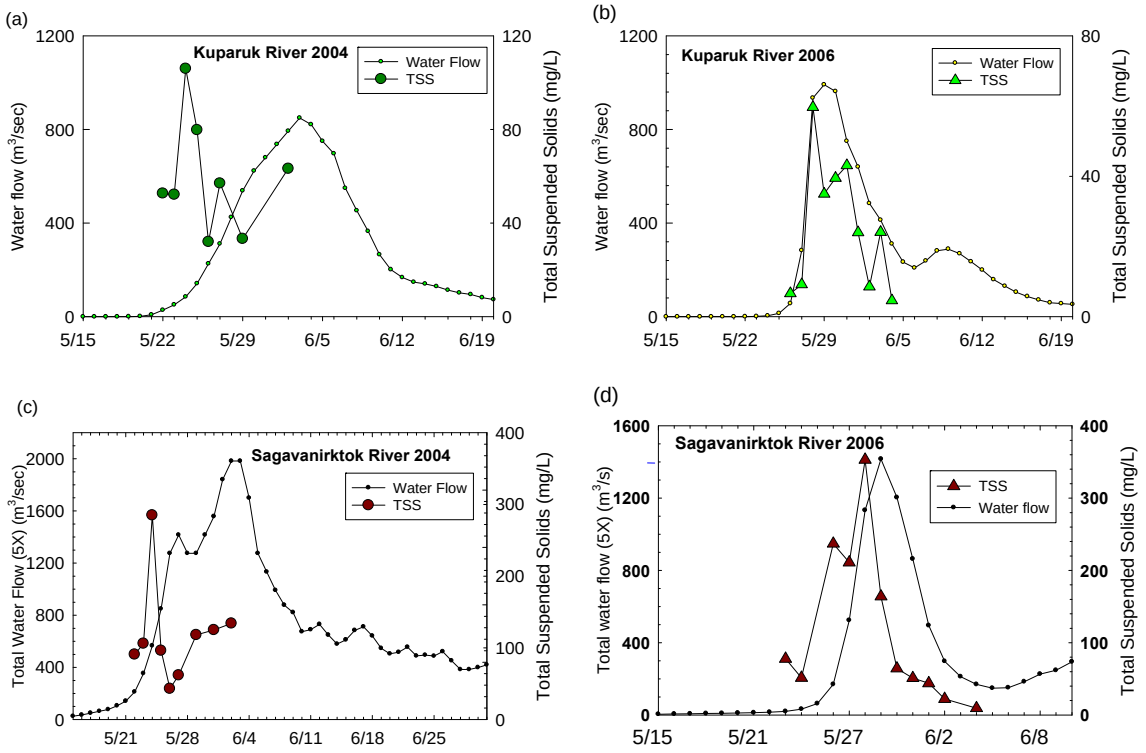

Figure 3-5. Water flow and total suspended solids for the Kuparuk and Sagavanirktok rivers for May-June, 2004 and 2006. Water flow for Sagavanirktok River multiplied by 5 to provide extrapolation from U.S.G.S. gauge to river basin as described by Rember and Trefry (2004).

Concentrations of TSS for the Sagavanirktok and Kuparuk rivers for spring 2004 and 2006 (Figure 3-5, Table 3-2) ranged from ~10 to 353 mg/L and ~5 to 106 mg/L, respectively. Thus, the suspended matter load of the river water that was moving offshore under the ice varied on a daily basis. This trend made tracking the fate of the suspended sediments during freshwater-seawater mixing more difficult because the freshwater end-member value for TSS was variable.

In a manner similar to that observed in 2002 for the Sagavanirktok River (Trefry et al., 2004a), the onset of the 2004 melt occurred about May 20, with a period of refreezing several days later (Figure 3-5c). The impact of the weather on trends for concentrations of TSS was less dramatic in 2004 than observed in 2002 because the freezing event was less complete in the river in 2004 and did not stop flow. Nevertheless, the refreezing process during both 2002 and 2004 lowered peak levels of TSS to <300 mg/L relative to >600 mg/L during a year, such as 2001, when no period of refreezing occurred.

The Colville River was sampled 13 times throughout the spring melt in 2001 and only three times during peak flow in 2006 (Table 3-2). Based on somewhat more limited sampling, the Colville River seems to carry a very high sediment load (Table 3-2).

Table 3-2. Mean, maximum and minimum concentrations of total suspended solids (TSS) in the Kuparuk, Sagavanirktok and Colville rivers during May-June for the years listed.

River and Year		n	TSS – Mean (mg/L)	TSS – Max. (mg/L)	TSS- Min. (mg/L)
Kuparuk	2006	10	25	60	4.6
	2004	8	60	106	32
	2002	14	19	120	0.5
	2001	10	27	67	1.8
Sagavanirktok	2006	13	130	353	9.5
	2004	11	127	285	43
	2002	26	92	244	3.5
	2001	27	158	609	14
Colville	2006	3	722	785	637
	2001	13	343	545	42

3.3 Particulate Metals and Organic Carbon in River Water

Data for particulate metals and organic carbon were obtained during spring for the Sagavanirktok and Kuparuk rivers during 2001, 2002, 2004 and 2006 and for the Colville River during 2001 and 2006 (Tables 3-3 and 3-4). In addition to these data for the spring floods, data for rivers in summer 2004, 2005 and 2006 are discussed in Section 3. Data for summer 2000, 2001 and 2002 were presented and discussed in Trefry et al. (2004b).

The composition of suspended matter in rivers can provide a geochemical signature that may allow differentiation between incoming natural suspended sediments and anthropogenic contributions from industrial activity in the coastal Beaufort Sea. Furthermore, changes in the composition of the river-borne particles may help identify future shifts in mechanical and chemical weathering in the Brooks Range and across the North Slope that may be related to changing climate and other processes.

Summary data for major elements (Al, Fe, Ca, K and Mg), trace metals (As, Ba, Cu, Ni, Pb and Zn) and POC for suspended sediments collected from the three rivers during the ANIMIDA and cANIMIDA Projects are presented in Tables 3-3 and 3-4. Differences in the Al content of the suspended sediments were observed with Colville>Sagavanirktok> Kuparuk (Table 3-4 and Figure 3-6). In contrast, concentrations of Ca are about 8 to 10 times greater in the Sagavanirktok River than in the Kuparuk or Colville rivers (Table 3-4 and Figure 3-6). These differences are directly related to the greater abundance of aluminum-bearing phases (clay minerals) in the Colville River relative to the

Table 3-3. Concentrations of particulate metals and organic carbon (POC) in the Kuparuk and Colville rivers during May-June for years listed.

River		Al (%)	As (µg/g)	Ba (µg/g)	Ca (%)	Cu (µg/g)	Fe (%)	K (%)	Mg (%)	Ni (µg/g)	Pb (µg/g)	Zn (µg/g)	POC (%)
Kuparuk 2006 (n= 10)	Mean	5.2	7.1	593	1.08	26.6	3.8	1.40	0.74	41.7	17.0	148	4.7
	Std. Dev.	± 1.0	± 2.1	± 103	± 0.47	± 3.9	± 0.5	± 0.27	± 0.12	± 6.2	± 3.8	± 25	± 2.1
	Min.	3.5	4.7	450	0.63	20.5	3.2	1.08	0.56	33.1	12.1	109	2.6
	Max.	6.6	11.6	725	2.2	34.1	4.6	2.02	0.96	49.7	23.7	191	7.8
Kuparuk 2004 (n= 8)	Mean	6.2	8.1	671	0.74	34.0	4.1	1.44	0.69	41.7	5.6	121	3.3
	Std. Dev.	± 0.4	± 3.8	± 72	± 0.12	± 5.1	± 0.2	± 0.16	± 0.05	± 2.4	± 0.6	± 6	± 1.0
	Min.	5.5	3.9	573	0.63	28.7	3.7	1.29	0.60	38.2	5.0	112	1.6
	Max.	6.7	13.1	805	0.89	45.1	4.3	1.72	0.73	44.5	6.5	130	4.9
Kuparuk 2002 (n=13)	Mean	4.0	14.6	537	0.9	28.4	4.5	1.1	0.6	48.8	18.9	152	5.3
	Std. Dev.	± 1.5	± 3.7	± 237	± 0.2	± 6.0	± 0.8	± 0.3	± 0.2	± 11.3	± 3.8	± 62	± 3.1
	Min.	2.6	7.4	358	0.6	17.6	2.7	0.8	0.5	28.6	10.3	81	1.7
	Max.	7.5	17.6	1219	1.1	38.5	5.4	1.6	1.1	63.8	24.6	263	10.9
Kuparuk 2001 (n=8)	Mean	4.4	16.6	562	1.0	31.4	3.7	1.1	0.5	43.8	15.1	110	4.8
	Std. Dev.	± 1.0	± 8.1	± 98	± 0.2	± 4.6	± 0.3	± 0.2	± 0.2	± 7.6	± 5.1	± 23	± 1.5
	Min.	2.7	10.2	497	0.8	25.7	3.1	0.6	0.12	29.0	11.9	82	2.8
	Max.	5.8	29.7	743	1.5	37.2	4.2	1.3	0.69	53.6	22.5	126	5.9
Colville 2006 (n= 3)	Mean	7.7	10.3	939	0.87	36.8	4.8	2.13	1.31	57.9	19.6	128	2.2
	Std. Dev.	± 0.2	± 0.2	± 35	± 0.19	± 1.9	± 0.3	± 0.09	± 0.11	± 5.2	± 1.7	± 3	± 0.1
	Min.	7.5	10.2	903	0.68	35.3	4.5	2.05	1.20	52.2	17.7	125	2.1
	Max.	7.9	10.5	973	1.05	39.0	5.1	2.22	1.41	62.3	20.9	131	2.3
Colville 2001 (n= 5)	Mean	8.3	14.2	989	0.7	40.8	5.0	1.9	1.1	68.7	24.0	130	2.2
	Std. Dev.	± 0.3	± 1.3	± 125	± 0.1	± 2.3	± 0.3	± 0.3	± 0.2	± 10.0	± 6.8	± 11	± 0.6
	Min.	8.00	12.6	887	0.58	36.9	4.66	1.29	0.78	59.9	19.8	116	1.7
	Max.	8.86	15.3	1190	0.92	42.6	5.34	2.06	1.17	81.2	36.0	147	3.3

Table 3-4. Concentrations of particulate metals and organic carbon (POC) in the Sagavanirktok River and mean values for the Kuparuk, Colville and Sagavanirktok rivers during May-June for the years listed.

River		Al (%)	As (µg/g)	Ba (µg/g)	Ca (%)	Cu (µg/g)	Fe (%)	K (%)	Mg (%)	Ni (µg/g)	Pb (µg/g)	Zn (µg/g)	POC (%)
Sagavanirktok 2006 n=12	Mean	6.0	8.4	555	7.9	29.6	3.5	1.67	1.17	49.3	15.5	145	2.0
	Std. Dev.	± 1.2	± 1.6	± 96	± 2.4	± 5.3	± 0.6	± 0.32	± 0.09	± 6.8	± 4.5	± 35	± 0.5
	Min.	4.7	4.7	433	3.6	23.2	2.9	1.32	1.06	26.8	11.0	109	1.2
	Max.	7.8	7.8	780	10.0	40.9	4.6	2.36	1.34	41.5	26.8	209	3.0
Sagavanirktok 2004 n=9	Mean	6.1	10.7	654	7.4	31.0	3.4	1.52	1.07	45.7	11.7	133	1.1
	Std. Dev.	± 0.5	± 3.6	± 53	± 0.7	± 4.4	± 0.1	± 0.10	± 0.02	± 3.9	± 1.4	± 14	± 0.2
	Min.	5.2	5.4	578	6.3	23.6	3.1	1.35	1.04	40.0	9.8	115	0.8
	Max.	6.9	17.0	733	8.2	38.6	3.5	1.65	1.09	51.4	13.6	161	1.5
Sagavanirktok 2002 n=23	Mean	6.2	14.3	698	8.9	33.3	3.5	1.7	1.1	52.1	11.9	142	1.6
	Std. Dev.	± 1.1	± 4.3	± 160	± 1.7	± 5.7	± 0.6	± 0.3	± 0.1	± 6.4	± 4.1	± 31	± 0.3
	Min.	5.0	9.0	541	4.8	25.6	2.8	1.4	1.0	42.4	4.3	116	1.2
	Max.	8.8	24.5	1110	10.9	45.4	4.7	2.5	1.2	65.0	23.2	214	2.4
Sagavanirktok 2001 n =22	Mean	5.6	11.1	702	6.7	32.8	3.3	1.7	0.8	60.9	18.0	123	1.6
	Std. Dev.	± 0.9	± 1.6	± 113	± 1.0	± 2.8	± 0.4	± 0.2	± 0.1	± 5.1	± 2.0	± 7	± 0.49
	Min.	4.0	8.2	542	4.9	29.7	2.6	1.4	0.67	53.7	16.0	115	0.7
	Max.	7.7	13.4	1008	8.2	39.2	4.0	2.3	0.93	75.8	23.4	135	2.7
Kuparuk 2001-2, 2004, 2006	**Mean**	**5.0**	**11.6**	**591**	**0.9**	**30.1**	**4.0**	**1.3**	**0.6**	**44.0**	**14.2**	**133**	**4.5**
	Min.	2.6	3.9	358	0.6	17.6	2.7	0.6	0.5	28.6	5.0	81	1.6
	Max.	7.5	29.7	1219	2.2	45.1	5.4	2.0	1.1	63.8	24.6	264	7.8
Colville 2001, 2006	**Mean**	**8.0**	**12.2**	**964**	**0.8**	**38.8**	**4.9**	**2.0**	**1.2**	**63.3**	**21.8**	**129**	**2.2**
	Min.	7.5	10.2	887	0.58	35.3	4.5	1.3	0.8	52	18	116	1.7
	Max.	8.9	15.3	1190	1.05	42.6	5.3	2.2	1.4	81	36	147	3.3
Sagavanirktok 2001-2, 2004, 2006	**Mean**	**6.0**	**11.1**	**652**	**7.7**	**31.7**	**3.4**	**1.6**	**1.0**	**52.0**	**14.3**	**136**	**1.6**
	Min.	4.0	4.7	433	**3.6**	23	2.6	1.3	0.7	27	4	109	0.7
	Max.	8.8	24.5	1110	**10.9**	45	4.7	2.5	1.3	76	27	214	3.0

Sagavanirktok and Kuparuk rivers along with a much greater abundance of particulate calcite ($CaCO_3$) and dolomite ($CaMg(CO_3)_2$) in the Sagavanirktok River. Unfortunately, the differences in the Ca/Al ratios among the rivers were not easily observed in coastal sediments due to the addition of marine shells (carbonate) to the coastal sediments.

Previous studies have shown that the Sagavanirktok River drains primarily limestone deposits and has concentrations of dissolved Ca that are ~2 times higher than in the Kuparuk and Colville rivers (Telang et al., 1991). In addition to the Lisburne limestone and dolomite from the Tertiary, the Brooks Range also contains shales from the Triassic to Pennsylvanian age (Payne et al., 1951; Mull and Adams, 1989). The Gubik formation (Quaternary riverine and marine sediments) underlies the coastal plain and Quaternary sediments, older Cretaceous and Tertiary sandstones, conglomerates and siltstones are exposed in the foothills province (Payne et al., 1951; Mull and Adams, 1989). Distinctions in the composition of the source material among the rivers can help explain differences in concentrations of both particulate and dissolved trace metals among the rivers as described below.

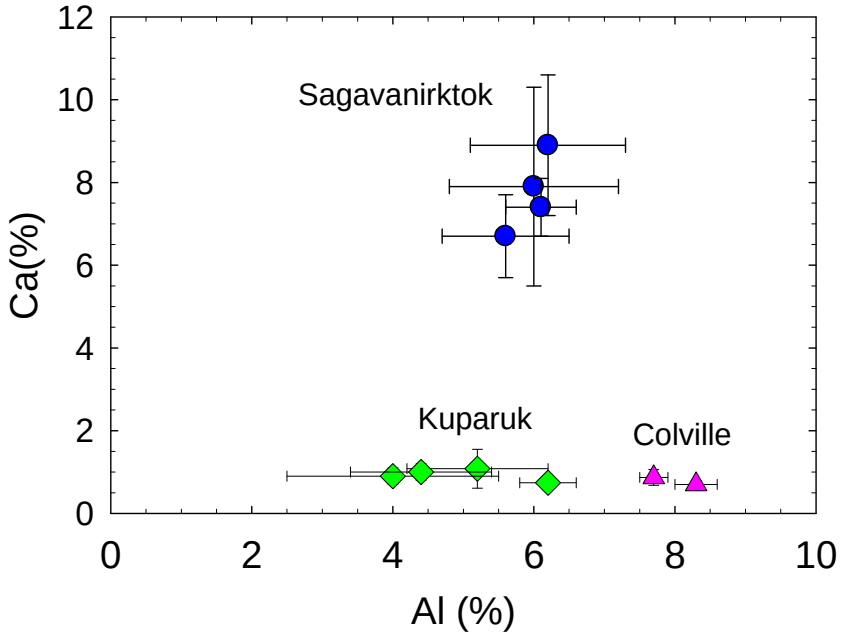

Figure 3-6. Concentrations of calcium (Ca) versus aluminum (Al) for suspended sediments from the Sagavanirktok (circles), Kuparuk (diamonds), and Colville (triangles) rivers during 2001, 2002, 2004 and 2006. Markers show means and lines show standard deviations using data from Tables 3-3 and 3-4.

Differences in the K and Mg concentrations of river suspended sediments also were observed among the rivers with an overall trend of Colville>Sagavanirktok>Kuparuk (Table 3-4 and Figure 3-7). However, these differences were much less distinct than those previously shown for Ca (Figure 3-6). In fact, the K/Al plot shows a good linear relationship and a near zero y-intercept for the combined annual averages for all three rivers (Figure 3-7a). This trend suggests that the source minerals bearing K (most likely illite clays with some micas and potassium feldspars) are similar enough for each river that the linear variations are due to differences in the relative amounts of K phases in the suspended sediments. A similar relationship between Mg and Al supports common source minerals, such as chlorite, for Mg (Payne et al., 1951).

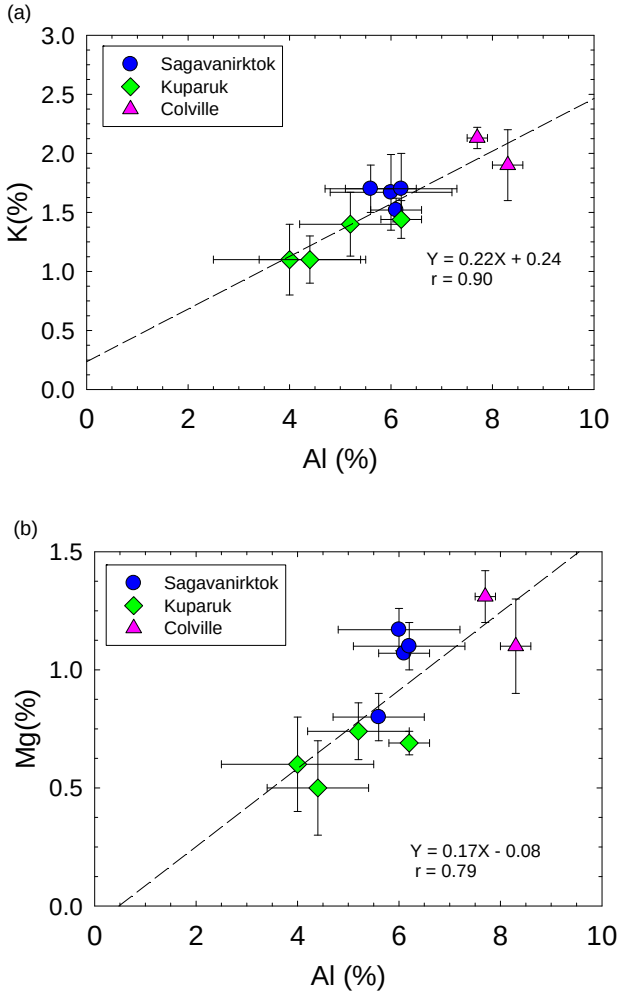

Figure 3-7. Concentrations of (a) potassium (K) and (b) magnesium (Mg) versus aluminum (Al) for suspended sediments from the Sagavanirktok (circles), Kuparuk (diamonds) and Colville (triangles) rivers during the spring floods of 2001, 2002, 2004 and 2006 (data from Tables 3-3 and 3-4).

Concentrations of trace metals in river suspended matter provide another possible point of reference for differentiating among river sources of sediment and for comparison with bottom sediment in the cANIMIDA study area. Such comparisons may enable us to determine whether incoming suspended particles have been modified by chemical processes in marine sediments or if metal concentrations have been enhanced by anthropogenic inputs.

Average concentrations of particulate Ba, Cu, Fe, Ni and Pb in the Colville River averaged ~20 to ~50% higher than concentrations found in suspended particles from the Sagavanirktok and Kuparuk rivers (Tables 3-3 and 3-4). However, particles from the Colville River also had higher concentrations of Al, suggesting that sources of suspended sediments to the Colville River, from farther to the west in the Brooks Range, are richer in fine-grained aluminosilicates or less diluted by non-aluminosilicate minerals (Tables 3-3 and 3-4). When concentrations of particulate Fe were plotted versus Al (Figure 3-8), the results for the Sagavanirktok River fit the same Fe/Al trend reported for sediments in the coastal Beaufort Sea (Trefry et al., 2003). For most of the suspended sediment samples from the Kuparuk and Colville rivers, concentrations of Fe were as much as ~10% higher than predicted from the sediment data (Figure 3-8). Concentrations of dissolved Fe averaged 3 to 4 times more in the Kuparuk and Colville rivers than in the Sagavanirktok River as described in the next section (3.4). Such excess dissolved Fe enhances the formation of Fe hydrous oxides and an increase in levels of particulate Fe as described by Rember and Trefry (2004).

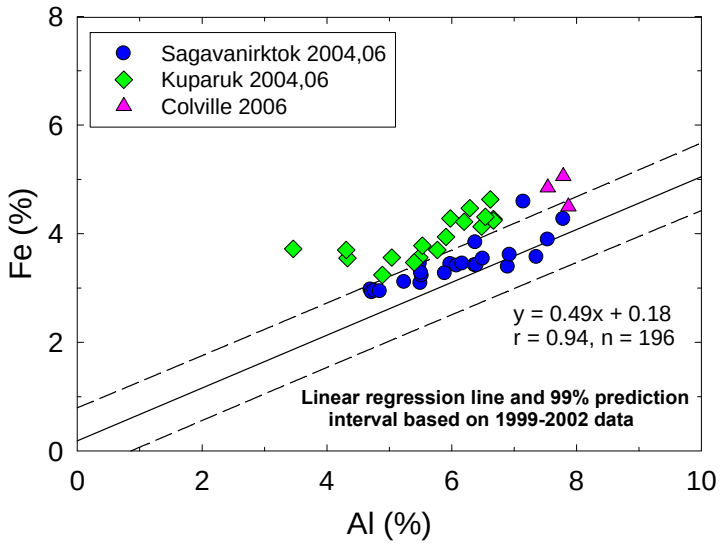

Figure 3-8. Concentrations of iron (Fe) versus aluminum (Al) for suspended sediments from the Sagavanirktok (circles), Kuparuk (diamonds) and Colville (triangles) rivers during May-June 2004 and 2006. Solid line is from a linear regression for sediment data from the ANIMIDA study area and dashed lines show 99% prediction interval for sediment data.

More than 85% of the data points for Ba, Cu, Cr, Ni and Pb in suspended sediments from the three rivers during 2004 and 2006 plotted below the upper prediction intervals on the metal versus Al graphs (Figures 3-9 and 3-10). The higher metal concentrations, that plotted at <25% above the upper prediction interval, were from the Kuparuk River that typically carried lower amounts of TSS with more variable metal concentrations (Table 3-3). About 20% of the data points for Zn in suspended sediments plotted above the upper prediction interval on Figure 3-10c. In the case of Zn, as well as Ba, Cu, Cr, Ni and Pb, some of the observed anomalies may be due to anthropogenic inputs of metals from industrial activities on the North Slope; however, no data were available to support this statement. With the large data base from 2000 to 2006, river particles may provide a useful long-term tool for monitoring inputs of potential metal contaminants from land to the cANIMIDA study area.

Concentrations of POC (as a % of TSS) varied by factors of 2 to 5 in each of the rivers for the 2004 and 2006 data with the highest average (4.5%) and maximum value (7.8%) in the Kuparuk River (Table 3-4).

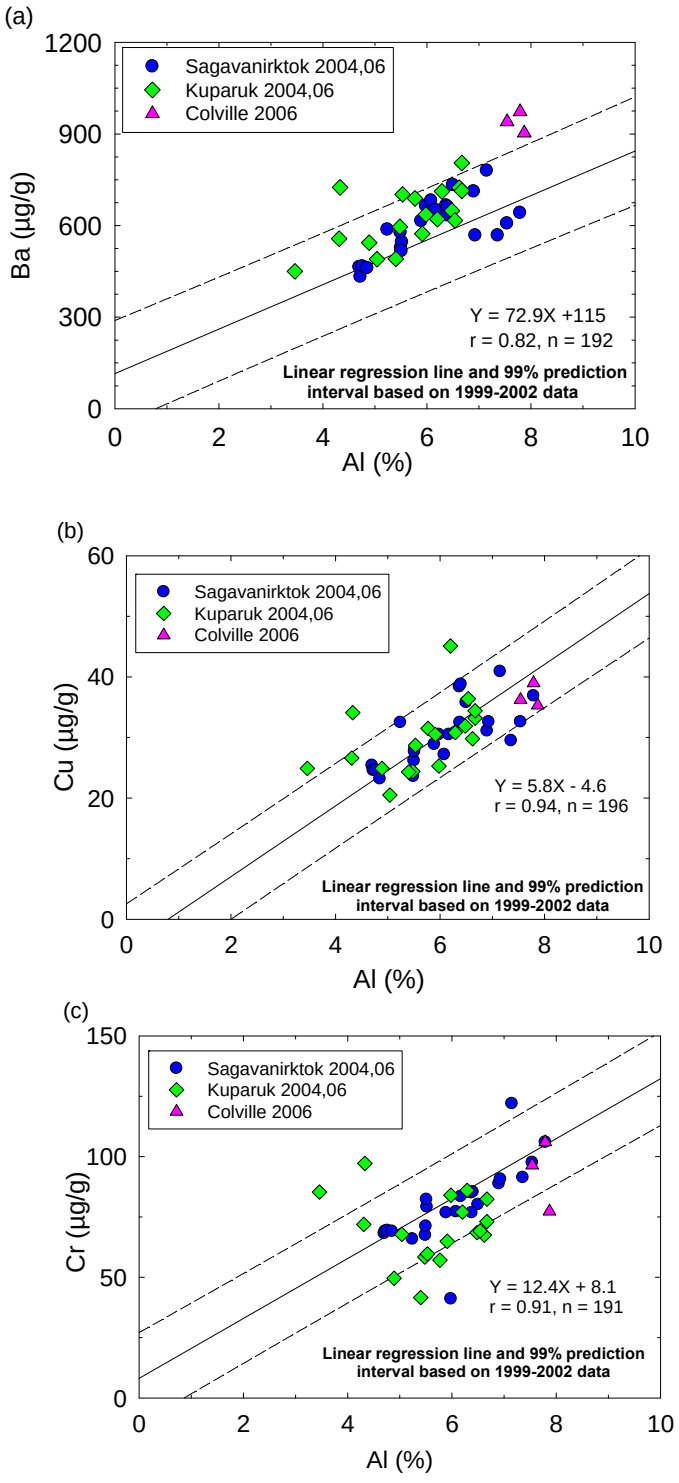

Figure 3-9. Concentrations of (a) barium (Ba), (b) copper (Cu) and (c) chromium (Cr) versus aluminum (Al) for suspended sediments from the Sagavanirktok (circles), Kuparuk (diamonds), and Colville (triangles) rivers during May-June 2004 and 2006. Solid lines are from linear regressions for sediment data from the ANIMIDA study area and dashed lines show 99% prediction intervals for sediment data.

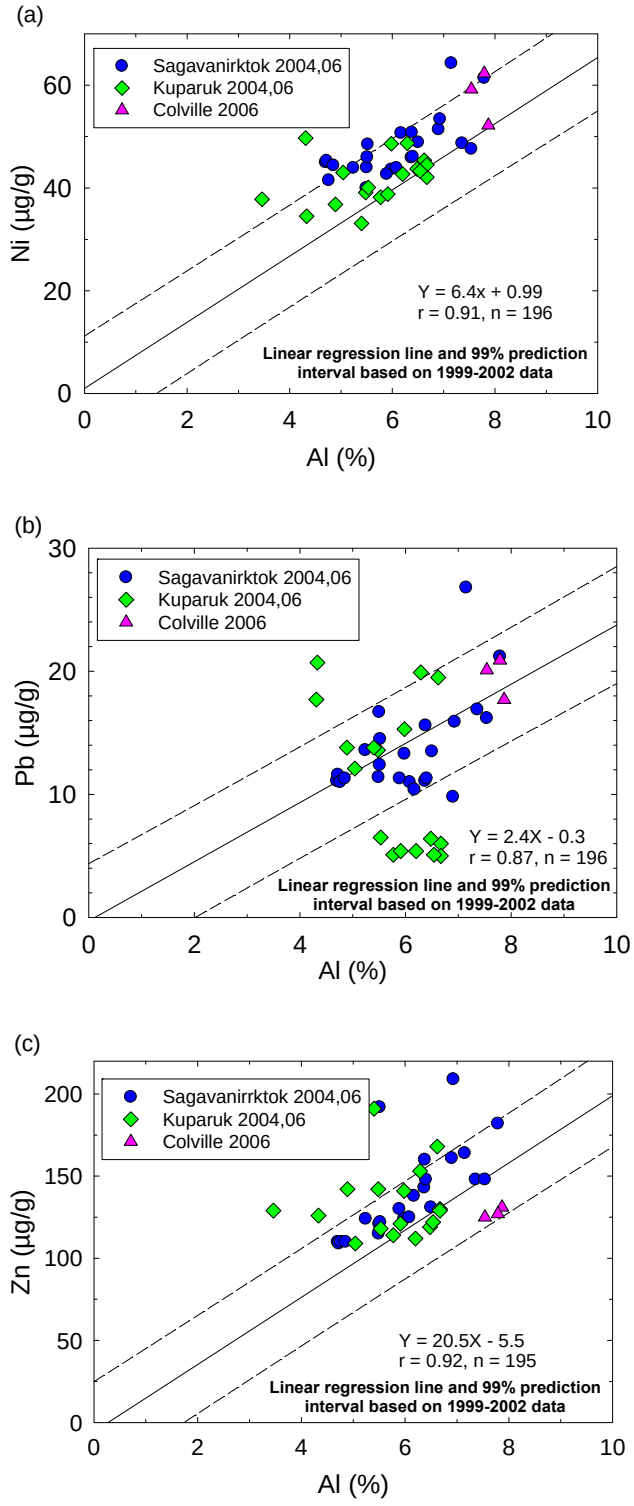

Figure 3-10. Concentrations of (a) nickel (Ni), (b) lead (Pb) and (c) zinc (Zn) versus aluminum (Al) for suspended sediments from the Sagavanirktok (circles), Kuparuk (diamonds) and Colville (triangles) rivers during May-June 2004 and 2006. Solid lines are from linear regressions for sediment data from the ANIMIDA study area and dashed lines show 99% prediction intervals for sediment data.

3.4 Dissolved Metals in River Water

Previous studies showed that concentrations of dissolved trace metals can be quite variable during the spring floods and reach maximum concentrations during peak flow (Rember and Trefry, 2004; Trefry et al., 2004b). This trend for maximum concentrations of dissolved trace metals during peak flow in spring is influenced by the discharge of soil interstitial water and shallow surface water that is diluted by snow melt and flushed from surrounding soils into the rivers. During the short summers, the arctic coastal plain is covered with pools of standing water and lakes where trace metals are leached from soils. The permafrost, along with a topography that averages <2 m on the coastal plain, inhibit lateral water flow during the summer months, thereby extending the residence time of the surface water in the system (McNamara et al., 1998). Then, after the long frozen winter (8 to 9 months), increased surface runoff in the spring provides a direct pathway for the release of accumulated and freshly leached metals into the rivers from the thawing ponds and soils.

Mean concentrations for dissolved metals in the Kuparuk, Sagavanirktok and Colville rivers during May-June 2001, 2002, 2004 and 2006, along with multi-year means for each river, are presented in Tables 3-5 and 3-6. During May-June 2004 and 2006, average concentrations of dissolved Fe (filtered at 0.4 μm) in the Sagavanirktok River were 41 and 43 μg/L, respectively, and maximum concentrations of dissolved Fe were 65 and 67 μg/L, respectively (Table 3-6, Figure 3-11a, b). Peak concentrations of dissolved Fe were generally observed within 3-7 days of peak flow (Figure 3-11a,b).

The trend of maximum concentrations of dissolved Fe during peak flow also were observed for the Kuparuk River; however, peak concentrations of dissolved Fe in the Kuparuk River were 1.7 to 3.9 times higher than found for the Sagavanirktok River (Tables 3-5 and 3-6 and Figure 3.11c). Higher concentrations of DOC and lower pH in the Kuparuk River (peak DOC of 14 mg/L and pH of 7.35) than the Sagavanirktok River (peak DOC of 9 mg/L and pH of 7.90) favor enhanced leaching and transport of dissolved Fe.

Similar trends to those observed for dissolved Fe were found for concentrations of dissolved Cu (Figure 3-12a) as well as Mn. The other trace metals listed in Tables 3-4 and 3-5 showed smaller relative variations in concentrations over the May-June sampling period during 2004 and 2006 than observed for Fe or Cu.

In contrast, concentrations of dissolved Ba and Ca varied by <10% during the May-June period in the Sagavanirktok River (Figure 3-12b,c) and the Kuparuk River (Tables 3-5 and 3-6). These observations are consistent with those of Rember and Trefry (2004) who noted that concentrations of these two elements were not enhanced by flushing from soils during peak flow.

Table 3-5. Concentrations of dissolved metals in the Kuparuk and Colville rivers during May-June for the years listed.

River		As (µg/L)	Ba (µg/L)	Ca (mg/L)	Cd (µg/L)	Cr (µg/L)	Cu (µg/L)	Fe (µg/L)	Mg (mg/L)	Mn (µg/L)	Ni (µg/L)	Pb (µg/L)	Zn (µg/L)
Kuparuk 2006 (n=10)	Mean	0.089	25.2	13.3	0.008	0.115	0.57	148	1.5	31	0.50	0.038	0.82
	Std. Dev.	± 0.028	± 19.1	± 10.2	± 0.004	± 0.022	± 0.19	± 58	± 0.9	± 28	± 0.08	± 0.013	± 0.57
	Min.	0.061	16.8	7.2	0.003	0.078	0.35	57	0.9	7	0.62	0.020	0.37
	Max.	0.153	79.3	41.6	0.013	0.152	0.99	259	3.9	94	0.36	0.062	2.37
Kuparuk 2004 (n=8)	Mean		7.0	4.4	0.014		0.21	135	0.7	26	0.20	0.011	0.35
	Std. Dev.	0.041	± 1.5	± 1.3	± 0.003	0.085	± 0.14	± 25	± 0.2	± 3	± 0.10	± 0.008	± 0.19
	Min.	(n = 1)	3.5	3.4	0.010	(n = 1)	0.05	96	0.5	21	0.11	0.003	0.16
	Max.		8.6	7.0	0.019		0.49	166	1.0	30	0.42	0.023	0.69
Kuparuk 2002 (n=19)	Mean		26.4	16.0	0.012		0.28	81	1.6	5.4	0.89	0.030	0.29
	Std. Dev.	-	± 3.9	± 4.3	± 0.012	-	± 0.12	± 51	± 0.33	± 5.5	± 0.08	± 0.013	± 0.15
	Min.		18.0	8.1	0.003		0.16	17	0.9	0.5	0.81	0.016	0.11
	Max.		31.8	21.2	0.038		0.56	172	2.0	14.6	1.0	0.066	0.64
Kuparuk 2001 (n=5)	Mean		21.9	11.3			0.77	116	1.4	9.1	1.1	0.047	0.33
	Std. Dev.	-	± 3.1	± 4.0	-	-	± 0.05	± 77	± 0.4	± 9.0	± 0.1	± 0.017	± 0.6
	Min.		18.0	6.6			0.72	47	1.0	1.1	1.0	0.022	0.27
	Max.		28.6	15.1			0.86	232	1.8	20.7	1.2	0.060	0.41
Colville 2001 (n=5)	Mean		51.1	9.7			2.1	131	2.9	34	2.0	0.081	0.20
	Std. Dev.	-	± 3.1	± 2.8	-	-	± 0.5	± 102	± 0.8	± 21	± 0.2	± 0.038	± 0.11
	Min.		46.7	5.7			1.5	60	1.8	10	1.7	0.053	0.12
	Max.		54.0	11.9			2.7	282	3.6	53	2.3	0.124	0.33
Colville 2006 (n=2)	Mean	0.137	48.3	8.9	0.008	0.116	2.1	166	2.3	9.2	1.18	0.039	0.38
	Std. Dev.	± 0.031	± 3.0	± 1.0	± 0.002	± 0.008	± 0.3	± 33	± 0.3	± 1.3	± 0.02		± 0.12
	Min.	0.115	46.2	8.2	0.007	0.111	1.9	143	2.1	8.3	1.17	0.039	0.30
	Max.	0.159	50.4	9.6	0.010	0.122	2.4	189	2.5	10.2	1.20	0.039	0.47

Table 3-6. Concentrations of dissolved metals in the Sagavanirktok River and averages for the Kuparuk, Colville and Sagavanirktok rivers during May-June for the years listed.

River		As (µg/L)	Ba (µg/L)	Ca (mg/L)	Cd (µg/L)	Cr (µg/L)	Cu (µg/L)	Fe (µg/L)	Mg (mg/L)	Mn (µg/L)	Ni (µg/L)	Pb (µg/L)	Zn (µg/L)
Sagavanirktok 2006 (n=12)	Mean	0.069	25.2	29.0	0.012	0.147	0.79	43	4.4	11.0	0.54	0.031	1.0
	Std. Dev.	± 0.016	± 1.9	± 2.7	± 0.004	± 0.027	± 0.38	± 13	± 0.8	± 3.5	± 0.11	± 0.006	± 1.0
	Min.	0.054	22.6	25.4	0.007	0.118	0.46	27	3.3	5.2	0.42	0.021	0.3
	Max.	0.108	28.0	32.6	0.016	0.206	1.6	67	5.5	17.3	0.82	0.039	3.6
Sagavanirktok 2004 (n=9)	Mean	0.068	19.0	22.4	0.018	0.096	0.50	41	3.4	10.8	0.43	0.013	0.28
	Std. Dev.	± 0.015	± 1.8	± 1.9	± 0.006	± 0.010	± 0.17	± 19	± 0.6	± 2.4	± 0.08	± 0.006	± 0.08
	Min.	0.048	16.1	20.3	0.010	0.080	0.34	14	2.6	7.9	0.33	0.007	0.19
	Max.	0.086	22.6	25.5	0.025	0.110	0.88	65	4.4	15.1	0.53	0.023	0.40
Sagavanirktok 2002 (n=21)	Mean	-	29.9	33.3	0.015	-	0.34	31	1.1	8.8	0.82	0.017	0.22
	Std. Dev.		± 2.1	± 3.9	± 0.019		± 0.16	± 29	± 0.1	± 5.8	± 0.11	± 0.010	± 0.17
	Min.		25.8	24.1	0.006		0.06	4	1.0	1.3	0.68	0.006	0.03
	Max.		33.5	37.0	0.062		0.59	101	1.2	20.2	1.0	0.040	0.63
Sagavanirktok 2001 (n =22)	Mean	-	31.7	26.7	-	-	0.56	22	5.4	9.2	1.08	0.018	0.16
	Std. Dev.		± 2.0	± 3.7			± 0.26	± 23	± 1.4	± 4.9	± 0.13	± 0.012	± 0.08
	Min.		27.4	21.2			0.23	2.8	3.2	2.9	0.79	0.008	0.08
	Max.		35.1	32.6			0.96	72	7.2	18.2	1.27	0.040	0.31
Kuparuk 2001-2, 2004, 2006	**Mean**	**0.065**	**20.1**	**11.2**	**0.011**	**0.10**	**0.46**	**120**	**1.3**	**18**	**0.7**	**0.032**	**0.45**
	Min.	0.041	3.5	3.4	0.003	0.08	0.05	17	0.5	0.5	0.1	0.003	0.11
	Max.	0.153	79.3	41.6	0.038	0.15	0.99	259	3.9	94	1.2	0.066	2.37
Colville 2001, 2006	**Mean**	**0.14**	**50**	**9.3**	**0.008**	**0.12**	**2.1**	**148**	**2.6**	**22**	**1.6**	**0.060**	**0.29**
	Min.	0.12	46	5.7	0.007	0.11	1.5	60	1.8	8	1.2	0.039	0.12
	Max.	0.16	54	11.9	0.010	0.12	2.7	282	3.6	53	2.3	0.124	0.47
Sagavanirktok 2001-2, 2004, 2006	**Mean**	**0.068**	**26.4**	**27.8**	**0.015**	**0.122**	**0.55**	**34**	**3.6**	**10.0**	**0.72**	**0.020**	**0.42**
	Min.	**0.050**	16.1	20.3	0.006	0.080	0.06	**4**	1.0	1.3	0.33	0.006	0.03
	Max.	**0.110**	35.1	37.0	0.062	0.206	1.6	**101**	7.2	20.2	1.27	0.040	3.6

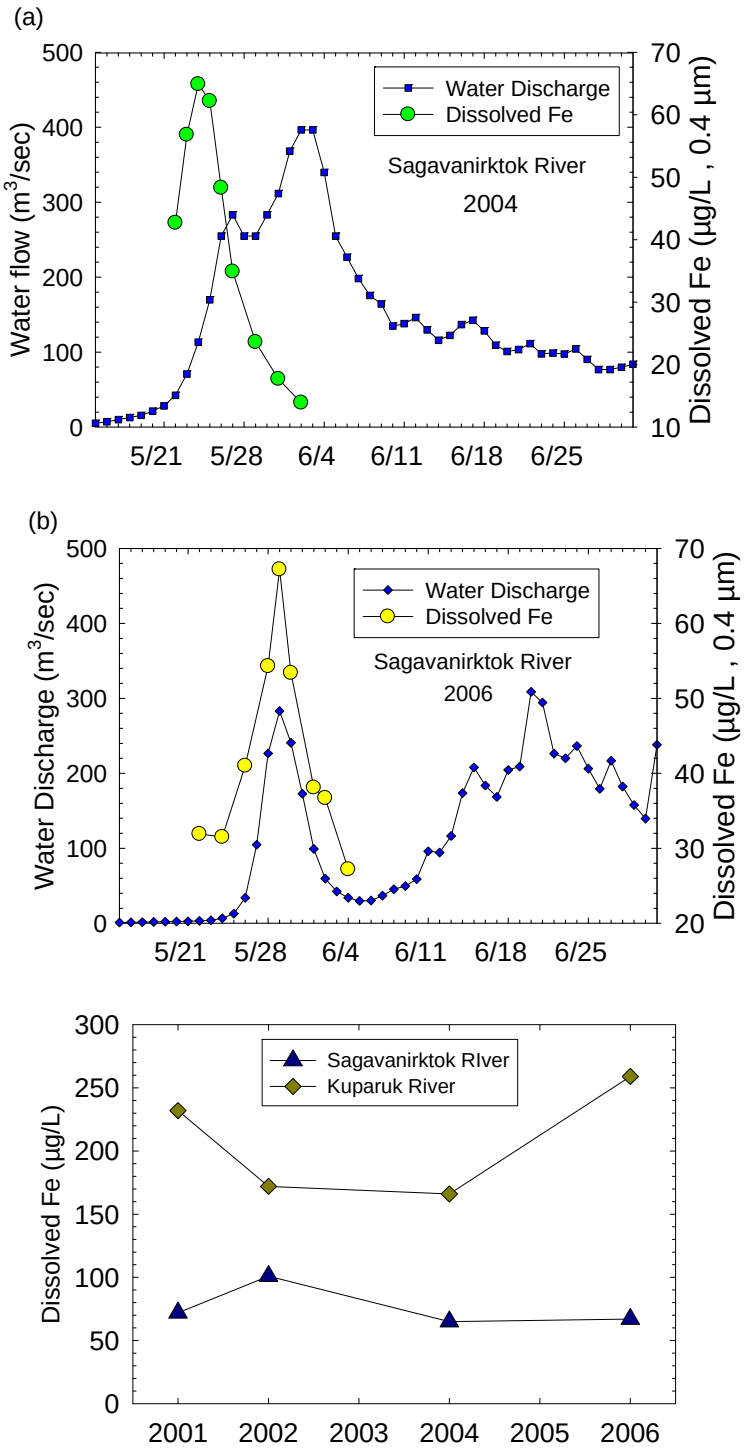

Figure 3-11. Concentrations of dissolved Fe (0.4 µm pore size membrane filter) and water discharge in (a) the Sagavanirktok River for May-June 2004 and (b) 2006 and (c) peak concentrations of dissolved Fe (0.4 µm pore size membrane filter) in the Sagavanirktok and Kuparuk rivers for May-June 2001, 2002, 2004 and 2006.

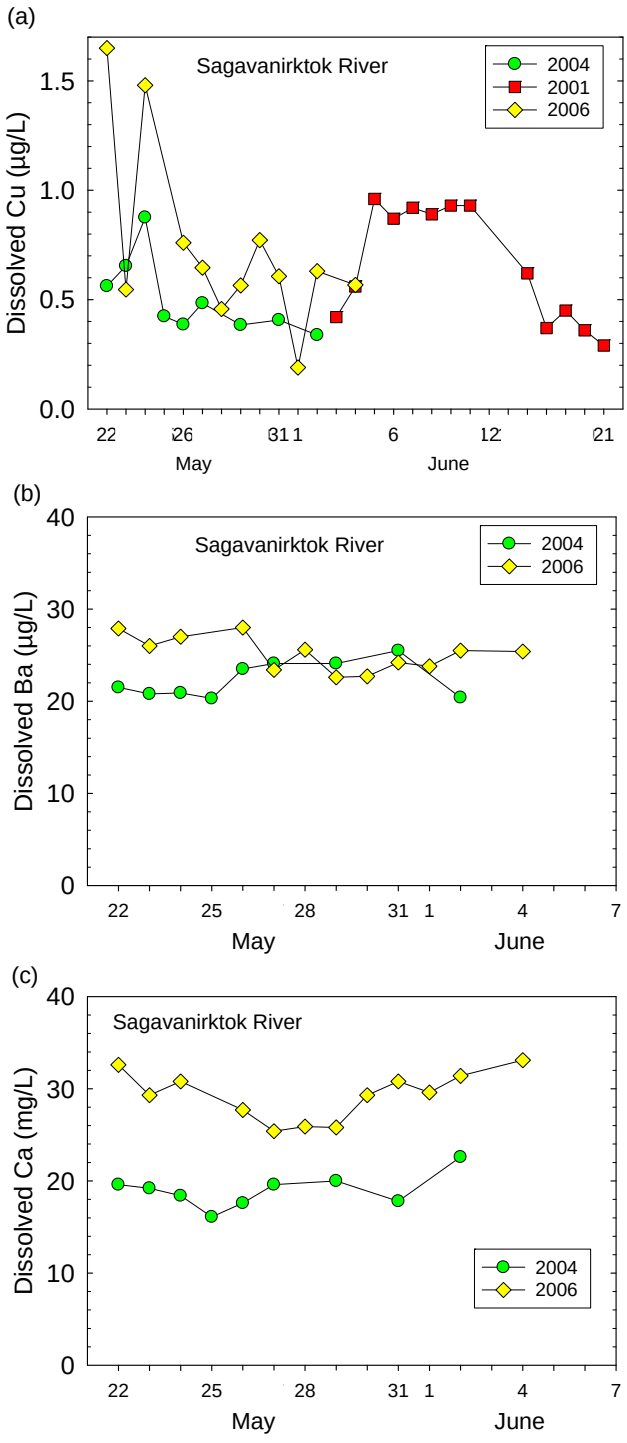

Figure 3-12. Concentrations of (a) dissolved copper (Cu), (b) dissolved barium (Ba) and (c) dissolved calcium (Ca) in the Sagavanirktok River for May-June of 2004 and 2006.

4. PARTITIONING OF METALS BETWEEN PARTICULATE AND DISSOLVED PHASES IN RIVER WATER

The chemical forms of metals in rivers and coastal seawater are an important component for understanding chemical reactions and biological uptake of metals. Values for the percent of total metal (dissolved + particulate) per liter that was dissolved (passed through a 0.4 μm filter) varied considerably among the different metals (Table 4-1). In the Sagavanirktok River during the cANIMIDA Project (2004 and 2006), the following ranges were found:

<10% dissolved/liter	As, Cr, Fe, Pb, Zn
10-30% dissolved/liter	Cd, Cu, K, Mn, Ni
30-50% dissolved/liter	Ba
70-80% dissolved/liter	Ca, Mg, Na

The trends for percent of total metal that was dissolved were similar for the Colville River (2006) and for the Kuparuk River in 2004 (Table 4-1). In 2006, the lower values for TSS and the longer period of peak flow of water for the Kuparuk river yielded higher values for % dissolved metal than observed during 2004 (Table 4-1). Although considerably variability was observed for the percent of total river-borne metal that was dissolved, the trends in values from this study are generally similar to those reported by Martin and Meybeck (1979) for average world rivers (Table 4-1).

A simple distribution coefficient (K_d) has been used to provide one perspective on metal partitioning between particulate and dissolved phases. As an example, concentrations of dissolved and particulate Ba varied by a factor of 2 to 3 among rivers (Figure 4-1). However, concentrations of dissolved Ba varied in proportion to concentrations of particulate Ba (Figure 4-1). Therefore, a K_d can be used to model the behavior of dissolved and particulate Ba during the spring samples of river water. Distribution coefficients were calculated in this study using

$$K_d = \frac{\text{(concentration of particulate metal in μg metal/g particles)}}{\text{(concentration of dissolved metal in μg metal/g water)}}$$

where the conceptual perspective is shown below by considering that dissolved Ba^{2+} can adsorb and desorb from suspended particles in a predictable manner.

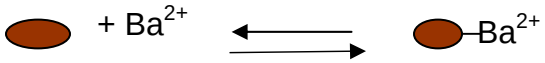

Despite significant differences in concentrations of dissolved and particulate Ba among rivers, the K_d values calculated for Ba were statistically equal (t-test, $\alpha = 0.05$), with the following average for all samples collected from the Sagavanirktok River (where $K_d = 2.3 \pm 0.3 \times 10^4$ or average $\log K_d = 4.36$), Kuparuk River ($2.6 \pm 0.5 \times 10^4$, $\log K_d = 4.42$) and Colville River ($2.1 \pm 0.4 \times 10^4$, $\log K_d = 4.32$; Figure 4-1). These results suggest that partitioning of Ba between dissolved and particulate phases is a quasi-equilibrium

Table 4-1. Means and standard deviations (SD) for percent of total metal in rivers that was dissolved during May-June for the years listed.

River		As (%)	Ba (%)	Ca (%)	Cd (%)	Cr (%)	Cu (%)	Fe (%)	K (%)	Mg (%)	Mn (%)	Ni (%)	Pb (%)	Zn (%)
Sagavanirktok 2006 (n=12)	Mean ±SD	12.8 ± 12.6	37.9 ± 19.7	76.1 ± 19.2	26.5 ± 19.5	3.0 ± 2.8	27.3 ± 16.9	2.3 ± 1.7	35.6 ± 17.7	77.7 ± 16.1	22.8 ± 15.3	15.2 ± 11.9	3.1 ± 2.0	9.9 ± 10.2
Sagavanirktok 2004 (n=9)	Mean ±SD	6.6 ± 3.1	23.0 ± 8.1	73.1 ± 10.8	22.7 ± 11.8	1.4 ± 0.7	14.0 ± 5.2	1.3 ± 0.9	19.9 ± 8.1	74.1 ± 11.0	15.2 ± 6.5	9.2 ± 5.0	1.4 ± 1.5	2.3 ± 1.6
Kuparuk 2006 (n=10)	Mean ±SD	41.8 ± 24.4	62.5 ± 23.5	97.6 ± 2.0	44.4 ± 22.3	10.2 ± 7.3	51.9 ± 18.7	19.3 ± 13.0	75.6 ± 15.1	85.9 ± 12.1	52.7 ± 25.8	40.5 ± 20.9	11.8 ± 6.7	25.5 ± 20.2
Kuparuk 2004 (n=8)	Mean ±SD	14.2 (n=1)	16.5 ± 7.0	90.9 ± 3.3	38.7 ± 12.2	2.0 (n=1)	9.3 ± 4.1	6.1 ± 3.0	41.5 ± 11.9	62.4 ± 11.9	35.9 ± 11.6	8.2 ± 4.0	3.6 ± 2.3	5.3 ± 3.0
Colville 2006 (n=2)	Mean ±SD	1.7 ± 0.3	6.4 ± 0.4	-	2.6 ± 0.7	0.2 ± 0	7.2 ± 1.2	-	-	-	-	–	0.3 ± 0	0.4 ± 0.1
World Rivers[1]	-	44	19	62	-	2.5	19	0.2	14	40	2	5	2	17

[1]Martin and Meybeck (1979).

Table 4-2. Distribution coefficients (log K_d)[a] for metals in rivers during May-June for the years listed.

River		As	Ba	Ca	Cd	Cr	Cu	Fe	K	Mg	Mn	Ni	Pb	Zn
Sagavanirktok 2006 (n=12)	Mean ±SD	5.11 ± 0.11	4.36 ± 0.08	3.33 ± 0.33	4.68 ± 0.15	5.78 ± 0.13	4.62 ± 0.20	5.61 ± 1.15	4.32 ± 0.35	3.37 ± 0.34	4.75 ± 0.17	4.98 ± 0.10	5.71 ± 0.17	5.32 ± 0.29
Sagavanirktok 2004 (n=9)	Mean ±SD	5.20 ± 0.20	4.55 ± 0.04	3.53 ± 0.05	4.58 ± 0.12	5.89 ± 0.11	4.82 ± 0.18	5.99 ± 0.24	4.64 ± 0.11	3.52 ± 0.08	4.78 ± 0.11	5.04 ± 0.08	5.99 ± 0.22	5.71 ± 0.10
Kuparuk 2006 (n=10)	Mean ±SD	4.91 ± 0.21	4.44 ± 0.19	2.96 ± 0.11	4.85 ± 0.24	5.80 ± 0.15	4.70 ± 0.13	5.45 ± 0.18	4.16 ± 0.12	3.75 ± 0.21	4.63 ± 0.41	4.94 ± 0.07	5.68 ± 0.19	5.33 ± 0.24
Kuparuk 2004 (n=8)	Mean ±SD	4.99	5.01 ± 0.10	3.25 ± 0.09	4.48 ± 0.15	5.90	5.32 ± 0.35	5.50 ± 0.10	4.43 ± 0.08	4.04 ± 0.10	4.54 ± 0.08	5.37 ± 0.22	5.81 ± 0.34	5.61 ± 0.23
Colville 2006 (n=2)	Mean ±SD	4.89 ± 0.10	4.29 ± 0.01	2.95 ± 0.03	4.70 ± 0.11	5.88 ± 0.04	4.25 ± 0.06	5.47 ± 0.06	4.24 ± 0	3.75 ± 0.02	5.05 ± 0.04	4.68 ± 0.03	5.70 ± 0.04	5.55 ± 0.15

$$^{a}K_d = \frac{\text{(Concentration of particulate metal in µg metal/g particles)}}{\text{(concentration of dissolved metal in µg metal/g water)}}$$

controlled process between free Ba^{2+} and suspended particles. Considering the large variations in water discharge, TSS, and concentrations of organic carbon, the apparent uniformity of the distribution coefficients for Ba indicates that discharge, TSS and organic carbon have little impact on the partitioning of Ba between dissolved and particulate phases.

Values for K_d also were calculated using the equation shown below that includes concentrations of TSS; however, no significant differences were found between the two K_ds for any metals (data in Appendices).

$$K_d = \frac{\text{(Concentration of particulate metal in µg metal/g particles)}}{\text{(concentration of dissolved metal in µg metal/g water)}} \text{ x } \frac{1}{\text{TSS (in g/mL)}}$$

The broader implication of these results for the biogeochemistry of Ba and other metals in rivers is potentially important. Do concentrations of particulate and dissolved Ba in other rivers follow similar behavior? Unfortunately, investigators have seldom determined both particulate and dissolved Ba concentrations for the same sample in rivers and the only data identified to date are for concentrations of particulate and dissolved Ba

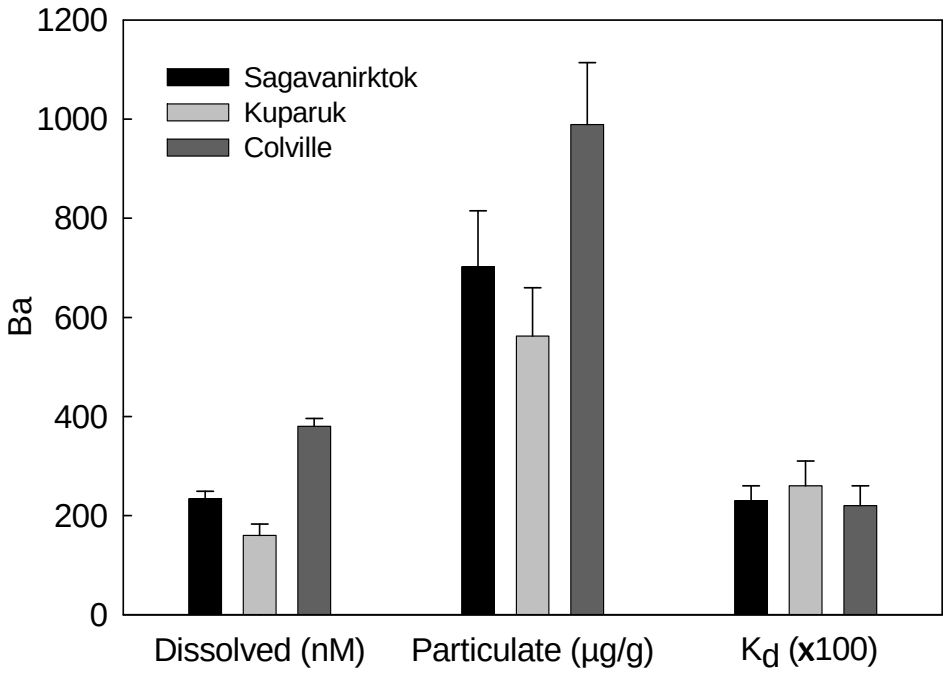

Figure 4-1. Average concentrations of dissolved and particulate barium (Ba) and distribution coefficients (K_d) for Ba in the Sagavanirktok, Kuparuk and Colville rivers.

from another northern Alaskan River, the Kuskokwim River (Wang, 1999), the average K_d based on 5 samples was $2.6 \pm 0.6 \times 10^4$ ($\log K_d = 4.42$). These preliminary results suggest that differences between the North American and Eurasian concentrations for dissolved Ba such as those found by Guay and Falkner (1998) are linked to geology by being dependent upon the Ba concentrations of river particles and thus the mineralogy of the drainage basin.

The use of a K_d is more complicated in rivers and seawater when concentrations of DOC change. For example, increased concentrations of dissolved Cu, Pb, and Zn in rivers during peak discharge occur despite relatively constant concentrations of particulate metals. These results suggest that a K_d is less likely to explain dissolved concentrations of these metals. During peak discharge, K_d values ($\times 10^4$) for Cu (4.4), Pb (116) and Zn (67) were 40 to 50% lower than during off-peak discharge in the Sagavanirktok River. In contrast, concentrations of DOC were ~40% greater during peak discharge. Strong correlations between dissolved metals and DOC suggest that elevated concentrations of organic ligands during peak discharge alter partitioning of Cu, Pb and Zn between dissolved and particulate phases. Thus, K_d values, are potentially more useful in low or more uniform DOC riverine environments. Results from previous studies in rivers have shown that distribution coefficients for Cu, Pb and Zn often have order-of-magnitude differences where a large fraction of the variance can be explained by concentrations of DOC (Shafer et al., 1999).

5. DISPERSION OF RIVER WATER, SEDIMENTS AND CHEMICALS UNDER ICE IN THE BEAUFORT SEA

5.1 Overview

The high water flow from rivers during the spring floods is carried to a Beaufort Sea that is covered with ~2-m thick, land-fast ice. Thus, the river water flows out above and below the ice. The fresh and relatively warm (slightly >0° C) discharge from the rivers flows out onto and then under the land-fast ice where it mixes with the colder marine waters (-1.8° C) forming a 1-2 m thick under-ice lens of brackish waters that can extend >15 km offshore. This under-ice mixing takes place in the absence of wind and wave effects and sets the stage for the estuarine conditions and stratification that dominate nearshore regions during the early to mid open-water time period. Furthermore, river water that is not advected off the shelf can retain its distinct geochemical signature and move with the local circulation (Granskog et al., 2005; Weingartner et al., 1999).

The main objectives of the under-ice tracking of river water during the spring melt were to identify general flow patterns and behavior of freshwater, dissolved and particulate chemicals, and potential contaminants from the Sagavanirktok and Kuparuk rivers. This information can be used to help predict dispersion patterns for freshwater, suspended sediments, dissolved chemicals and potential contaminants originating from activities on the North Slope of Alaska. The under-ice movement of freshwater plumes is an important component of potential spill trajectories as well as biogeochemical models during the period of maximum river discharge when these plumes provide a means for offshore transport of potential contaminants.

The 2004 study was designed to take a broad look at under-ice flow over a large area between the Sagavanirktok and Kuparuk rivers with sampling at 28 stations. During 2006, sampling was focused at 15 stations along three transects, two from the Kuparuk River and one from the Sagavanirktok River, all of which were along the main flow path of the respective rivers as determined during the 2004 study. Replicate sampling was carried out at several stations each year to examine the time history of change over the breakup time period at select locations as well as changes along transects extending offshore. Sampling consisted of collecting water samples, hydrographic profiles, under-ice currents, ice cores, and snow samples. In addition, time series measurements of temperature, conductivity, and turbidity were collected from ice-mounted moorings at five locations during the spring of 2006. Hydrographic profiles and/or water samples were analyzed for TSS, pH, temperature, conductivity (salinity), turbidity, transmissivity, dissolved and particulate metals, nutrients, and a suite of other constituents. Data presented in this report focus on results from 2004 and 2006.

Electronic instrumentation used during the 2004 and 2006 cANIMIDA study included a Seabird SEACAT SBE-19 CTD equipped with temperature, conductivity, pressure, and transmissivity sensors, an Aanderaa real-time current profiling system, and YSI SONDE recorders that were equipped with temperature, conductivity, pressure, and turbidity that were used for both profiling and time series measurements. As previously stated, water

samples were collected with a non-contaminating peristaltic pump and Teflon weighted sampling hose and ice cores were collected with a 4-inch diameter stainless steel Sipre corer. On-ice logistics were accomplished with two snowmobiles equipped with freight sleds for transporting personnel and equipment to the sampling sites from the Prudhoe Bay STP located at the terminus of the West Dock Causeway.

During the breakup of the Kuparuk and Sagavanirktok Rivers, river water initially flowed out over the bottom-fast ice before encountering ice cracks, seal holes, and other breaks in the ice surface that allowed most of the river water to make its way through and under the ice canopy. Typically, over-ice flow extended 5 to 10 km from the river mouths and would sometimes recede after finding passages down through the ice, whereas the under-ice plume of mixed river water was transported up to 15 to 20 km offshore before encountering offshore barrier islands or the shear zone. As will be shown below, at least 50% of the total flow of the Sagavanirktok River during the study period could be accounted for as being under ice within the somewhat limited area that was sampled.

5.2 Dispersion of River Water Under Ice in the Beaufort Sea during Spring 2004

River water flow began in both rivers on May 20, 2004. River water, seawater, and ice cores were collected from May 23 to June 2, 2004 during the landfast ice period while rivers were at high flow. As previously described, river water was sampled daily and seawater was collected over a nine-day period through holes drilled in the ice at 28 stations (Figure 5-1 and Table 5-1). Vertical profiles of salinity, temperature and turbidity also were obtained at each location. Sampling through the ice was limited to nine days by the time of onset of the floods, weather conditions, and accessibility when nearshore areas flooded above the ice.

Three aerial photographs are shown to help provide a better perspective of the sampling area. Figure 5-2 shows a view looking north with water flow from the Kuparuk River moving across the shallow water (1-2 m deep) inside the barrier islands (e.g., Stump Island). Then, the flow from the Kuparuk River moved north adjacent to the causeway at West Dock (STP and Pt. McIntyre), under an ice road to Northstar Island and out into the coastal Beaufort Sea. Four sampling stations that were part of the SK transect are shown in the upper part of the photo. The ice at these stations was 1.7 to 2.0 m thick (Table 5-1). The K transect is west of the area shown on Figure 5-2, but is shown on Figure 5-1. Without the causeway at West Dock, sampling at offshore locations would not have been possible with snow machines because ice along the coast was flooded.

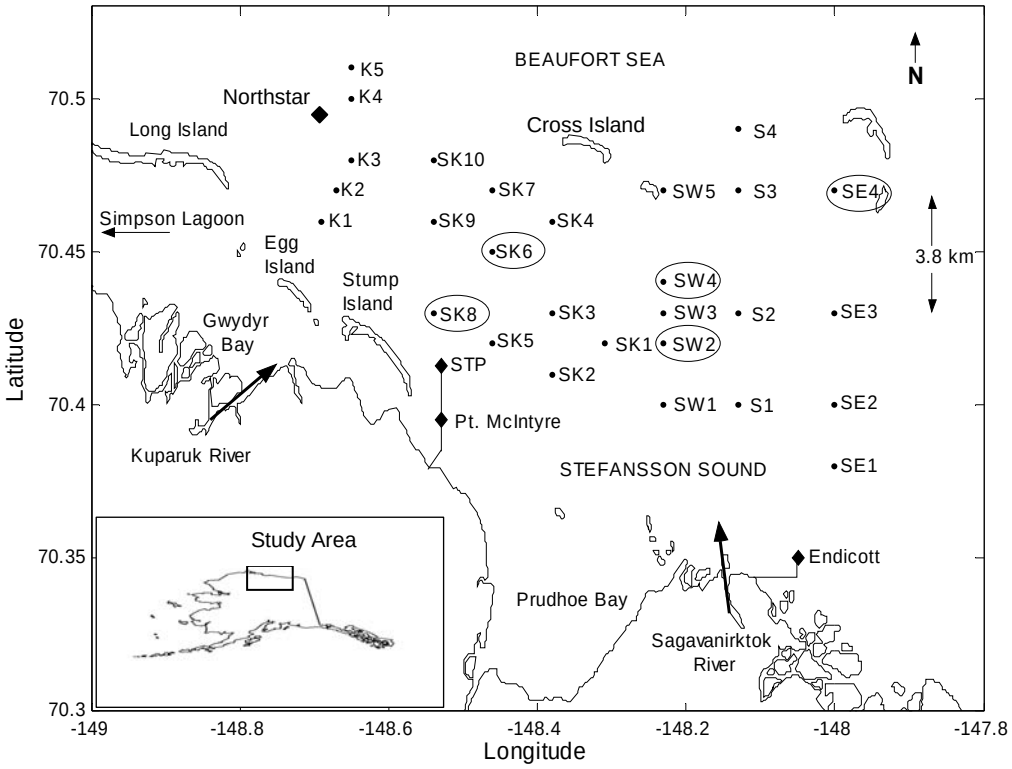

Figure 5-1. Sampling sites in Stefannsson Sound with inset map of Alaska showing study area during May-June 2004. Causeways connecting the Seawater Treatment Plant (STP), Pt. McIntyre, and Endicott Island to shore are shown by the solid lines. Stations numbers in ovals identify locations where ice cores also were collected. Arrows show approximate direction of primary river outflow. Map of coastline from the NGDC [2005].

Table 5-1. Coordinates, sampling dates, total depths, and ice thickness for water stations occupied during May-June 2004.

Station	Latitude (N)	Longitude (W)	Sample Date	Total Depth (m)	Ice Thickness (m)
SE1	70°22.97'	147°59.99'	May 27	4.2	1.9
SE2	70°24.00'	147°59.98'	May 27	4.6	1.7
SE3	70°26.00'	148°00.00'	May 27	4.9	2.4
SE4	70°28.00'	148°00.00'	May 27	3.8	1.9
S1	70°24.00'	148°08.00'	May 27,31	3.2	1.9
S2	70°25.86'	148°08.00'	May 31	4.8	1.8
S3	70°28.00'	148°08.00'	May 31	4.0	1.9
S4	70°29.60'	148°08.03'	May 31	9.1	1.9
SW1	70°24.23'	148°13.98'	May 25	2.3	1.9
SW2	70°25.00'	148°13.98'	May 25,28	3.2	1.9
SW3	70°25.79'	148°13.96'	May 25	5.0	1.8
SW4	70°26.59'	148°13.97'	May 25,28,31	6.3	1.9
SW5	70°28.19'	148°13.93'	May 28	2.3	2.0
SK1	70°25.00'	148°18.80'	May 25,28	2.0	2.2
SK2	70°24.49'	148°22.97'	May 30	1.2	2.0
SK3	70°25.83'	148°22.98'	May 28	4.6	1.9
SK4	70°27.45'	148°22.99'	May 30	5.5	2.0
SK5	70°25.12'	148°27.64'	May 30	2.9	2.0
SK6	70°26.75'	148°27.65'	May 29, June 2	3.2	1.9
SK7	70°28.36'	148°27.65'	May 30	5.1	1.9
SK8	70°25.60'	148°32.50'	May 30, June 2	3.2	1.9
SK9	70°27.72'	148°32.50'	May 29	7.0	1.9
SK10	70°29.04'	148°32.46'	May 30	7.7	1.7
K1	70°27.66'	148°41.29'	May 23	5.1	1.9
K2	70°28.32'	148°40.07'	May 23	7.3	1.9
K3	70°29.00'	148°38.78'	May 24,29	8.7	1.8
K4	70°29.80'	148°38.74'	May 29	10.0	1.9
K5	70°30.60'	148°38.89'	May 29	11.0	1.9

Figure 5-2. Aerial photograph with view to the north showing the spring outflow from the Kuparuk River. Approximate locations of selected stations are shown on the photograph for orientation and perspective. K transect was to the west.

Figure 5-3 shows a view looking south from the STP across the incoming flow from the Kuparuk River to the drainage basin of the river. Some ponds in the drainage basin were still frozen; however, a considerable amount of snow-free ground can be seen in the photograph.

An aerial view of the Sagavanirktok River delta (Figure 5-4) shows the main channel of the river with any flow that might be transported to the east being forced northward by the causeway to Endicott Island. The clear demarcation between ice and water on the upper right-hand portion of the figure is along a causeway. The approximate locations of some nearshore stations along the SK, SW, S and SE transects are shown on the photograph (Figure 5-4) for comparison with the more complete map of sampling stations in Figure 5-1.

One objective of the under-ice study was to trace the dispersion of freshwater and the second was to track the mixing and movement of suspended sediments and dissolved chemicals. A representative set of salinity and temperature profiles for the Kuparuk River (K) Transect (stations K1, K3 and K4) shows the sharp vertical pycnocline due to the flow of river water under the ice and above seawater (Figure 5-5). The profiles also show increasing salinity in the surface water with increasing distance offshore. No detectable

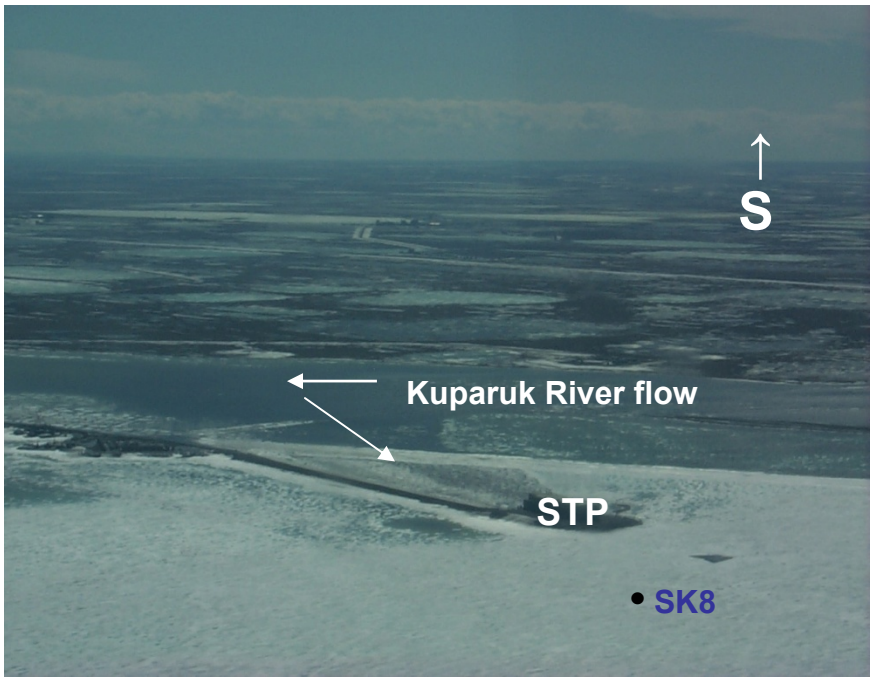

Figure 5-3. Aerial photograph with view to the south showing the spring outflow from the Kuparuk River. The approximate location of station SK8 is shown on the photograph for orientation and perspective.

Figure 5-4. Aerial photograph with view to the north showing the spring outflow from the Sagavanirktok River. The approximate locations of selected stations are shown on the photograph for orientation and perspective.

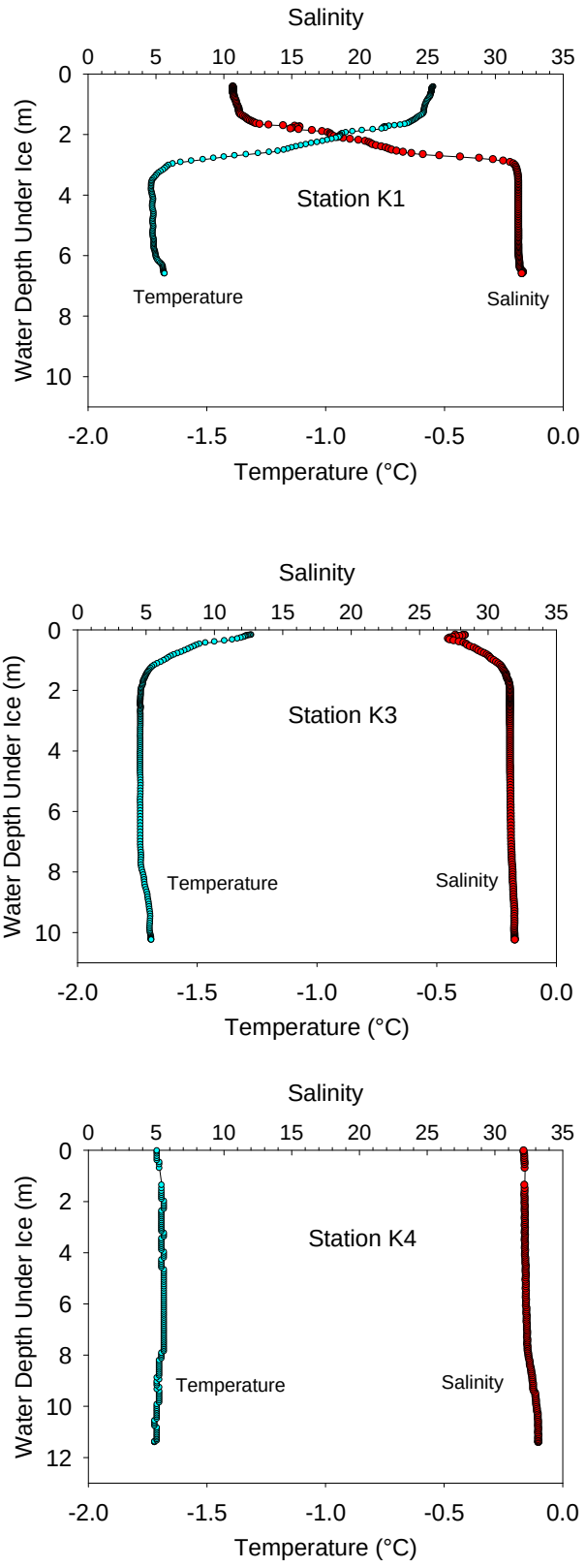

Figure 5-5. Vertical profiles for salinity and temperature for stations K1, K3 on May 23, 2004 and station K4 on May 29, 2004, all located offshore of the mouth of the Kuparuk River.

fraction of river water was detected at station K4, even near the end of the sampling period on May 29 (Figure 5-5).

Another example of temporal shifts in salinity can be seen with data from station SW4 at the mouth of the Sagavanirktok River (Figure 5-6). Over just six days, the salinity in the surface water decreased from ~18 to 5 and the width (thickness) of the pycnocline increased by ~2 m (Figure 5-6). Vertical profiles for salinity and temperature are available for all stations in papers and appendices provided with the attached CD.

In 2004, strong haloclines and thermoclines were observed near the mouth of the Sagavanirktok River at Stations SE0 and SE1 (Figure 5-7). River water mixed along a frontal zone as the under-ice plume extended offshore to stations SE2 and SE3 (Figure 5-7). Turbidity in the under-ice river plume decreased with distance from the river mouth as shown for the transect from nearshore station SE0 to offshore station SE3 in Figure 5-7. This trend is consistent with data for TSS (in Section 5.3) that show settling of suspended sediments from the water column. The influence of runoff from both the Kuparuk and Sagavanirktok rivers extended >15 km from their respective mouths where the under-ice plume encountered the barrier islands and the shear zone offshore of Northstar and Cross Islands (see Figure 5-1 for map on page 45). Horizontal contour maps of temperature, salinity and turbidity at a depth of 2 m (~0.5 m below the ice canopy) show the under-ice plume extending well offshore (Figure 5-8). In contrast, turbidity was found to decrease from nearshore to offshore as suspended sediments settled from the water column (Figure 5-8). The under-ice plume associated with the Sagavanirktok River had much higher concentrations of suspended sediments than the Kuparuk River as show with the turbidity data in Figure 5-8c.

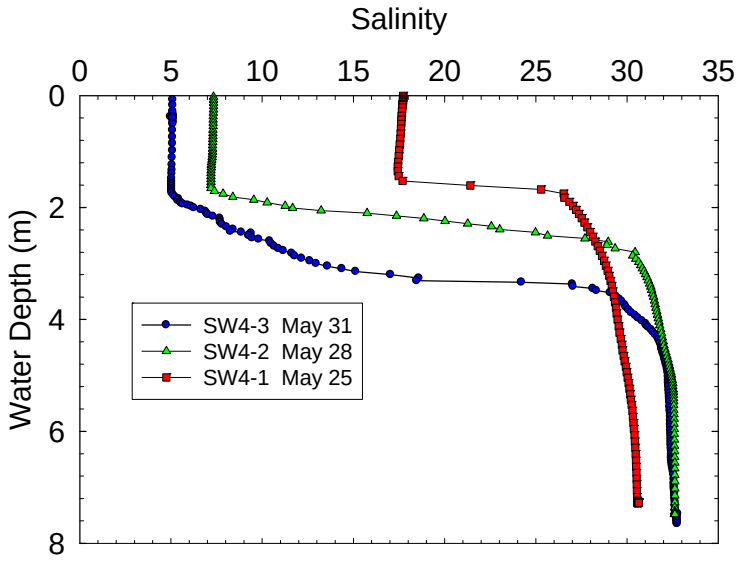

Figure 5-6. Vertical profiles of salinity for station SW4 on May 25, May 28 and May 31, 2004.

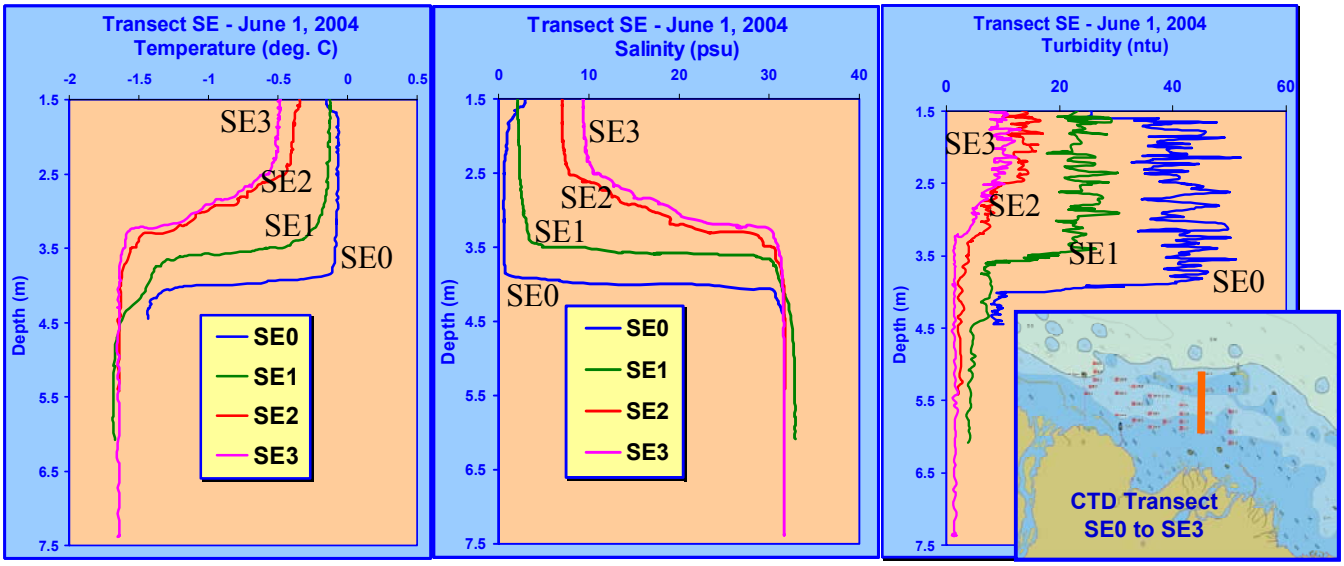

Figure 5-7. Under-ice vertical profiles of temperature, salinity, and turbidity taken along the SE transect starting near the bottom-fast ice zone and extending offshore beyond the barrier islands just south of the offshore shear zone, 1 June 2004.

Using only temperature and salinity, the relative contributions and dispersion patterns of freshwater to the coastal Beaufort Sea from the two river sources could not be distinguished. Distinct differences in turbidity patterns at the mouths of the two rivers were observed (e.g., Figure 5-8c) due to the higher suspended sediment load of the Sagavanirktok River; however, the behavior of the TSS during mixing was non-conservative and thus turbidity was not useful for following the seaward progression of freshwater from the two rivers. Two additional variables, $\delta^{18}O$ and dissolved silica, did prove to be useful tracers for the two rivers and were used to determine the relative amounts of river water, seawater and sea ice melt at each station as described in the cANIMIDA paper by Alkire and Trefry (2006) and summarized below.

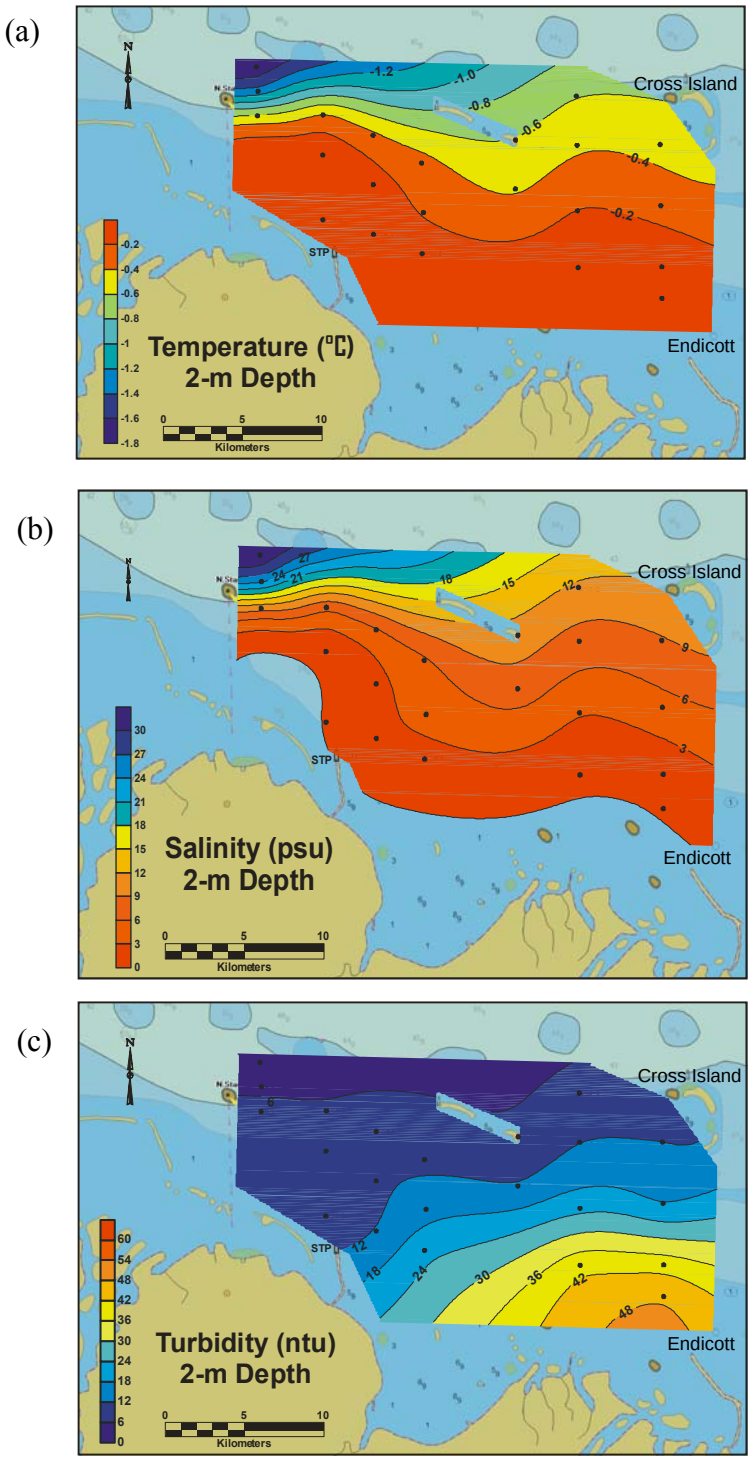

Figure 5-8. Under-ice horizontal contour maps of temperature, salinity and turbidity isoclines at 2-m water depth (~0.5 m below the ice canopy) that depicts flow from both the Sagavanirktok and Kuparuk Rivers, 1 June 2004.

Three tracers, salinity, $\delta^{18}O$ and dissolved silica, provided distinct geochemical fingerprints that were used to calculate the relative contributions of four water masses, Sagavanirktok River (SR), Kuparuk River (KR), Sea Ice Melt (SIM) and Polar Mixed Layer (PML), to individual water samples and to trace the under-ice dispersion of freshwater. Some background perspective on use of $\delta^{18}O$ and silica as tracers is provided below. Temperature was excluded as a tracer due to the small range between end-members (-1.8°C in seawater to 0.5°C in river water), daily variations in rivers (0.1 to 0.5°C), and solar heating of surface waters, as observed by Macdonald et al. (1989). In addition, errors with the OMP calculations increased significantly when temperature was included in the endmember matrix.

The $\delta^{18}O$ of water (e.g., $^{1}H^{1}H^{18}O$ versus $^{1}H^{1}H^{16}O$) is zero for standard mean ocean water (SMOW) where

$$\delta^{18}O = \frac{(^{18}O/^{16}O)_{sample} - (^{18}O/^{16}O)_{standard}}{(^{18}O/^{16}O)_{standard}} \times 1000$$

and SMOW is the standard. The $\delta^{18}O$ of freshwater in rivers becomes more negative (richer in ^{16}O relative to the standard) at higher latitudes due to a process called Rayleigh distillation whereby cycles of evaporation and rainfall north of the equator favor the transport of the lighter isotope (^{16}O) away from the equator. Thus, the SR and the KR had $\delta^{18}O$ values of -21.7 and – 23.0, respectively, relative to -3.4 in Beaufort Sea water (PML) and -0.8 in SIM (Figure 5-9). These differences present $\delta^{18}O$ as a second tracer, one that is independent of salinity.

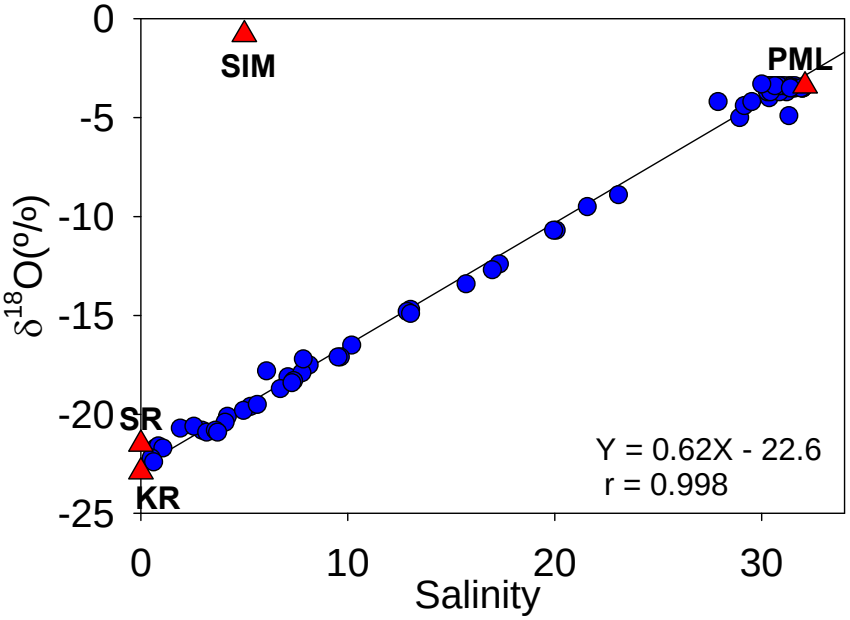

Figure 5-9. $\delta^{18}O$ versus salinity for water collected in Stefannsson Sound from May 23-31, 2004. Endmember values for the Sagavanirktok River (SR), Kuparuk River (KR), Sea Ice Melt (SIM), and Polar Mixed Layer (PML) are marked with solid triangles. The equation and correlation coefficient (r) were calculated from a linear regression analysis.

The strong linear relationship between salinity and $\delta^{18}O$, coupled with marked differences in endmember values for each parameter, yielded two variables that facilitated discrimination between river water and seawater (Figure 5-9). However, the data for salinity and $\delta^{18}O$ could not be used to effectively differentiate SR from KR water. Despite daily variations in the concentrations of dissolved silica for the SR, silica could be used to distinguish between water from the SR and KR because the endmember values for each river were significantly different (Figure 5-10). Concentrations of dissolved silica in the SIM also were distinct and helped to better define the contribution from sea-ice melt (Figure 5-10). Some of the data points that plotted between the river mixing lines in Figure 5-10 were from samples with a mixture of SR and KR water (i.e., the SK stations as described in more detail below). Data points for some of the SW stations plotted below the SR-PML mixing line due to variations in the silica endmember for the SR. Numerous runs of the OMP analysis (with variations in the endmember value for silica throughout the observed range for the SR) do not altered water mass fraction calculations by more than 10%. Furthermore, data for the K stations, as well as stations SK8, SK9, SK10, and SK6 (closest to KR outflow), plotted on or very close to the KR-PML mixing line. Dissolved silica was essentially conservative in the study area because

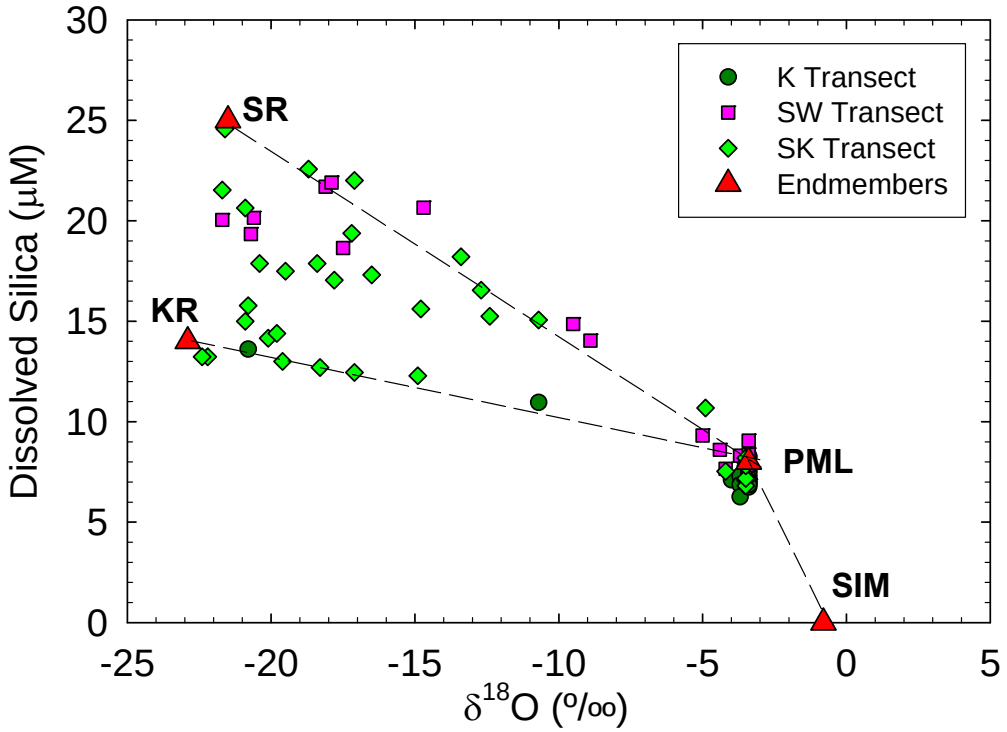

Figure 5-10. Concentrations of dissolved silica versus $\delta^{18}O$ for water collected from Stefannsson Sound from May 23-31, 2004. Endmember values for the Sagavanirktok River (SR), Kuparuk River (KR), Sea Ice Melt (SIM), and Polar Mixed Layer (PML) are marked with solid triangles. Dashed lines connecting the end-member data points show simple mixing lines (conservative behavior) between end-members.

the seasonal landfast ice cover restricted growth of phytoplankton, thereby greatly reducing the amount of biological uptake in the surface water (Granskog et al., 2005; Guay and Falkner, 1997; Weingartner and Okkonen, 2001). Macdonald et al. (1989) successfully used dissolved silica in combination with salinity and $\delta^{18}O$ in a similar water mass analysis for the Mackenzie River estuary in the Canadian Arctic (~500 km eastward) within limited space and time scales.

Results from the OMP analysis helped determine the fraction of SR water under ice in Stefannsson Sound during the study period. An example of the seaward advancement of the SR plume over time is shown using data from the SW transect for May 25 and 28 (Figure 5-11a, b). On May 25, the top 1 m of the water column at stations SW1 to SW3 contained 61 to 84% SR water (Figure 5-11a). Three days later, an increase in the percent

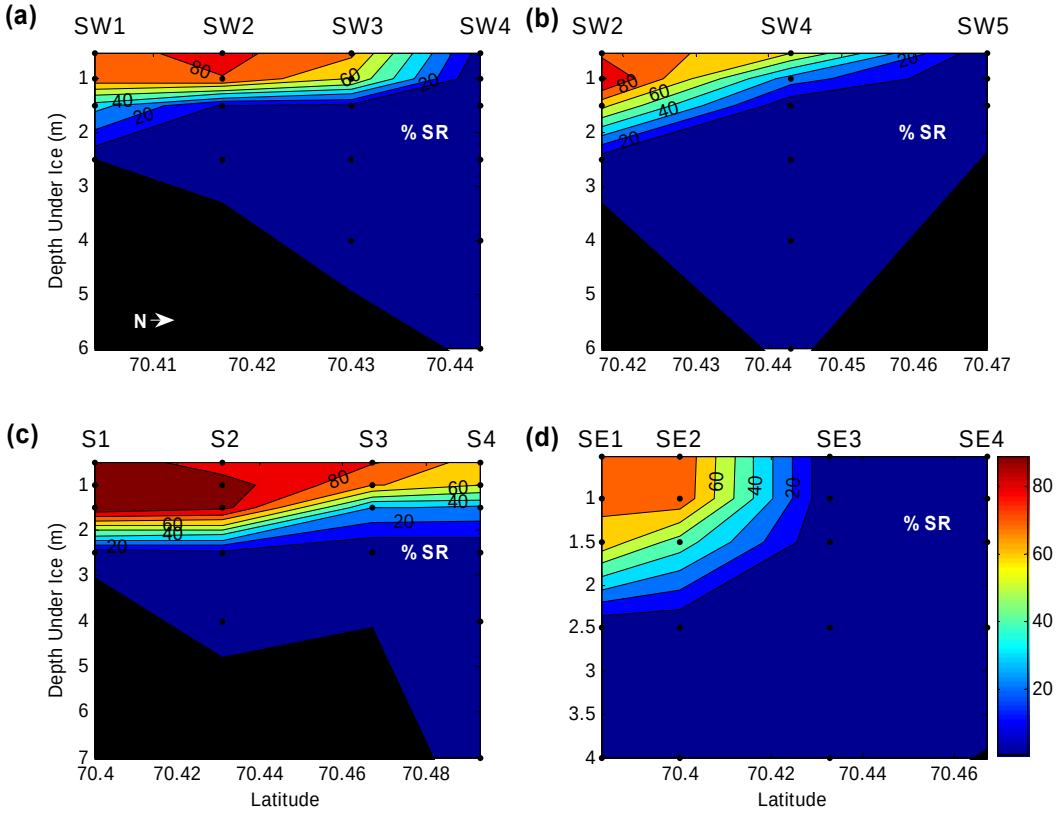

Figure 5-11. Percent of water sample that was Sagavanirktok River (SR) water for (a) samples from the SW transect sampled on May 25, (b) samples from the SW transect sampled on May 28, (c) samples from the S transect sampled on May 31, and (d) samples from the SE transect sampled on May 27. Black area shows the seafloor where pertinent. Black dots show sampling depths. Contour interval is 10%.

and depth of penetration of SR water was observed along the SW transect (Figure 5-11b). For example, the fraction of SR water increased from 10 to 63% at 1.5 m for station SW2 from 2 to 29% at 1 m for station SW4 (Figure 5-11). The increased fractions of SR water along the SW transect showed both the seaward and vertical progression of the SR plume

The largest fractions of SR water (≥90%) were found at depths of 0.5 to 1.5 m along the S1-S4 transect on May 31 (Figure 5-11c). Samples in the top 1 m at station S4 contained >60% SR water, even though station S4 was 16.7 km offshore and was the most seaward station sampled (Figure 5-1, page 45). The higher fractions of SR water observed along the S transect were partly due to the May 31 sample date. However, station SW4 was re-sampled on May 31 when it had a SR water fraction of 62% at 1 m depth. This fraction was similar to values of 73% and 62% (on May 31) at stations S3 and S4 that were located ~2.7 and 5.6 km farther north, respectively (Figure 5-1, page 45). Therefore, regardless of time, the SR plume progressed predominately along the S transect, as discussed in more detail below.

East of the S transect, the SR plume extended ~6.3 km seaward with ≥70% SR water in the top 1 m of the water column at stations SE1 and SE2 (Figure 5-11d). However, no detectable SR water was found at stations SE3 and SE4. Collectively, the OMP results supported movement of the SR plume seaward primarily along the S transect and secondarily along the SW transect with some eastward movement along the SE transect closer to shore.

A layer of water with a salinity of 25 to 30 was observed beneath the SR plume at ~2.5 m for all stations due to entrainment of denser waters below the pycnocline (Garvine and Monk, 1974; McLaughlin et al., 2002). As the plume shoaled and the water depth increased (moving offshore), this water layer widened below the plume and surfaced ahead of the front. The observed trend suggested mixing of SR water with another layer of lower salinity water that was deeper (>1.5 m) in the water column at stations seaward of the SR plume. This additional source of lower salinity water was attributed to inputs of sea-ice melt (SIM) that was pulled downward beneath the seaward-moving plume front via convergence due to a shoreward flow at depth as suggested by Garvine and Monk (1974) and Macdonald et al. (1989). The percent of SIM was generally <20% throughout the study area, with larger fractions present at stations farther offshore due to greater melting in the vicinity of offshore barrier islands. However, at some nearshore stations (SW1, S1, SE1, and SE2), >10% of SIM was calculated for some water samples. These larger fractions of SIM nearshore may have formed by heat advected directly by the river water or indirectly via the increased absorption of solar radiation from turbid river water flowing above the ice canopy (Knauss, 1996).

Overall, results from the OMP analysis suggest that the SR plume was a single, large structure that moved predominately northward along the S and SW transects and spread >15 km to the west and ~5 km to the east of the S transect (Figure 5-12, and discussed in more detail below). Turbulent mixing near the mouth of the SR created a well-mixed, fresher water column that advected seaward with increasing discharge to form a well-stratified flow beneath the ice farther offshore (Geyer et al., 2004;

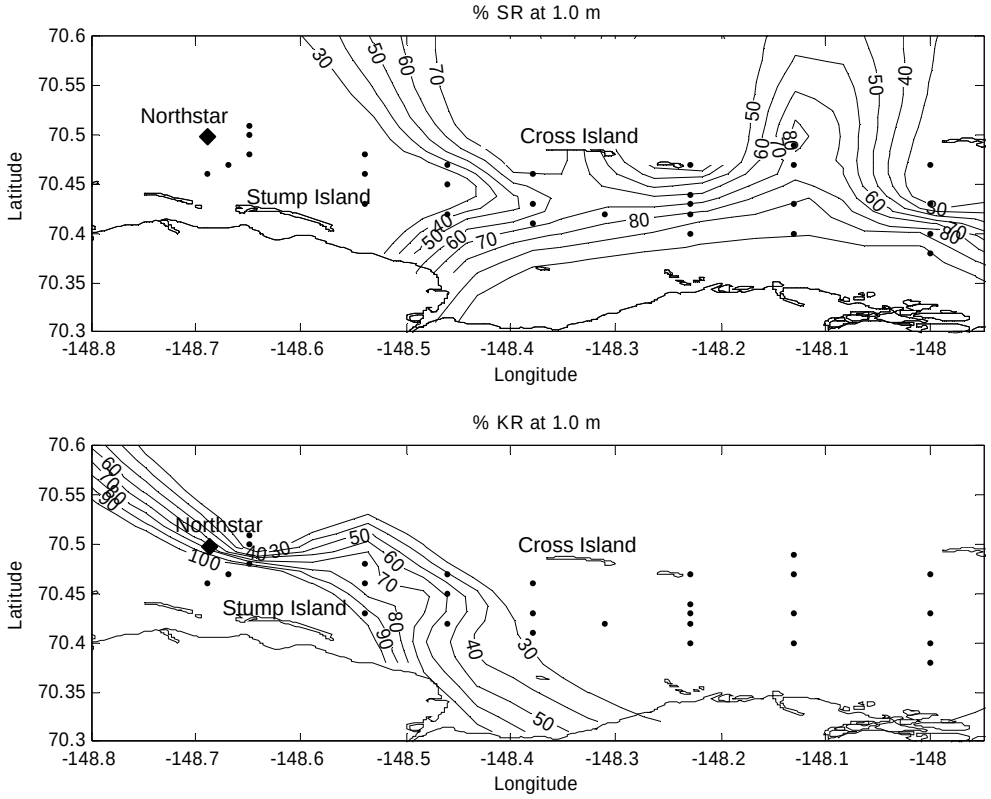

Figure 5-12. Quasi-synoptic view of the percent Sagavanirktok River (SR) water (top) and Kuparuk River (KR) water (bottom) at 1.0 m for May 27-31. Water mass fractions were rounded to the nearest 10%.

Garvine and Monk, 1974). The spread of the SR plume was limited by entrainment, lateral mixing, and buoyancy forcing (Chao, 1988; Garvine and Monk, 1974; Nishino, 2002; Weingartner et al., 1999).

Results from the SK stations (SK2-SK10), sampled on May 29 and 30, show the movement of SR water westward as well as the interaction between SR and KR plumes as they converged beneath the ice (Figure 5-13). Flow from the KR that moved eastward toward the SK stations was channeled by barrier islands and man-made causeways just north of the river mouth that effectively re-directed the plume alongshore.

Approximately equal fractions of ~40-50% SR and KR water were found in the top 1 to 1.5 m of the water column at stations SK5 (Figure 5-13a,c) and SK7 (Figure 5-13b,d), where the two plumes met. The distribution of the water mass fractions illustrated in Figure 5-13 suggest a northward flow of plume water as a result of convergence at or shoreward of station SK5 between the SR plume moving west and the KR plume moving east (Figure 5-13a,c). For example, the eastward flow of the KR plume, with maximum

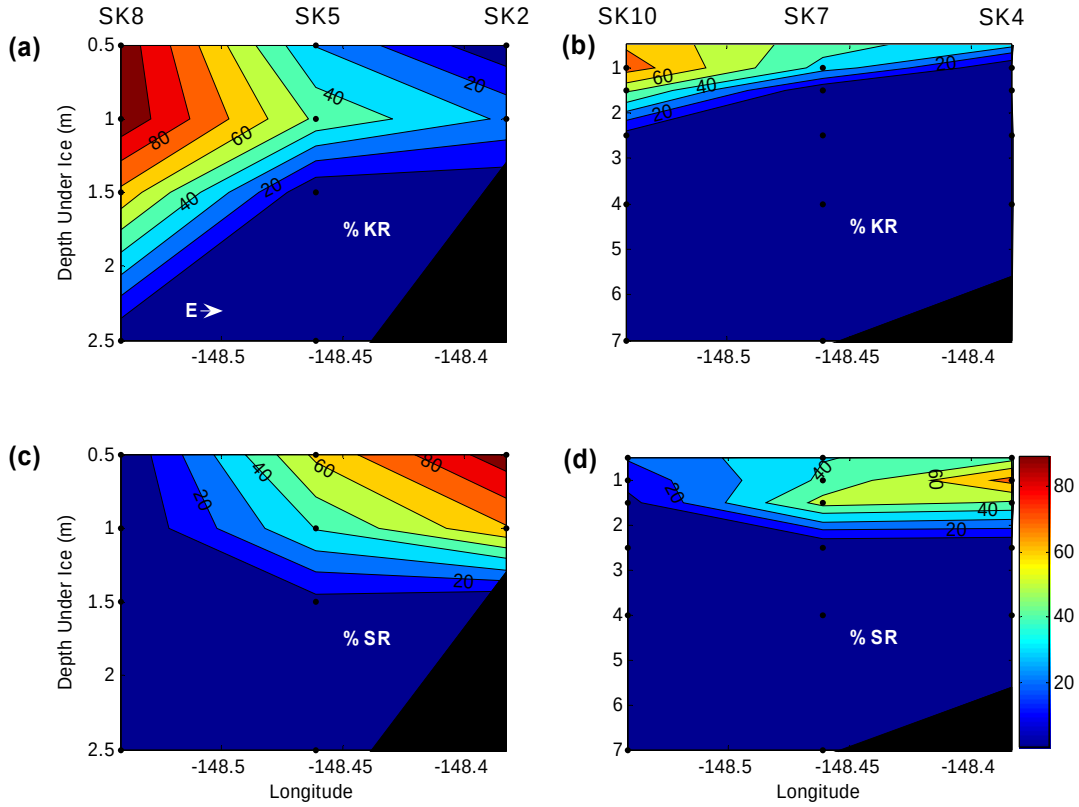

Figure 5-13. Percent of water sample that was (a) Kuparuk River (KR) water and (c) Sagavanirktok River (SR) water for stations SK8, SK5, and SK2; and (b) Kuparuk River (KR) water and (d) Sagavanirktok River (SR) water for stations SK10, SK7, and SK4. All stations were sampled on May 30. Black shows the seafloor where pertinent. Black dots show sampling depths. Contour interval is 10%.

fractions of KR at stations SK8 (Figure 5-14a) and SK10 (Figure 5-14c), was driven upward to ~1 m depth by increased mixing with SR water that was moving westward and downward from SK2 (Figure 5-14b) and SK4 (Figure 5-14d). As the two plumes converged, a northward flow may have been generated and guided by the shallower bottom topography to the east (Jones and Anderson, 1986; McLaughlin et al., 1996; Weingartner et al., 1998). As a result, the KR plume appears to have forced the westward flowing SR water to the north (Figure 5-12) and increased the offshore movement of freshwater.

No SR water was identified at station SK8 and <20% SR water was found at station SK10 (Figure 5-14c). Thus, the SR plume did not flow farther west than station SK5, but it was advected north to stations SK6 and SK7 (Figures 5-12 and 5-14d). The small fraction of SR water at stations SK8 and SK10 suggested that the portion of the KR plume that was closer to shore forced SR water to the north (Figure 5-13). In contrast,

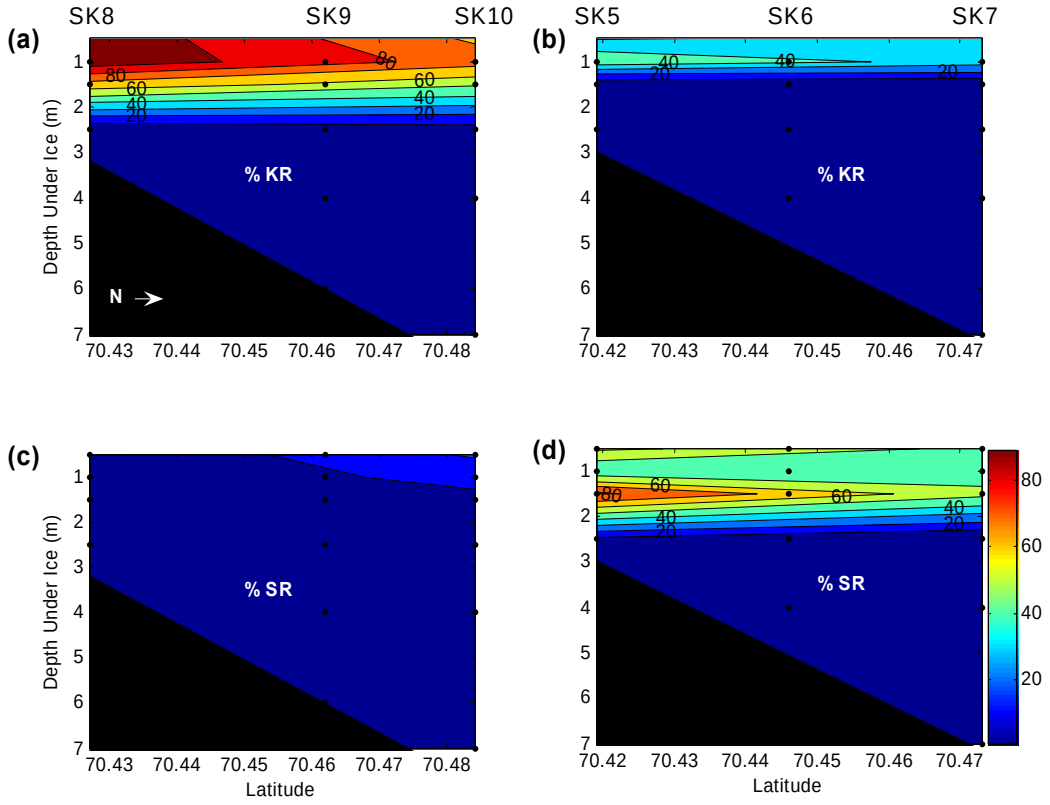

Figure 5-14. Percent of water sample that was (a) Kuparuk River (KR) water and (c) Sagavanirktok River (SR) water for stations SK8, SK9, and SK10; and (b) Kuparuk River (KR) water and (d) Sagavanirktok River (SR) water for stations SK5, SK6, and SK7. All stations sampled on May 30. Black shows the seafloor where pertinent. Black dots show sampling depths. Contour interval is 10%.

KR water was abundant to >2 m depth for stations SK8 to SK10 (Figure 5-14a) as a result of further re-direction northward by the causeway connecting Point McIntyre and the STP to shore (Figure 5-1, page 45) as well as the westward moving SR plume. As a result of mixing between the two plumes along the SK5, SK6, and SK7 transect (meridional), more SR water was advected along the 1.5 m isobath as the SR and KR plumes merged and mixed in the top 1 m of the water column. Furthermore, the decrease in the fraction of KR water east of stations SK8, SK9, and SK10 showed the seaward deflection of the plume due to interaction with the SR water (Figure 5-14a, b). The KR plume was mixed more easily by turbulence with the oppositely-flowing local circulation. However, the presence of the KR plume was sufficient to force westward-spreading SR water north (Figure 5-14), increasing the possibility of advection to the outer continental shelf. Such interaction among the many rivers along the northern coast of Alaska may aid in the transport of freshwater off the shelf between barrier islands via convergence of alongshore flows (Weingartner et al., 1999) and steering by bottom topography (Carmack et al., 1997; McLaughlin et al., 2002; Swift et al., 1997).

Currents under the ice averaged 7.2 ± 3.2 cm/sec at 309 ± 76° (n = 40). The current data were categorized as surface (1 and 1.5 m) and sub-surface (≥2.5 m) based on the observed 1-1.5 m thickness of the SR plume. Surface currents, with an average magnitude of 6 ± 3 cm/sec at 313 ± 115° (n = 17) were not significantly different from sub-surface currents that averaged 8 ± 3 cm/sec at 303 ± 34° (n = 23). These results suggest that a landward flow present in the top layer of the water column under ice prior to the spring floods, as inferred by Matthews (1981) and Weingartner and Okkonen (2001), reversed during high river discharge. Water flow in Stefannsson Sound was northwestward and parallel to the shoreline for the entire study period in agreement with results from Matthews (1981) and Weingartner and Okkonen (2001). Exceptions to this trend occurred only where there were mixing fronts, changes in bathymetry, or barrier islands (Granskog et al., 2005). Maximum current velocities of ≥10 cm/sec in this study were generally found in regions of plume fronts.

Weak relationships ($r^2 \leq 0.33$) were observed among alongshore and cross-shore current magnitudes, changes in sea level height, and stage height. Thus, local circulation was most likely forced by the baroclinic pressure/density gradient set up by the initial high discharge of river water over the saline shelf water (Carmack et al., 1989; Geyer et al., 2004; Harms et al., 2000). We also observed that the northwestward flow of the local circulation contradicts the usual eastward deflection of northward moving waters due to the Coriolis force. This resultant flow was most likely due to the influence of the high intensity of the river runoff (Harms et al., 2000) as well as possible forcing from the larger scale anti-cyclonic Beaufort Gyre offshore (Weingartner and Okkonen, 2001).

Mixing gradients were calculated using the fractions of SR water along isobaths between stations. These gradients helped to quantitatively support qualitative inferences of SR water movement based on the distributions of water mass fractions. Calculations were carried out for the top 1.5 m of the water column where differences in the SR water mass fractions between stations were >10 %. Gradients were calculated in % km^{-1} as follows:

$$\text{Gradient } (z) = ([\%\ \text{River}]_2 - [\%\ \text{River}]_1) / L$$

where flow was assumed to be from station 1 to station 2 (subscripts 1 and 2) along a given sampling depth (z = 0.5, 1, or 1.5 m) and L = distance (in kilometers) between stations. The calculation yielded negative gradients along an assumed flow pathway and positive gradients when opposite the proposed flow. The following simplifying assumptions were applied to the gradient calculations: (1) a single source was selected for the SR water at what was believed to be the primary outflow and (2) gradient calculations assumed all river water entering the study area did so via only this outflow.

Flow pathways were determined by comparing horizontal gradients (e.g., 1 m, Table 5-2) and assumed that smaller gradients (<-5% km^{-1}) represented primary flow pathways and

Table 5-2. Selected gradients for the percent of Sagavanirktok River (SR) water between stations along the 1 m isobath.

Sample Date	Station 2	SR_2 (%)	Station 1	SR_1 (%)	ΔSR/L (%/km)
May 25	SK1	31	SR	100	-7
	SK1	31	SW2	80	-13
	SW1	75	SR	100	-3
	SW2	80	SW1	75	-
	SW4	2	SW2	80	-27
	SW3	61	SW2	80	-13
	SW4	2	SW3	61	-41
May 27	S1	70	SR	100	-5
	S1,SE1	70,72	SE1,SE2	72,78	-
	SE1	72	SR	100	-4
	SE3	0	SE2	78	-21
May 28	SK1	76	SR	100	-2
	SK1	76	SW2	92	-5
	SW2	92	SR	100	-
	SW4	29	SW2	92	-22
	SW5	0	SW4	29	-10
May 30	SK2	69	SR	100	-3
	SK5	41	SR	100	-4
	SK5	41	SK2	69	-9
	SK8	0	SK5	41	-13
	SK4	74	SR	100	-2
	SK4	74	SK2	69	-
	SK7	42	SK4	74	-9
	SK7	42	SK5	41	-
	SK10	14	SK7	42	-9
	SK10	14	SK5	41	-3
May 31	S1, S2	99,96	SR, S1	100,99	-
	S3	73	S2	96	-6
	S4	62	S3	73	-4
	SW4	62	S2	96	-9
	SW4	62	SR	100	-3

larger gradients ($\geq$-10% km^{-1}) represented a resistance to flow or shear that was identified where physical barriers or water mass fronts were present. For example, on May 25, two possible flow pathways of SR water to station SK1 along the 1 m isobath were chosen, one from the SR mouth (ΔSR/L = -69%/10.5 km = -7% km^{-1}) and the other from station SW2 (ΔSR/L = -44%/3.3 km = -16% km^{-1}). The two gradients suggested that SR water more likely flowed directly from the mouth of the SR because it would have been less mixed by approximately a factor of two along that route.

The flow pathways determined by comparing horizontal gradients in this manner are shown schematically in Figure 5-15. Generally, mixing (larger gradients) was comparatively lower in a cross-shore (N-S) versus alongshore (E-W) direction, indicating a preferential seaward advection of SR water. The presence of relatively unmixed SR water (≥90% SR) from the SR mouth to stations closest to the shore (e.g., SK1, SW1, S1, and SE1) indicated a large and increasing pool of SR water located shoreward of these stations. Mixing fronts were consistently observed between stations located farther offshore (e.g., SW4 and SW5) with magnitudes >20% km^{-1}, marking the limits of the spread of SR water. Small mixing gradients (≤4% km^{-1}) observed between the SR mouth and the SK stations confirmed a large westward spread of SR water.

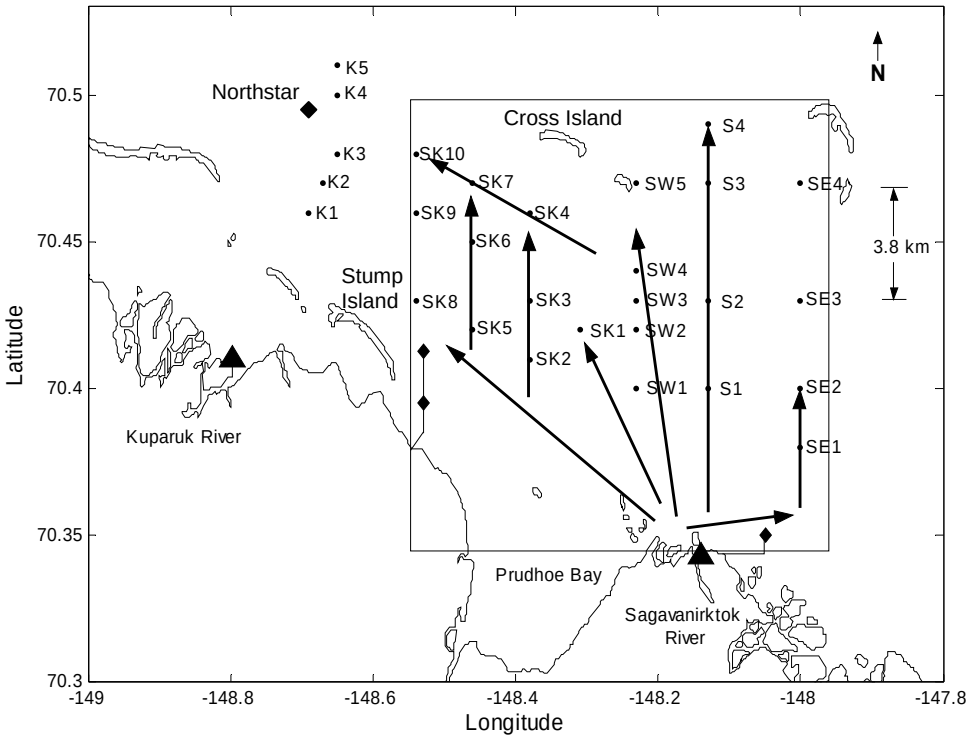

Figure 5-15. Qualitative flow pathways for Sagavanirktok River (SR) water according to lowest negative gradients and the calculated area of influence of the SR plume (rectangle). Solid triangles show the locations of the SR and Kuparuk River (KR) outflows in gradient calculations. The lengths of arrows show the distance over which the SR plume was observed.

A freshwater budget was calculated for the SR discharge using the water mass fractions from the OMP analysis. The total amount of SR water was calculated as water depth equivalents (in meters) for each station by summing the distribution of water mass fractions over the water column to a depth of 2.5 m (no river water was observed below this depth during the study). Water mass fractions were assumed to be evenly distributed between sampling depths. The top 0.5 m of the water column under ice was assumed to be homogeneous.

Data from stations that were re-occupied during the study were used to estimate the rate of change in SR water for the entire sampling area. These rates were then utilized to estimate the total SR water at each station at the end of the study (June 2), and thereby obtain the discharged water depth equivalent for the study area (Table 5-3). Some values were adjusted so that the depth equivalent of SR water was $\leq$2.5 m, and data for stations SK1 and SK2 were adjusted so that values did not exceed their total bottom depths of 1.5 and 1.0 m, respectively.

The comprehensive sum of SR water in the study area was 34.7 m, ~14 % of which flowed east to stations SE1 and SE2, ~35% flowed west to the SK stations, and ~50% flowed north to the SW (28%) and S (22%) stations. Overall, ~65% of the SR discharge identified during this study was found east of Prudhoe Bay. These observations supported the primary movement of SR water northward along the S transect with an influence from both the local circulation and KR plume (Figure 5-15).

The depth equivalent of SR water at individual stations was averaged to obtain a value of 1.6 ± 0.7 m. This average value was multiplied by the relative area of SR plume influence (~315 km^2), to yield a total volume in the study area on June 2, 2004 of 0.5 ± 0.2 km^3. Based on the U.S.G.S. data, the measured total SR flow during our study period was ~1 km^3 (includes 5X multiplier from Rember and Trefry, 2004, that was based on a determination that the U.S.G.S. gauge accounts for only ~20% of the total SR flow). Therefore, on June 2, 2004, the calculated 0.5 km^3 of SR water that was under the ice at the mouth of the SR in the coastal Beaufort Sea accounted for only ~50% of the total discharge based on the U.S.G.S. The discrepancy between the two values for flow was most likely due to several factors including the following: movement of water away from our sampling area in the Beaufort Sea, open water closer to shore that was not included in the calculation, possible errors in gauge measurements at flood stages, use of the 5X multiplier, and water that was above ice during our sampling period. Any above-ice water will eventually re-enter the water column via strudel holes or during the sea ice melt and consequent break-up in July (Reimnitz and Bruder, 1972).

Table 5-3. Contribution of Sagavanirktok River (SR) water to individual stations on June 2, 2004, by using an average rate of 0.2 m day^{-1}. Underlined numbers in the adjusted final column were modified as described in text.

Station	Initial (m)	Days to June 2, 2004	Final (m)	Adjusted Final (m)	Percent of SR Total
SW1	1.2	8	2.8	2.5	7.2
SW2	1.5	5	2.5	2.5	7.2
SW3	0.8	8	2.4	2.4	6.9
SW4	1.1	2	1.5	1.5	4.3
SW5	0.0	5	1.0	1.0	2.9
SE1	1.4	6	2.6	2.5	7.2
SE2	1.3	6	2.5	2.5	7.2
S1	2.0	2	2.4	2.4	6.9
S2	1.8	2	2.2	2.2	6.3
S3	1.2	2	1.6	1.6	4.6
S4	1.0	2	1.4	1.4	4.0
SK1	1.1	5	2.1	1.5	4.3
SK2	0.9	3	1.5	1.0	2.9
SK3	0.8	5	1.8	1.8	5.2
SK4	1.0	3	1.6	1.6	4.6
SK5	1.3	3	1.9	1.9	5.5
SK6	0.4	0	0.4	0.4	1.2
SK7	0.9	3	1.5	1.5	4.3
SK8	0.5	0	0.5	0.5	1.5
SK9	0.4	4	1.2	1.2	3.5
SK10	0.2	3	0.8	0.8	2.3
SUM			**(36.2)**	**34.7**	100
AVG				**1.6 ± 0.7**	

5.3 Dispersion of Sediments and Chemicals Under Ice in the Beaufort Sea during Spring 2004

The data in Figure 5-16 show that concentrations of TSS did not follow a simple mixing trend versus salinity and that some of the particles settled out of the surface layer of the incoming fresh water. All data points, excluding one data point from the mixing zone, plotted below a simple mixing line between the seawater end-member of ~1 mg/L and the lowest value for TSS in the river of 43 mg/L (Figure 5-16). Thus, concentrations of TSS in offshore samples are 15 to 90% lower than predicted from the smallest simple mixing

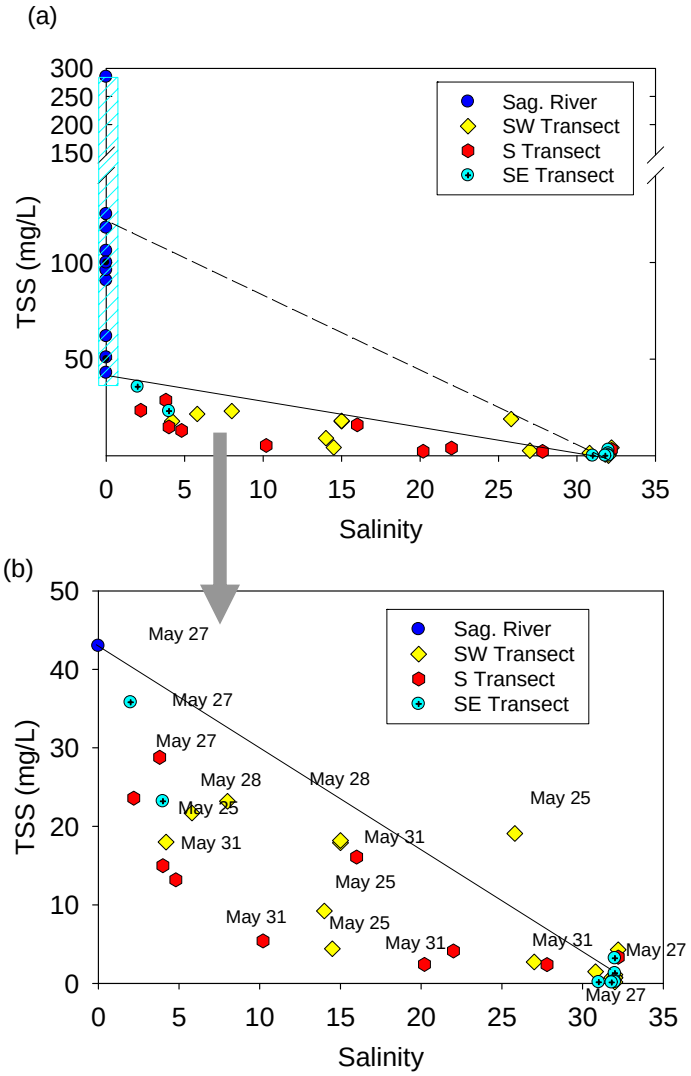

Figure 5-16. Total suspended solids (TSS) versus salinity (a) full-scale for TSS and for (b) TSS at 0 to 50 mg/L for the Sagavanirktok River and offshore in Stefannsson Sound during May-June 2004. Dashed line on (a) shows simple mixing line between TSS of average river water (127 mg/L) and seawater (1 mg/L). Solid line on (a) and (b) shows simple mixing line between lowest value for TSS in river water during peak flow (43 mg/L) and a value of 1 mg/L for seawater.

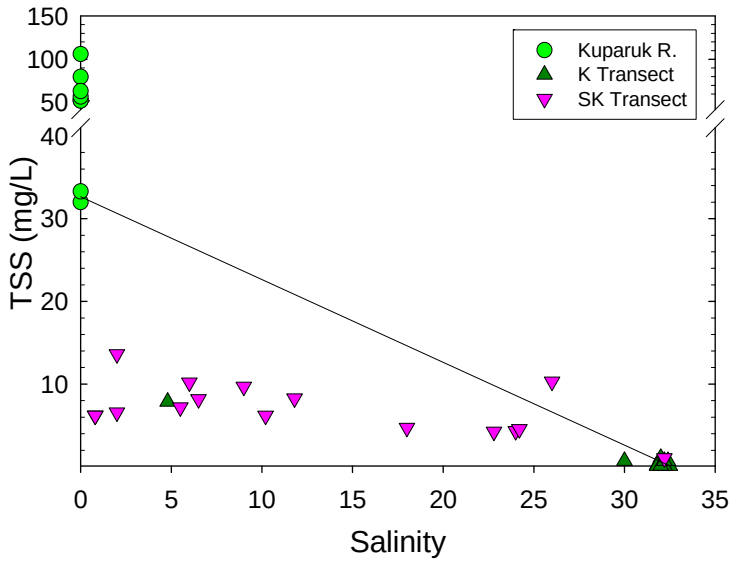

Figure 5-17. Salinity versus total suspended solids (TSS) for water samples collected in the Kuparuk River and along the K and SK Transects during May-June 2004. Solid line on graph shows simple mixing line between lowest value for TSS in river water during peak flow (32 mg/L) and a value of 1 mg/L for seawater.

gradient for particles along the pathway of the Sagavanirktok River plume. A similar trend was observed for the Kuparuk River. Concentrations of TSS along the mixing zone in the Kuparuk River decreased sharply and showed settling of >50% of the suspended sediments (Figure 5-17). Concentrations of TSS in samples with salinities >30 averaged 1 mg/L and ranged from 0.1 to 4 mg/L (Figures 5-16 and 5-17).

A laboratory determination of turbidity was made for all discrete water samples. Results from the laboratory samples correlated well with concentrations of TSS (Figure 5-18). Values for TSS were about 1.3 times the values for turbidity (Figure 5-18).

Vertical profiles also are available for *in situ* turbidity. At station SW4, the first of the vertical profiles for turbidity (May 25) shows a thin layer of suspended sediments at the surface with a gradual decrease across the pycnocline (Figure 5-19). After three days (from May 25 to May 28), the layer of suspended sediment thickened as the layer of fresh water thickened (Figure 5-19). No significant changes in turbidity occurred after an additional three days (May 31). However, when turbidity was viewed as a function of salinity for station SW4, the turbidity on May 31 was about half of the turbidity on May 28 for the same salinity (turbidity on Figure 5-20 and salinity on Figure 5-6, page 50). This trend is most likely related to a combination of mixing and thickening of the plume and continued settling of particles from the under-ice plume.

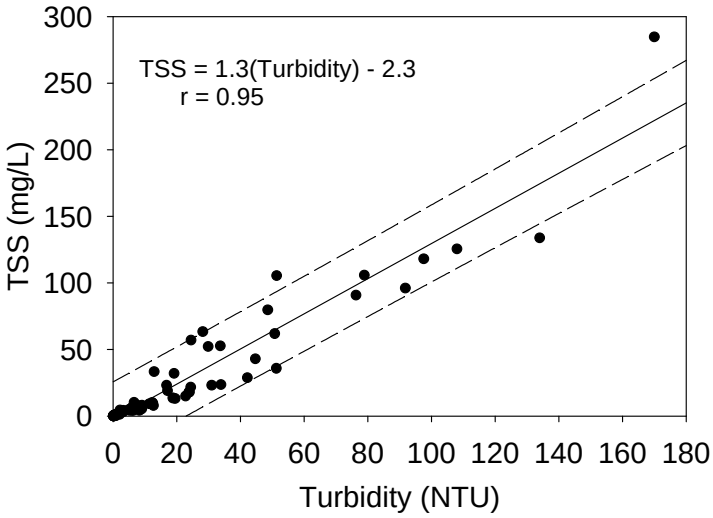

Figure 5-18. Total suspended solids (TSS) versus turbidity for samples collected during spring 2004. The solid line, equation and correlation coefficient (r) from are from a linear regression analysis. Dashed lines show 95% prediction interval.

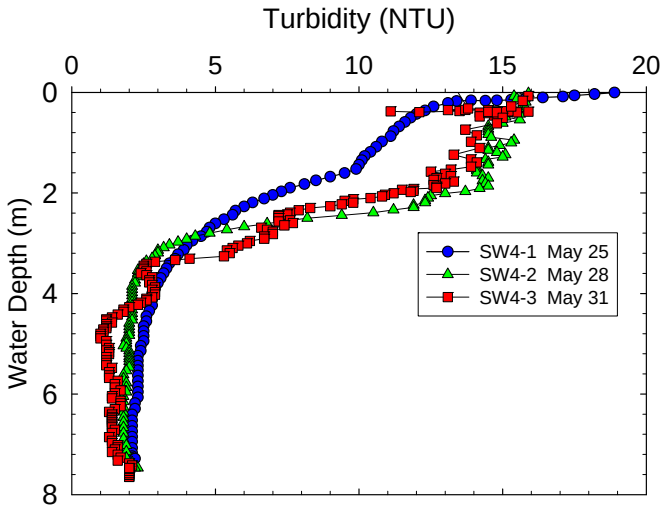

Figure 5-19. Vertical profiles of turbidity for station SW4 on May 25, May 28 and May 31, 2004. Salinity profiles for the same station and dates are shown on Figure 5-6, page 50.

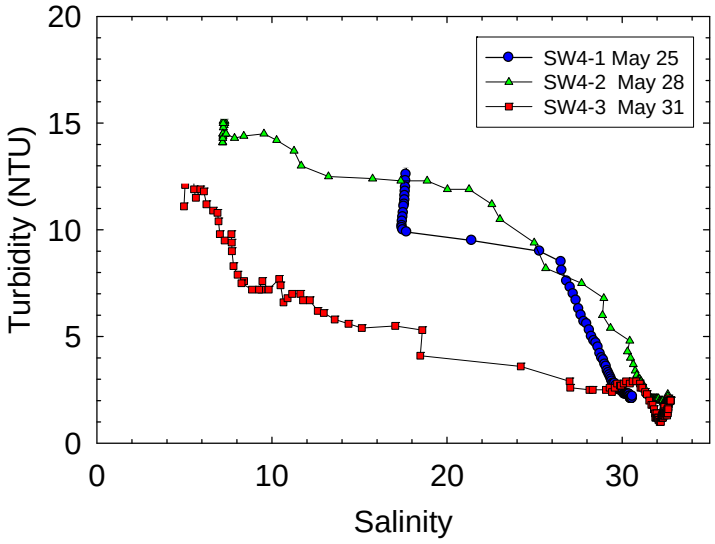

Figure 5-20. Salinity versus turbidity for station SW4 on May 25, May 28 and May 31, 2004. Vertical profiles for salinity and turbidity for this station on the above dates are shown on Figures 5-6 and 5-19, respectively.

Some links between river inputs of suspended sediments and local sedimentation rates can be made with available data from the cANIMIDA Project. Our previous results showed that sedimentation rates ranged from ~0.04 cm/yr to ~0.10 cm/yr with several sites having little or no net accumulation of sediment during at least the past 50 years (Figure 5-21 after Trefry et al., 2003). At two sites, we identified 3 to 5 cm thick layers of sediment that were deposited since development began during the 1960s (Figure 5-21). Our overall results are consistent with those of Naidu et al. (2001) for the same area, namely that sedimentation rates and isotope activities are very low. We also know from our previous work that the presence of fine-grained sediment at a given location can vary from year to year and that the sediment movement along much of the shallow, coastal Beaufort Sea is quite dynamic.

The low sedimentation rates at stations P01 and E01 (Figure 5-21) can be supported by comparison with data for river inputs of suspended sediments. For example, the Sagavanirktok River, the major river source of sediments to this area, is estimated to have an annual sediment load of about 6 x 10^5 metric tons (Rember and Trefry, 2004). The depositional area for this sediment in the coastal Beaufort Sea is about 1000 km^2 to yield an estimated deposition rate of ~0.04 cm/y, based on a sediment bulk density of 1.6 g/cm^3 ([0.6 x 10^{12} g dry sediment/10 x 10^{12} cm^2] x [(1.6 g wet sediment/$cm^{3)}$/(2.6 g dry sediment/cm^3)]). This calculated value is consistent with results from direct determinations of sedimentation rate.

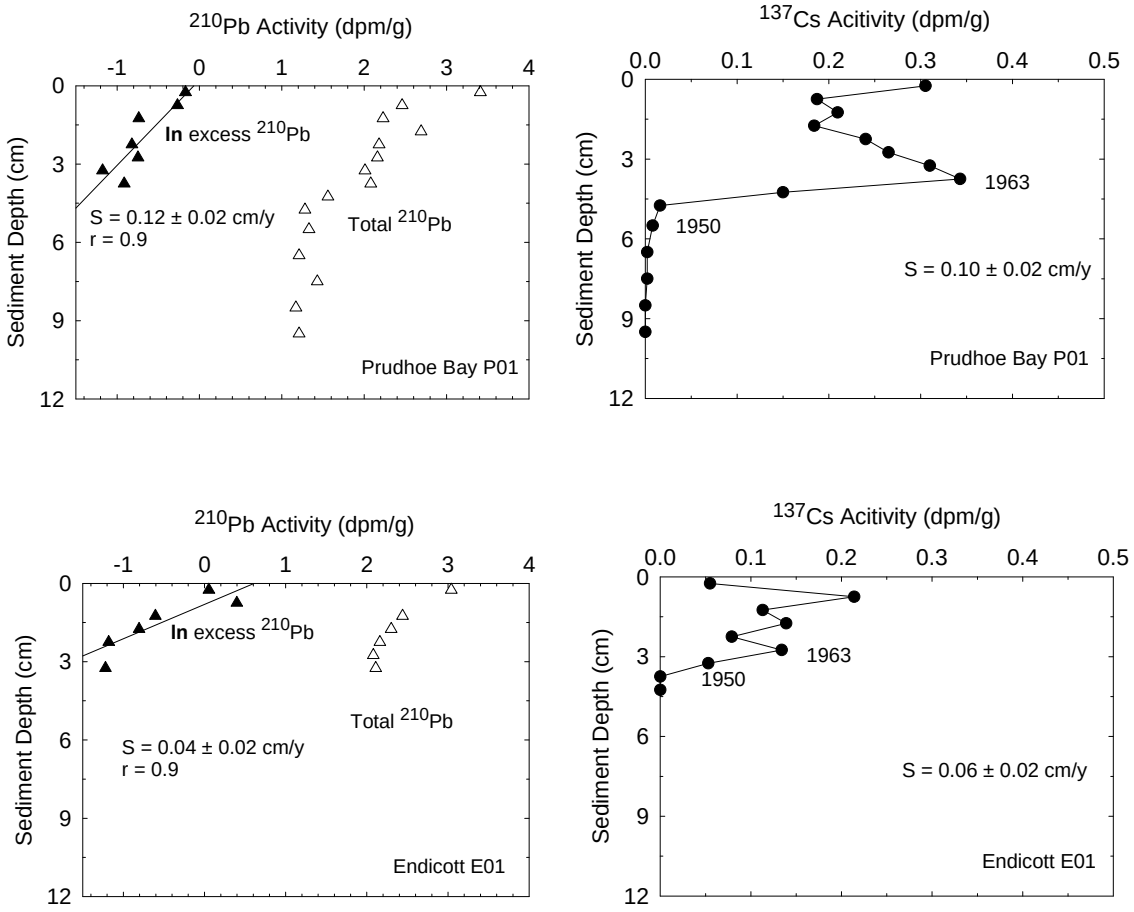

Figure 5-21. Vertical profiles for the activities of total ^{210}Pb, excess ^{210}Pb and ^{137}Cs for sediment cores from stations in Prudhoe Bay and east of Endicott Island.

Concentrations of dissolved and particulate metals were traced under ice across the freshwater-seawater mixing zones in a manner similar to that described previously for salinity, dissolved silica, δ^{18}O and suspended sediments. The data are used here as follows: (1) to describe how the mixing process influences concentrations of dissolved and particulate metals and (2) to obtain a better perspective about concentrations of metals in suspended sediments relative to bottom sediments. Concentrations of dissolved and particulate metals may provide a useful and more sensitive short-term (days to months) integrator of any future metal contamination than bottom sediments (Trefry et al., 2003). Concentrations of dissolved and particulate metals also provide an important link with biological uptake of potentially toxic metals. However, the complexities of natural trends for dissolved and particulate metals must be well understood in order to use them as tracers of contamination and bioaccumulation in the ecosystem. The metals chosen for study in this project represent a combination of metals selected by MMS and us because of their usefulness as tracers of potential contamination in the study area.

Concentrations of dissolved As followed a strong positive trend versus salinity across the freshwater-seawater mixing zone, even when data for both the Sagavanirktok and Kuparuk rivers were combined on the same graph (Figure 5-22). Concentrations of dissolved As in both the Sagavanirktok (0.068 ± 0.015 µg/L) and Kuparuk (0.041 µg/L) rivers were low relative to seawater values of 1.0 ± 0.1 µg/L (Figure 5-22). The observed trend supports simple mixing of dissolved As under the ice with no easily detectable biological or physical removal or addition of dissolved As over the one to two week study period (Figure 5-22). The large range of dissolved As concentrations at a salinity of 32 (the polar mixed layer) was most likely the effect of long-term (many months) biological and inorganic processes. Figure 5-22 also supports the statement that the primary source of dissolved As to the coastal water of the cANIMIDA study area was from upwelling of deeper, offshore water with advection into Stefannsson Sound, not from river runoff.

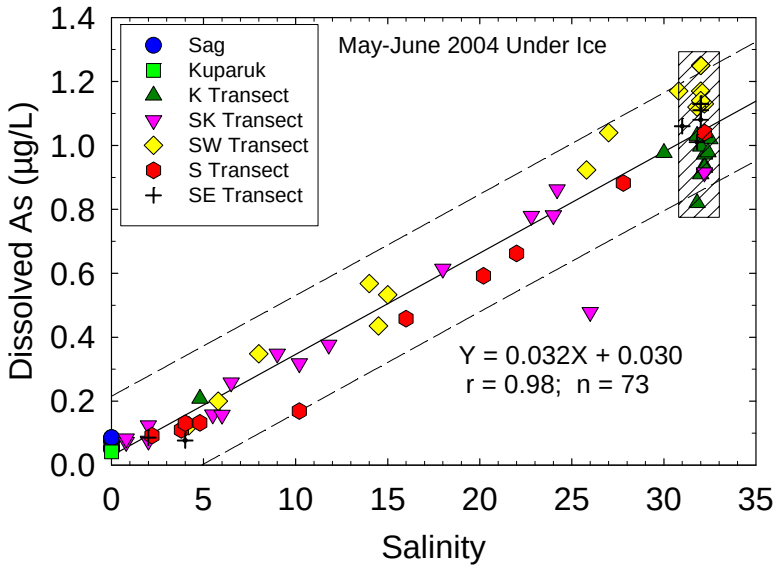

Figure 5-22. Concentrations of dissolved As versus salinity for water samples collected under ice across the mixing zones from the Sagavanirktok and Kuparuk rivers to the coastal Beaufort Sea. Shaded area was drawn to emphasize the range of dissolved As concentrations in the polar mixed layer. Line and equation are from a linear regression. Dashed lines show 95% prediction interval.

When the data for As in suspended matter collected under ice were plotted versus particulate Al, >80% of the data points plotted within the 99% prediction interval developed using sediment data from the coastal Beaufort Sea (Figure 5-23a) as previously described by Trefry et al. (2003). However, 10 data points for samples from the K Transect and two for the SW Transect plotted above the upper confidence interval. Each of these samples of suspended matter contained a lower Al content (at 1-5% Al) relative to river particles, suggesting that they contained more As-rich organic matter as described by Trefry et al. (2004a).

Precautions to avoid contamination during sampling are always an important component to obtaining reliable data and thus data quality must be evaluated. The highest

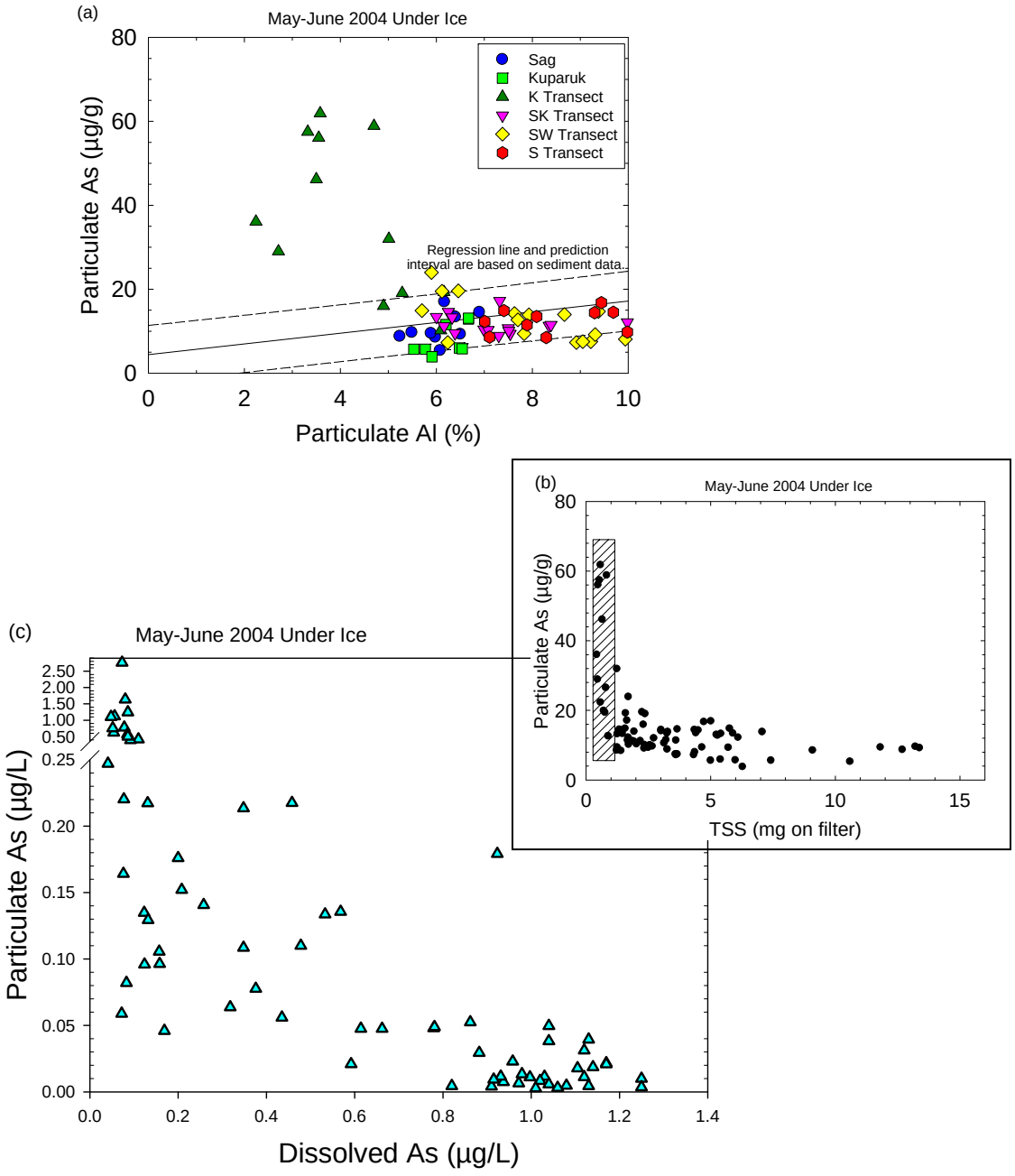

Figure 5-23. Concentrations of (a) particulate As (µg/g) versus particulate Al, (b) particulate As (µg/g) versus total suspended sediments (TSS), shaded area highlights range in As concentrations at low values of TSS and (c) particulate As (in µg/L) versus dissolved As (µg/L) for water samples collected in the rivers and under ice in the coastal Beaufort Sea. Line and equation on (a) are from a linear regression based on previous Beaufort Sea data from Trefry et al. (2003). Dashed lines on (a) show 95% prediction interval from previous data.

concentrations of particulate As from this study were found for samples when <1 mg of particles was collected on the filter (Figure 5-23b). However, the particulate As concentrations in samples with <1 mg of material ranged from 8 to 60 µg/g and included samples with both high and low values (Figure 5-23b). Coupled with the strong connection between low Al and high As (Figure 5-23a), the likelihood of contaminated samples seemed low considering the precautions taken during sampling and analysis. Similar trends for As in suspended sediments for this study area were previously reported by us during the ANIMIDA Project (Trefry et al., 2004a).

Based on the absolute amount of As per liter of sample, river water contained >90% particulate As whereas seawater (the polar mixed layer at a salinity of 32) <5% particulate As (Figure 5-23c). Along the freshwater-seawater mixing gradient (with linearly increasing concentrations of dissolved As), the decrease in concentrations of particulate As (in µg/L) was much sharper than the increase in concentrations of dissolved As. This trend of higher concentrations of dissolved As at higher salinity also supports upwelling of offshore waters, rather than desorption of As from river particles, as the primary source of dissolved As in Stefannsson Sound. A more detailed assessment of the biogeochemistry of As is presented in Section 7.

The plot showing concentrations of particulate Cu versus particulate Al is very similar to that observed for particulate As versus particulate Al with some higher concentrations of Cu at lower concentrations of Al (Figure 5-24a). The observed Cu enrichment is for the same samples of suspended matter that were enriched with As. In addition to the Cu-rich samples, samples from the SW and S transects are Cu-poor relative to Al (plot below the lower prediction interval based on typical regional sediments). Such a decrease in particulate Cu concentrations and the Cu/Al ratio could be due to desorption of Cu across the freshwater-seawater mixing zone as described for other rivers for Ba and Cd (Hanor and Chan, 1977) or addition of some more Al-rich (or Cu-poor) suspended matter in the area of transects SW and S as discussed below.

In contrast with As, concentrations of dissolved Cu in the Sagavanirktok River (0.5 ± 0.2 µg/L) are similar to those in offshore samples (0.5 ± 0.2 µg/L) and both are higher than values of 0.2 ± 0.1 µg/L in the Kuparuk River (Figure 5-24). Thus, it is difficult to see any significant deviations from a conclusion of no change or simple dilution across the freshwater-seawater mixing zone for dissolved Cu by viewing the complete data set on one graph (Figure 5-24b). Any other trends for Cu versus salinity seem to be masked by expected temporal variations in concentrations of Cu in the rivers during high flow and subsequent impacts on concentrations of dissolved Cu in offshore waters as well as by possible desorption of Cu as particles enter seawater.

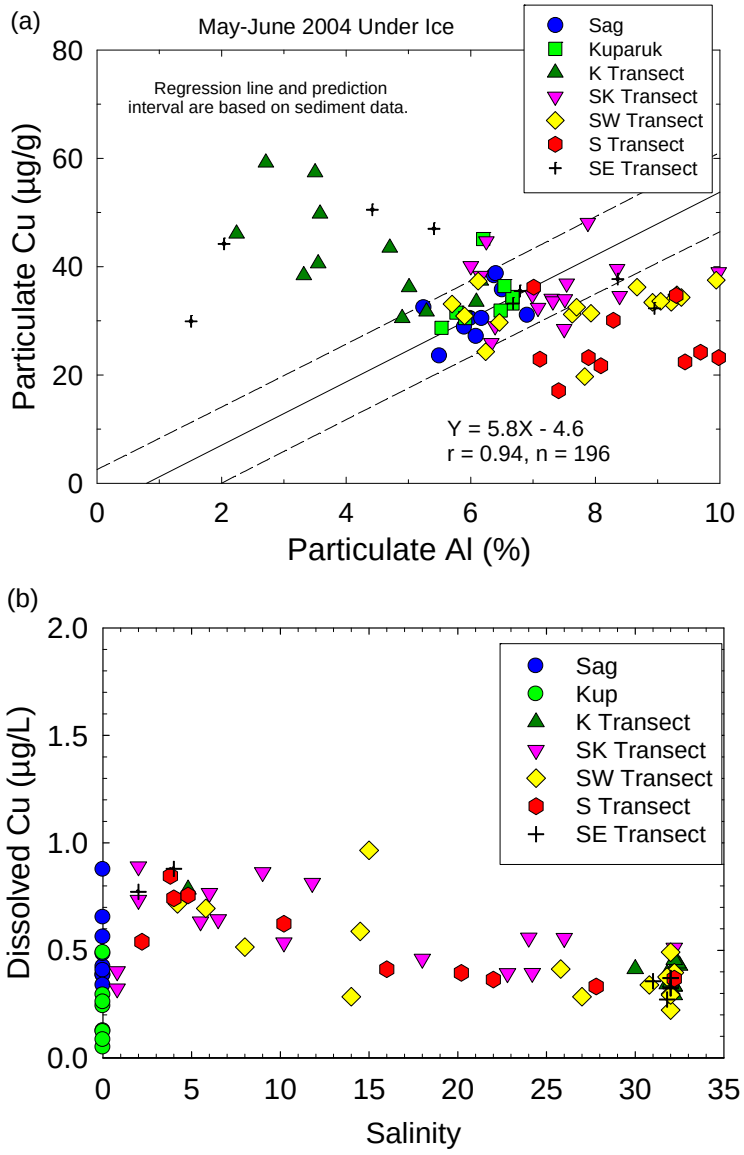

Figure 5-24. (a) Concentrations of particulate Cu versus particulate Al and (b) concentrations of dissolved Cu versus salinity for samples from the Sagavanirktok and Kuparuk rivers and the coastal Beaufort Sea. Line and equation on (a) are from a linear regression. Dashed lines on (a) show 95% prediction interval.

However, Figure 5-25a shows that when dissolved Cu concentrations for just the S and SE transects are plotted versus salinity, a relatively strong negative relationship was observed (river water data are excluded from linear regression in Figure 5-25a). This trend suggests that Cu was not very reactive during mixing. Some high particulate Cu/Al ratios at a salinity of ~32 (Figure 5-25b) as well as at dissolved Cu concentrations of 0.3-0.4 µg/L (Figure 5-25c) support the possibility of biological Cu enrichment as previously discussed.

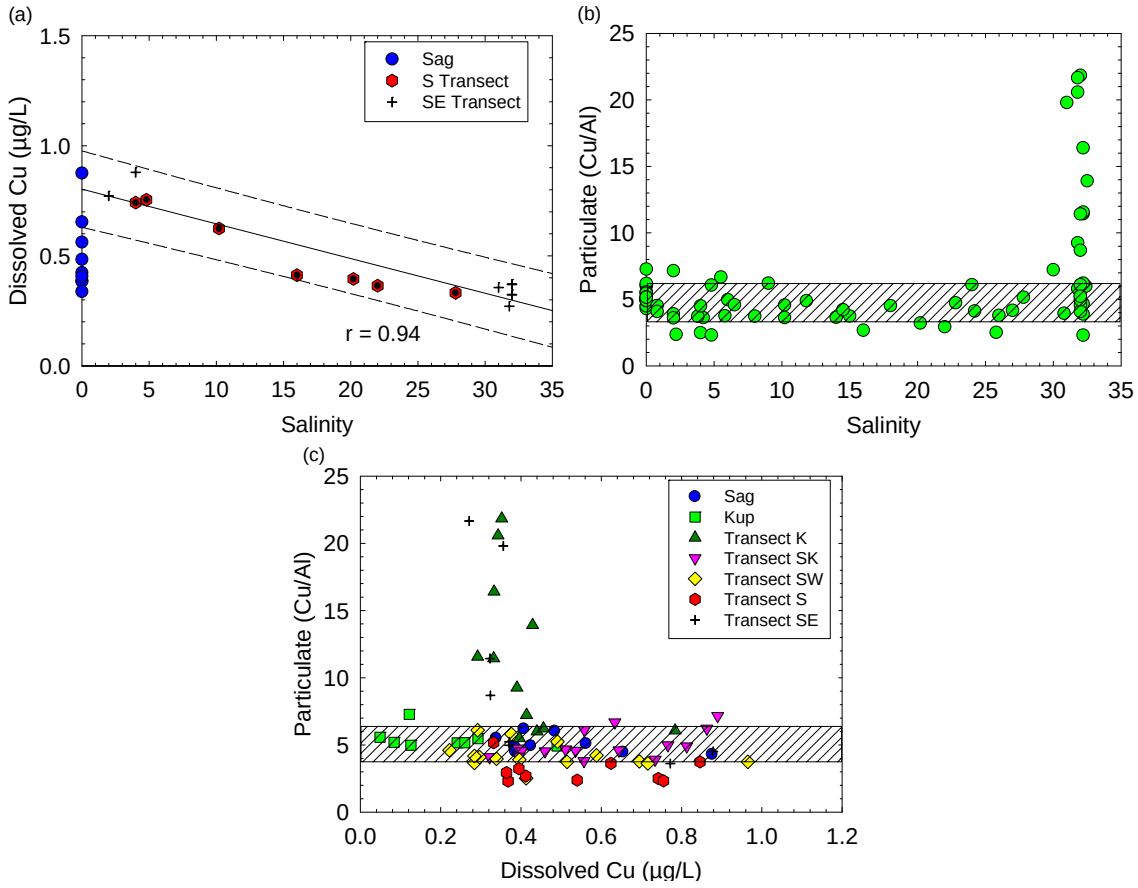

Figure 5-25. (a) Concentrations of dissolved Cu versus salinity, (b) particulate Cu/Al ratio for suspended matter versus salinity and (c) concentrations of particulate Cu/Al versus dissolved Cu. Line and correlation coefficient (r) on (a) are from a linear regression. Dashed lines on (a) show 95% prediction interval. Shaded area on graphs shows typical range of Cu/Al in bottom sediments from the coastal Beaufort Sea.

Concentrations of particulate Fe were skewed to the high side of the Fe/Al ratio obtained for bottom sediments in the cANIMIDA area (Figure 5-26a). Data points that exceeded the upper prediction interval for Fe/Al in sediments were predominantly for suspended sediments from the Kuparuk River and adjacent K and SK Transects (Figure 5-26a). A trend of slightly higher particulate Fe concentrations, relative to Al, in the Kuparuk River was observed consistently during the ANIMIDA Project (Rember and Trefry, 2004; Trefry et al., 2004a). The Kuparuk River drains mainly arctic tundra and the river water contains higher concentrations of DOC and dissolved Fe (Rember and Trefry, 2004). The higher Fe/Al ratio in suspended sediments under the ice is consistent with previous observations. However, the impact of such particles on bottom sediments in the study area seems limited based on the narrow 99% prediction interval for Fe/Al in Figure 5-26a. This observation is consistent with a lower sediment load for the Kuparuk River and trapping of incoming particles by the Kuparuk delta and adjacent barrier islands.

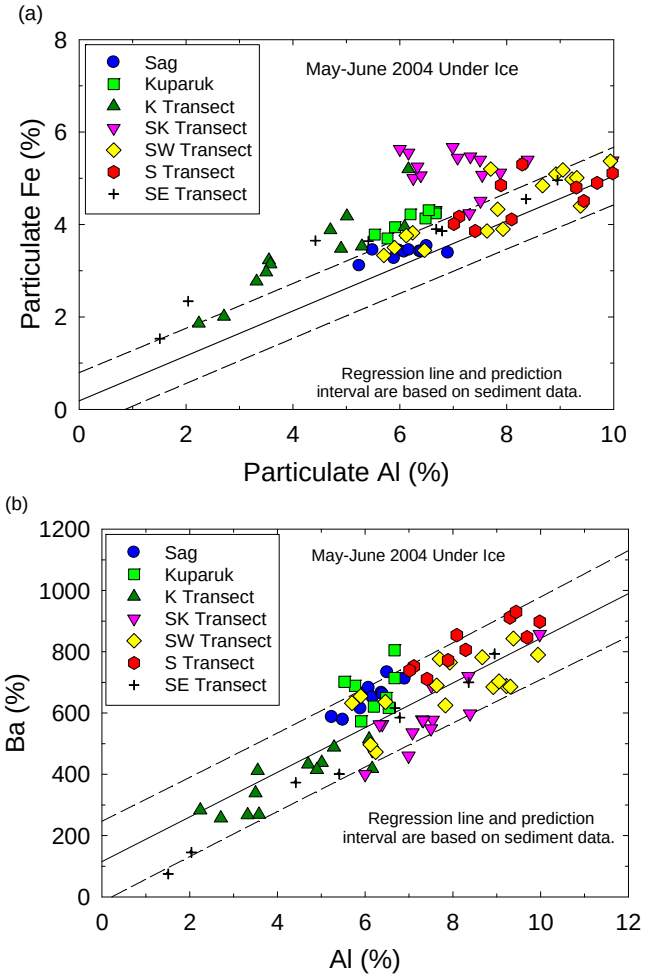

Figure 5-26. Concentrations of particulate (a) Fe and (b) Ba versus particulate Al for samples from the Sagavanirktok and Kuparuk rivers and the coastal Beaufort Sea. Solid lines are from a linear regression and dashed lines show 95% prediction intervals based on sediment data for the coastal Beaufort Sea from Trefry et al. (2003).

Very few deviations were observed for particulate Ba/Al in suspended sediments relative to trends predicted from bottom sediments (Figure 5-26b). This observation is consistent with previous data sets, as was the occasionally higher Ba/Al ratio for suspended sediments from the Kuparuk River.

The plot for particulate Cr versus particulate Al (Figure 5-27a) is similar to the Fe versus Al graph (Figure 5-26a) in that some data points from the K and SK transects plot above the upper confidence interval based on the sediment data (Figure 5-27a). In contrast, the data for Cr in particles from the Kuparuk River plotted on the lower half within the prediction interval rather than above the upper prediction interval as observed for Fe. When particulate Cr values were plotted versus concentrations of particulate Fe (Figure 5-27b), most of the data for the K and SK transects plotted within the prediction interval

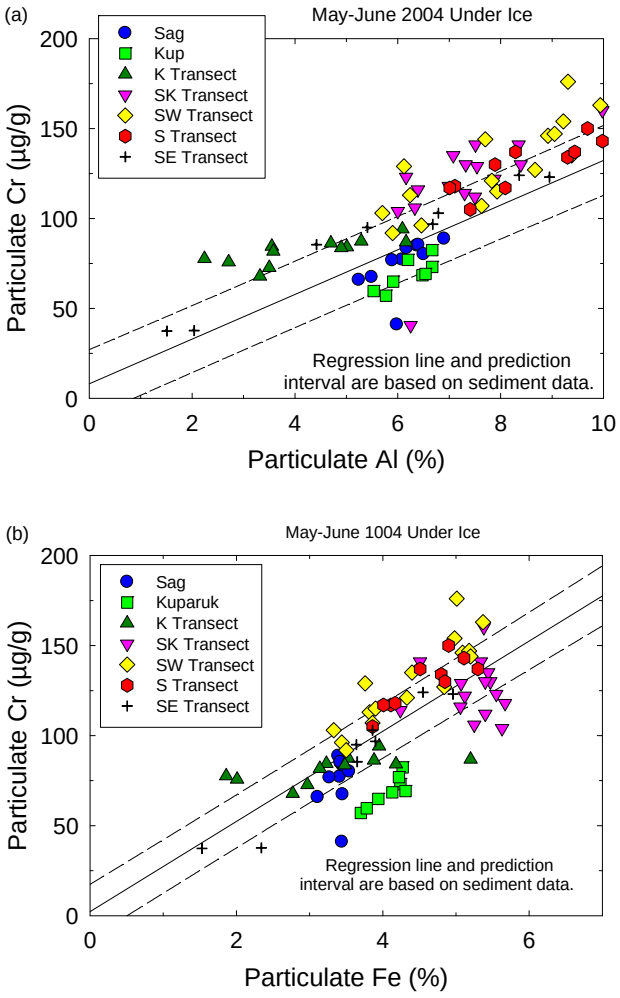

Figure 5-27. Concentrations of (a) particulate Cr versus Al and (b) particulate Cr versus Fe for samples from the Sagavanirktok and Kuparuk rivers and the coastal Beaufort Sea. Solid lines are from a linear regression and dashed lines show 95% prediction intervals based on sediment data for the coastal Beaufort Sea from Trefry et al. (2003).

for Cr/Fe in bottom sediments; however, the Kuparuk River samples and selected other samples plotted below the lower prediction interval.

No discernible shifts in concentrations of dissolved Cr were observed across the freshwater-seawater mixing zone under ice (Figure 5-28). Based on the observations in Figure 5-28, Cr was not very reactive during mixing under the ice. The low values for dissolved Cr in some low salinity samples from the SK transect may be related to lower concentrations of dissolved Cr in the Kuparuk River than shown by the single data point available for the river.

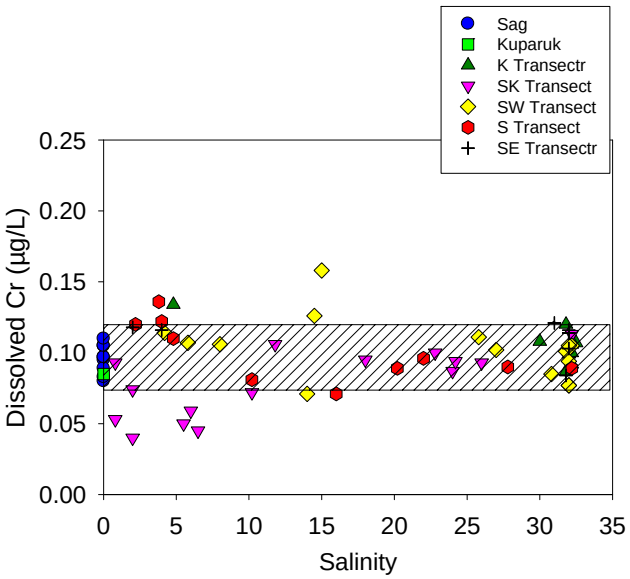

Figure 5-28. Concentrations of dissolved Cr versus salinity for water samples collected under ice across the mixing zones from the Sagavanirktok and Kuparuk rivers to the coastal Beaufort Sea. Shaded area was drawn to show the range in concentrations of dissolved Cr in both river water and the polar mixed layer.

Concentrations of particulate Cd follow the same trend previously described for As and Cu with high concentrations in samples with a lower Al content that were collected at higher salinity (Figure 5-29). In the case of Cd, the anomalously high concentrations of particulate Cd were 4 to 12 times greater than in typical Al-rich suspended or bottom sediments (Figure 5-29a). Enrichment of Cd in sediments due to diagenetic processes (e.g., Gobeil et al., 1997) is not likely to have played a role in the observed Cd enrichment of suspended particles because the highest sediment Cd value that has been observed and linked to such processes in the cANIMIDA study area was 0.4 µg/g (Trefry et al., 2003). Data for plankton show that Cd concentrations were typically in the range of 1 to 10 µg/g, dry wt. Suspended matter from our study with 50% of the typical values for Al (i.e., 4% instead of 8%) contained Cd at about 2 µg/g (dry wt.) that would extrapolate to a reasonable value of 4µg/g at 0% Al (all plankton or organic matter).

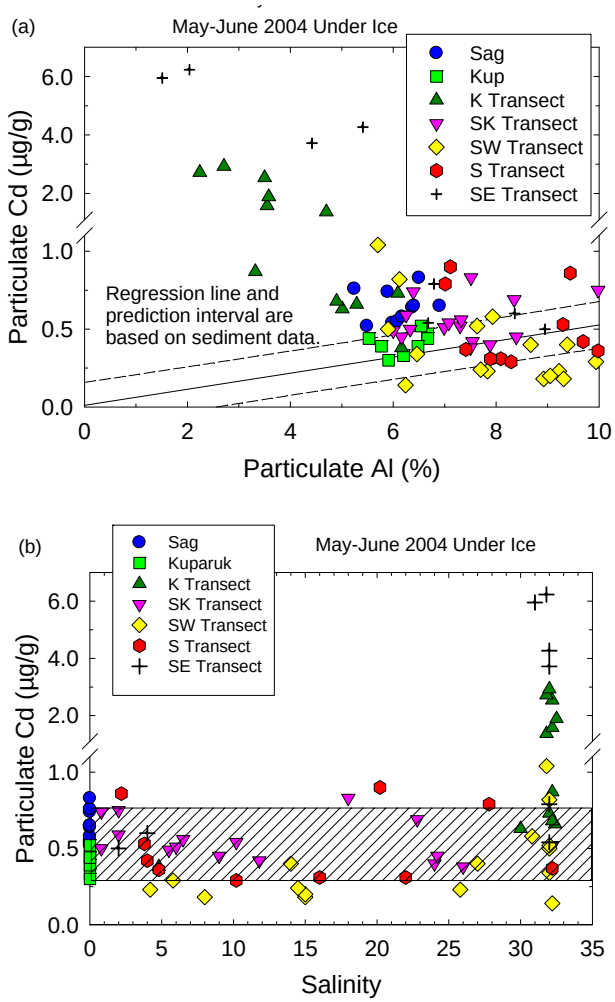

Figure 5-29. (a) Concentrations of particulate Cd versus particulate Al and (b) concentrations of particulate Cd versus salinity for samples from the Sagavanirktok and Kuparuk rivers and the coastal Beaufort Sea. Solid line on (a) is from a linear regression and dashed lines show 95% prediction intervals based on sediment data for the coastal Beaufort Sea from Trefry et al. (2003). Shaded area on (b) highlights typical range for dissolved Cu at salinity values <31.

Because the high concentrations of Cd were found for samples with low concentrations of TSS (in mg/L) and with a low total mass of TSS on the filter (Figure 5-30), the question of sample contamination is once again discussed. However, at TSS concentrations of <0.3 mg/L (Figure 5-30a), with a total mass of TSS on the filter that was <1 mg (Figure 5-30b), a ten-fold range in concentrations of particulate Cd was observed. Coupled with the clear negative relationship between particulate Al and Cd (Figure 5-29a), as well as similar trends for As and Cu, and the precautions taken during sample collection and processing, the argument against contamination during sampling and handling seems reasonable.

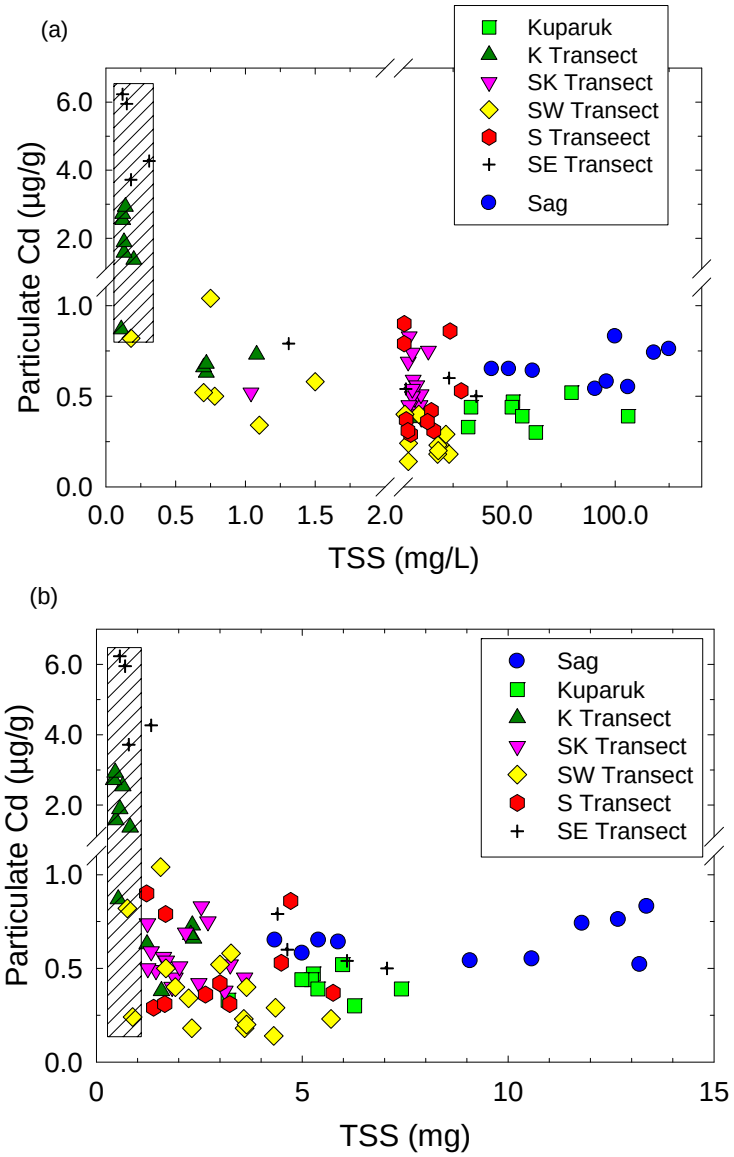

Figure 5-30. Concentrations of particulate Cd as a function of (a) concentrations of total suspended solids (TSS) and (b) as total mass of TSS on the filter for water samples collected in the rivers and under ice in the coastal Beaufort Sea. Shaded area shows range in concentrations of particulate Cd at low values for TSS as mg/L or as mg total mass.

Concentrations of dissolved Cd increased from 0.016 ± 0.005 µg/L in the rivers to 0.067 ± 0.013 µg/L in samples at salinities of 32 (Figure 5-31). However, considerable scatter was observed in the data for salinity versus dissolved Cd, and the correlation coefficient was 0.73 (Figure 5-31). As discussed previously for As, river water contained 50-90% particulate Cd and seawater (at a salinity of 32) contained<5% particulate Cd (Figure 5-32). In contrast with As, concentrations of dissolved Cd along the freshwater-seawater mixing gradient may be influenced by desorption of Cd. However, as shown for As, the

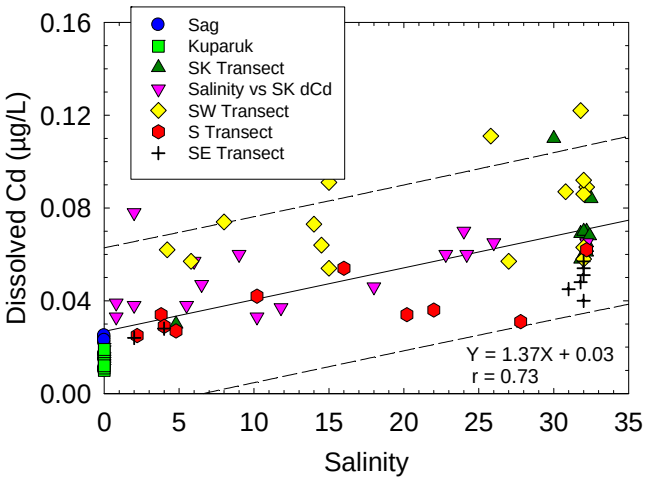

Figure 5-31. Concentrations of dissolved Cd versus salinity for water samples collected under ice across the mixing zones from the Sagavanirktok and Kuparuk rivers to the coastal Beaufort Sea. Solid line and equation are from a linear regression calculation, r is the correlation coefficient and the dashed lines show the 95% prediction interval.

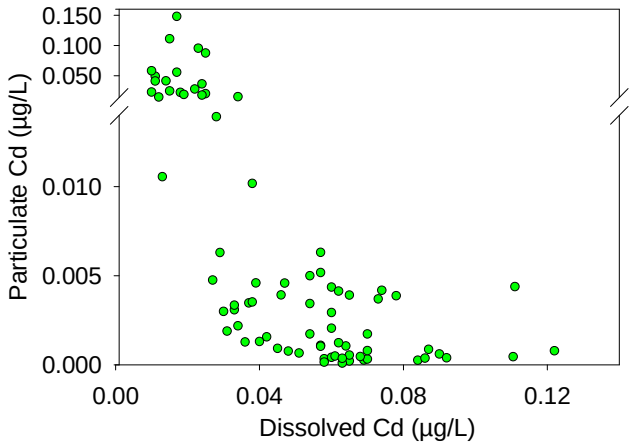

Figure 5-32. Concentrations of particulate Cd versus dissolved Cd for water samples collected in the rivers and under ice in the coastal Beaufort Sea.

relationship between particulate and dissolved Cd seems to suggest that the main source of dissolved Cd in the study area is from upwelling from deeper, offshore water.

Concentrations of particulate Zn did not vary greatly from the predicted trend with Al (Figure 5-33) because the concentrations of Zn in the suspended aluminosilicates were generally as high as or higher than found in plankton. In contrast, concentrations of As, Cu and Cd in plankton were much greater than found for aluminosilicates and thus the anomalies at low concentrations of Al reflected the higher levels of these three metals in plankton.

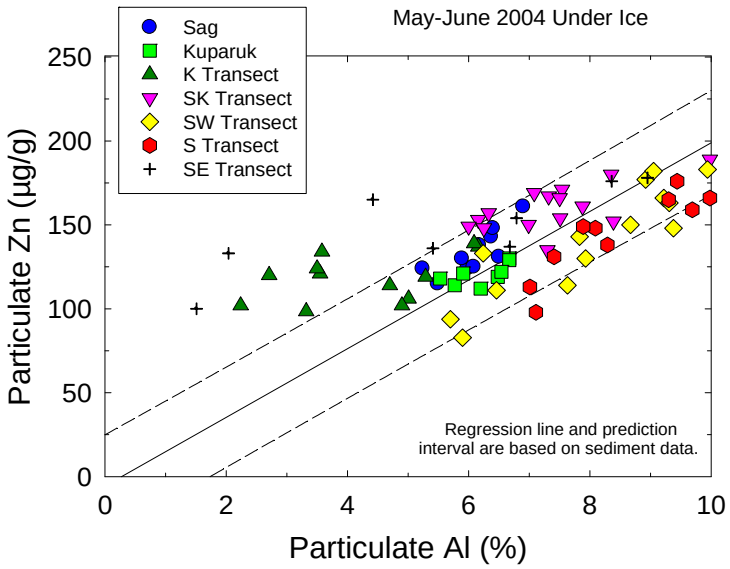

Figure 5-33. Concentrations of particulate Zn versus particulate Al for samples from the Sagavanirktok and Kuparuk rivers and the coastal Beaufort Sea.

The data for particulate Pb (Figure 5-34) show a mix of trends that seem to follow trends previously discussed for Cr. Some high concentrations of particulate Pb were found at a variety of locations and some low concentrations were found for the Kuparuk River (Figure 5-34). The same argument used against contamination for other metals can be used for Pb (Figure 5-35).

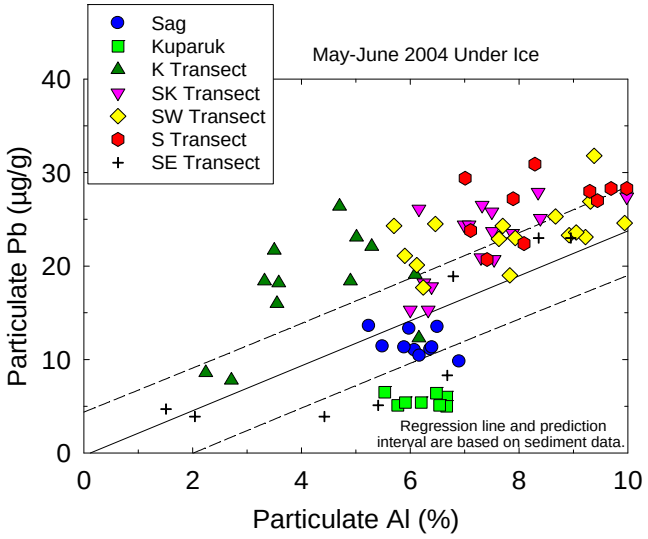

Figure 5-34. Concentrations of particulate Pb versus particulate Al for samples from the Sagavanirktok and Kuparuk rivers and the coastal Beaufort Sea.

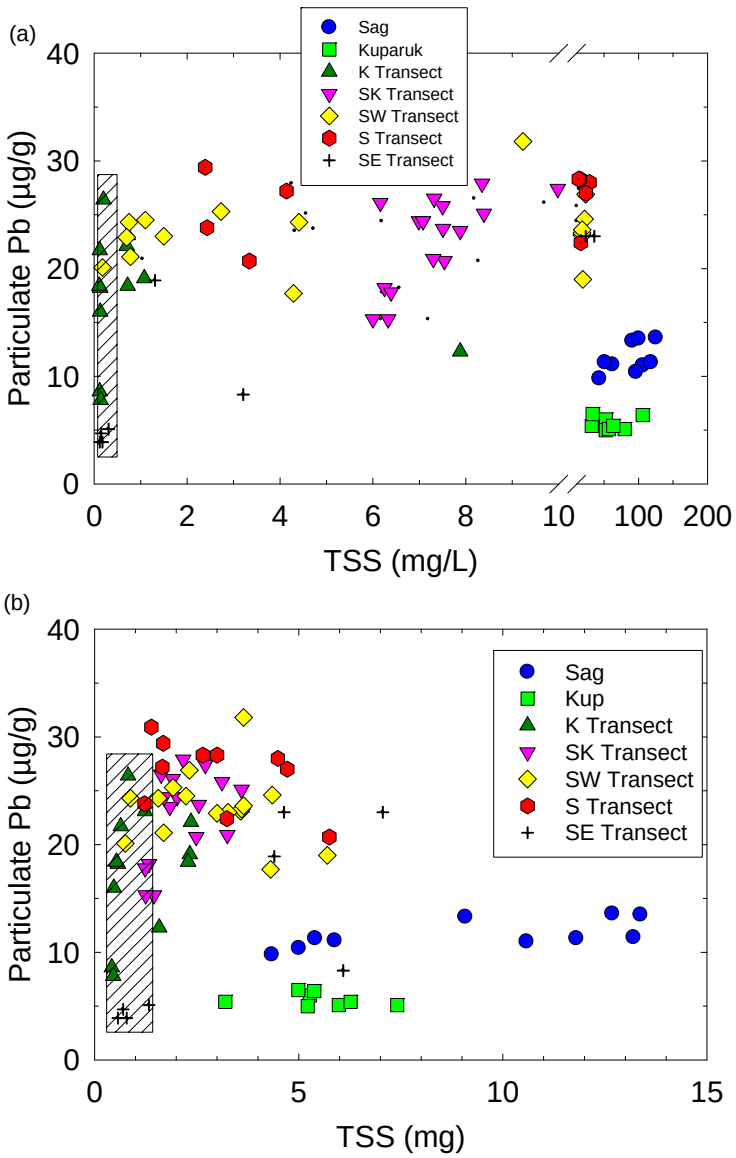

Figure 5-35. Concentrations of particulate Pb as a function of (a) concentrations of total suspended solids (TSS) and (b) as total mass of TSS on the filter for water samples collected in the rivers and under ice in the coastal Beaufort Sea. Shaded area shows range in concentrations of particulate Pb at low values for TSS as mg/L or as mg total mass.

5.4 Dispersion of Water Under Ice in the Beaufort Sea during Spring 2006

Offshore sampling was carried out at 15 stations plus 5 moorings from May 22 through June 2, 2006 (Figure 5-36, Table 5-4). Sampling was focused along three transects, two from the Kuparuk River and one from the Sagavanirktok River (Figure 5-36), all of which were along the main flow path of the respective rivers as determined during the 2004 study.

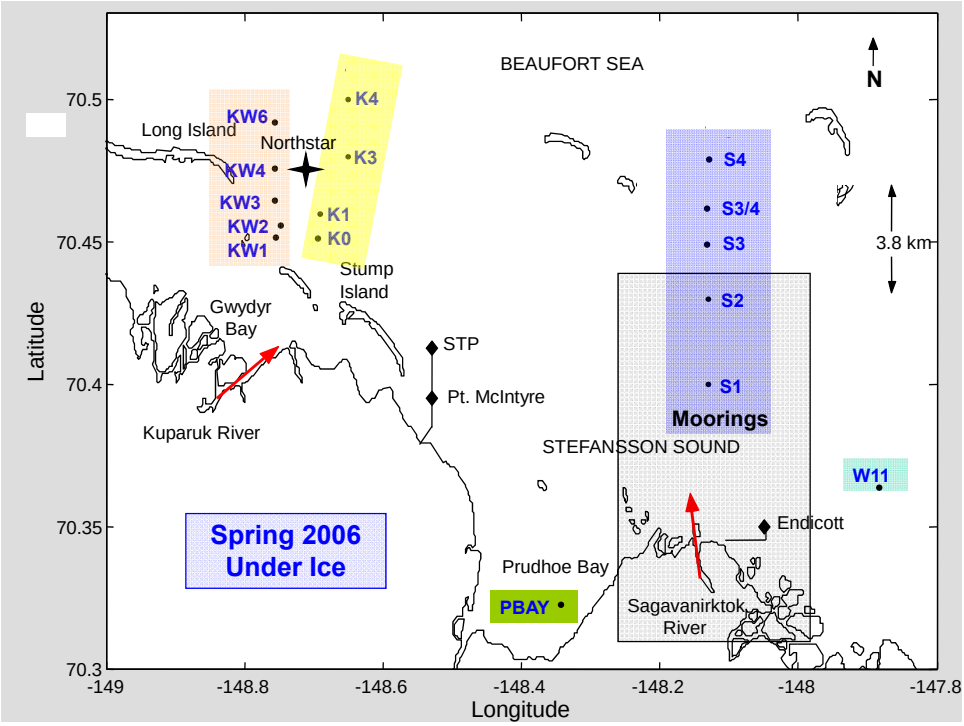

Figure 5-36. Map showing sampling stations for the May-June 2006 under-ice study in the coastal Beaufort Sea.

Table 5-4. Coordinates, sampling dates, total depths and ice thickness for water stations occupied during study during May-June 2006.

Station	Latitude (N)	Longitude (W)	Sample Date	Total Depth (m)	Ice Thickness (m)
K0	70°26.919'	148°43.001'	May 28	4.2	1.3
K1	70°27.645'	148°41.339'	May 26,28,29,31	6.8	1.3
K3	70°29.015'	148°38.773'	May 26,31	10.4	1.6
K3	70°29.015'	148°38.773'	May 31	4.0	1.9
K4	70°29.810'	148°38.739'	May 31	12.4	1.6
KW1	70°27.079'	148°45.158'	May 28	3.9	1.3
KW2	70°27.183'	148°44.763'	May 29	4.8	1.6
KW3	70°27.782'	148°44.763'	May 29,31	5.2	1.6
KW4	70°28.382'	148°44.763'	May 29,31	6.6	1.7
KW6	70°29.582'	148°44.763'	May 31	11.6	1.7
PBAY	70°20.000'	148°21.000'	May 23	2.7	1.4
R1	70°26.585'	148°21.879'	May 27, Jun 1	6.8	1.6
SOND0	70°23.000'	148°08.000'	May 24,26,30	3.5	1.8
SOND1	70°24.000'	148°08.000'	May 24,26,27,30	4.8	1.4
SOND2	70°25.500'	148°08.000'	May 22,24,26,27,30 Jun 1	5.8	1.5
SOND3	70°27.000'	148°08.000'	May 22,24,26,30 Jun 1	7.9	1.6
SOND3.5	70°27.750'	148°08.000'	May 30	5.8	1.7
SOND4	70°28.500'	148°08.000'	May 23,24,26,30	6.3	1.6
SOND5	70°29.250'	148°08.000'	Jun 2	11.8	1.6
SOND6	70°30.000'	148°08.000'	Jun 2	11.7	1.8
W11	70°21.992'	147°52.787'	May 23	5.4	1.5

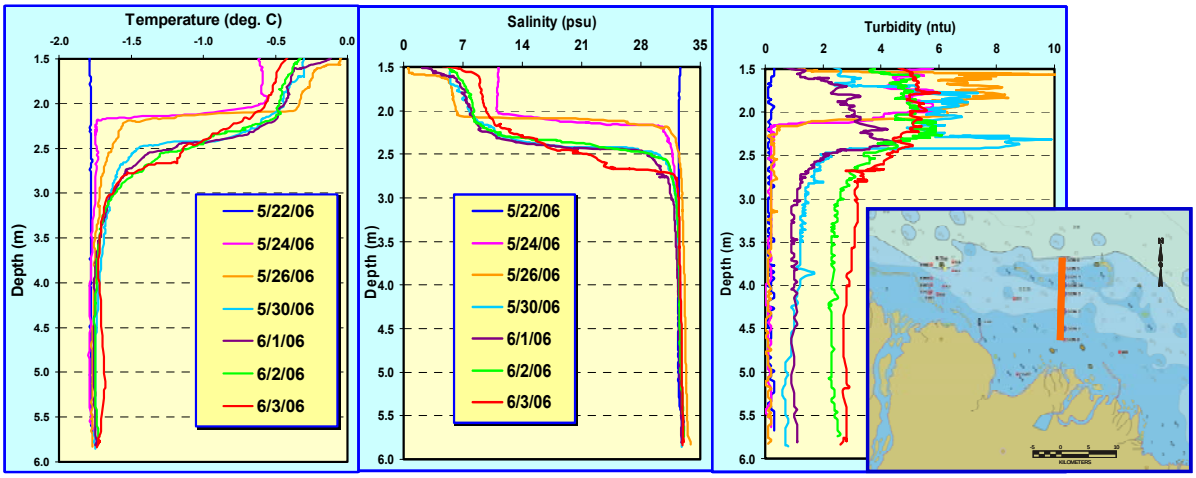

Figure 5-37. Vertical profiles of temperature, salinity, and turbidity taken at station S2 over a 10-day period during May-June 2006. The accompanying map depicts the station location along with the location of the onshore-offshore transect for salinity that is presented in Figure 5-38 below.

Vertical profiles of salinity, temperature, and turbidity in 2006 were similar to those seen during prior years (Figure 5-37). The first survey was conducted on May 22 prior to the breakup of the Sagavanirktok River, with subsequent surveys taking place during under-ice transport of river runoff. Vertical profiles of temperature and salinity from Station S2 show a very sharp pycnocline during the May 24 and 26 surveys, with some vertical mixing taking place and a gradual thickening of the plume during the May 30 to June 3 surveys (Figure 5-37). The plume was found to be about 2 m thick at the inshore locations and gradually mixed and thinned to less than 1 m further from shore (Figures 5-37, 5-38). In the spring of 2006, the under-ice plume was found to extend beyond the barrier islands (Reindeer and Cross Islands), but did not extend as far as the beginning of the shear zone which was located approximately 1 km beyond the barrier islands at the time of the survey. In 2004, the plume was found to extend to the edge of the shear zone which appeared to provide an underwater barrier of ice to increased spreading of the plume in the offshore direction.

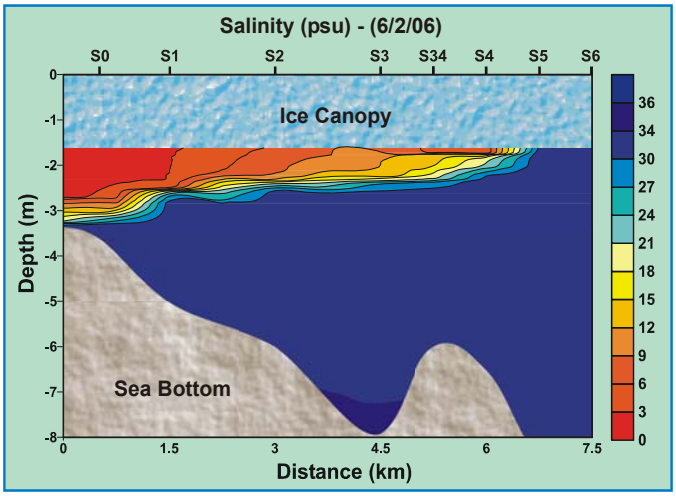

Figure 5-38 Vertical contour map of salinity along an onshore-offshore transect extending from Station S0 near shore to Station S6 beyond the barrier islands, June 2, 2006 (refer to above map in Figure 5-37 for transect location).

Turbidity and TSS concentrations did not follow the same mixing trends found for salinity as sediment particles were found to settle out of the water column. This pattern can be clearly seen in the turbidity profile where concentrations increase in the lower water column over time even though these bottom waters are marine and unmixed in terms of salinity and temperature characteristics (Figure 5-37).

Five moorings were deployed during 2006 from the ice surface with sensors located at a depth of 2 m (~0.5 m below the ice canopy). Three of the time series plots from these moorings show trends from Station SON-1 near shore to Station SON-4 located 4.5 km offshore (Figure 5-39). At the time of deployment on May 22, the Sagavanirktok River plume had already reached SON-1; salinity decreased and temperature increased over the next few days. The under-ice plume first reached SON-3, located 3 km from SON-1, about 6 days later; another 3 days passed before the plume reached SON-4 located 1.5 km from SON-3. Based on these two traverse times for the plume, the under-ice plume and associated currents were traveling at approximately 5 to 6 cm/s (0.5 km/day). These under-ice current estimates agree with the ADCP under-ice current measurements made by Weingartner (2006) during the breakup of the Sagavanirktok River in 2002 and with our data for 2004 that showed an average under-ice current of 7 ± 3 cm/sec (page 60). The time series plots for turbidity indicated that turbidity initially increased but later decreased as particles settled out. In contrast, the plots for salinity and temperature showed consistent trends of increasing temperature and decreasing salinity in the plume as a function of time.

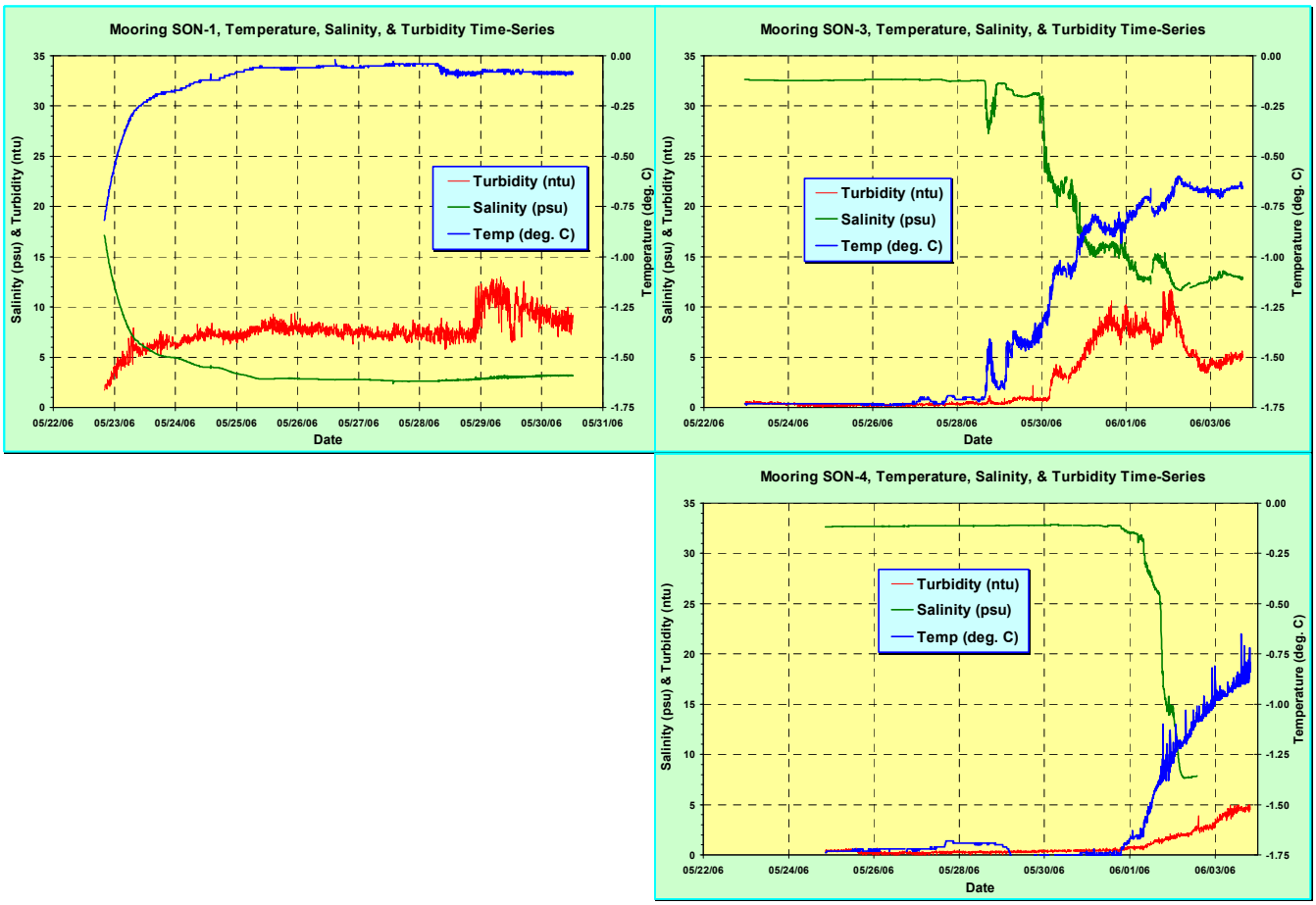

Figure 5-39. Time series plots for temperature, salinity and turbidity obtained during a 2-week period during spring breakup of 2006. Measurements were obtained along an onshore-offshore transect extending from Station SON-1 near shore to SON-4 located just inshore of the barrier islands.

5.5 Dispersion of Sediments and Chemicals Under Ice in the Beaufort Sea during Spring 2006

Concentrations of dissolved As increased linearly across the freshwater-seawater mixing zone from the Sagavanirktok River under-ice into the Beaufort Sea (Figure 5-40a). The trend was similar to that observed during May-June 2004 with a similar slope and range in concentrations of dissolved As at the seawater endmember. The trend for dissolved Cd was similar to that observed for As because concentrations increased with increasing salinity (Figure 5-40b). For both As and Cd, the trends once again reinforce the observation that the key sources of As and Cd were from upwelling of deeper water on to the shelf. The trend for Ba was opposite of that observed for As and Cd with a linear decrease offshore and data that support a minor degree of desorption of Ba from particles at low salinities (Figure 5-40c). Trends for Cr, Cu and Zn show relatively uniform values from salinities of 2 to 32; however, in each case, the higher concentrations observed in the rivers were not observed in the coastal Beaufort Sea (Figures 5-40d and 5-41 a,b)

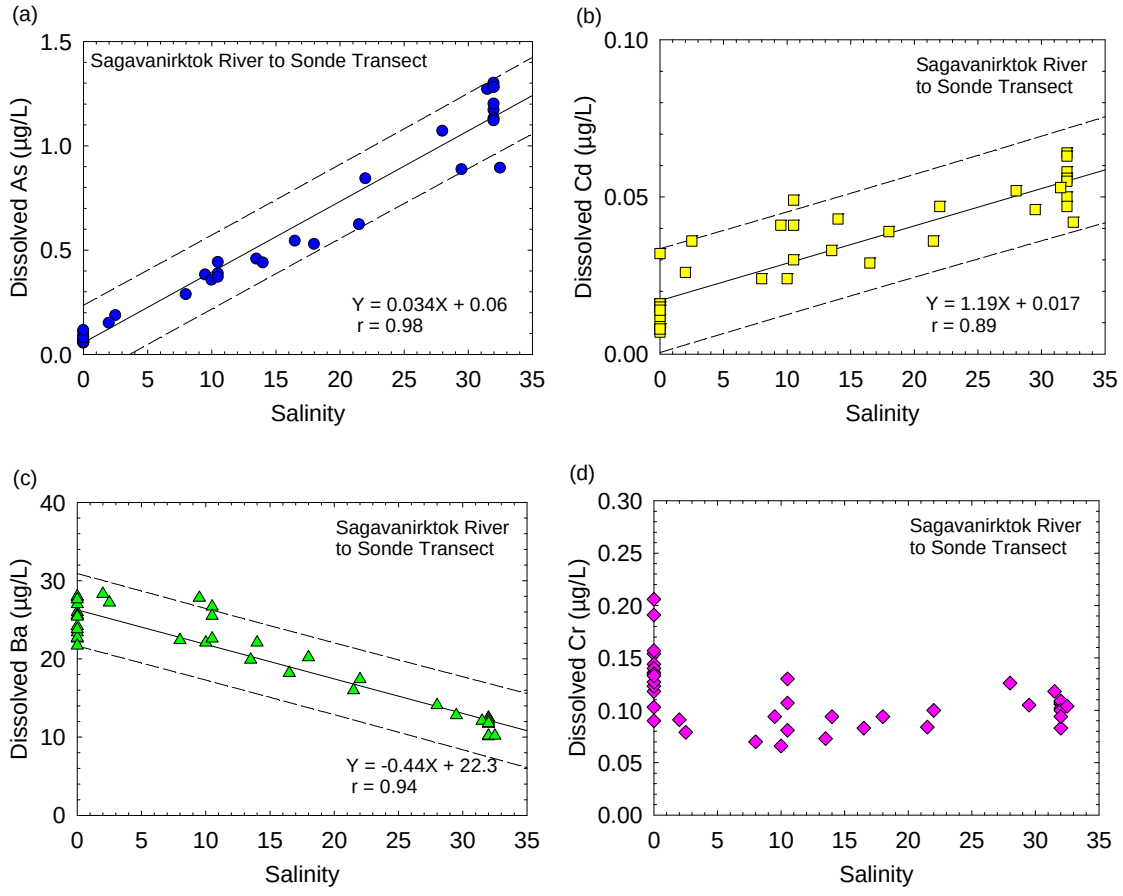

Figure 5-40. Concentrations of dissolved (a) As, (b) Cd, (c) Ba and (d) Cr versus salinity across the freshwater-seawater mixing zone from the Sagavanirktok River to the Coastal Beaufort Sea. Solid lines and equations are from linear regression calculations. Dashed lines shows 95% prediction intervals and r is the correlation coefficient.

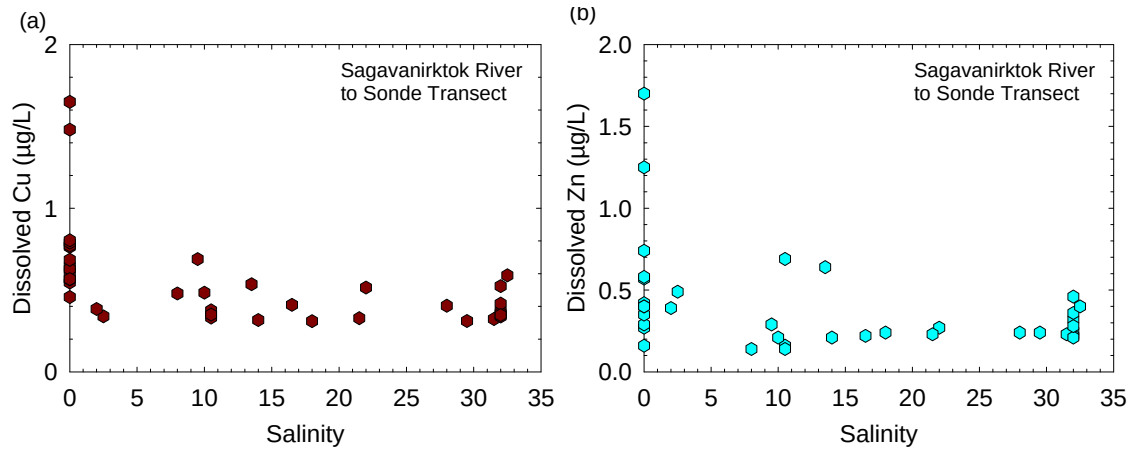

Figure 5-41. Concentrations of dissolved (a) Cu and (b) Zn versus salinity across the freshwater-seawater mixing zone from the Sagavanirktok River to the Coastal Beaufort Sea.

Concentrations of TSS were very low along the freshwater-seawater mixing zone from the Sagavanirktok River with all TSS values at salinities >2 equal to <10 mg/L, except for one value of 20 mg/L (Figure 5-42a). In 2004, most of the TSS concentrations at salinities of 2 to 20 were >10 mg/L with at least half >20 mg/L (Figure 5-16, page 65). This trend is most likely due to the much higher flow and longer duration of high flow for the Sagavanirktok River in 2004 relative to 2006 (Figure 3-2, page 20).

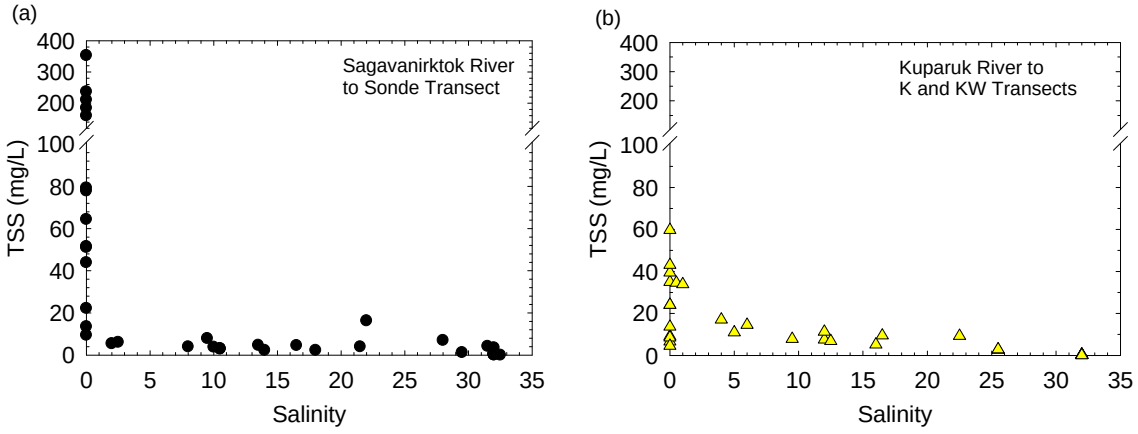

Figure 5-42. Concentrations of total suspended solids (TSS) versus salinity for the freshwater-seawater mixing zones from the (a) Sagavanirktok River and (b) Kuparuk River to the coastal Beaufort Sea during May-June 2006.

The TSS versus salinity plots in Figure 5-42 point out the six-fold difference in peak concentrations of TSS in the Kuparuk River versus the Sagavanirktok River during May-June 2006. On a relative basis, concentrations of TSS in the Kuparuk River decreased by less along the salinity gradient than observed for the Sagavanirktok River; however, the absolute TSS values were similar along the two different freshwater-seawater mixing zones.

Concentrations of Fe for suspended sediments from the Sagavanirktok River and its seaward plume plotted within, or very close, to the 99% prediction interval developed for Fe versus Al using sediments from the coastal Beaufort Sea (Figure 5-43a). In contrast, most of the data points for the Kuparuk River and under-ice plume plotted above the upper prediction interval (Figure 5-43b). This has been a recurrent trend that emphasizes differences in the composition and drainage basins of the two rivers as well as supporting a much larger role for the Sagavanirktok River as a source of sediments to the cANIMIDA study area than the Kuparuk River.

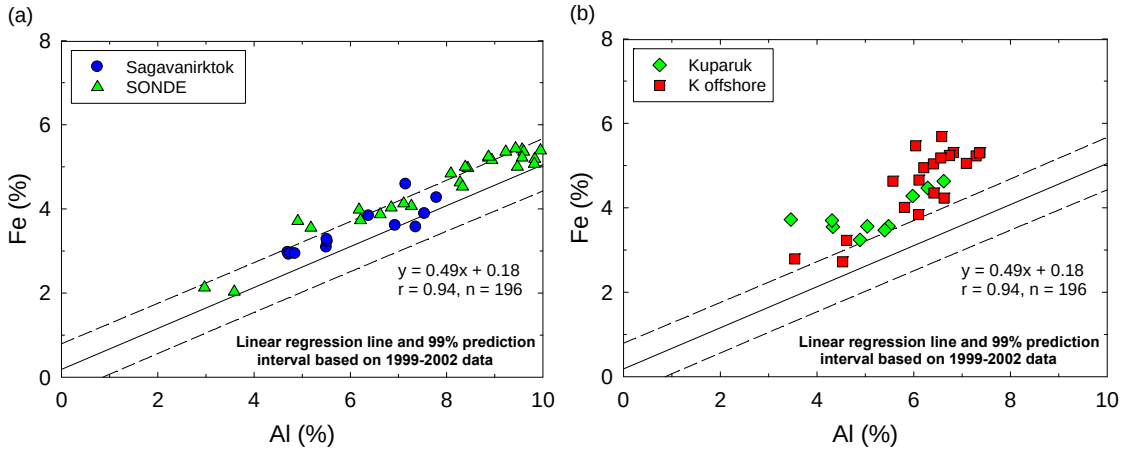

Figure 5-43. Concentrations of Fe versus Al for suspended sediments from the (a) Sagavanirktok River and (b) Kuparuk River and respective offshore, under-ice plumes in the coastal Beaufort Sea. Solid lines and equations are from linear regression analysis for the 1999-2002 data for bottom sediments from the coastal Beaufort Sea; dashed lines show 99% prediction intervals and r is the correlation coefficient (Trefry et al., 2003).

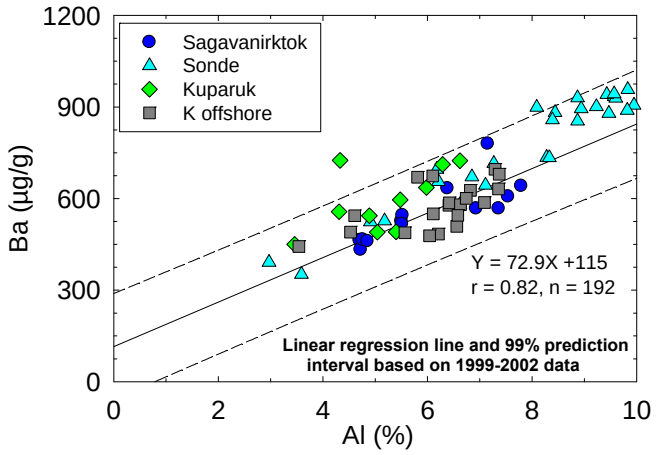

Figure 5-44. Concentrations of Ba versus Al for suspended sediments from the Sagavanirktok and Kuparuk rivers and their respective offshore, under-ice plumes in the coastal Beaufort Sea. Solid line and equation are from linear regressions for the 1999-2002 data for bottom sediments from the coastal Beaufort Sea; dashed lines show 99% prediction interval and r is the correlation coefficient (Trefry et al., 2003).

Concentrations of Ba for essentially all samples from each river and plume plotted within the 99% prediction interval established for bottom sediments in the coastal Beaufort Sea. (Figure 5-43). This trend supports and absence of any anthropogenic Ba inputs or reactions for particles from either river as they are carried seaward under the ice.

Most concentrations of Pb, Cr, Cu and Zn for samples of suspended sediments from the Sagavanirktok River and plume plot within the 99% prediction intervals for bottom sediments from the coastal Beaufort Sea (Figure 5-45). In contrast, a few data points for Cr and Cu, and many data points for Pb and Zn, from the Kuparuk River and under-ice plume plot above the upper prediction interval on the metal versus Al template for bottom sediments from Trefry et al. (2003) in Figure 5-45. Some of the Pb and Zn concentrations may have an anthropogenic origin; however, the elevated concentrations of Fe in the Kuparuk River and plume samples may indicate natural scavenging of Fe oxides that also contain Pb and Zn.

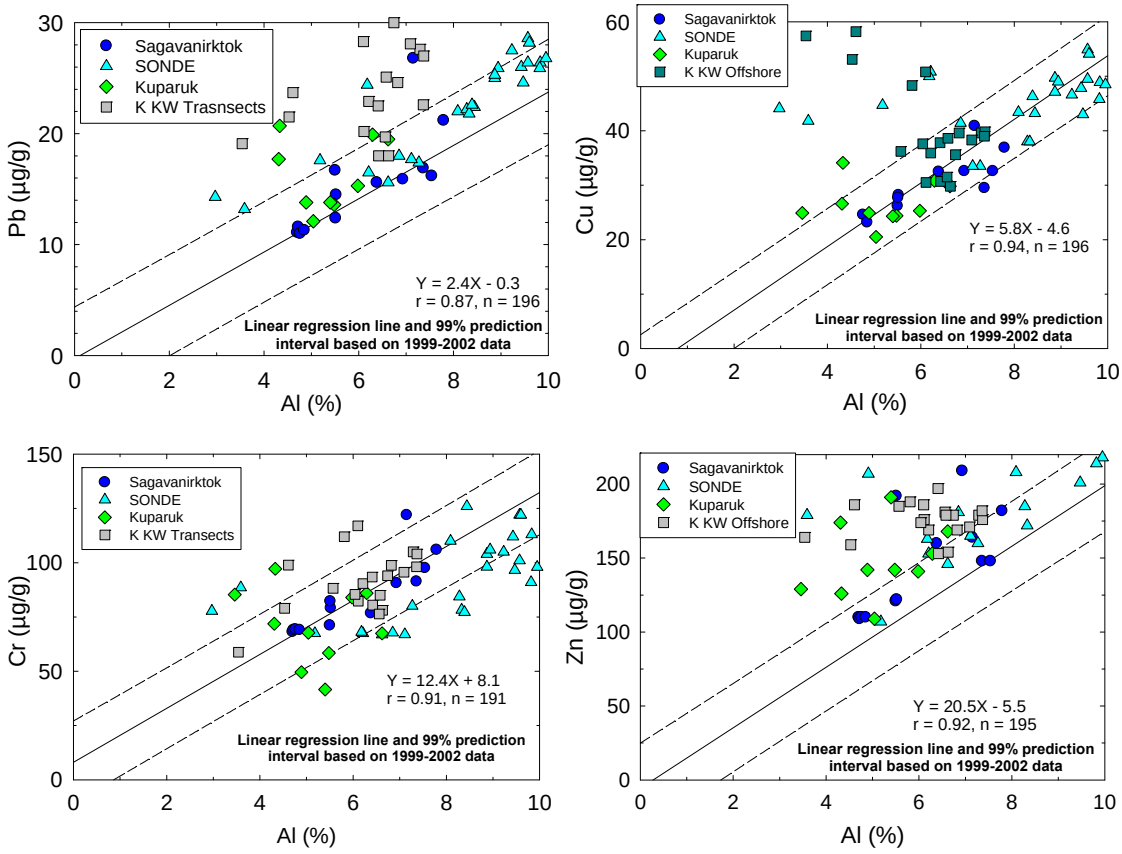

Figure 5-45. Concentrations of Al versus (a) Pb, (b) Cu, (c) Cr and (d) Zn for suspended sediments from the Sagavanirktok and Kuparuk rivers and their respective offshore, under-ice plumes in the coastal Beaufort Sea. Solid lines and equations are from linear regression analysis for the 1999-2002 data for bottom sediments from the coastal Beaufort Sea; dashed lines show 99% prediction intervals and r is the correlation coefficient (Trefry et al., 2003).

6. THE DISTRIBUTION OF SUSPENDED SEDIMENTS AND CHEMICALS DURING THE OPEN-WATER PERIOD

6.1 Overview

Vertical profiles for salinity, temperature and turbidity, as well as water samples for suspended sediments and dissolved and particulate metals were collected during the summers of 2004, 2005 and 2006 from the coastal Beaufort Sea. All the data are tabulated in the Appendices. Data from a modest sampling program for rivers also were collected during the summer period during the cANIMIDA Project and will be presented first. The format for this section combines some overviews of the complete data set as well as some specific studies that were carried out within a given year.

6.2 Suspended Sediments and Trace Metals in Rivers: Summer 2004, 2005 and 2006

Sampling of rivers during summer has been carried out to maintain a long-term data base for TSS and particulate and dissolved metals (Tables 6-1, 6-2, 6-3 and 6-4). Values for TSS in the Kuparuk River during summer 2004, 2005 and 2006 averaged 1.0 mg/L, about 25 to 60 times lower than during the spring floods (Table 6-2). Only one value for TSS of 1.4 mg/L was obtained for the Kuparuk River during summer 2004 (Table 6-2). This concentration of TSS was higher than typical values of 0.2-0.6 mg/L in previous years and in two out of three samples in 2005 and 2006. The slightly higher concentrations observed were most likely due to increased construction activity in the area west of the bridge where we sampled. Concentrations of TSS in the Sagavanirktok River were more variable during summer with a range of 0.5 to 53.4 mg/L (Table 6-1). An increase in TSS values >1-2 mg/L was typically linked to a rain event that raised flow and TSS (Table 6-1). During 2004, a rain storm raised water flow rate and concentrations of TSS in the Sagavanirktok River to 53 mg/L on August 3. All TSS values during summer were 10 to >300 times lower than during the spring melt.

At typical levels of TSS in summer (~2 mg/L), concentrations of particulate metals and organic carbon in the Sagavanirktok River were lower than in spring (Tables 6-1) but close to results obtained during summer for previous years (Trefry et al., 2004a). After the 2004 rainstorm, the concentrations of particulate metals increased to levels that were closer to those for particulate metals in spring 2004, except for Pb (Table 6-1). The rain seems to have carried in particles that were slightly more Pb-rich than typically observed (duplicate samples with Pb at 19.0 and 19.9 μg/g), perhaps representing a contribution from road runoff or deposition with rain.

Concentrations of dissolved metals in the Sagavanirktok River following the summer rain in 2004 were higher than in the pre-rain river water with concentrations of Cu and Pb ~3 times greater following the rain (Tables 6-3).

Table 6-1. Concentrations of particulate metals and organic carbon (POC) in the Sagavanirktok River for the seasons and years listed.

River		Al (%)	As (μg/g)	Ba (μg/g)	Cd (μg/g)	Cr (μg/g)	Cu (μg/g)	Fe (%)	Pb (μg/g)	Zn (μg/g)	TSS (mg/L)	POC (%)
Sagavanirktok Summer 2004 (n=2)	-	4.12 6.66	9.9 10.3	561 743	1.12 0.71	105 102	38.0 32.0	3.35 3.87	10.7 19.4	87.9 144	1.45 53.4	0.6 1.0
Sagavanirktok Spring 2004 (n=9)	Mean Std. Dev. Min. Max.	6.1 ± 0.5 5.2 6.9	10.7 ± 3.6 5.4 17.0	654 ± 53 578 733	0.65 ± 0.11 0.52 0.83	74.0 ± 14.5 41.1 88.8	31.0 ± 4.4 23.6 38.6	3.4 ± 0.1 3.1 3.5	11.7 ± 1.4 9.8 13.6	133 ± 14 115 161	127 ± 83 43 285	1.1 ± 0.2 0.8 1.5
Sagavanirktok Summer 2005 (n=2)	-	4.53 4.18	11.6 12.0	668 644	1.00 1.39	102 96	35.1 28.8	3.46 3.48	11.7 12.0	117 106	1.36 0.50	-
Sagavanirktok Summer 2006 (n=1)	-	6.91	7.6	625	0.67	113	31.8	3.65	19.3	167	8.9	1.3
Sagavanirktok 2006 (n=12)	Mean Std. Dev. Min. Max.	6.0 ± 1.2 4.7 7.8	8.4 ± 1.6 4.7 7.8	555 ± 96 433 780	0.53 ± 0.08 0.44 0.70	84.1 ± 16.7 68.2 122	29.6 ± 5.3 23.2 40.9	3.5 ± 0.6 2.9 4.6	15.5 ± 4.5 11.0 26.8	145 ± 35 109 209	131 ± 100 9.5 353	2.0 ± 0.5 1.2 3.0

Table 6-2. Concentrations of particulate metals and organic carbon (POC) in the Kuparuk River during the seasons and years listed.

River		Al (%)	As (µg/g)	Ba (µg/g)	Cd (%)	Cr (µg/g)	Cu (µg/g)	Fe (%)	Pb (µg/g)	Zn (µg/g)	TSS (mg/L)	POC (%)
Kuparuk Summer 2004 (n= 1)	-	3.44	7.6	551	0.20	43.7	29.4	3.06	15.7	131	1.35	3.9
Kuparuk Spring 2004 (n= 8)	Mean Std. Dev. Min. Max.	6.2 ± 0.4 5.5 6.7	8.1 ± 3.8 3.9 13.1	671 ± 72 573 805	0.41 ± 0.07 0.30 0.52	69.0 ± 8.5 57.1 82.4	34.0 ± 5.1 28.7 45.1	4.1 ± 0.2 3.7 4.3	5.6 ± 0.6 5.0 6.5	121 ± 6 112 130	59.5 ± 24.3 32 130	3.3 ± 1.0 1.6 4.9
Kuparuk Summer 2005 (n=2)	-	3.47 2.44	20.6 6.3	667 495	0.70 2.56	97.6 85.8	25.2 18.6	3.28 2.39	17.0 5.9	96.5 59.3	2.0 0.19	1.1
Kuparuk Summer 2006 (n=1)	-	4.01	12.4	448	6.6	76.6	31.9	4.59	38.0	155	0.39	8.6
Kuparuk Spring 2006 (n= 10)	Mean Std. Dev. Min. Max.	5.2 ± 1.0 3.5 6.6	7.1 ± 2.1 4.7 11.6	593 ± 103 450 725	0.53 ± 0.12 0.35 0.71	70.9 ± 17.6 41.6 97.2	26.6 ± 3.9 20.5 34.1	3.8 ± 0.5 3.2 4.6	17.0 ± 3.8 12.1 23.7	148 ± 25 109 191	25.4 ± 18.6 4.6 59.7	4.7 ± 2.1 2.6 7.8

Table 6-3. Concentrations of dissolved metals in the Sagavanirktok River for the season and year listed.

River		As (µg/L)	Ba (µg/L)	Cd (µg/L)	Cr (µg/L)	Cu (µg/L)	Pb (µg/L)	Zn (µg/L)
Sagavanirktok Summer 2004 (n=2)	-	0.126 0.174	38.0 31.8	0.009 0.003	0.166 0.160	0.233 0.661	0.004 0.010	0.18 0.21
Sagavanirktok Spring 2004 (n=9)	Mean Std. Dev. Min. Max.	0.068 ± 0.015 0.048 0.086	19.0 ± 1.8 16.1 22.6	0.018 ± 0.006 0.010 0.025	0.096 ± 0.010 0.080 0.110	0.50 ± 0.17 0.34 0.88	0.013 ± 0.006 0.007 0.023	0.28 ± 0.08 0.19 0.40
Sagavanirktok Summer 2005 (n=2)	-	0.096 0.102	41.6 44.8	0.003 0.004	0.108 0.137	0.264 0.196	0.004 0.004	0.14 0.13
Sagavanirktok Summer 2006 (n=1)	-	0.076	35.8	0.033	0.126	0.547	0.007	0.17
Sagavanirktok Spring 2006 (n=12)	Mean Std. Dev. Min. Max.	0.069 ± 0.016 0.054 0.108	25.2 ± 1.9 22.6 28.0	0.012 ± 0.004 0.007 0.016	0.147 ± 0.027 0.118 0.206	0.79 ± 0.38 0.46 1.6	0.031 ± 0.006 0.021 0.039	1.0 ± 1.0 0.3 3.6

Concentrations of dissolved metals in the Kuparuk River during summer showed variations that were similar to those observed for the Sagavanirktok River with overall higher values for As and Cu and lower concentrations of Cd, and Pb in the Kuparuk River relative to the Sagavanirktok River (Tables 6-3 and 6-4).

The percent of total metal in the rivers that was dissolved increased greatly during summer due to much lower values for TSS during summer (Table 6-5). For example, the % dissolved Ba in the Sagavanirktok River increased from an average of ~30% in May-June to >97% in summer 2005 (Table 6-5 and Table 4-1 on page 39). Even the % dissolved Pb increased from <5% in May-June to >20% in summer for the Sagavanirktok River. Similar trends were found for each year when spring and summer data were compared.

Values for log K_d in the summer samples were within the range of values found for spring for As, Cr and Zn in the Sagavanirktok River, but lower in summer than spring for Ba, and higher in summer than spring for Cd, Cu, and Pb. For the Kuparuk River, the log K_d values for summer were within the range of values for spring for As, Cu, Pb and Zn, lower for Ba and Cu and higher for Cd. To some degree, the distribution coefficients are conditional constants that respond to variations in mineralogy and surface area of the particles. Overall, the K_d values provide a first order approximation of the dissolved concentrations of metals as a function of metal concentrations of the suspended sediments.

Table 6-4. Concentrations of dissolved metals in the Kuparuk River for the season and year listed.

River		As (µg/L)	Ba (µg/L)	Cd (µg/L)	Cr (µg/L)	Cu (µg/L)	Pb (µg/L)	Zn (µg/L)
Kuparuk Summer 2004 (n=1)	-	0.161	35.8	0.002	0.147	0.858	0.014	0.28
Kuparuk Spring 2004 (n=8)	Mean Std. Dev. Min. Max.	0.041 (n = 1)	7.0 ± 1.5 3.5 8.6	0.014 ± 0.003 0.010 0.019	0.085 (n = 1)	0.21 ± 0.14 0.05 0.49	0.011 ± 0.008 0.003 0.023	0.35 ± 0.19 0.16 0.69
Kuparuk Summer 2005 (n=2)	-	0.080 0.084	41.8 52.2	0.002 0.002	0.083 0.088	0.635 0.630	0.013 0.013	0.22 0.18
Kuparuk Summer 2006 (n=1)	-	0.081	40.6	0.012	0.081	0.626	0.019	0.11
Kuparuk Spring 2006 (n=10)	Mean Std. Dev. Min. Max.	0.089 ± 0.028 0.061 0.153	25.2 ± 19.1 16.8 79.3	0.008 ± 0.004 0.003 0.013	0.115 ± 0.022 0.078 0.152	0.57 ± 0.19 0.35 0.99	0.038 ± 0.013 0.020 0.062	0.82 ± 0.57 0.37 2.37
Colville Summer 2006 (n=1)	-	0.141	59.0	0.012	0.107	1.06	0.026	0.13

Table 6-5. Data (for n =2) for summer 2005 and means and standard deviations [SD] for data summaries (May-June 2004-6) showing percent of total metal in rivers that was dissolved and log K_d.

River	**% Dissolved**	As (%)	Ba (%)	Cd (%)	Cr (%)	Cu (%)	Pb (%)	Zn (%)	TSS (mg/L)
Sagavanirktok Summer 2005 (n=2)	-	85.9 94.5	97.9 99.3	68.8 85.3	43.7 74.2	84.7 93.2	20.0 40.2	46.7 71.2	1.36 0.50
Kuparuk Summer 2005 (n=2)	-	65.9 98.6	96.9 99.8	58.7 80.8	29.7 84.7	92.6 99.5	27.6 92.2	53.2 94.2	2.0 0.19
May-June 2004-6 Sagavanirktok [Kuparuk]		10 [28]	30 [39]	25 [41]	2 [6]	20 [30]	2 [8]	6 [15]	129 [43]
River	**Log K_d**	As	Ba	Cd	Cr	Cu	Pb	Zn	TSS (mg/L)
Sagavanirktok Summer 2005 (n=2)	-	5.08 5.07	4.21 4.16	5.52 5.54	5.98 5.85	5.12 5.17	6.47 6.48	5.92 5.91	1.36 0.50
Kuparuk Summer 2005 (n=2)	-	5.41 4.88	4.20 3.98	5.54 6.11	6.07 5.99	4.60 4.47	6.12 5.66	5.64 5.52	2.0 0.19
May-June 2004-6 Sagavanirktok [Kuparuk]		5.15 [4.95]	4.46 [4.72]	4.63 [4.66]	5.84 [5.85]	4.72 [5.01]	5.85 [5.74]	5.85 [5.74]	129 [43]

6.3 Suspended Sediments and Trace Metals Offshore – Summer 2004, 2005, 2006

6.3.1 Sampling Locations, Hydrography and Total Suspended Solids

Sampling in the coastal Beaufort Sea during July-August 2004 was carried out at 10 of the same stations studied during May-June 2004 as well as at 11 of the traditional locations as shown below.

Stations from Under Ice Study during May-June 2004 (Figure 5-1):
K1, K2, K3, SW2, SW4, SW5, SE1, SE2, SE3, SE4

Traditional Stations (Figure 6-1):
N01, N23, N24, L01, L04, L17, 3A, 5(5), 5(10), PB1

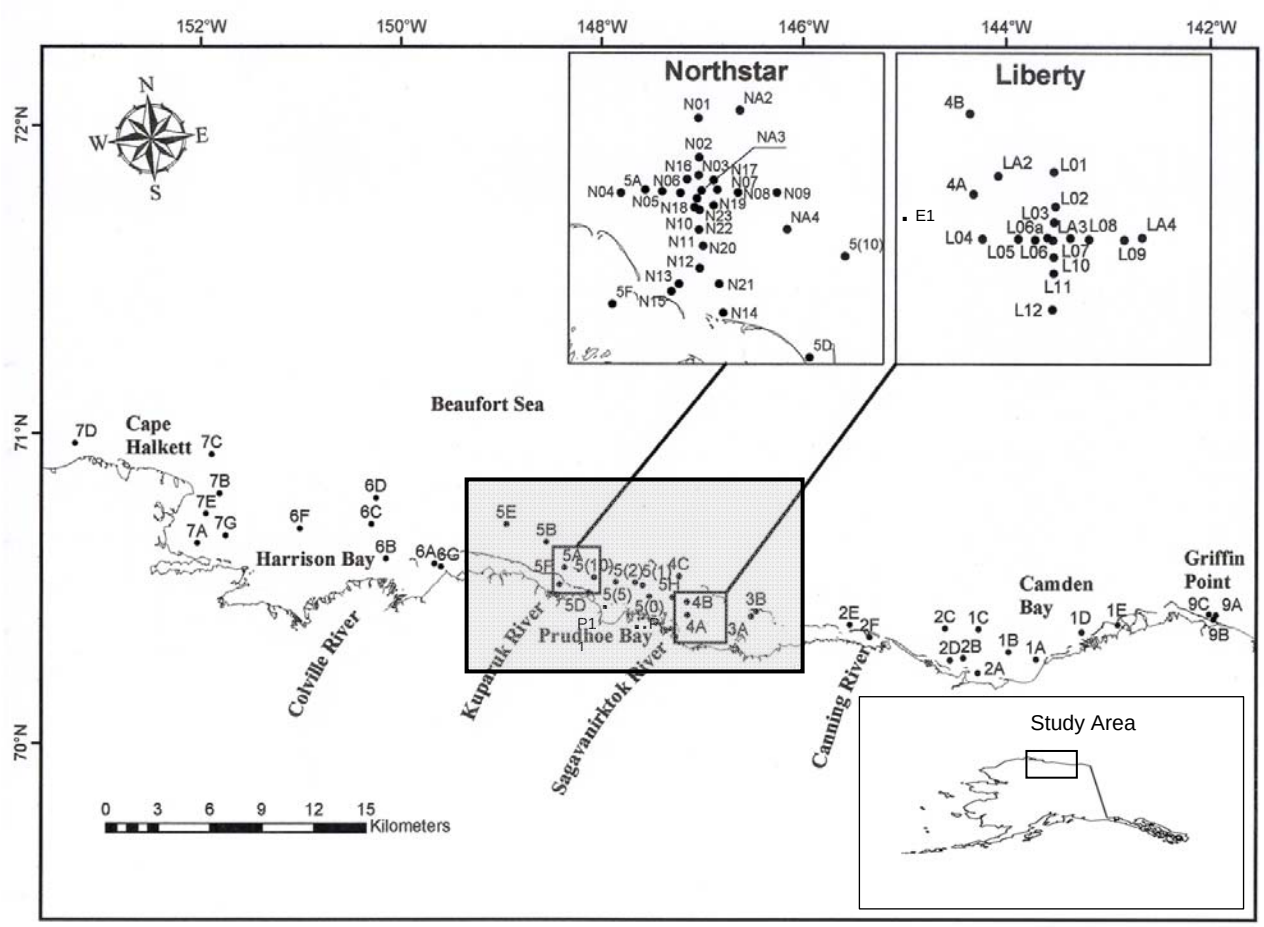

Figure 6-1. Map showing the western portion of the coastal Beaufort Sea with inset maps of Alaska, the oil production site at Northstar Island and a possible future drilling site at Liberty Prospect. The Task 3 and 4 portions of the cANIMIDA study focus mainly on the area shown in the shaded box.

During July-August 2005, sampling was carried out at the following locations:

Along the salinity gradient from the Sagavanirktok River (n = 18)

Northstar stations: N06, N08 and N23 (n = 9)

Liberty and Boulder Patch Stations: Dunton DS11 area (n = 9), L01A, L01B, L01C, L17, L17A, L17B, L18, BP01 (n = 31)

Beaufort Sea Monitoring Program (BSMP) stations: 1A, 1C, 1E, 2A, 2F, 2G, 4A, 4B (n = 16)

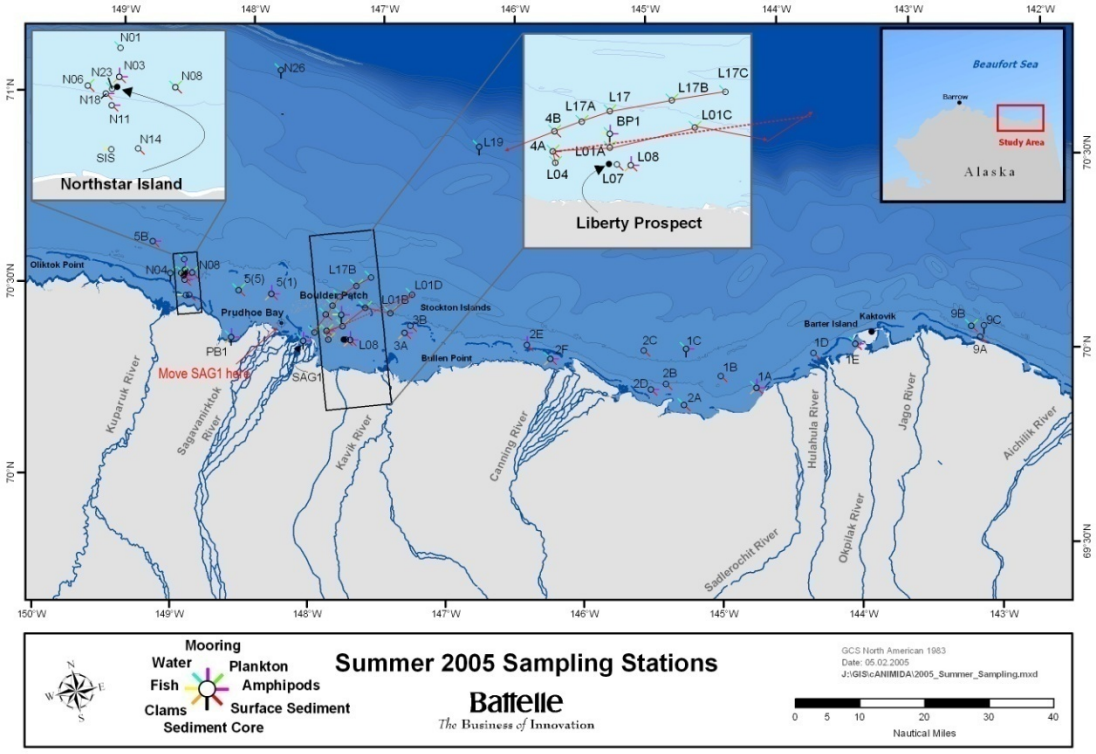

Figure 6-2. Map showing cANIMIDA study area in the Beaufort Sea along the northern coast of Alaska. Inset map in upper right-hand corner shows study area on map of Alaska. The other two inset maps show the area around Northstar Island and Liberty Prospect. Map shows sampling stations from 2005 summer field season. Map courtesy of Battelle.

The 2005 sampling focused more on the area from the mouth of the Sagavanirktok River to seaward of the barrier islands. A detailed discussion of the biogeochemistry of As and Hg from the 2005 sampling expedition is described in Section 7. Additional data and discussion of the 2005 data are included in this section as an overview of the open waters of the cANIMIDA study area during 2004, 2005 and 2006.

During July-August 2006, sampling was carried out at the following locations that are shown on Figures 6-1 and 6-2 as well as the map for summer 2006 that is Figure 1-2 (page 5):

Along the salinity gradient from the Sagavanirktok River (n = 12)

Northstar stations: N01, N08, N14 and N23 (n = 12)

Liberty (and BSMP) Stations: L08, L17, L22, 5(5) (n = 14)

Typically, salinities in the upper layer of the water column increase between early June and late July as break-up of the ice cover is followed by mixing due to wind. For example, at station K1, the salinity in the upper 2 m increased from ~11 on May 23, 2004, under ice, to ~23 during the open-water period (Figure 6-3). The bottom water was essentially unchanged. The water column at station K1 was still stratified. A similar change was observed for station SW4 with a progression of fresher and fresher water in the surface layer during late May reversing by early August (Figure 6-4).

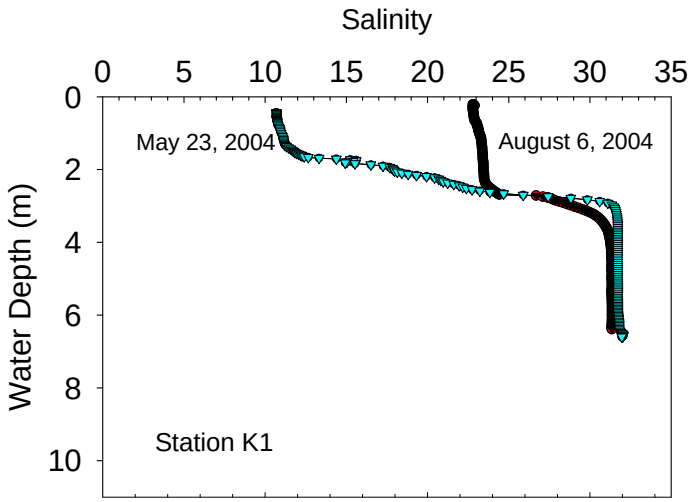

Figure 6-3. Vertical profiles for salinity at station K1 on May 23 and August 6, 2004.

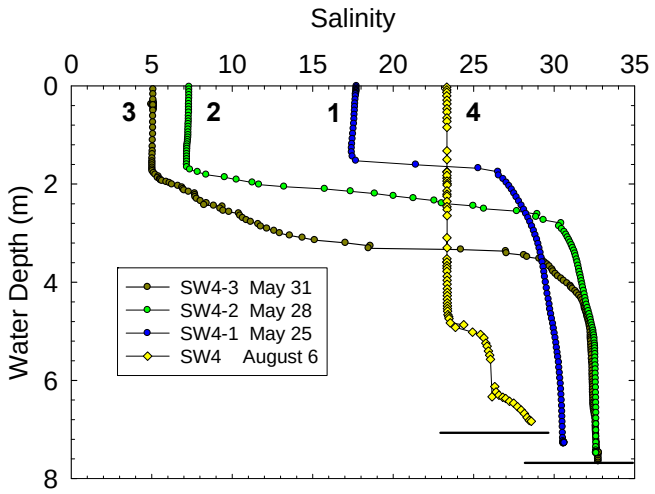

Figure 6-4. Vertical profiles for salinity at station SW4 during three days in May and on August 5, 2004. Numbers at the top of each profile show the chronological sequence for data collection with a gap of >2 months between profile 3 and 4. Lines at base of profiles show seafloor.

Turbidity was enhanced throughout the water column at most sites in late-July and August, 2004 (e.g., August in Figure 6-5). Both salinity and turbidity were uniform to a depth of ~5 m at station SW4 in August 2004 due to active mixing during relatively strong winds (10-15 kts) on 2-3 days before sampling (Figures 6-4 and 6-5). Similar trends to that shown for station SW4 were observed for most, but not all stations during

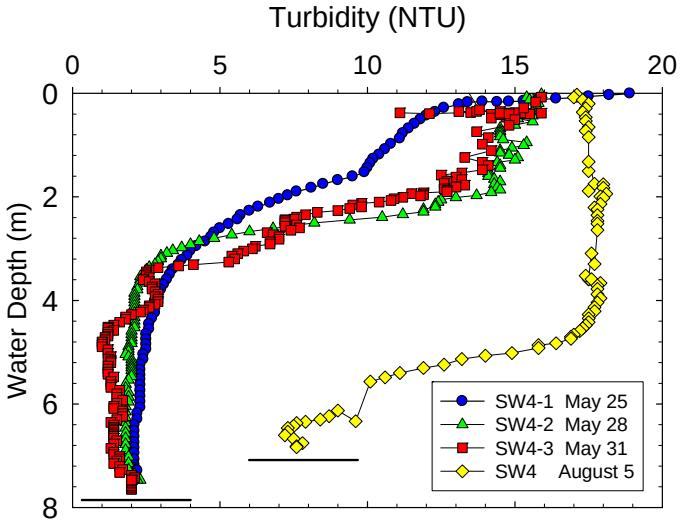

Figure 6-5. Vertical profiles for turbidity for dates specified in May and August 2004. Lines at base of profiles show seafloor.

summer 2004. However, in shallow water (<5 m), such as at station L17, the salinity and turbidity profiles were uniform from top to bottom.

The data in Table 6-6 show the mean, maximum and minimum values for TSS for all stations in the study area and for stations in the area of Northstar Island for 1999-2002 and 2004-2006. These data show higher mean concentrations of TSS in 1999, 2000 and 2004 relative to 200

1, 2002, 2005 and 2006 in the cANIMIDA area collectively as well as in the area of Northstar Island (Table 6-6). The very high TSS concentrations in 1999 are anomalous relative to the complete data set. Northstar Island was not constructed until winter 2000. However, much of the 1999 data were collected following a 5-day storm with >20 knot winds. In contrast, 2002, 2005 and 2006 data, for example, were collected during relatively calm conditions with considerable sea ice throughout the study area. During the 2000, 2001 and 2004 sampling periods, conditions were moderate with 5 to 15 knot winds during most of the sampling period. Furthermore, more samples from deeper water, seaward of the barrier islands are included in the mean values for 2005 and 2006. During 2004, relative calm was encountered during most of the study period as reflected in the low mean value for TSS in the Northstar area and in much of the rest of the study area (Table 6-6). The strong winds discussed above late in the 2004 study period yielded the high maximum value of 64 mg/L east of Endicott (Table 6-6).

The overall absolute values for TSS and turbidity during the open-water period were directly related wind conditions as discussed previously (Trefry et al., 2004a) and summarized in Table 6-7. Thus, during a given summer, the mean and range of measured values for TSS typically reflected the winds and weather. As an interesting aside, a layer of sediment only 0.02 cm thick would need to be resuspended and mixed through the water column of 8 m to yield TSS concentrations of 40 mg/L (details in Figure 6-6).

The data presented here and from many vertical profiles and horizontal tows presented in previous reports (Trefry et al., 2004a) show no significant differences in turbidity or concentrations of TSS in proximity (within 100 to 500 m) to Northstar Island relative to other locations in the ANIMIDA study area. This result is consistent with the coarse-grained composition of the original sand and gravel used to construct the island and the armoring that covers the slope of the island to the seafloor. Data for turbidity also were collected and are tabulated in the Appendices. The equation in Figure 6-7 can be used to convert turbidity values to TSS.

Table 6-6. Summary data for total suspended solids (TSS) for all stations in the ANIMIDA and cANIMIDA study area during the open-water period and for a subset of stations in the area of Northstar Island.

All Stations Year	n	TSS Mean ± SD (mg/L)	TSS Maximum (mg/L)	TSS Minimum (mg/L)
1999	31	30 ± 27	119	2.9
2000	51	8.2 ± 4.8	26	1.7
2001	34	5.1 ± 2.1	8.7	0.9
2002	32	2.1 ± 1.3	4.4	0.2
2004	45	13 ± 16	64	0.5
2005	65	1.7 ± 1.4	6.7	0.3
2006	26	1.3 ± 0.7	4.0	0.4

Northstar Area Year	n	TSS Mean ± SD (mg/L)	TSS Maximum (mg/L)	TSS Minimum (mg/L)
1999	17	38 ± 33	119	2.9
2000	35	7.3 ± 4.0	16	1.7
2001	15	4.1 ± 1.8	6.3	0.9
2002	11	2.5 ± 1.5	4.4	0.2
2004	15	6.2 ± 4.8	16	0.5
2005	9	1.4 ± 0.8	3.6	0.8
2006	12	1.1 ± 0.4	2.1	0.6

Table 6-7. Trends in concentrations of total suspended solids (TSS) in the coastal Beaufort Sea as a function of wind and ice conditions for water depths <10 m.

Wind and Ice Conditions when TSS data were obtained	Typical Range in TSS concentrations
TSS Under ice	TSS typically 0.1 to 0.5 mg/L
TSS in Open Water	
Winds calm to 5 knots (0 to 2.5 m/sec)	TSS typically 1 to 4 mg/L
Winds 5 to 10 knots (2.5 to 5 m/sec)	TSS typically 3 to 8 mg/L
Winds 10 to 20 knots (5 to 10 m/sec)	TSS typically 5 to 15 mg/L
Winds >20 knots (>10 m/sec)	TSS typically 50 to 100 mg/L

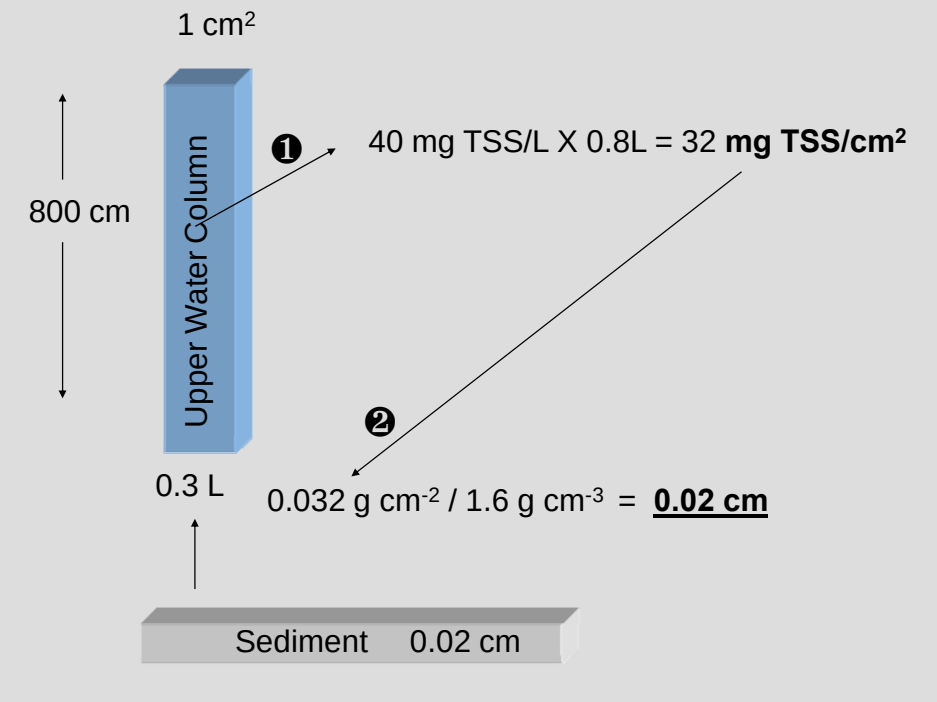

Figure 6-6. Schematic representation of the thickness of a layer of bottom sediments that would need to be resuspended in an 8-m deep water column to produce a value for total suspended solids (TSS) of 40 mg/L. The calculation can be described as follows: (1) the integrated amount of suspended sediments in the 8 m of the water column as [800 cm x 1 cm^2 x 40 mg/1000 cm^3 = 32 mg TSS], (2) TSS of 32 mg or 0.032 g divided by wet weight density of 1.6 g cm^{-3} yields thickness of sediment of 0.02 cm, the calculated thickness of a layer of sediment that would need to be resuspended to yield a TSS of 40 mg/L.

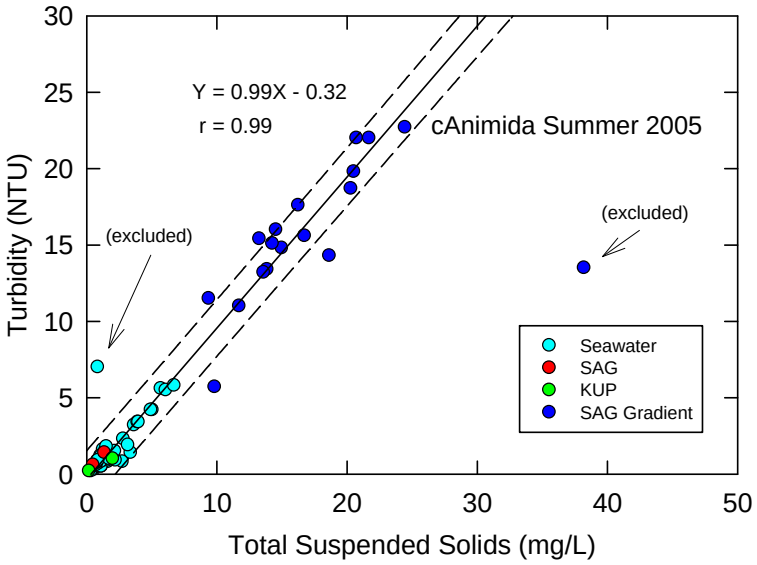

Figure 6-7. Turbidity versus total suspended solids for samples from the open Beaufort Sea during summer 2005. Solid line and equation are from a linear regression, r is the correlation coefficient and the dashed lines show a 95% prediction interval.

6.3.2 Particulate Metals

Concentrations of particulate metals in the open-waters of the Beaufort Sea were variable as a function of the organic matter and clay content. The grand averages for 2000, 2001, 2002, 2004, 2005 and 2006 in Table 6-8 show some interannual variability; however, most of the variations are due to differences in the composition of the suspended sediments as shown by variations in concentrations of Al and Fe and generally comparable shifts in concentrations of trace metals. Average concentrations of Al, Fe and trace metals in bottom sediments (Table 6-8) are lower than found in suspended sediments because the bottom sediments contain more quartz sand and carbonate shell material that dilutes concentrations of trace metals. Thus, any comparisons of metal concentrations between suspended sediments and bottom sediments are made by using metal/Al ratios.

Concentrations of particulate metals in the Northstar area were not significantly different from values obtained throughout the cANIMIDA area during 2004, 2005 and 2006 with the exception of Cd in 2004 and Pb in 2006. As explained below, the Cd observation is most likely due to increased organic matter (plankton) as shown by the lower Al content in the 2004 samples of suspended sediment from the Northstar area. The slightly increased Pb may be related to trace amounts of input from flaring or island activities.

Table 6-8. Mean concentrations of particulate metals for water collected from the coastal Beaufort Sea and near Northstar Island (NS) during the open-water season.

Year	Al (%)	As (µg/g)	Ba (µg/g)	Cd (µg/g)	Cr (µg/g)	Cu (µg/g)	Fe (%)	Pb (µg/g)	Zn (µg/g)
2000 (n = 51)	7.4	21	738	0.66	104	40	4.3	30	154
2001 (n = 34)	8.0	21	775	0.49	111	48	4.8	27	132
2002 (n = 32)	5.9	28	564	0.72	82	39	4.1	21	103
2004 Area wide (n = 42)	6.9	22	680	0.54	105	31	4.0	19	137
2004 NS (n = 7)	6.3	18	674	0.91	90	38	3.8	21	144
2005 Area wide (n = 65)	4.9	22	507	1.4	99	31	3.6	19	124
2005 NS (n = 9)	5.0	27	581	1.0	106	27	3.7	18	108
2006 Area wide (n=26)	5.7	25	574	1.1	88	36	3.9	22	161
2006 NS (n = 12)	5.7	26	598	1.0	84	39	4.1	30	163
Beaufort Sea Bottom Sediment (Trefry et al.,2003)	3.9	11	394	0.22	57	19	2.3	10	70

Some concentrations of Cd in suspended sediments show a good fit to the sediment prediction intervals, whereas others show a negative trend versus Al for data that plotted above the upper prediction interval on the Cd versus Al plot (Figure 6-7). The higher concentrations of Cd at lower Al values can be tied to Cd values in plankton that were at values of several µg/g. In contrast, the higher As values found for suspended sediments at lower concentrations of Al cannot be related to plankton because all plankton had As concentrations <8 µg/g as discussed in Section 7. The excess As is most likely bound to fine-grained Fe oxides as also discussed in Section 7.

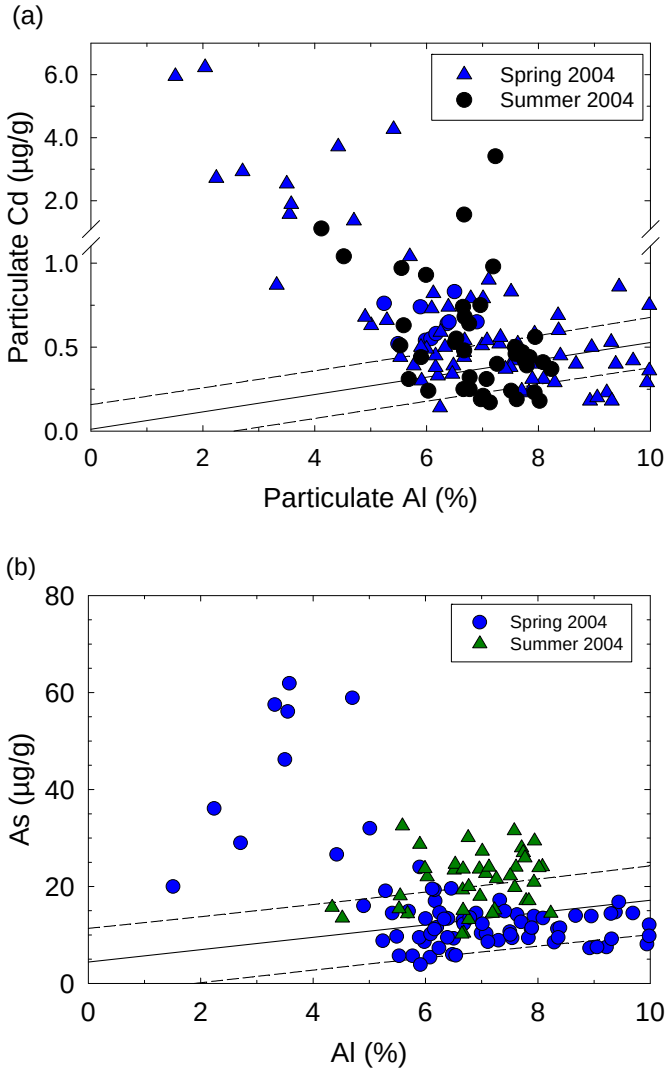

Figure 6-8. Concentrations of particulate (a) Cd and (b) As versus particulate Al for samples collected during May-June (Spring) and July-August (Summer) 2004. Solid and dashed lines show the linear regression fit and prediction interval based on data for bottom sediments from Trefry et al. (2003).

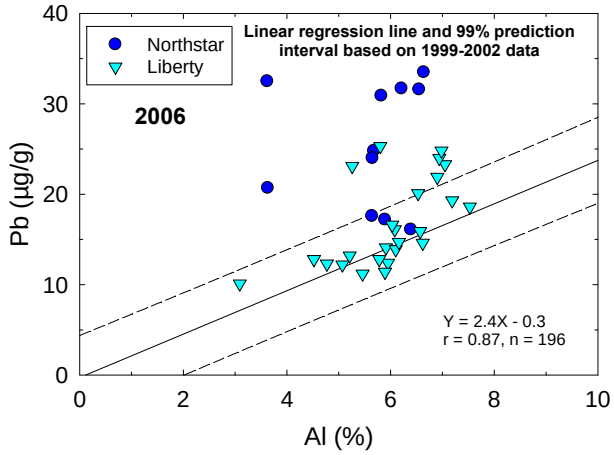

Figure 6-9. Concentrations of particulate Pb versus particulate Al for water samples collected during July-August (Summer) 2006. Solid and dashed lines show the linear regression fit and prediction interval based on data for bottom sediments from Trefry et al. (2003).

In some cases, such as for Pb (Figure 6-9), the anomalously high Pb values cannot be linked with plankton or Fe oxides and may be the result of minor anthropogenic inputs. In the case of Pb, some elevated values have been found in nearshore areas such as very near Northstar Island and near Endicott and may be related to flaring or other activities.

Concentrations of dissolved trace metals were determined for samples of saline water from the coastal Beaufort Sea during both the ANIMIDA and cANIMIDA Projects (Table 6-9). Concentrations of dissolved As. Cr and Pb were lower than reported values for surface seawater worldwide (Table 6-9). Lower As concentrations were found because As values increase with increasing salinity as previously discussed. In contrast, concentrations of dissolved Cd, Cu and Zn were higher than in typical surface seawater (Table 6-9). Concentrations of dissolved Cd in summer were about 50% lower than values obtained for winter. In the rivers, concentrations of dissolved Cd at 14 to 18 ng/L were lower than in seawater at any time of year (Table 6-9). Concentrations of dissolved Ba were similar to those in surface seawater, except during 2000 and 2001 when a greater number of nearshore samples were collected. Concentrations of dissolved Ba in rivers averaged 20, 26 and 50 µg/L for the Kuparuk, Sagavanirktok and Colville rivers, respectively (Table 3-6, page 35).

All metal concentrations seem to be at background values and these values are well below the EPA water quality criteria for chronic impacts in marine waters (Table 6-9). Furthermore, concentrations of dissolved metals were not significantly different in the Northstar area relative the overall cANIMIDA study area (Table 6-9).

Table 6-9. Mean concentrations of dissolved metals and salinity for water collected from the coastal Beaufort Sea and near Northstar Island during the open-water season.

Year	Salinity	As (µg/L)	Ba (µg/L)	Cd (ng/L)	Cr (ng/L)	Cu (µg/L)	Hg (ng/L)	Pb (ng/L)	Zn (µg/L)
2000 (n = 49)	22	0.49	26.8	20	65	0.54	0.5	5	0.20
2001 (n = 34)	17	0.38	31.9	21	94	0.64	1.3	10	0.16
2002 (n = 31)	20	0.51	14.2	27	73	0.47	0.9	7	0.11
2004 Area wide (n = 42)	23	0.72	13	43	111	0.36	-	10	0.16
2004 NS (n =7)	25	0.81	12	44	105	0.40	-	11	0.14
2005 Area wide (n = 65)	27	0.93	10.6	48	91	0.31	0.7	10	0.32
2005 NS (n = 9)	25	0.88	11.5	38	89	0.30	0.8	15	0.28
2006 Area wide (n = 26)	23	0.60	13	35	92	0.31	-	8	0.17
2006 NS (n =12)	21	0.56	14	31	85	0.31		7	0.20
Average Surface Seawater[a]	35	1.2	13	1	156	0.10	0.2	20	0.1
EPA Marine Water Quality Standards[b]	Chronic	36	-	8800	50,000	2.4	25	8,100	81

[a] Donat and Bruland (1995).
[b] EPA (2006)

The observed enrichment of dissolved Cd in the coastal Beaufort Sea during summer is consistent with the global Cd/P relationship for seawater (Figure 6-9); however, such high concentrations of dissolved Cd are unusual for surface seawater. The cANIMIDA study area has notably low concentrations of dissolved nitrate such that the N:P ratio of the seawater inside the barrier islands during summer is typically <1 (rather than 16:1) as shown on Figure 6-11. Dissolved Cd, phosphate and nitrate move onto the inner shelf during upwelling of deeper, offshore water. Carmack and Macdonald (2002) showed for the Canadian Beaufort Sea that seawater (salinity 34) at several hundred meters water depth has an N/P ratio of ~8:1. As this water is moved up onto the outer shelf, the N/P ratio is <5:1 (salinity of 30-32). Increased depletion of nitrate, relative to phosphate continues into the nearshore area (such as Stefannsson Sound) such that the N/P ratio becomes <1 in summer and the Cd/P ratio is consistent with global seawater values. However, in winter, concentrations of dissolved Cd are high (~50 ng/L) when concentrations of dissolved phosphate are low (<0.1 µM).

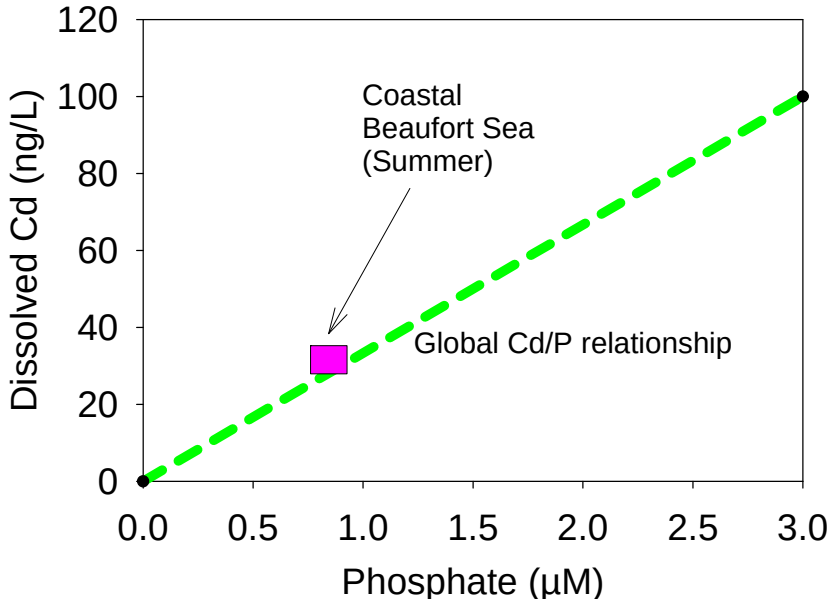

Figure 6-10. Concentrations of dissolved Cd and phosphate in the coastal Beaufort Sea versus the global trend for seawater (after Broecker and Peng, 1982).

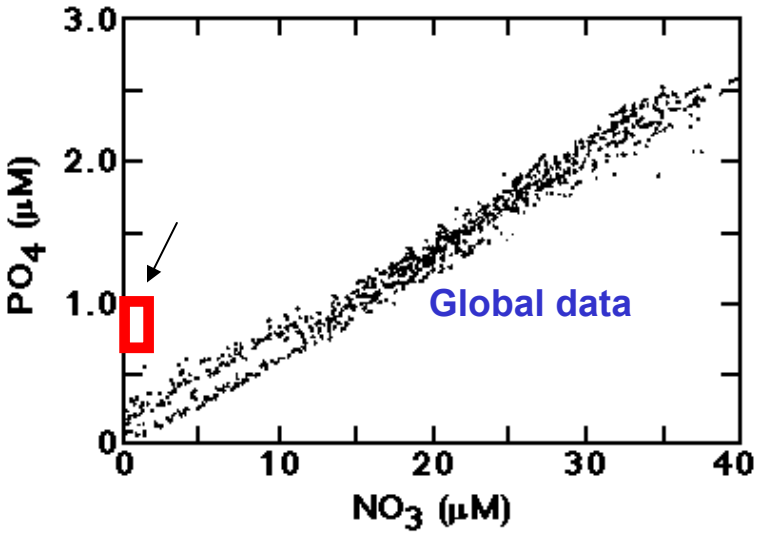

Figure 6-11. Concentrations of nitrate versus phosphate from global data sets (after Broecker and Peng, 1982) with an arrow pointing to a box that represents data for the study area in the coastal Beaufort Sea during summer.

As discussed previously, concentrations of dissolved Cd in the rivers are lower than in offshore water and thus upwelling was viewed as an important source of dissolved Cd to the study area. Suspended matter with lower concentrations of Al contains high concentrations of Cd in both spring (under ice) and summer (Figure 6-7). Such enrichment is typical of plankton and was also observed Cu.

7. BIOGEOCHEMISTRY OF ARSENIC AND MERCURY IN THE COASTAL BEAUFORT SEA

During summer 2005, the offshore study included a more detailed investigation of As and Hg in the coastal Beaufort Sea that is presented here as modified from Semmler (2006).

7.1 Arsenic

Concentrations of dissolved As were very low (0.03 to 0.17 µg/L) in the Sagavanirktok and Kuparuk rivers during summer 2005. These values are similar to or lower than concentrations reported for other uncontaminated rivers (0.13 to 0.54 µg/L, Table 7-1). Worldwide, concentrations of dissolved As in rivers vary as a function of drainage basin characteristics including geology and climate (Andreae et al., 1983; Andreae and Froelich, 1984) and contamination from anthropogenic sources such as industrial effluents (e.g., van der Sloot et al., 1985).

Concentrations of dissolved As in the coastal Beaufort Sea (S ~ 30 to 32) ranged from 0.8 to 1.4 µg/L during summer 2005. These values agree well with concentrations of 0.9 to 1.3 µg/L previously reported by Trefry et al. (2004b) for the coastal Beaufort Sea, and are within the range for typical seawater concentrations (Table 7-1). Dissolved As is found at higher concentrations in the ocean than in uncontaminated freshwater due to its long residence time of 39,000 year in seawater (Broecker and Peng, 1982).

As previously introduced, concentrations of dissolved As typically increase linearly with increasing salinity across a freshwater-seawater mixing zone, although deviations from this behavior has been observed in some estuaries, particularly those with anthropogenic sources of As (Andreae *et al*., 1983; Sanders, 1985; van der Sloot *et al*., 1985; Seyler and Martin, 1990; Yao *et al*., 2006). Concentrations of dissolved As in water samples collected from the mixing zone of the Sagavanirktok River during summer 2005 were 8 to 57% lower than the concentrations predicted by conservative mixing between river water and seawater end members (Figure 7-1), suggesting removal of As at intermediate salinities.

To determine whether this "missing" dissolved As at intermediate salinities was associated with suspended particles, "expected" concentrations of particulate As (As_p) were calculated based on the mass ratio of As to Fe in suspended sediments from the Sagavanirktok (Sag) River using the following equation:

$$\text{Expected } As_p\ (\mu g/g) = \left(\frac{As_p}{Fe_p}\right)_{Sag} \times \text{ Actual } Fe_p(\%)$$

Table 7-1. Concentrations of dissolved As in selected rivers and in seawater.

Location	Dissolved As (µg/L)			Ref.
	Mean	SD	Range	
Rivers				
Sagavanirktok River[a]	0.11	0.04	0.07 – 0.17	1, 2
Kuparuk River[a]	0.09	0.06	0.03 – 0.16	1
Yukon River	0.48	-	-	3
St. Lawrence River	0.54	-	-	3
Krka River	0.13	-	-	4
Susquehanna River (Chesapeake Bay)	0.18	-	-	5
Po River	1.5	0.4	0.96 – 2.07	6
Tejo River (Portugal)	4.4	-	-	7
Rhine River (the Netherlands)	7.5	-	-	8
Average of European rivers	3.5	-	-	3
Seawater				
Coastal Beaufort Sea (S ~ 30 to 32)	-	-	0.8 – 1.4	1, 2
Pacific Ocean (S. California coastal)	1.5	-	-	9
Surface Atlantic Ocean (S ~ 35)	1.5	-	-	3
Adriatic Sea (Po River mixing zone)	1.1	0.2	0.93 – 1.42	6

Notes: [a] During low flow conditions in July and August.

References: (1) This study; (2) Trefry *et al*., 2004b; (3) Andreae and Froelich, 1984; (4) Seyler and Martin, 1991; (5) Sanders, 1985; (6) Pettine *et al*., 1997; (7) Andreae *et al*., 1983; (8) van der Sloot *et al*., 1985; (9) Andreae, 1979.

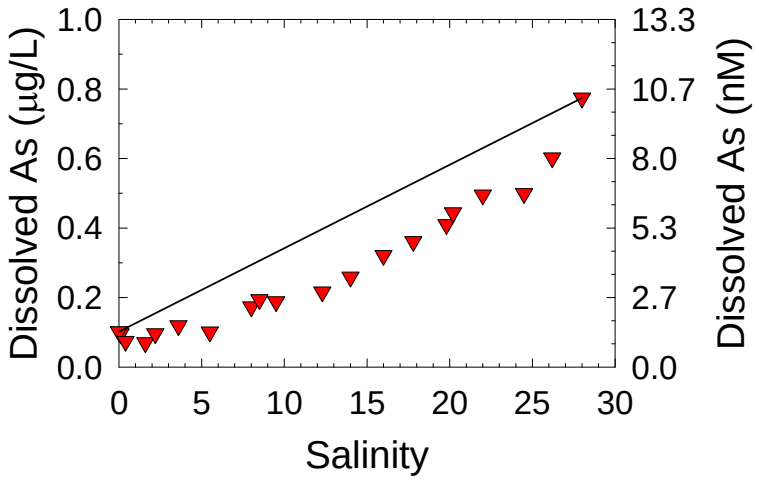

Figure 7-1. Concentrations of dissolved As versus salinity across the freshwater-seawater mixing zone from the Sagavanirktok River to the coastal Beaufort Sea during summer 2005. The solid line is a conservative mixing line between river water and seawater.

This calculation is based on the assumption that the Sagavanirktok River was the predominant source of suspended solids to the mixing zone. The average mass ratio of As_p to particulate Fe (Fe_p) in the Sagavanirktok River during the summers of 2000 to 2002 and 2004 to 2005 $[(\frac{As_p}{Fe_p})_{Sag}]$ was 2.78 ± 0.46 x 10^{-4} (n = 9). The expected As_p concentrations were then subtracted from the actual As_p concentrations to yield an estimated "excess" As on the particles as follows:

$$\text{Excess } As_p \text{ (µg/L)} = \text{Actual } As_p \text{ (µg/L)} - [\text{Expected } As_p \text{ (µg/g)} \times \text{TSS (g/L)}]$$

When values for excess As_p (converted to µg/L) calculated for each sample were added to the corresponding concentrations of dissolved As and plotted as a function of salinity, they provided a better fit to the river water and seawater end-members and the conservative mixing line than the uncorrected data (Figure 7-2). This observation suggests that dissolved As was being removed by suspended particles across the freshwater-seawater mixing zone by means of biological uptake or scavenging of As by suspended sediments. Biological removal of As by phytoplankton seems to be of minor importance because the estimated contribution of organic matter to TSS along the salinity gradient is < 10% based on concentrations of POC (0.8 to 3.3%), indicating that phytoplankton constitute only a small fraction of the suspended matter. Furthermore, concentrations of As in phytoplankton collected during this study were low (4.2 ± 2.6

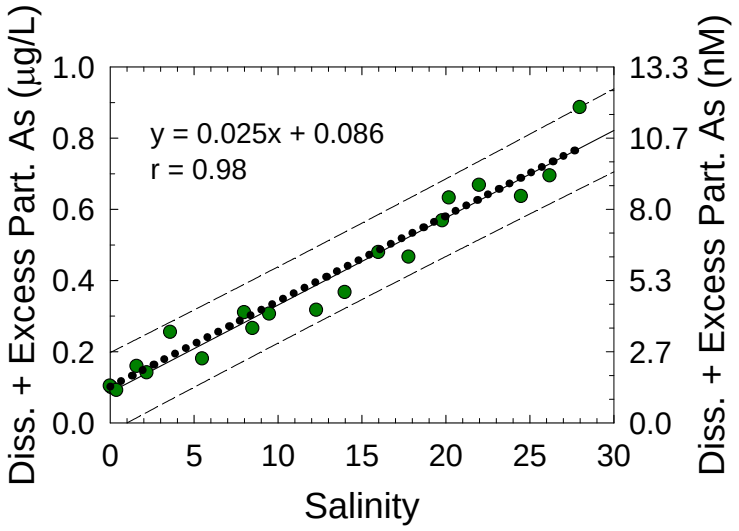

Figure 7-2. Concentrations of dissolved plus excess particulate As versus salinity across the freshwater-seawater mixing zone from the Sagavanirktok River to the coastal Beaufort Sea. The dotted line is the conservative mixing line from Figure 7-1 for dissolved As across the freshwater-seawater mixing zone. The underlying solid line is from the linear regression for dissolved + excess As versus salinity; the dashed lines show the corresponding the 95% prediction interval.

µg/g, n = 9) compared to concentrations of particulate As in the salinity gradient (18.2 ± 4.3 µg/g, n = 20), as discussed later.

Previous studies have shown that colloidal Fe in river water flocculates upon entering the freshwater-seawater mixing zone in an estuary (e.g., Boyle et al., 1977), resulting in the precipitation of Fe oxides and oxyhydroxides with coprecipitation of As (e.g., Howard et al., 1984; van der Sloot et al., 1985). This process provides a possible removal mechanism for dissolved As across the freshwater-seawater mixing zone in this study.

The distribution of dissolved reactive phosphate (DRP) across the freshwater-seawater interface was similar to that observed for dissolved As (Figure 7-3a), and dissolved As correlated strongly with DRP across the salinity gradient (r = 0.99, Figure 7-3b). Concentrations of DRP were 3 to 53% lower than the concentrations predicted by a conservative mixing line between river water and seawater (Figure 7-3a); however, no particulate P data were obtained. One possible conclusion is that DRP may be removed across the freshwater-seawater mixing zone by a mechanism similar to that described for dissolved As. Phosphate is known to adsorb strongly to and coprecipitate with Fe oxides and oxyhydroxides (Pierce and Moore, 1982; Fox, 1990; Feely et al., 1991), suggesting that scavenging or coprecipitation with Fe oxides also was a possible mechanism for removal of DRP across the salinity gradient.

The salinity of surface seawater in Stefannsson Sound during July and August 2005 was within the range observed at the seaward end of the Sagavanirktok River salinity gradient. However, concentrations of dissolved As were higher in coastal seawater than in the mixing zone and were highly variable (0.48 to 1.34 µg/L, n = 50), especially at S = 28

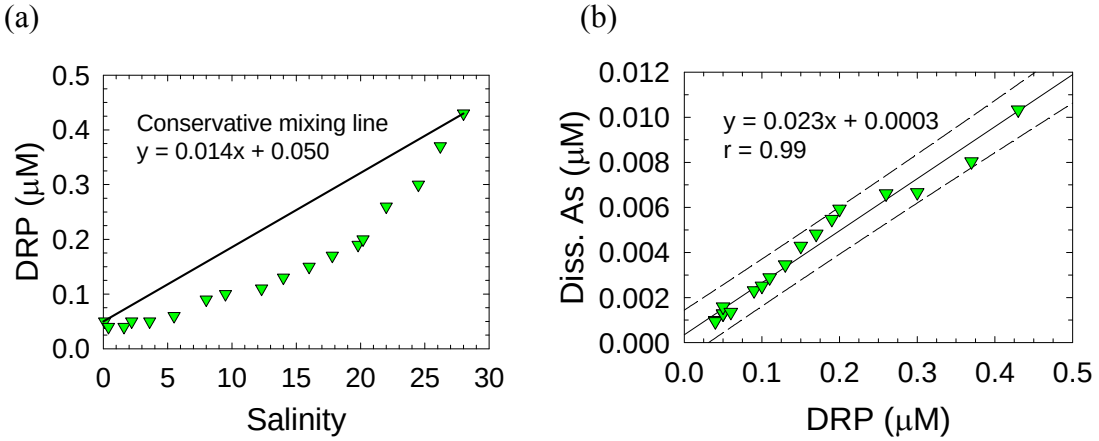

Figure 7-3. (a) Concentrations of dissolved reactive phosphate (DRP) versus salinity and (b) concentrations of dissolved As versus DRP across the freshwater-seawater mixing zone from the Sagavanirktok River to the coastal Beaufort Sea. Solid line in (a) shows a conservative mixing line between river water and seawater and in (b) a least squares linear regression line with dashed lines showing 95% prediction interval.

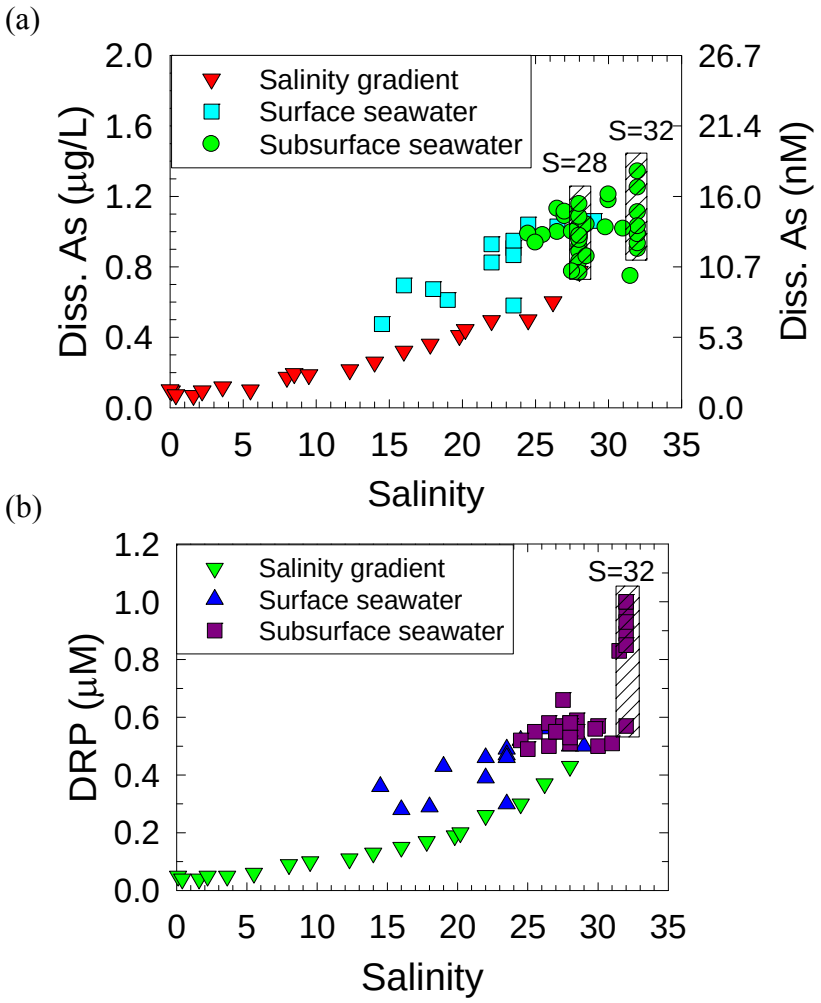

Figure 7-4. Concentrations of (a) dissolved As and (b) dissolved reactive phosphate (DRP) versus salinity across the freshwater-seawater mixing zone from the Sagavanirktok River to the coastal Beaufort Sea, and in surface and subsurface seawater in Stefannsson Sound (data for all three water types identified with separate markers).

(0.77 to 1.16 µg L^{-1}, n = 13) and S = 32 (0.90 to 1.34 µg/L, n = 8, Figure 7-4a). Concentrations of DRP were higher in coastal seawater than along the very nearshore salinity gradient; DRP values also were variable, especially at S = 32 (0.57 to 1.0 µM, n = 7). The variability in concentrations of dissolved As and DRP in Stefannsson Sound appears to be related to a combination of the following: (1) dilution by sea ice meltwater, (2) upwelling of offshore seawater onto the continental shelf, and (3) scavenging by or coprecipitation with Fe oxides. Biological uptake by phytoplankton did not appear to be an important mechanism controlling concentrations of dissolved As and DRP during this study, as discussed later.

Vertical profiles for dissolved As generally followed salinity at stations 4B, L17A, and L17 on July 31, and stations L18, L01A, and L01B on August 3 (Figure 7-5) with higher concentrations and greater stratification in the deeper, more saline water. Total water depths ranged from 6.0 m (4B) to 13.6 m (L17B) along the July 31 transect, and from 3.9 m (L18) to ~ 12 m (L01C) along the August 3 transect. Concentrations of dissolved As were lowest at all depths at stations L17B and L01C, despite the fact that the salinity of deeper water ($\geq$ 4 m) was higher at these stations than for similar depths at nearshore stations (Figure 7-5). However, this trend was not observed in vertical profiles for DRP or dissolved NO_3^- (Figure 7-5). In addition, the ratio of dissolved As to DRP was lower at all depths at stations L17B and L01C than at all other locations along the two transects. The dissolved As/DRP ratios at stations L17B and L01C were similar to the value previously reported by Feely et al. (1991) for the North Atlantic Ocean (1.5×10^{-2}; Figure 7-6). The similarity of the dissolved As to DRP ratios at stations L01C and L17B with that of the North Atlantic Ocean suggests that offshore seawater that upwells onto the continental shelf of the Beaufort Sea may originate in the North Atlantic Ocean. Seawater from the Pacific Ocean enters the Beaufort Sea via the Alaskan Coastal Current and flows along the continental slope of the Beaufort Sea over deeper water originating from the Atlantic Ocean which contributes to this current by upwelling (e.g., Pickart, 2004; Weingartner, 2006). The continental shelf receives some input of offshore seawater by upwelling (e.g., Aagaard et al., 1981; Macdonald et al., 1987; Weingartner, 2006). Thus, the variability in concentrations of dissolved As at stations L01C and L17B appears to be controlled, to some extent, by upwelling and mixing of offshore seawater with coastal seawater in Stefannsson Sound.

Suspended sediments collected during summer 2005 from Stefannsson Sound (n = 21) were enriched in As and Fe relative to Al (Figure 7-7a). Concentrations of As_p (14.5 to 53.0 µg/ g, n = 21) and Fe_p (2.4 to 5.9%, n = 21) in most suspended sediment samples plot above the 95% prediction intervals established by Trefry *et al*. (2003) for As versus Al and Fe versus Al in bottom sediments collected from the coastal Beaufort Sea during the summers of 1999 through 2001 (Figure 7-7). These observations support the presence of iron oxides, most likely on clay particles, as the source of Fe enrichment. Scavenging of As by iron oxides is the most likely explanation for observed As enrichment in suspended particles. Concentrations of As in phytoplankton (4.2 ± 2.6 µg/g, n = 9) and zooplankton (2.3 ± 1.1 µg/g, n = 9) collected from Stefannsson Sound during summer 2005 were too low to account for the high concentrations of As found in suspended sediments. Likewise, resuspension of bottom sediments cannot account for the high concentrations of As_p because concentrations of As in surface bottom sediments collected during summer 2005 (9.8 ± 3.8 µg g^{-1}, n = 38) fit well within the 95% prediction intervals of Trefry et al. (2003). Thus, scavenging of As by iron oxides seems to be a common occurrence in the study area and a reasonable explanation for the As-rich particles found in the water column.

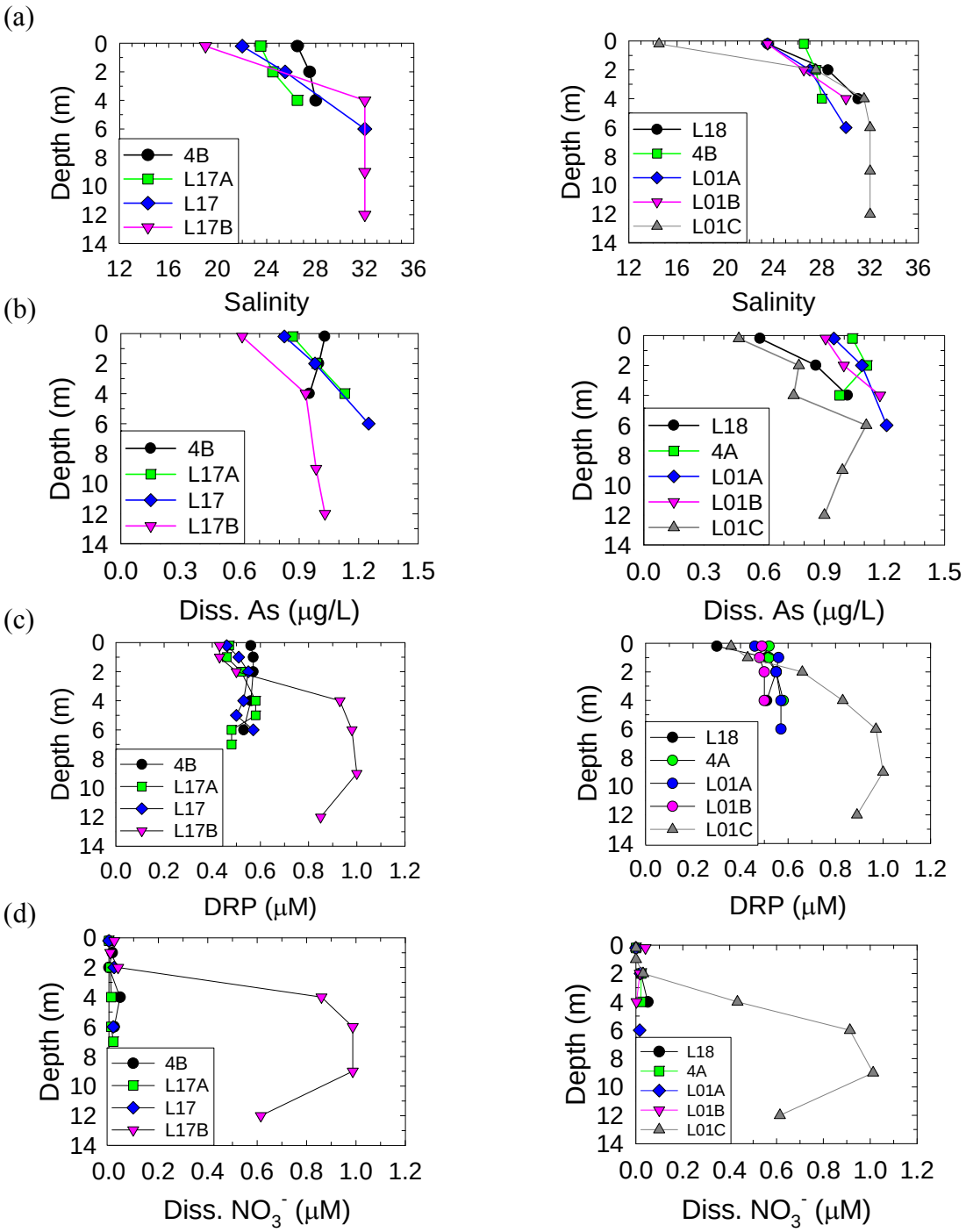

Figure 7-5. Vertical profiles of (a) salinity, (b) dissolved As, (c) dissolved reactive phosphate (DRP), and (d) dissolved NO_3^- on July 31 (left) and August 3 (right) in Stefannsson Sound. Stations are listed in order of increasing distance from shore.

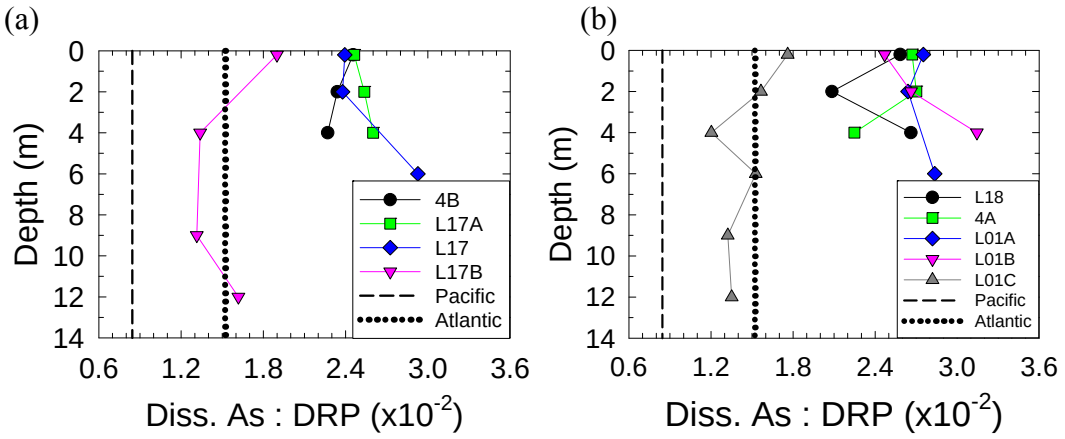

Figure 7-6. Vertical profiles of the ratio of dissolved As to dissolved reactive phosphate (DRP) on (a) July 31 and (b) August 3 in Stefannsson Sound. Dotted and dashed lines show ratio of dissolved As to DRP in North Atlantic and North Pacific Oceans, respectively (Feely et al., 1991 and references therein).

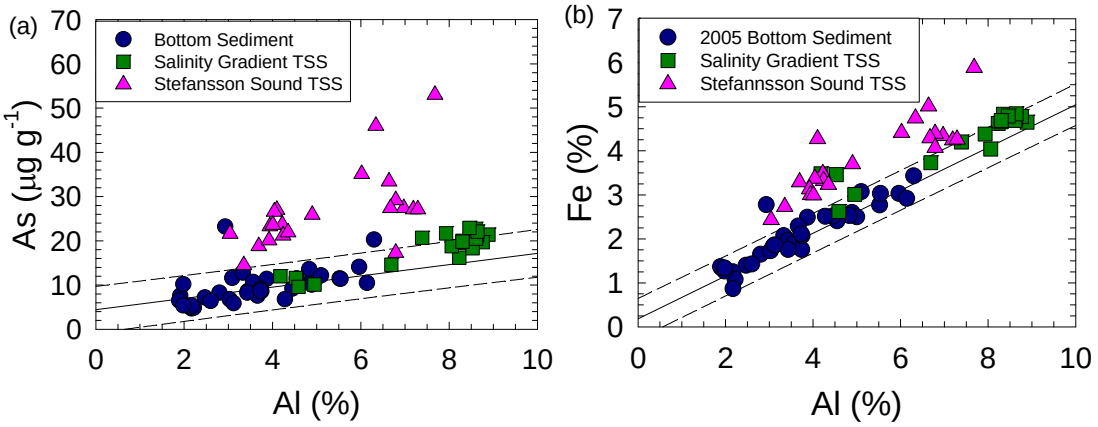

Figure 7-7. Concentrations of (a) As versus Al and (b) Fe versus Al in total suspended solids (TSS) and bottom sediments collected from Stefannsson Sound during summer 2005. Solid lines are from a linear regression and dashed lines are 95% prediction intervals for bottom sediments from the coastal Beaufort Sea collected in 1999 through 2001 (Trefry *et al*., 2003; n = 194; data points not shown).

Concentrations of As in phytoplankton, zooplankton, amphipods, clams and fish collected during summer 2005 are presented in Table 7-2. Enrichment factors (EF) were determined as the ratio of the average concentration of As in tissue (in µg/g dry weight) to the average concentration in water (in µg/g of water) or tissue belonging to the next lower tropic level (Table 7-2). The EF between surface seawater and phytoplankton was ~5,000, indicating that bioaccumulation of dissolved As by phytoplankton was occurring. However, this process seemed to have little influence on the concentrations of dissolved As in the water column due to the relatively high concentrations (1 to 1.5 µg/L) that occur naturally in seawater. No significant differences were found for concentrations of As between phytoplankton and zooplankton ($t = 1.444$, $p > 0.05$, $df = 16$) or between zooplankton and fish ($t = 0.451$, $p > 0.05$, $df = 27$; Figure 7-8). Concentrations of As were significantly greater in amphipods than in zooplankton ($t = 8.563$, $p < 0.001$, $df = 18$), and also were significantly greater in clams than in phytoplankton ($t = 5.770$, $p < 0.001$, $df = 11$; Figure 7-8). Enrichment factors between successive trophic levels ranged from 0.55 (between phytoplankton and zooplankton) to 4.9 (between zooplankton and amphipods).

Table 7-2. Concentrations of As in surface seawater (dissolved), phytoplankton, zooplankton, amphipods (*Anonyx* sp.), clams (*Astarte* sp.) and fish collected from the coastal Beaufort Sea during summer 2005.

Sample Type	As Concentration (µg/g)			
	Mean	SD	Range	N
Surface seawater[a] (S = 14.5 to 29)	0.83×10^{-3}	0.19×10^{-3}	$(0.48\text{-}1.06) \times 10^{-3}$	14
Phytoplankton[b,c]	4.2 (6.7)	2.6 (4.6)	0.8 – 7.9 (1.4 – 15.3)	9
Zooplankton[b,c]	2.3 (4.7)	1.1 (2.0)	1.2 - 4.1 (2.41 – 8.31)	9
Amphipods (*Anonyx* sp.)	11.2	3.6	5.0 – 17.4	11
Clams (*Astarte* sp.)	13.0	2.2	11.3 – 16.0	4
Fish[d]	2.5	1.5	0.8 – 7.4	20

Notes: [a] Dissolved concentrations in seawater are in µg/mL
[b] Concentrations of phytoplankton and zooplankton are sediment-corrected using ratios to Fe (uncorrected concentrations are in parentheses) as described by Semmler (2006, copy attached with CD).
[c] Details of phytoplankton and zooplankton species composition are in the Appendix
[d] Average of concentrations found in Arctic char, Arctic cisco, Arctic flounder, four-horn sculpin, and humpback broad whitefish

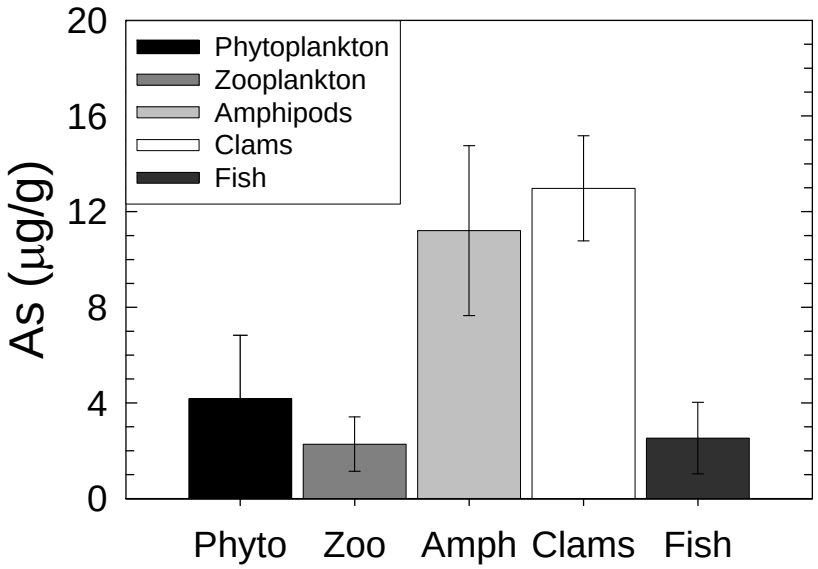

Figure 7-8. Average concentrations of As in phytoplankton, zooplankton, amphipods (*Anonyx* sp.), clams (*Astarte* sp.) and fish collected from Stefannsson Sound during summer 2005.

Concentrations of As in organisms collected during summer 2005 from Stefannsson Sound (Table 7-2 and Figure 7-8) compare well with values previously reported by others. For example, Lindsay and Sanders (1990) reported an average concentration of 8.6 µg/g in cultured phytoplankton exposed to ambient water from the Patuxent River (average concentration of dissolved As = 0.71 µg/L). A review by Neff (1997) tabulated average concentrations of As of 2.1 µg/g (0.2 to 24.4 µg/g, n = 4) in zooplankton, 10.4 µg/g (< 0.6 to 214 µg/g, n = 151) in bivalves, and 5.6 (0.05 to 449.5 µg/g, n = 156) in fish.

7.2 Mercury

Concentrations of total dissolved Hg in the Sagavanirktok and Kuparuk rivers during August 2005 were similar to concentrations reported for other Arctic rivers, including the Lena and Ob rivers in Russia, and were ~ 2 to 3 times lower than average concentrations reported for the St. Lawrence, Garonne, Rhône, and Seine rivers (Table 7-3). Trefry et al. (2004b) previously reported average concentrations for total dissolved Hg of ~ 2 ng/L in the Sagavanirktok, Kuparuk and Colville rivers. Concentrations of dissolved mono-methylmercury (CH_3Hg^+) were undetectable (< 0.019 ng/L) in the Sagavanirktok and Kuparuk rivers during low flow conditions in August 2005.

Table 7-3. Concentrations of total dissolved Hg (TDHg) and dissolved CH_3Hg^+ in selected rivers, estuaries and seawater.

Location	TDHg (ng/L)			Dissolved CH_3Hg^+ (ng/L)			Ref.
	Mean	SD	Range	Mean	SD	Range	
Rivers and Estuaries							
Sagavanirktok River (August, 2005, n = 3)	0.81	0.41	0.5- 1.1	< 0.019	-	-	1
Kuparuk River (August 2005, n = 3)	1.03	0.39	0.8- 1.3	< 0.019	-	-	1
Lena River[a]	1.0	0.1	0.9 – 1.1	-	-	-	2
Ob River[a]	0.6	0.1	-	-	-	-	2
Yenisei River[a]	0.3	0.1	-	-	-	-	2
St. Lawrence River[a]	2.4	0.6	-	-	-	-	3
Garonne River (Gironde Estuary, France)[a]	3.0	-	-	-	-	-	4
Rhône River[a]	1.6	0.7	0.6 – 2.6	-	-	-	5
Loire River[a]	0.82	0.42	0.4 – 2.0				6
Seine River[a]	2.3	1.9	0.5 – 7.9				6
Ochlockonee Estuary[b]	3.2	1.6	0.7 – 6.0	0.08	-	0.06 – 0.09	7
Seawater							
Coastal Beaufort Sea (S = 14.5 to 32) August, 2005 (n = 38)	0.69	0.12	0.5 – 0.9	-	-	< 0.019 – 0.046	1,8
North Atlantic Ocean (surface)[b]	0.23	0.20	0.1 – 0.5	-	-	-	7
South and Equatorial Atlantic Ocean (surface)[a,c,d]	0.56	-	-	<0.01 (MDL)	-	-	9
Laptev Sea (Arctic Ocean; S = 32.6, depth = 35 m)[a]	0.80	-	-	-	-	-	2
Kara Sea (Arctic Ocean; S ~34, depth = 30-45 m)[a]	2.0	1.5	0.4 – 3.4	-	-	-	2
North Sea and English Channel (surface, S ~34-35)[d]	0.29	0.06	0.2 – 0.4	0.03	0.02	0.02 – 0.06	10
Equatorial Pacific Ocean (Mixed layer, 0-100 m)[d]	-	-	-	<0.01 (MDL)	-	-	11
Equatorial Pacific Ocean (>100 m)[d]	-	-	-	-	-	<0.01 (MDL)-116	11
Arctic Ocean (75°N, 14°W to 16°E)[b]	-	-	-	-	-	<0.005 (MDL) – 0.16	12

Notes: [a] Filtered using 0.8 µm glass fiber filters; [b] Filtered using 0.45 µm filters; [c] Dissolved Hg obtained by subtracting particulate Hg (0.02 ± 0.01 ng/g) from total Hg (unfiltered; 0.58 ± 0.34 ng/L); [d] CH_3Hg^+ reported as total CH_3Hg^+ (unfiltered)

References: (1) This study; (2) Coquery *et al*., 1995; (3) Cossa *et al*., 1988; (4) Cossa and Noël, 1987; (5) Cossa and Martin, 1991; (6) Coquery *et al*., 1997; (7) Guentzel *et al*., 1996; (8) Trefry *et al*., 2004b; (9) Mason and Sullivan, 1999; (10) Leermakers *et al*., 2001; (11) Mason and Fitzgerald, 1993; (12) Pongratz and Heumann, 1998.

Concentrations of total dissolved Hg (TDHg) in Stefannsson Sound averaged 0.69 ± 0.12 ng/L (0.50 to 0.90 ng/L, n = 38, Table 7-3). Trefry et al. (2004b) previously reported concentrations of 0.70 ± 0.39 ng/L (0.30 to 1.50 ng/L, n = 8) in the coastal Beaufort Sea during August 2000 and 2001. Concentrations of dissolved CH_3Hg^+ were undetectable (< 0.019 ng/L) in 12 of the 17 seawater samples collected during summer 2005. The exceptions included one sample collected at station L18 (0.025 ng/L) and four samples collected at station L01C (0.022 to 0.046 ng/L). In the 15 samples with concentrations of both TDHg and dissolved CH_3Hg^+, CH_3Hg^+ accounted for <3.8 to 7.3% of the TDHg.

Concentrations of TDHg averaged 1.0 ± 0.2 ng/L (n = 9) across the freshwater-seawater mixing zone during summer 2005 (Figure 7-9) with no significant trend as a function of salinity (r = 0.14). Similar distributions of TDHg were previously observed by Coquery

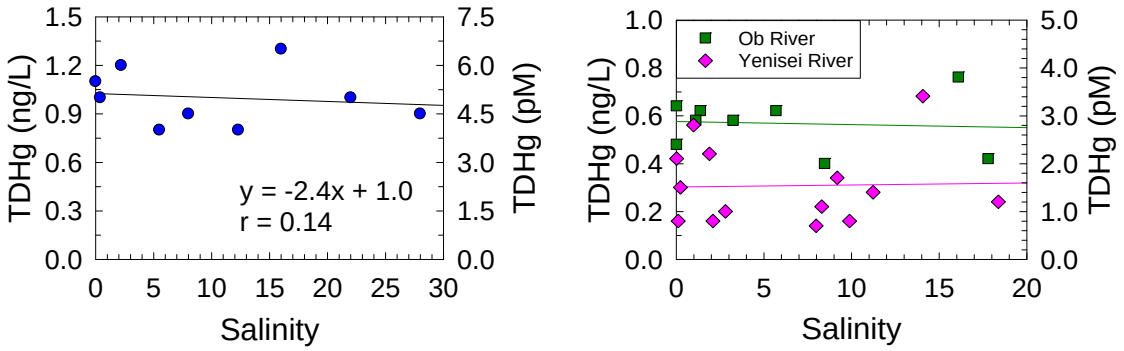

Figure 7-9. Concentrations of total dissolved Hg (TDHg) versus salinity from the (a) Sagavanirktok River across the freshwater-seawater mixing zone to the coastal Beaufort Sea, and (b) Ob and Yenisei estuaries (plotted using data from Coquery et al., 1995).

et al. (1995) in two Arctic estuaries, the Ob and the Yenisei (Figure 7-9b), and by Coquery et al. (1997) in the Loire and Seine estuaries, with variable concentrations and no clear trend as a function of salinity. The behavior of TDHg in the Loire and Seine estuaries was attributed to a combination of several factors, including anthropogenic inputs from industrial activities, seasonal variations in water flow, association with colloids, and complexation with dissolved organic matter (Coquery et al., 1997).

Concentrations of TDHg in Stefannsson Sound (0.69 ± 0.12 ng/L, n = 38) were significantly lower than concentrations of 1.0 ± 0.2 ng/L observed across the freshwater-seawater mixing zone ($t = 6.47$, $p < 0.001$, $df = 45$; Figure 7-10). Concentrations of TDHg appear to be controlled by a combination of processes including: (1) upwelling of

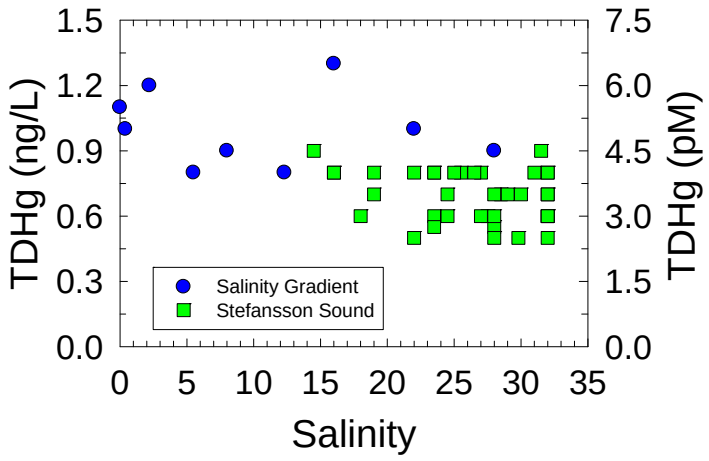

Figure 7-10. Concentrations of total dissolved Hg (TDHg) versus salinity from the Sagavanirktok River across the freshwater-seawater mixing zone to the coastal Beaufort Sea and in Stefannsson Sound.

offshore seawater onto the continental shelf, (2) input of dissolved Hg to surface waters from organic matter and/or sediment released from melting sea ice during summer, and (3) biological productivity. Biological productivity was low during summer 2005 and thus it is probably of minor importance in controlling the concentrations of total dissolved Hg in Stefannsson Sound. However, productivity may play a role in the distribution of dissolved CH_3Hg^+, as discussed later in this section. The lower concentrations of TDHg in coastal seawater relative to the freshwater-seawater mixing zone could be the result of upwelling of offshore seawater having lower concentrations of TDHg. Concentrations of TDHg in the North Atlantic Ocean (Guentzel et al., 1996) and Northeast Pacific Ocean (Gill and Bruland, 1987) are similar and range from ~ 0.1 to 0.5 ng/L and ~ 0.2 to 0.6 ng/L, respectively. Thus, mixing of river and intermediate-salinity waters (TDHg = 1.0 ± 0.2 ng/L) with offshore seawater originating from the North Atlantic and/or North Pacific Oceans may account for the lower concentrations of TDHg found in Stefannsson Sound (0.69 ± 0.12 ng/L).

Vertical profiles of TDHg were relatively uniform with depth at stations 4A and L01A (CV = 4.9% and 7.5%, respectively) and increased with depth at station L18 on August 3 (Figure 7-11). Concentrations of TDHg at station L01C were similar in magnitude to those found at stations nearer to shore but showed greater variation (± 20.5%; 0.6 to 0.9 ng/L). Although this distribution does not clearly show dilution of dissolved Hg at depth by upwelling of offshore seawater or input of dissolved Hg near the surface from melting sea ice, these processes may occur simultaneously and compete with each other to produce the observed variability.

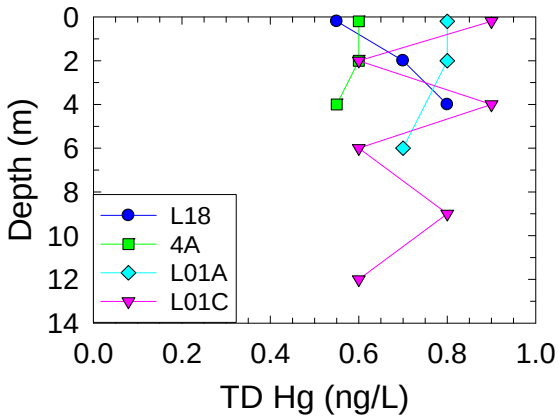

Figure 7-11. Vertical profiles of total dissolved Hg (TD Hg) at stations along a transect sampled on August 3 in Stefannsson Sound. Stations are listed in order of increasing distance from shore.

Concentrations of dissolved CH_3Hg^+ at station L01C increased from the surface (< 0.019 ng/L) to a mid-depth maximum of 0.046 ng/L at 4 m (Figure 7-12). The observed distribution of dissolved CH_3Hg^+ may be produced by biological activity in Stefannsson Sound, although the biomass of plankton was estimated to be low (< 600 µg/L) in Stefannsson Sound during this study. Alternatively, this distribution could be the result of upwelling of offshore seawater onto the continental shelf. Pongratz and Heumann (1998) found that concentrations of both CH_3Hg^+ and $(CH_3)_2Hg$ were elevated at the boundary of pack ice in the Arctic and Antarctic Oceans, corresponding to high biological productivity (Meyerdierks, 1996 from Pongratz and Huemann, 1998). In addition, CH_3Hg^+ is thought to be the main product of decomposition of $(CH_3)_2Hg$ (Mason and Fitzgerald, 1993; Mason et al., 1995b, Pongratz and Heumann, 1998), and $(CH_3)_2Hg$ accumulates in deep ocean waters over long periods of time (> 5 years, Mason et al., 1995b). Mason et al. (1995) and Mason and Fitzgerald (1993) reported that $(CH_3)_2Hg$ and CH_3Hg^+ were not found in surface waters of the North Atlantic or Equatorial Pacific Oceans, respectively, but were detectable in deeper waters below the thermocline. Concentrations in deep waters ranged from < 0.002 (MDL) to 0.07 ng/L for $(CH_3)_2Hg$ and were at or below the MDL (0.01 ng/L) for CH_3Hg^+ in unfiltered samples from the North Atlantic Ocean (Mason et al., 1995). Values ranged from 0.008 to 0.15 ng/L for $(CH_3)_2Hg$ and < 0.01 (MDL) to 125 ng/L for CH_3Hg^+ in unfiltered samples from the Equatorial Pacific Ocean (Mason and Fitzgerald, 1993). Pongratz and Heumann (1998) reported concentrations of dissolved (< 0.45 µm) CH_3Hg^+ and $(CH_3)_2Hg$ of ~ 0.1 to 3 ng/L in surface waters of the North Atlantic (40 to 51° N, 10° W), adjacent to areas of anthropogenic inputs. Thus, upwelling of seawater originating from the deeper waters of the Atlantic or Pacific Oceans and/or influenced by higher concentrations within the region of the pack ice boundary may be a source of CH_3Hg^+ to the coastal waters of Stefannsson Sound. This hypothesis is supported by the observation that concentrations of dissolved As, DRP, and dissolved NO_3^- also were highest at intermediate depths and at stations located farthest offshore in Stefannsson Sound.

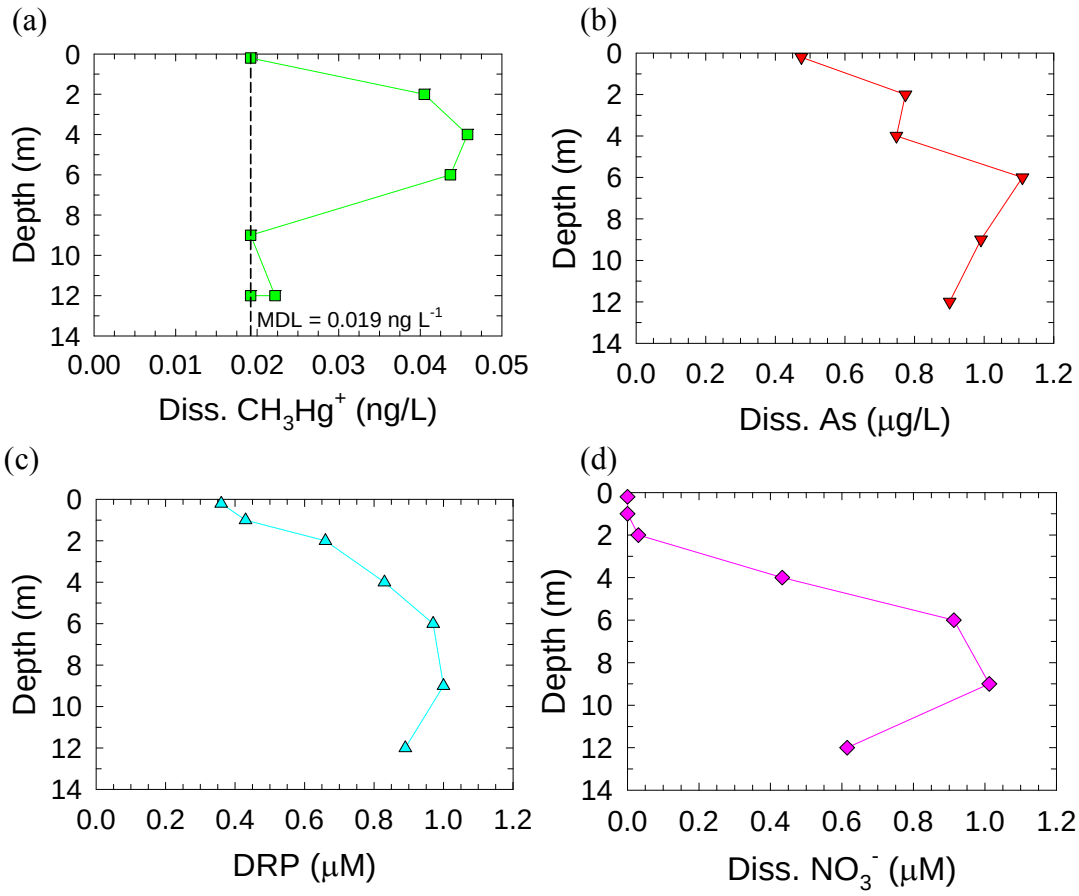

Figure 7-12. Vertical profiles of (a) dissolved CH_3Hg^+, (b) dissolved As, (c) dissolved reactive phosphate (DRP), and (d) dissolved NO_3^- at L01C on August 3.

Enrichment factors for total Hg and CH_3Hg^+ (Table 7-4) were determined by the same method as described for As (using tissue concentrations expressed in µg/g dry weight). The enrichment factor for TDHg between surface seawater and phytoplankton averaged about 28,000. Concentrations of total Hg in zooplankton were significantly greater (EF = 2.8) than concentrations of total Hg in phytoplankton collected from Stefannsson Sound during summer 2005 ($t = 2.62$, $p < 0.05$, $df = 10$; Table 7-4 and Figure 7-13). Concentrations of CH_3Hg^+ in zooplankton also were significantly greater (EF = 7.1) than in phytoplankton ($t = 4.10$, $p < 0.01$, $df = 7$; Table 7-4 and Figure 7-13). Monomethylmercury accounted for an average of 4% and 10% of the total Hg in phytoplankton and zooplankton, respectively, and no significant difference was found for the % CH_3Hg^+ between phytoplankton and zooplankton ($t = 1.23$, $p > 0.05$, $df = 7$).

Table 7-4. Concentrations of Hg and CH_3Hg^+ in surface seawater (dissolved), phytoplankton, zooplankton, amphipods (*Anonyx* sp.), clams (*Astarte* sp.) and fish collected from the coastal Beaufort Sea during summer 2005.

Sample Type	Concentration (ng/g)[a]			
	Mean	SD	Range	n
Total Hg				
Surface seawater (S = 14.5 to 32)[a]	0.69×10^{-3}	0.12×10^{-3}	$0.50 – 0.90 \times 10^{-3}$	38
Phytoplankton	19.6	13.4	11.2 – 39.7	4
Zooplankton	55.4	30.7	29.6 – 105.1	8
Amphipods (*Anonyx* sp.)	78.0	28.2	46.4 – 116.6	10
Clams (*Astarte* sp.)	53.5	18.4	42.6 – 80.9	4
Fish[b]	106.2	64.2	30.0 – 266.0	20
Methylmercury				
Surface seawater (S = 14.5 to 32)[a,c]	0.025×10^{-3}	0.025×10^{-3}	< 0.019 – 0.0458	15
Phytoplankton	0.60	0.56	0.22 – 1.24	3
Zooplankton	4.25	1.94	2.21 – 6.66	6

Notes: [a] Dissolved concentrations in seawater are in ng/mL
[b] Average of concentrations found in Arctic char, Arctic cisco, Arctic flounder, four horn sculpin, and humpback broad whitefish
[c] Average and standard deviation were determined using the MDL as the concentration for samples in which CH_3Hg^+ was undetectable

Concentrations of total Hg were significantly greater (EF = 2.7) in clams than in phytoplankton ($t = 2.84$, $p < 0.05$, $df = 8$) and also were significantly greater (EF = 1.9) in fish than in zooplankton ($t = 2.13$, $p < 0.05$, $df = 26$; Table 7-4 and Figure 7-13a). No significant difference was found for concentrations of total Hg between zooplankton and amphipods ($t = 1.63$, $p > 0.05$, $df = 16$; Table 7-4 and Figure 7-13b).

Concentrations of total Hg in zooplankton collected from Stefannsson Sound during summer 2005 compare well with concentrations found by Stern and Macdonald (2005) in zooplankton (*Calanus hyperboreus*) from the Canadian Basin of the Beaufort Sea (85 ± 9 ng/g) and from the Chukchi Plateau and Mendeleev Basin of the Arctic Ocean (48 ± 3 ng/g). Stern and Macdonald (2005) also reported concentrations of CH_3Hg^+ in *C. hyperboreus* of ~ 5 to 20 ng/g (~ 10 to 30% of the total Hg), slightly higher than concentrations found during this study (Table 7-4). Atwell *et* al. (1998) also determined concentrations of total Hg in zooplankton (*C. hyperboreus*) from Lancaster Sound, Northwest Territories, Canada, and found a similar average concentration of 60 ± 10 ng/g. In contrast, Rezai *et al*. (2003) reported much lower average concentrations of total Hg (2.08 ± 0.25 ng/g) in zooplankton (unidentified species) from Malacca Straits. Concentrations of total Hg in *Astarte* sp. clams collected from Stefannsson Sound during this study (53 ± 18 ng/g) were similar to concentrations of total Hg of 70 ± 10 ng/g reported by Atwell *et al*. (1998) in *Mya truncata* (a filter-feeding clam) from Lancaster Sound. Stern and Macdonald (2005) reported concentrations of total Hg in Arctic cod

(*Boreogadus saida*) from the Canadian Basin of the Beaufort Sea (270 ± 40 ng/g) and from the Chukchi Plateau and Mendeleev Basin (85 ± 5 ng/g), adjusted for variability in $\delta^{15}N$ and body length. Atwell *et al*. (1998) reported similar concentrations of total Hg in Arctic cod (190 ± 30 ng/g) from Lancaster Sound. Bloom (1989) reported concentrations of total Hg of 43.0 ± 3.1 ng/g and 65.3 ± 1.8 ng/g in Chinook Salmon (*Oncorhynchus tshawytscha*) and Pacific Halibut (*Hippoglossus stenolepis*), respectively. Corresponding concentrations of CH_3Hg^+ were 41.8 ± 4.2 ng/g in Chinook Salmon (97.2% of the total Hg) and 55.5 ± 8.0 ng/g in Pacific Halibut (85.0% of the total Hg; Bloom, 1989). These concentrations of total Hg in various species of fish are in agreement with those found in fish collected from Stefannsson Sound during summer 2005.

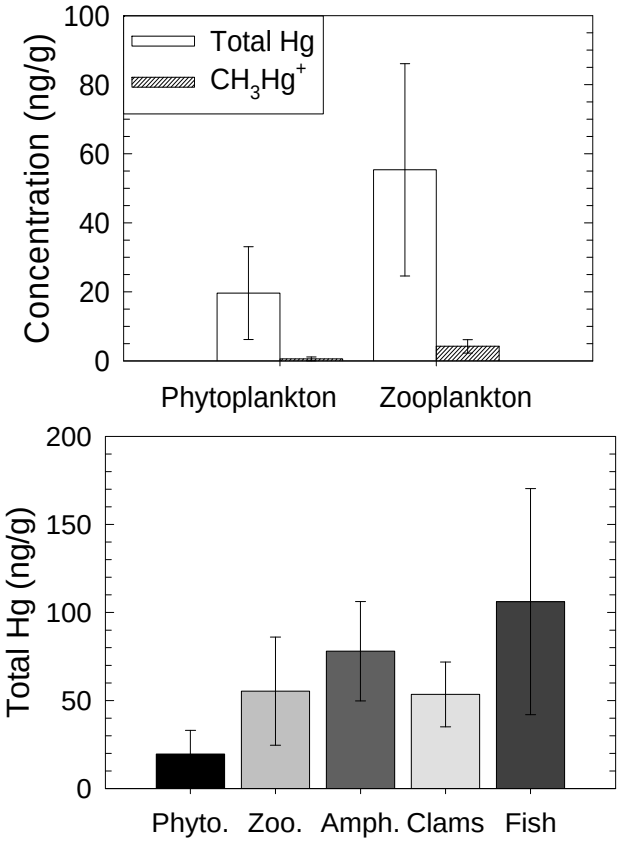

Figure 7-13. Concentrations of (a) total Hg and CH_3Hg^+ in phytoplankton and zooplankton and (b) total Hg in phytoplankton, zooplankton, amphipods, clams, and fish collected from Stefannsson Sound during summer 2005.

8. CONCLUSIONS

Key findings and conclusions from Tasks 3 and 4 of the cANIMIDA Project are as follows:

- During May-June 2004 and 2006, maximum concentrations of total suspended solids (TSS) ranged from 60 mg/L (2006) to 106 mg/L (2004) in the Kuparuk River and 285 mg/L (2004) to 353 mg/L (2006) in the Sagavanirktok River. All TSS values in rivers during summer were 10 to >300 times lower than during the spring melt. About 90% of the annual transport of TSS from the two rivers occurs during the spring floods.

- More than 85% of the data points for Ba, Cu, Cr, Ni and Pb in suspended sediments from the three rivers during 2004 and 2006 were within predicted ratios to Al for Beaufort Sea sediments. This overall continuity shows strong support for river particles as a key source for metals in coastal sediments as well as showing that concentrations of these metals in Beaufort Sea sediments are not significantly influenced by anthropogenic inputs or diagenetic processes.

- A trend of maximum concentrations of dissolved trace metals in rivers during peak flow in spring, first observed during the ANIMIDA Project, was again observed in some cases in the 2004 and 2006 data. This trend is natural and influenced by the discharge of soil interstitial water and shallow surface water that is diluted by snow melt and flushed from surrounding soils into the rivers. In contrast, concentrations of major elements such as Ca, or even Ba, varied by <10% over the May-June period in the rivers.

- A simple distribution coefficient (K_d) was used to describe metal partitioning between particulate and dissolved phases. For example, the K_d values calculated for Ba in the Sagavanirktok, Kuparuk and Colville rivers were statistically equal, suggesting that partitioning of Ba between dissolved and particulate phases is a quasi-equilibrium controlled process between free Ba^{2+} and suspended particles. Reasonably good agreement in K_d values among rivers and seasons also was found for Cd, Cu, Cr, Pb and other metals. The K_d relationship can be used to help explain and predict concentrations of dissolved metals in area rivers.

- During the spring floods, water from the Sagavanirktok River was traced beneath the ice, relatively undiluted, to a distance of ~6 to 8 km offshore and ~8 to 10 km alongshore in ~3 days. The SR plume was ~1.0 to 1.5 m thick with the majority of the river water ($\geq$60%) in the top 1 m over an area of ~315 km^2. This information can be used to help predict potential spill trajectories under ice as well as transport pathways for freshwater, suspended sediments and dissolved chemicals in the coastal Beaufort Sea.

- Offshore transport and dispersion of spring floodwater under the ice canopy during a given year was linked to the seasonal river hydrographs with noticeable inter-annual variations. For example, in 2004, river flow was higher and a thicker under-ice plume formed and extended farther from shore.

- Concentrations of TSS, under ice, along the freshwater-seawater mixing zone into the Beaufort Sea decreased sharply and showed settling of >50% of the suspended sediments within 10 km of the river mouths.

- No significant differences in concentrations of TSS were found due to oil and gas operations near Northstar Island relative to the overall cANIMIDA study area.

- Concentrations of dissolved trace metals were lower than reported values for surface seawater worldwide and well below the EPA water quality criteria for chronic impacts in marine waters. No significant differences in concentrations of dissolved trace metals were observed near Northstar Island relative to the overall cANIMIDA study area during the 2004, 2005 and 2006 study period.

- Concentrations of particulate metals during the open-water season showed the variable importance of scavenging by iron oxides (e.g., As), uptake by biota (e.g., Cd) and possibly some anthropogenic inputs (e.g., Pb) to metal distributions. Concentrations of particulate metals near Northstar Island were not different than in the overall cANIMIDA area, with the exception of Cd in 2004 (plankton) and Pb in 2006 (possibly anthropogenic).

- With respect to potential contaminants from offshore activities, the overall conclusion of this study is that concentrations of suspended sediments, as well as dissolved and particulate metals, are at background levels throughout the study area, with a possible minor exception for Pb in some suspended particles during 2006. The data produced during cANIMIDA provide a strong baseline for future, long-term monitoring.

9. REFERENCES

Aagaard, K., L.K. Coachman and E.C. Carmack (1981) On the halocline of the Arctic Ocean. Deep-Sea Res., Part A 28:529-545.

Alkire, M.B. and J.H. Trefry (2006) Transport of spring floodwater from rivers under ice to the Alaskan Beaufort Sea. Journal of Geophysical Research 111: C12008, doi:10.1029/2005JC003446, 2006.

Andreae, M.O. (1979) Arsenic speciation in seawater and interstitial waters: the influence of biological-chemical interactions on the chemistry of a trace element. Limnology and Oceanography 24:440-452.

Andreae, M.O., J.T. Byrd and P.N. Froelich Jr. (1983) Arsenic, antimony, germanium, and tin in the Tejo Estuary, Portugal: modeling a polluted estuary. Environmental Science and Technology 17:731-737.

Andreae, M.O. and P. N. Froelich Jr. (1984) Arsenic, antimony, and germanium biogeochemistry in the Baltic Sea. Tellus 36B:101-117.

Arnborg L., H.J. Walker and J. Peippo (1967) Suspended load in the Colville River, Alaska, 1962. Geog. Annaler 49A:131-144.

Atwell, L., K.A. Hobson and H.E. Welch (1998) Biomagnification and bioaccumulation of mercury in an arctic marine food web: insights from stable nitrogen isotope analysis. Canadian Journal of Fisheries and Marine Sciences 55:1114-1121.

Bloom, N. (1989) Determination of picogram levels of methylmercury by aqueous phase ethylation, followed by cryogenic gas chromatography with cold vapour atomic fluorescence detection. Canadian Journal of Fisheries and Aquatic Sciences 46:1131-1140.

Boyle, E.A., J.M. Edmond and E.R. Sholkovitz (1977) The mechanism of iron removal in estuaries. Geochimica et Cosmochimica Acta 41:1313-1324.

Broecker, W.S. and T.-H. Peng. (1982) Tracers in the Sea. Lamont-Doherty Geological Observatory, Palisades, NY, 690 pp.

Carmack, E.C., R.W. Macdonald and J.E. Papadakis (1989) Water mass structure and boundaries in the Mackenzie shelf estuary. Journal of Geophysical Research 94:18043-18055.

Carmack, E.C., K. Aagaard, J.H. Swift, R.W. Macdonald, F.A. McLaughlin, E.P. Jones, R.G. Perkin, J.N. Smith, K.M. Ellis and L.R. Killius (1997) Changes in temperature and tracer distribution within the Arctic Ocean: results from the 1994 Arctic Ocean section. Deep Sea Res., Part II 44:1487-1502.

Carmack, E.C. and R.W. Macdonald (2002) Oceanography of the Canadian shelf of the Beaufort Sea: a setting for marine life. Arctic 55:29-45.

Chao, Shenn-Yu (1988) River-forced estuarine plumes, Journal of Physical Oceanography 18:72-88.

Coquery, M., D. Cossa and J.M. Martin (1995) The distribution of dissolved and particulate mercury in three Siberian estuaries and adjacent Arctic coastal waters. Water, Air, and Soil Pollution 80:653-664.

Coquery, M., D. Cossa and J. Sanjuan (1997) Speciation and sorption of mercury in two macro-tidal estuaries. Marine Chemistry 58:213-227.

Cossa, D. and J. Noël (1987) Concentrations of mercury in near shore surface waters of the Bay of Biscay and in the Gironde Estuary. Marine Chemistry 20:389-396.

Cossa, D., C. Gobeil and P. Courau (1988) Dissolved mercury behaviour in the Saint Lawrence Estuary. Estuarine, Coastal and Shelf Science 26:227-230.

Cossa, D. and J.-M. Martin (1991) Mercury in the Rhône delta and adjacent marine areas. Marine Chemistry 36:291-302.

Craig P.C. and P. J. McCart (1975) Classification of stream types in Beaufort Sea drainages between Prudhoe Bay, Alaska, and the Mackenzie Delta, N.W.T., Canada. Arctic Alpine Research **7:**183-198.

Donat, J.R. and K.W. Bruland (1995) Trace elements in the oceans. In:B. Salbu and E. Steinnes (Eds.) Trace Elements in Natural Waters, CRC Press, Boca Raton, FL, pp. 247-281.

Feely, R.A., J.H. Trefry, G.J. Massoth and S. Metz (1991) A comparison of the scavenging of phosphorus and arsenic from seawater by hydrothermal iron oxyhydroxides in the Atlantic and Pacific Oceans. Deep-Sea Research 38:617-623.

Fox, L.E. (1990) Geochemistry of dissolved phosphate in the Sepik River and Estuary, Papua, New Guinea. Geochimica et Cosmochimica Acta 54:1019-1024.

Garvine, R.W. and J.D. Monk (1974) Frontal structure of a river plume, Journal of Geophysical Research 79:2251-2259.

Geyer, W.R., P.S. Hill and G.C. Kineke (2004) The transport, transformation and dispersal of sediment by buoyant coastal flows. Continental Shelf Research 24:927-949.

Gill, G.A. and K.W. Bruland (1987) Mercury in the northeast Pacific. EOS Transactions of the American Geophysical Union 68:1763.

Gobeil, C., R.W. Macdonald and B. Sundby (1997) Diagenetic separation of cadmium and manganese in suboxic continental margin sediments. Geochimica et Cosmochimica Acta 61:4647–4654.

Gordeev V.V., J.-M. Martin, I.S. Sidorov and M.V. Sidorova (1996) A reassessment of the Eurasian input of water, sediment, major elements, and nutrients to the Arctic Ocean. American Journal of Science 296:664-691.

Grasshoff, K. (1976) Methods of Seawater Analysis. Verlag Chemie, New York, 317 pp..

Granskog, M.A., J. Ehn and M. Niemela (2005) Characteristics and potential impacts of under-ice river plumes in the seasonally covered Bothnian Bay (Baltic Sea), Journal of Marine Systems 53:187-196.

Guay, C.K. and K. K. Falkner (1997) Barium as a tracer of Arctic halocline and river waters. Deep-Sea Research, Part II 44:1543-1569.

Guay C.K. and K.K. Falkner (1998) A survey of dissolved barium in the estuaries of major Arctic rivers and adjacent seas. Continental Shelf Research 18:859-882.

Guentzel, J.L., R.T. Powell, W.M. Landing and R.P. Mason (1996) Mercury associated with colloidal material in an estuarine and an open-ocean environment. Marine Chemistry 55:177-188.

Hanor, J. S. and L.H. Chan (1977) Non-conservative behavior of barium during mixing of Mississippi River and Gulf of Mexico waters. Earth and Planetary Science Letters 37:242-250.

Harms, I.H., M.J. Karcher and D. Dethleff (2000) Modeling Siberian river runoff – implications for contaminant transport in the Arctic Ocean. Journal of Marine Systems 27:95-115.

Hinrichsen, H.H. and M. Tomczak (1993) Optimum multiparameter analysis of the water mass structure in the western North Atlantic Ocean. Journal of Geophysical Research 98:10155-10169.

Howard, A.G., M.H. Arbab-Zavar and S. Apte (1984) The behaviour of dissolved arsenic in the estuary of the River Beaulieu. Estuarine, Coastal and Shelf Science 19:493-504.

Jones, E.P. and L.G. Anderson (1986), On the origin of the chemical properties of the Arctic Ocean halocline. Journal of Geophysical Research 91:10759-10767.

Karstensen, J. (2005) Optimum multi-parameter (OMP) analysis user group, Lamont-Doherty Earth Observatory, Columbia University. (Available at http://www.ldeo.columbia.edu/%7Ejkarsten/omp_std/).

Knauss, J. A. (1996) Introduction to Physical Oceanography, 2nd Ed., Prentice-Hall, Inc., Upper Saddle River, 309 pp.

Leermakers, M., S. Galletti, S. De Galan, N. Brion and W. Baeyens (2001) Mercury in the southern North Sea and Scheldt Estuary. Marine Chemistry 75:229-248.

Lindsay, D.M. and J.G. Sanders (1990) Arsenic uptake and transfer in a simplified estuarine food chain. Environmental Toxicology and Chemistry 9:391-395.

Lock M.A., T.E. Ford, D.M. Fiebig, M.C. Miller, M. Hullar, M. Kaufman, J.R. Vestal, B.J. Peterson and J.E. Hobbie (1989) A biogeochemical survey of rivers and streams in the mountains and foothills province of arctic Alaska. Archives of Hydrobiology 115:499-521.

Macdonald, R.W., C.S. Wong and P.E. Erickson (1987) The distribution of nutrients in the southeastern Beaufort Sea: implications for water circulation and primary production. Journal of Geophysical Research 92(C3):2939-2952.

Macdonald, R.W., E.C. Carmack, F.A. McLaughlin, K. Iseki, D.M. Macdonald and M.C. O'Brien (1989) Composition and modification of water masses in the Mackenzie Shelf Estuary. Journal of Geophysical Research 94:18057-18070.

Mackas, D.L., K. L. Denman and A. F. Bennett (1987) Least-square multiple tracer analysis of water mass composition. Journal of Geophysical Research 92:2907-2918.

Martin, J-M. and M. Meybeck (1979) Elemental mass-balance of material carried by major world rivers. Marine Chemistry 7:173-206.

Mason, R.P. and W.F. Fitzgerald (1993) The distribution and biogeochemical cycling of mercury in the equatorial Pacific Ocean. Deep-Sea Research I 40:1897-1924.

Mason, R.P., K.R. Rolfhus W.F. and Fitzgerald (1995) Methylated and elemental mercury cycling in surface and deep ocean waters of the North Atlantic. Water, Air, and Soil Pollution 80:665-677.

Mason, R.P. and K.A. Sullivan (1999) The distribution and speciation of mercury in the South and equatorial Atlantic. Deep-Sea Research II 46:937-956.

Matthews, J.B. (1981) Observations of under-ice circulation in a shallow lagoon in the Alaskan Beaufort Sea. Ocean Management 6:223-234.

McLaughlin, F.A., E.C. Carmack, R.W. Macdonald and J.K.B. Bishop (1996) Physical and geochemical properties across the Atlantic/Pacific water mass front in the southern Canadian Basin. Journal of Geophysical Research 101:1183-1197.

McLaughlin, F.A., E.C. Carmack, R.W. Macdonald, A.J. Weaver and J. Smith (2002) The Canada Basin, 1989-1995: upstream events and far-field effects of the Barents Sea. Journal of Geophysical Research 107:1, doi:10.1029/2001JC000904.

McNamara J.P., D.L. Kane and L.D. Hinzman (1998) An analysis of streamflow hydrology in the Kuparuk River Basin, Arctic Alaska: a nested watershed approach. Journal of Hydrology 206:39-57.

Meyerdierks, D. (1996) Ph.D. Dissertation, University of Bremen, Germany.

Mull, C.G. and K.E. Adams (1989) Dalton Highway, Yukon River to Prudhoe Bay, Alaska: Alaska Division of Geological and Geophysical Surveys, Guidebook **7**, v. 1 and 2.

Naidu, A.S., J.J. Goering, J.J. Kelley and M.I. Venkatesan (2001) Historical changes in trace metals and hydrocarbons in the inner shelf sediments, Beaufort Sea: prior and subsequent to petroleum-related industrial developments. Final Report to MMS, OCS Study 2001-061, 80 pp.

Nakashima, S., R.E. Sturgeon, S.N. Willie, and S.S. Berman (1988) Determination of trace elements in sea water by graphite-furnace atomic absorption spectrometry after preconcentration by tetrahydroborate reductive precipitation. Analytica Chimica Acta 207:291-299.

Neff, J.M. (1997) Ecotoxicology of arsenic in the marine environment. Environmental Toxicology and Chemistry. 16:917-927.

NGDC (2005), National Geophysical Data Center, NOAA Satellite and Information Service, Coastline Extractor. (Available at http://rimmer.ngdc.noaa.gov/mgg/coast/getcoast.html).

Nishino, S. (2002). Buoyancy- and eddy-driven circulation in the Atlantic layer of the Canada Basin. Journal of Geophysical Research 107:1,doi:10.1029/2000JC000286.

Payne T.G., S.W. Dana, W.A. Fischer, S.T. Yuster, P.D. Krynine, R.H. Morris, E. Lathram E. and H. Tappan H. (1951) Geology of the arctic slope of Alaska. U.S Geol. Survey Oil and Gas Investigations. Map OM-126.

Pettine, M., D. Mastroianni, M. Camusso, L. Guzzi and W. Martinotti (1997) Distribution of As, Cr, and V species in the Po-Adriatic mixing area, (Italy). Marine Chemistry. 58:335-349.

Pickart, R.S. (2004) Shelfbreak circulation in the Alaskan Beaufort Sea: Mean structure and variability. Journal of Geophysical Research. 109:C04024.

Pierce, M.L. and C.B. Moore (1982) Adsorption of arsenite and arsenate on amorphous iron hydroxide. Water Research 16:1247-1253.

Pongratz, R. and K.G. Heumann (1998) Determination of concentration profiles of methyl mercury compounds in surface waters of polar and other remote oceans by GC-AFD. International Journal of Environmental Analytical Chemistry 71:41-56.

Reimnitz, E. and K.F. Bruder (1972) River discharge into an ice-covered ocean and related sediment dispersal, Beaufort Sea, coast of Alaska. Geological Society of America Bulletin 83:861-866.

Reimnitz, E. and S.C. Wolf (1998) Are north slope surface alluvial fans pre-Holocene relicts? U.S.G.S. Professional Paper 1605, 9 pp.

Rember R.D. and J.H. Trefry (2004), Increased concentrations of dissolved trace metals and organic carbon during snowmelt in rivers of the Alaskan Arctic. Geochimica Cosmochimica Acta 68:477, doi:10.1016/S0016-7037(03)00458-7.

Rezai, H., F.M. Yusoff and C.K. Yap (2003) Mercury in zooplankton from the Malacca Straits. Indian Journal of Marine Sciences. 32:240-243.

Sanders, J.G. (1985) Arsenic geochemistry in Chesapeake Bay: dependence upon anthropogenic inputs and phytoplankton species composition. Marine Chemistry 17: 329-340.

Semmler, C.M. (2006) Sources, cycling, and fate of arsenic and mercury in the coastal Beaufort Sea. M.S. Thesis, Florida Institute of Technology, Melbourne, FL,70 pp.

Strickland, J.D.H. and T.R. Parsons. (1972) A practical handbook of seawater analysis. Bulletin of Fisheries Research Board of Canada, 167:207-211.

Seyler, P. and J.-M. Martin (1990) Distribution of arsenite and total dissolved arsenic in major French estuaries: dependence on biogeochemical processes and anthropogenic inputs. Marine Chemistry 29:277-294.

Seyler, P. and J.-M. Martin (1991) Arsenic and selenium in a pristine river-estuarine system: the Krka (Yugoslavia). Marine Chemistry 34:137-151.

Shafer M.M., J.T. Overdier, H. Phillips, D. Webb, J.R. Sullivan and D.E. Armstrong (1999) Trace metal levels and partitioning in Wisconsin Rivers. Water Air and Soil Pollution 110:273-311.

Stern, G.A. and R.W. Macdonald (2005) Biogeographic provinces of total and methyl mercury in zooplankton and fish from the Beaufort and Chukchi Seas: results from the SHEBA drift. Environmental Science and Technology 39:4707-4713.

Swift, J.H., E.P. Jones, K. Aagaard, E.C. Carmack, M. Hingston, R.W. Macdonald, F.A. McLaughlin and R.G. Perkin (1997), Waters of the Makarov and Canada Basins. Deep-Sea Res., Part II 44:1503-1529.

Szakács, O, A. Lasztity and Z.S. Horvath (1980) Breakdown of organic mercury compounds by hydrochloric acid-permanganate or bromine monochloride solution for the determination of mercury by cold vapour atomic absorption spectrometry. Analytica Chimica Acta 209:147-156

Telang S.A. (1985) Transport of carbon and minerals in the Mackenzie River. In: Degens E.T., Kempe S. and Herrera R. (Eds) Transport of Carbon and Minerals in Major World Rivers. Pt 3. Mitt. Geol.-Palaont. Inst. Univ. Hamburg, SCOPE/UNEP Soderbd. 58:337-344.

Telang S.A., R. Pocklington, A.S. Naidu, E.A. Romankevich, I.I. Gitelson and M.I. Gladeyshev (1991) Carbon and mineral transport in major North American, Russian Arctic, and Siberian Rivers: the St. Lawrence, the Mackenzie, the Arctic Alaskan Rivers, the Arctic Basin Rivers in the Soviet Union, and the Yenisei. In: Degens E.T., S. Kempe and J.E. Richey (Eds) Biogeochemistry of Major World Rivers. SCOPE Report 42, John Wiley, Chichester, 75-104.

Thompson, R.O. and R. J. Edwards (1981), Mixing and water mass formation in the Australian Sub-Antarctic. Journal of Physical Oceanography 11:1399-1406.

Tomczak, M. (1981a), An analysis of mixing in the frontal zone of South and North Atlantic Central Water off North-West Africa, Progress in Oceanography 10:172-192.

Tomczak, M. (1981b), A multiparameter extension of temperature/salinity diagram techniques for the analysis of non-isopycnal mixing, Progress in Oceanography 10:147-171.

Trefry, J.H., R.D. Rember, R.P. Trocine and J.S. Brown (2003) Trace metals in sediments near offshore oil exploration and production sites in the Alaskan Arctic. Environmental Geology 45:149-160.

Trefry, J.H., R.D. Rember, R.P. Trocine and M. Savoie (2004a) Sources, concentrations and dispersion pathways for suspended sediment in the coastal Beaufort Sea. Final Report to MMS,OCS Study MMS 2004-032.

.

Trefry, J.H., R.D. Rember, R.P., Trocine and J.S. Brown (2004b) Partitioning of potential contaminants between dissolved and particulate phases in waters of the coastal Beaufort Sea. Final Report to MMS,OCS Study MMS 2004-031.

USGS (2005), U.S. Geological Survey, Water Resources, Real-Time Data for Alaska, gauge #15908000. (Available at http://nwis.waterdata.usgs.gov/ak/nwis/discharge/?site_no=15908000&agency_cd=USGS).

van der Sloot, H.A., D. Hoede, J. Wijkstra, J.C. Duinker and R.F. Nolting (1985) Anionic species of V, As, Se, Mo, Sb, Te, and W in the Scheldt and Rhine Estuaries and the Southern Bight (North Sea). Estuarine, Coastal and Shelf Science 21:633-651.

Wang, B. (1999) Spatial distribution of chemical constituents in the Kuskokwim River, Alaska. U.S.G.S Water-Resources Investigations Report 99-4177, 1-33.

Weingartner, T.J., D.J. Cavalieri, K. Aagaard and Y. Sasaki (1998) Circulation, dense water formation, and outflow on the northeast Chukchi shelf. Journal of Geophysical Research 103:7647-7661.

Weingartner, T.J., Y. Sasaki, V. Pavlov and M. Kulakov (1999) The Siberian Coastal Current: A wind- and buoyancy-forced Arctic coastal current. Journal of Geophysical Research 104:29697-29713.

Weingartner, T.J. and S.R. Okkonen (2001) Beaufort Sea nearshore under ice currents: Science, analysis and logistics. Final Report, OCS Study MMS 2001-068.

Weingartner, T. (2006) Circulation, thermohaline structure, and cross-shelf transport in the Alaskan Beaufort Sea. Final Report to the Minerals Management Service, OCS Study MMS 2006-031. 58 pp.

Yao, Q.-Z., J. Zhang, X.-G. Qin, H. Xiong and L.-X. Dong (2006) The behavior of selenium and arsenic in the Zhujiang (Pearl River) Estuary, South China Sea. Estuarine, Coastal and Shelf Science 67:170-180.

ACKNOWLEDGEMENTS

We thank the Minerals Management Service (MMS), U.S. Department of Interior, for support and encouragement during this project. We especially thank Dick Prentki of MMS, the COTR for the study, for his participation in field exercises, for scientific consultation, and for his unwavering enthusiasm for ANIMIDA and cANIMIDA. Support and advice from Cleve Cowles and Tom Ahlfeld of MMS also are greatly appreciated. We thank Greg Durell and John Hardin of Battelle for their leadership and enthusiasm in cANIMIDA as Project Manager and Field Leader, respectively. The Peer Review Group for cANIMIDA played a very helpful role in the study and we thank the members of the group: Dr. Kenneth Lee, Dr. B.J. Presley and Dr. Damian Shea. In the field, the efforts of Mark Mertz (TEG Oceanographic Services, Inc.) as ship captain, Gary Lawley (Kinnetic Laboratories, Inc.) as physical oceanographers and snow machine leaders, and Debra Woodall (Florida Institute of Technology) as members of the water team, were indispensable and are greatly appreciated. We thank BP for logistical support and accommodations throughout the project with special recognition to Dr. Bill Streever and Mr. Wilson Cullor. Use of laboratory facilities at the Seawater Treatment Plant (STP) at West Dock and the support and interest shown by the staff at the STP were very important to us and we sincerely thank them.

The Department of the Interior Mission

As the Nation's principal conservation agency, the Department of the Interior has responsibility for most of our nationally owned public lands and natural resources. This includes fostering sound use of our land and water resources; protecting our fish, wildlife, and biological diversity; preserving the environmental and cultural values of our national parks and historical places; and providing for the enjoyment of life through outdoor recreation. The Department assesses our energy and mineral resources and works to ensure that their development is in the best interests of all our people by encouraging stewardship and citizen participation in their care. The Department also has a major responsibility for American Indian reservation communities and for people who live in island territories under U.S. administration.

The Minerals Management Service Mission

As a bureau of the Department of the Interior, the Minerals Management Service's (MMS) primary responsibilities are to manage the mineral resources located on the Nation's Outer Continental Shelf (OCS), collect revenue from the Federal OCS and onshore Federal and Indian lands, and distribute those revenues.

Moreover, in working to meet its responsibilities, the **Offshore Minerals Management Program** administers the OCS competitive leasing program and oversees the safe and environmentally sound exploration and production of our Nation's offshore natural gas, oil and other mineral resources. The MMS **Royalty Management Program** meets its responsibilities by ensuring the efficient, timely and accurate collection and disbursement of revenue from mineral leasing and production due to Indian tribes and allottees, States and the U.S. Treasury.

The MMS strives to fulfill its responsibilities through the general guiding principles of: (1) being responsive to the public's concerns and interests by maintaining a dialogue with all potentially affected parties and (2) carrying out its programs with an emphasis on working to enhance the quality of life for all Americans by lending MMS assistance and expertise to economic development and environmental protection.